UNIVERSIDAD AUTÓNOMA DE MADRID

FACULTAD DE CIENCIAS

DEPARTAMENTO DE BIOLOGÍA MOLECULAR

The role of epigenetic regulation in B-cell lymphomas

by

Daniel Martín Pérez

Tesis presentada en la Universidad Autónoma de Madrid para optar al grado de Doctor

Madrid 2010

This thesis, submitted for the degree of Doctor of Philosophy at the Unversidad Autónoma de Madrid, has been performed in the laboratory of Lymphoma Group at Spanish National Cancer Research Center (CNIO). The presented work was done under the guidance of Dr Margarita Sánchez-Beato Gómez and Dr Miguel Ángel Piris Pinilla. This work was supported by Ministerio de Educación y Ciencia (AP2005-3972, SAF2004-06952-C02-02, SAF2005-00221, and SAF2007-65957-C02-02) and the Ministerio de Sanidad y Consumo (G03/179, RD06/0020/0083 and RTICC RD06/0020/0107)

El trabajo presentado en esta memoria para optar al grado de doctor en la Universidad Autónoma de Madrid ha sido realizado en el laboratorio de Linfomas del Centro Nacional de Investigaciones Oncológicas (CNIO) bajo la dirección de la Dra Margarita Sánchez-Beato Gómez y del Dr Miguel Ángel Piris Pinilla. La realización de este trabajo ha sido posible gracias a la financiación del Ministerio de Educación y Ciencia (AP2005-3972, SAF2004-06952-C02-02, SAF2005-00221, y SAF2007-65957-C02-02) y el Ministerio de Sanidad y Consumo (G03/179, RD06/0020/0083 y RTICC RD06/0020/0107).

Anybody who has been seriously engaged in scientific work of any kind realizes that over the entrance to the gates of the temple of science are written the words: 'Ye must have faith'. It is a quality which the scientist cannot dispense with.

Max Planck

Where Is Science Going? (1932)

Dedicada a mi familia

ACKNOWLEDGEMENTS

I can't count how many people have helped me to arrive here, but they are a lot. To all of them I'd like to say THANK YOU! Now, I hope the reader can forgive me, but I'll switch to Spanish.

Este trabajo habría sido imposible sin la discusión, ayuda, motivación y/o ánimo que me ha aportado un gran número de personas. No es mi intención no ser agradecido con todas ellas, pero por cuestiones de espacio y memoria, no aparecerán todos sus nombres.

En primer lugar, quiero dar las gracias a mis codirectores **Miguel Ángel** y **May** por su orientación, ayuda e impulso. A Miguel Ángel porque siempre me ha hecho reflexionar sobre lo que daba por sentado y porque con sus comentarios (los cuales siempre me ha costado entender) me ha permitido profundizar en mis hipótesis. A May porque, simplemente, siempre ha estado conmigo al pie del cañón.

También tengo que agradecer su trabajo a las unidades del CNIO y a todos los colaboradores externos sin los cuales esta tesis habría durado muchos más años. A los estudiantes que he tenido a mi cargo, de los que tanto he aprendido y que me han ayudado; desde **Tamara** y **Sonia** hasta **Malia** y **Elena López**. También incluyo a **Bea (Charlize)**, que lleva muy poquito con nosotros pero está haciendo todo lo posible para que ponga aquí su nombre. Por supuesto, no puedo olvidarme de **Denise (D-NIS)** que se pasó un año peleando con clonaciones imposibles en vectores lentivirales y que se marchó (después de innumerables despedidas) dejándonos una gran amistad y los días DE, DED y variantes. Espero algún día poder leer también los agradecimientos de **TU** tesis.

Todos mis compañeros también han participado de alguna manera en esta tesis y por eso quiero agradecer su aportación a todos los componentes (pasados y presentes) del grupo de linfomas. Sólo nombraré a algunos por cuestiones de espacio. A **Abel**, porque fuiste una fuente de inspiración, porque aprendí mucho de ti y porque sé algo que vos no sabéis… ¡que yo no soy zurdo! A **Mar**, mi primera profesora y quien me enseñó a hacer maxipreps. A **María** y **Santi**, por resolver mis dudas sobre la patología de los linfomas. A **Elena (Mipro)** porque sin ti "El Kraken" no habría podido crecer tanto. A **MG,** que nunca ha dudado en ofrecer su ayuda con una sonrisa. A **Pier**, por ayudarme con muchísimos experimentos, por los consejos, por la música y porque, en un laboratorio lleno de mujeres, al final uno necesita hablar con un hombre de vez en cuando (**Alberto**, **Luis** y **Rubén**, que también me ayudaron en este aspecto).

Magda (Chaky), me has acompañado casi desde el principio y has sido una de las mejores compañeras que he podido tener nunca. Muchas gracias por contagiarme tu positividad y tus sueños, por regalarme tantas risas (y lágrimas) juntos y por nuestro próximo viaje a Polonia.

Lore (Lorelain), tienes el mérito de haber conseguido que deje de ser tan *friky* y me parezca a una persona normal. Eso es mucho. También te tengo que agradecer tu amistad (Ah, pero… ¿somos amigos?) y las largas conversaciones sobre la vida aderezados con tus pensamientos paralelos que tanto me han hecho reír.

Lina (Colina), es sorprendente lo bien que congeniamos en tan poco tiempo, aunque claro, tú ya me habías llevado a la cámara oscura. Gracias por tus comentarios críticos, por tu ENORME energía, por tu buen humor, por tu cariño y por dejarme ganar a los dardos de vez en cuando.

Beatriz S. (Espiridión), ¡qué jóvenes éramos cuando empezamos! Yo tan *friky* y tú tan formal. A ti te debo unos cuantos kilitos a base de cuajadas con "requemao", bombones y pasteles varios. Gracias por hacernos a todos las mañanas más dulces.

Helen (Hp), hace poco leí en los agradecimientos de otra tesis que habías sacado lo mejor de nosotros. No puedo estar más de acuerdo. Gracias por ser el alma de la fiesta, contigo es imposible estar de mal humor.

Espe (Superpatxi), gracias por apuntar todas las frases de Elena, por enseñarme la geografía de Euskadi y algo de euskera y por ser una chica tan dulce… en el fondo. Eskerrik asko.

Pilar, eres admirable en muchos sentidos. Me he beneficiado de tu sim/em-patía, de que tengas los pies en la tierra (aunque un poco desfocalizados) y te agradezco todo el cariño y los abrazos que me has dado.

Marién, gracias por esperarme siempre para desayunar (con todo lo que eso conlleva) y por leerme el horóscopo. **Elena Doménech (Perroflauta)**, llevas poco pero sigue así que vas por buen camino y gracias por arrugar la nariz cuando leas esto. **Cristina (Golden)**, es una pena que las fotos no reflejen el cariño que nos das a todos, en cualquier caso, gracias por dárnoslo.

Gracias a New York, a la compañía que tuve y a la limusina que nos llevó al aeropuerto.

En otros laboratorios del CNIO hay mucha gente que también me ha ayudado profesional o personalmente y a los que tengo especial afecto. Aquí entran **Ricardinho** y **Magda Z**, **Fabian (Caipira)** y nuestras clases de capoeira, **Gonzalo (San Gonzalo)**, y el comité de becarios del Retreat de 2006. También **Laura Cereceda,** a la que quiero agradecer que siempre me haya considerado "una más".

Fuera del CNIO también hay mucha gente a la que mencionar. A **Alfredo**, **David**, **Hugo** y **Miguel** del dpto. de Medicina de la UAH. Todo esto empezó con vosotros. A mis amigos de la facultad de Biología, especialmente a la **Dra. López (Anita)** y a la futura **Dra. Vázquez (Victoria)**, vosotras sí que sabéis por lo que se pasa ¿verdad? A **Lidia, Gema** y **Carlos**, por hacerme el mejor regalo que se puede hacer a alguien… cumplir un sueño. A mis amigos del Recuerdo y las tapas del EMYFA.

A mi familia, que me ha dado todo lo necesario para llegar aquí. Especialmente a mis padres, **Félix** y **Mª Jesús** dos grandísimas personas que me han ofrecido todas las oportunidades del mundo para que yo eligiese qué hacer con mi vida (y que me han alimentado realmente bien). Gracias por dejarme tropezar pero estar siempre ahí para levantarme de nuevo. También a mi hermana **Ruth** y a mi cuñado **Isra**, sois estupendos.

A **Sara**, que lleva ya 9 años aguantándome estoicamente. Gracias por todo este tiempo compartido y por ser mi apoyo más grande. Gracias también por ponerme todo fácil y por todo lo que has hecho por mí. Perdona que en estas líneas no quepa todo lo que quiero decirte.

Y como a mí me gusta dejarme lo mejor para el final, mis últimas GRACIAS van para **Beatriz Herreros (Maribel).** Hemos pasado juntos todas las fases del doctorado y has sido una compañera ejemplar, la mejor que se puede desear. Hemos diseñado juntos cientos de experimentos y discutido sobre resultados muy raros (el origen de las bandas de ectoplasmina) y has sabido mostrarme el lado positivo en los momentos malos. También has aguantado mis infinitas bromas. Gracias por la comprensión, el cariño los muchos buenos ratos y los malos (que también unen) y por ser una gran amiga.

A todos los que me han acompañado en este camino… ¡GRACIAS!

INDEX

INDEX ..... **I**

SUMMARY/RESUMEN ..... **VII**

ABBREVIATIONS ..... **XIII**

1. INTRODUCTION **1**

1.1. HEMATOLOGIC MALIGNANCIES: LYMPHOMAS 3

1.1.1. GENERAL ASPECTS 3

1.1.2. MANTLE CELL LYMPHOMA 3

1.1.2.1. EPIDEMIOLOGY 4

1.1.2.2. IMMUNOPHENOTYPE AND GENETIC FEATURES 5

1.1.3. DIFFUSE LARGE B CELL LYMPHOMA 7

1.1.3.1. EPIDEMIOLOGY 7

1.1.3.2. MOLECULAR PATHOGENESIS 8

1.1.3.3. RELATIONSHIP WITH EPSTEIN BARR VIRUS 9

1.2. MECHANISMS OF EPIGENETIC REGULATION 11

1.2.1. LEVELS OF EPIGENETIC REGULATION 11

1.2.2. THE POLYCOMB GROUP AS A REGULATOR OF GENE EXPRESSION 13

1.2.2.1. POLYCOMB TARGETING TO GENE PROMOTERS 16

1.2.2.2. POLYCOMB FUNCTIONS 17

1.2.2.3. POLYCOMB AND CANCER 18

1.2.3. MicroRNAS AND REGULATION OF GENE EXPRESSION 23

OBJECTIVES **27**

2. MATERIALS AND METHODS **31**

2.1. HUMAN TISSUE SAMPLES. ORIGIN, PROCESSING AND DIAGNOSIS 33

2.2. CELL CULTURE 35

2.2.1. CELL LINES 35

2.2.2. CULTURE AND CONSERVATION OF CELL LINES 36

2.3. ANTIBODIES 37

2.3.1. PRODUCTION OF SUZ12 MONOCLONAL ANTIBODY 38

2.4. IMMUNOHISTOCHEMISTRY 38

2.5. TISSUE MICROARRAYS 39

2.6. BACTERIAL STRAINS AND CULTURE 40

2.6.1. PROPAGATION CONDITIONS 40

2.7. POLYMERASE CHAIN REACTION (PCR) 40
2.8. CLONING OF PCR PRODUCTS 40
2.8.1. CLONING IN PENTR/D-TOPO VECTOR 40
2.8.2. CLONING IN PGL3 CONTROL VECTOR 41
2.9. CLONING OF shRNA IN LENTIVIRAL VECTORS 41
2.10. TRANSFECTION AND TRANSDUCTION TECHNIQUES 42
2.10.1. TRANSFECTION WITH FUGENE® HD 42
2.10.2. CALCIUM PHOSPHATE PRECIPITATION 43
2.10.3. MICROPORATION 43
2.10.4. TRANSDUCTION WITH LENTIVIRAL PARTICLES 44
2.11. LUCIFERASE ASSAYS 46
2.12. CHROMATIN IMMUNOPRECIPITATION (CHIP) AND CHIP-ON-CHIP 46
2.12.1. CHROMATIN IMMUNOPRECIPITATION (CHIP) 47
2.12.2. CHIP-ON-CHIP 50
2.12.3. DATA ANALYSIS 51
2.13. FLOW CYTOMETRY TECHNIQUES 52
2.13.1. ANALYSIS OF TRANSDUCTION EFFICIENCY 52
2.13.2. CELL COMPETITION ASSAYS 52
2.13.3. ANALYSIS OF APOPTOSIS BY ANNEXIN V STAINING 52
2.13.4. CELL CYCLE ANALYSIS BY PI STAINING 53
2.14. GENOMIC DNA EXTRACTION 53
2.15. RNA EXTRACTION 54
2.15.1. CELL LINES 54
2.15.1.1. EXTRACTION OF mRNA 54
2.15.1.2. EXTRACTION OF microRNA 54
2.15.2. .TISSUES 55
2.15.2.1. FROZEN TISSUES 55
2.15.2.2. FFPE TISSUES 55
2.16. RETROTRANSCRIPTION 56
2.16.1. mRNA 56
2.16.2. MicroRNA 57
2.17. REAL-TIME QUANTITATIVE PCR 57
2.18. GENE EXPRESSION MICROARRAYS 58
2.18.1. cDNA SYNTHESIS FROM TOTAL RNA 58

2.18.2. FLUORESCENT cRNA SYNTHESIS: IN VITRO TRASNSCRIPTION AND INCORPORATION OF FLUOROCHROMES 58
2.18.3. HYBRIDIZATION 59
2.19. MicroRNA EXPRESSION MICROARRAYS....60
2.19.1. LABELING 60
2.19.2. HYBRIDIZATION 60
2.20. BIOINFORMATIC TOOLS....61
2.20.1. MICROARRAY DATA ANALYSIS....61
2.20.1.1. GENE EXPRESSION MICROARRAYS 61
2.20.1.2. MicroRNA EXPRESSION MICROARRAYS....61
2.20.2. GENE SET ENRICHMENT ANALYSIS 61
2.20.3. INGENUITY PATHWAYS....62
2.21. TOTAL PROTEIN EXTRACTION 62
2.22. HISTONE EXTRACTION 62
2.23. WESTERN BLOTTING 62
2.24. ANALYSIS OF THE PRESENCE OF THE EPSTEIN-BARR VIRUS 63
2.24.1. ANALYSIS BY PCR 63
2.24.2. ANALYSIS BY IN SITU HYBRIDIZATION 64
2.25. FLUORESCENT IN SITU HYBRIDIZATION....64
3. RESULTS....67
RESULTS I....69
3.1. SUZ12 AND EZH2 PROTEIN EXPRESSION IN NORMAL HUMAN TISSUES 71
3.2. SUZ12 AND EZH2 PROTEIN EXPRESSION IN HUMAN TUMORS 72
3.3. COPY NUMBER CHANGES AT THE SUZ12 LOCUS....74
3.4. SUZ12 IN MANTLE CELL LYMPHOMAS....75
3.5. MicroRNA LOSSES MAY ACCOUNT FOR UPREGULATION OF SUZ12 IN SOME MCL CASES 83
3.6. SUZ12 DEFICIENCY COMPROMISES MCL VIABILITY....84
3.7. IDENTIFICATION AND FUNCTIONAL CLASSIFICATION OF SUZ12 GENOMIC TARGET GENES IN MCL....85
3.8. GENE EXPRESSION PROFILING IN SUZ12 DEFICIENT MCL CELLS AND IN MCL PATIENTS....91
3.8.1.CHANGES IN SUZ12 TARGETS AFTER SUZ12 SILENCING IN THE Z138 MCL-DERIVED CELL LINE....91

3.8.2.GENE EXPRESSION PROFILE IN MCL SAMPLES 91
3.9. PATHWAYS COREGULATED WITH SUZ12 IN MCL 92

RESULTS II 97

3.10. EBV microRNA EXPRESSION IN DLBCL CASES 99
3.11. EBV INFECTION CORRELATES WITH THE ABSENCE OF BCL6 PROTEIN 102
3.12. MicroRNA TARGET PREDICTION 103
3.13. EXPRESSION OF SELECTED microRNAS IN DLBCL PATIENTS 105
3.14. BCL6 PROTEIN AND microRNA EXPRESSION IN CELL LINES 108
3.15. MULTIPLE VIRAL microRNAS REPRESS BCL6 IN DLBCL 109
3.15.1. ASSESMENT OF THE INTERACTION BETWEEN EBV-ENCODED microRNAS AND THE 3' UTR OF BCL6 109
3.15.2. EFFECTS OF microRNAS ON ENDOGENOUS BCL6 PROTEIN 111
3.15.3. INHIBITION OF ENDOGENOUS EBV-ENCODED microRNAS AUGMENTS THE EXPRESSION OF BCL6 PROTEIN 112

4. DISCUSSION 115

4.1. SUZ12 AND THE PATHOGENESIS OF MANTLE CELL LYMPHOMA 118
4.2. REGULATION OF BCL6 BY EBV-ENCODED microRNAS 124
4.3. PERSPECTIVES 128

CONCLUSIONS/CONCLUSIONES 129

REFERENCES 133

APPENDIX (Publications) 157

SUMMARY/RESUMEN

There is increasing evidences showing that cancer is not only a genetic disease but also an epigenetic disease. The most important epigenetic regulators are the Polycomb and trithorax complexes and DNA methylation. Moreover several cancers show altered expression of microRNAs that also deregulate several genes. In this work, we have undertaken the study of SUZ12, a Polycomb group protein and the microRNAs (miRNA) expressed by the oncogenic Epstein Barr Virus (EBV) in different B-cell lymphoma types.

SUZ12 is a component of the Polycomb PRC2 complex, along with EZH2, that has been involved in embryonic stem cell differentiation. Various results coincide in showing that EZH2 plays an essential role in many cancer types, but this has not been as fully demonstrated for SUZ12. In the first part of this work, we report SUZ12 protein expression and genetic alterations in several tumors and especially in Mantle Cell Lymphoma (MCL), a tumor whose pathogenesis is not completely understood. Additionally, functional and genomic studies demonstrate that SUZ12 targets genes involved in central oncogenic pathways are associated with MCL pathogenesis and SUZ12 deficiency results in reduced viability of MCL cells. Our results support the hypothesis that the abnormal expression of SUZ12 in MCL may account for some of the still unexplained features of MCL, and lead us to propose a putative oncogenic role for SUZ12. These data suggest that drugs targeting the PRC2 complexes, such as LBH589, could be a rational therapeutic approach for MCL patients.

EBV is a very successful virus that infects B cells, inducing proliferation of EBV carrying B-lymphocytes. EBV infection disrupts the normal B cell program and abrogates the formation of normal germinal centers by infected B cells. BCL6 is a key transcriptional repressor required for germinal centre reaction and it has been shown to repress NF-κB in DLBCL. However, EBV positive DLBCL are usually BCL6-negative.

In the second part of this work, we have found a restricted cluster of viral microRNAs that is expressed in EBV-positive patients. By immunohistochemical studies we have found an almost perfect inverse correlation between EBV infection and BCL6 protein expression in cases of DLBCL. Using a bioinformatic approach we have found that several of these miRNAs can potentially target the 3'UTR of BCL6. Functional experiments have allowed us to demonstrate the effect of these miRNAs on BCL6. With these results we hypothesize that BCL6 downregulation might be necessary for DLBCL cells to survive in the context of EBV infection, probably in order to allow the activation of the NF-κB pathway.

Cada vez hay más evidencias que demuestran que el cáncer no es sólo una enfermedad genética, sino también epigenética. Los reguladores epigenéticos más importantes son los complejos Polycomb y Trithorax y la metilación del ADN. Además muchos tumores presentan una expresión alterada de microARNs que desorganizan la expresión de varios genes. En el presente trabajo, hemos abordado el estudio de SUZ12, una proteína del grupo Polycomb y de microARNs expresados por el virus de Epstein Barr en diferentes tipos de linfomas B.

SUZ12 es un componente del complejo Polycomb PRC2, junto a EZH2, que ha sido implicado en la diferenciación de células troncales embrionarias. Varios resultados coinciden en mostrar que EZH2 interpreta una función esencial en muchos tipos de cáncer, pero esto mismo no se ha demostrado totalmente para SUZ12. En la primera parte de este trabajo, mostramos alteraciones genéticas y en la expresión de SUZ12 en varios tumores, especialmente en linfoma de célula del manto, un tumor cuya patogenia no se entiende totalmente. Además, estudios genómicos y funcionales demostraron que SUZ12 regula genes implicados en vías de señalización oncogénicas asociadas con la patogenia del linfoma de célula del manto y que la deficiencia de esta proteína reduce la viabilidad de las células de este linfoma. Nuestros resultados avalan la hipótesis de que la expresión anormal de SUZ12 en linfoma del manto da cuenta de algunas de las características sin explicación de este tumor y nos permiten proponer una función oncogénica para SUZ12. Por otro lado, estos datos sugieren que fármacos que interfieren con los complejos PRC2, tales como el LBH589, pueden suponer una aproximación terapéutica alternativa para los pacientes de linfoma del manto.

El virus de Epstein Barr es un virus que infecta de manera muy eficiente células B induciendo la proliferación de estos linfocitos. Esta infección interfiere con el programa normal de desarrollo de las células B e impide la participación de estas células en la formación de centros germinales normales. BCL6 es un represor transcripcional clave requerido para la reacción del centro germinal y se ha demostrado que es capaz de inhibir la vía de NF-κB en linfoma difuso de células B grandes. Sin embargo, los casos de linfoma difuso positivos para el virus de Epstein Barr suelen ser negativos para BCL6.

En la segunda parte de este trabajo, hemos encontrado un grupo restringido de microARNs que se expresa en los casos de linfoma difuso positivos para el virus de Epstein Barr. Mediante estudios inmunohistoquímicos hemos encontrado una correlación inversa casi perfecta entre la presencia del virus y la expresión de BCL6 en estos casos. Mediante un análisis bioinformático hemos podido comprobar que muchos de estos microARNs pueden, potencialmente, inhibir BCL6. Experimentos funcionales nos ha permitido demostrar el efecto

de estos microARNs sobre BCL6. Con estos resultados podemos especular que la inhibición de BCL6 podría ser necesaria para la supervivencia de los linfomas difusos en el contexto de una infección por el virus de Epstein Barr, permitiendo la activación de la vía de NF-κB.

ABBREVIATIONS

aRNA	Amplified RNA
ATCC	American Type Culture Collection
ATM	Ataxia Telangiectasia Mutated
BART	BamH1-A Rightward Transcript
BHRF	BamH1-H Right reading Frame
BIRC	Baculoviral IAP Repeat-Containing protein
BL	Burkitt Lymphoma
BMI1	B lymphoma Mo-MLV Insertion region 1
BSA	Bovine Serum Albumin
CDK	Cyclin-Dependent Kinases
cDNA	Complementary DNA
ChIP	Chromatin Immunoprecipitation
CLL	Chronic Lymphocytic Leukemia
CNIO	Spanish National Cancer Research Centre
CSC	Cancer Stem Cell
Cy3	Cyanine 3-conjugated dUTP
Cy5	Cyanine 5-conjugated dUTP
DLBCL	Diffuse Large B Cell Lymphoma
DMSO	Dimethyl Sulphoxide
DNA	Deoxyribonucleic acid
dNTP	2'-Deoxyribonucleoside-5'-triphosphate
DSMZ	Deutsche Sammlung von Mikroorganismen und Zellkulturen
DTT	Dithiothreitol
EBV	Epstein Barr virus
EED	Embryonic Ectoderm Development
EZH2	Enhancer of Zeste Homologue 2
FAM	6-carboxyfluorescein
FBS	Fetal Bovine Serum
FDR	False Discovery Rate

FE	Feature Extraction
FL	Follicular Lymphoma
GEP	Gene Expression Profiling
GSEA	Gene Set Enrichment Analysis
H/E	Hematoxylin and Eosin
HDAC	Histone Deacetylase
HDACi	Histone Deacetylase Inhibitor
HL	Hodgkin Lymphoma
HSC	Hematopoietic Stem Cell
MCL	Mantle Cell Lymphoma
mRNA	Messenger RNA
miR	microRNA
miRNA	microRNA
NF-κB	Nuclear Factor Kappa B
NHL	Non-Hodgkin Lymphoma
PBS	Phosphate Buffered Saline
PcG	Polycomb Group
PCR	Polymerase Chain Reaction
PI	Propidium Iodide
PRC1	Polycomb Repressive Complex 1
PRC2	Polycomb Repressive Complex 2
Pre-miRNA	Precursor microRNA
Pri-miRNA	Primitive microRNA
PUMA	P53 Up-regulated Modulator of Apoptosis
Rb	Retinoblastoma
RNA	Ribonucleic Acid
RNAi	RNA Interference
rpm	Revolutions Per Minute
RT	Reverse Transcription

SDS	Sodium Dodecyl Sulfate
shRNA	Short Hairpin RNA
SMZL	Splenic Marginal Zone Lymphoma
SUZ12	Suppressor of Zeste 12
TIC	Tumor Initiating Cell
trxG	Trithorax Group
TMA	Tissue Microarrays
WB	Western Blot
WHO	World Health Organization

1. INTRODUCTION

1.1 HEMATOLOGIC MALIGNANCIES: LYMPHOMAS

1.1.1 GENERAL ASPECTS

The word lymphoma encompasses a series of B and T cell derived malignancies with very different courses and prognosis. They constitute around 4-5% of all newly diagnosed cancers in developed countries and its incidence has followed an increasing tendency in the last years (Altekruse et al., 2009).

Lymphomas are classified attending to their morphology, immunophenotype, clinical course as well as genetic and cytogenetic characteristics. Although lymphoma classification is dynamic and frequent revisions are published, there are two major categories recognized: Hodgkin lymphoma (HL, discovered by Thomas Hodgkin in 1832, being the first lymphoma to be described) and non-Hodgkin lymphoma (NHL). Non-Hodgkin lymphomas constitute 87.5% of all lymphomas and include neoplasms derived from B and T/NK cells. B cell lymphomas account for nearly 85% of all non-Hodgkin lymphomas though (Altekruse et al., 2009).

Lymphoma classification is complex (Table 1.1) and its extension is out from the scope of this work. Thus, due to their relevance for this doctoral thesis, only two lymphoma subtypes are going to be described: mantle cell lymphoma and diffuse large B cell lymphoma.

1.1.2 MANTLE CELL LYMPHOMA

Mantle cell lymphoma (MCL) is a type of high-grade (i.e. fast-growing or aggressive) small B cell lymphoma characterized by an abnormal proliferation of mature B lymphocytes. This lymphoma was first described in the 70's by Lennert (Stansfeld et al., 1988) and the concept of MCL was first introduced by Weisenburger and collaborators (Weisenburger et al., 1981). However it was not until 1992 that the International Lymphoma Study Group (ILSG) agreed on the denomination of this tumor as MCL (Banks et al., 1992). There are different morphologic variants: blastoid, pleomorphic, small cell and marginal zone-like. The blastoid and pleomorphic variants are larger cell types, have higher proliferation rates and are normally associated to a shorter survival (Argatoff et al., 1997; Bosch et al., 1998; Lardelli et al., 1990; Pileri and Falini, 2009; Swerdlow et al., 2008). High tumor cell proliferation is another factor that is associated to poor prognosis in MCL (Argatoff et al., 1997; Bosch et al., 1998).

Table 1.1. WHO 2008: the mature B-cell neoplasms (Swerdlow et al., 2008)
Chronic lymphocytic leukemia/small lymphocytic lymphoma
B-cell prolymphocytic leukemia
Splenic marginal zone lymphoma
Hairy cell leukemia
Splenic lymphoma/leukemia, unclassifiable
Splenic diffuse red pulp small B-cell lymphoma*
Hairy cell leukemia-variant*
Lymphoplasmacytic lymphoma
Waldenström macroglobulinemia
Heavy chain diseases
Alpha heavy chain disease
Gamma heavy chain disease
Mu heavy chain disease
Plasma cell mieloma
Solitary plasmacytoma of bone
Extraosseous plasmacytoma
Extranodal marginal zone B-cell lymphoma of mucosa-associated lymphoid tissue (MALT lymphoma)
Nodal marginal zone B-cell lymphoma (MZL)
Pediatric type nodal MZL
Follicular lymphoma
Pediatric type follicular lymphoma
Primary cutaneous follicle center lymphoma
Mantle cell lymphoma
Diffuse large B-cell lymphoma (DLBCL), not otherwise specified
T cell/histiocyte rich large B-cell lymphoma
DLBCL associated with chronic inflammation
Epstein-Barr virus (EBV)+ DLBCL of the elderly
Lymphomatoid granulomatosis
Primary mediastinal (thymic) large B-cell lymphoma
Intravascular large B-cell lymphoma
Primary cutaneous DLBCL, leg type
ALK+ large B-cell lymphoma
Plasmablastic lymphoma
Primary effusion lymphoma
Large B-cell lymphoma arising in HHV8-associated multicentric Castleman disease
Burkitt lymphoma
B-cell lymphoma, unclassifiable, with features intermediate between diffuse large B-cell lymphoma and Burkitt lymphoma
B-cell lymphoma, unclassifiable, with features intermediate between diffuse large B-cell lymphoma and classical Hodgkin lymphoma
Hodgkin Lymphoma
Nodular lymphocyte-predominant Hodgkin lymphoma
Classical Hodgkin lymphoma
Nodular sclerosis classical Hodgkin lymphoma
Lymphocyte-rich classical Hodgkin lymphoma
Mixed cellularity classical Hodgkin lymphoma
Lymphocyte-depleted classical Hodgkin lymphoma
*These represent provisional entities or provisional subtypes of other neoplasms.

1.1.2.1 EPIDEMIOLOGY

MCL is a relatively rare disease that constitutes only about 8-10% of all NHL in Europe and more frequently affecting middle-aged to elderly men (mean age at diagnosis: 60 years;

male:female ratio = 2-7:1) (Meusers et al., 1997; Swerdlow et al., 2008). It is thought to arise from the malignant transformation of B lymphocytes in the mantle zone of the lymphoid follicle (Figure 1.1). Most MCL patients (>70%) are diagnosed in a stage III-IV (i.e. with extranodal dissemination, bone-marrow involvement and leukemic spread). MCL is regarded as an aggressive incurable disease with a median survival of patients being 3-4 years and less than 15% of long-term survivors (Weigert et al., 2009). However, individual clinical behavior can vary substantially and survival times range between few months only to more than 10 years (Fernandez et al., 2010; Jares et al., 2007; Meusers et al., 1997; Orchard et al., 2003; Rosenwald et al., 2003b).

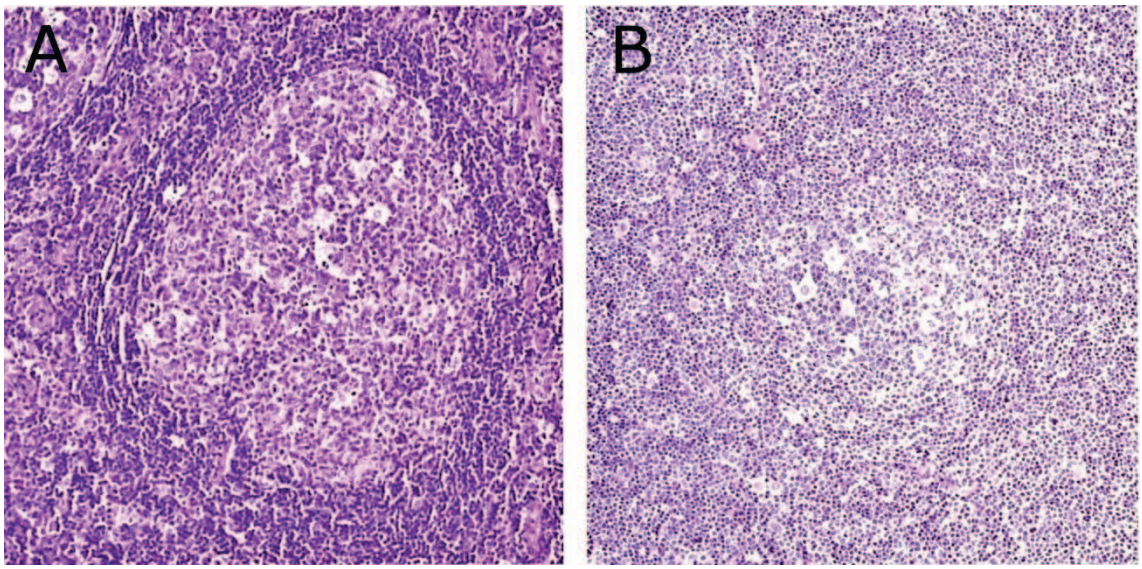

Figure 1.1. Comparison of the structure of a reactive follicle (A) and an early phase of mantle cell lymphoma (B). Despite of the tumoral cells that are invading the germinal center, the structure of the follicle, centered by a reactive germinal centre, can still be recognized.

1.1.2.2 IMMUNOPHENOTYPE AND GENETIC FEATURES

MCL is characterized by expression of the B-cell markers CD19, CD20, CD22, CD79a, SOX11 and BSAP/PAX5 (Jaffe, 2009; Jares and Campo, 2008; Mozos et al., 2009). MCL normally expresses high levels of IgM/D with more frequent lambda restriction (Jaffe, 2009; Jares and Campo, 2008). Most cases of MCL do not show mutation in V-gene sequences of Ig(V_H) genes but 15-40% of MCLs may carry somatic hypermutation, indicating a different origin in cells that

has passed through the germinal centre reaction (Camacho et al., 2003; Kienle et al., 2003; Orchard et al., 2003; Welzel et al., 2001).

Table 1.2. Common genetic alterations in mantle cell lymphoma (from Jares *et al.* 2007)

Chromosomal region*	Frequency (%)			Candidate gene	Functional process
	BAC array	SNP array (10 K)	Metaphase CGH		
Gains					
3q25-qter	31–50	27	32–70‡	?	?
4p12-13	57	?	7‡	?	?
7p21-22	16-34	?	27‡	?	?
8q21-qter	16-36	?	11–30‡	MYC	Cell growth, proliferation, apoptosis
9q22	?	?	16	SYK	Cell signaling
10p11-12	17	12	5-7‡	BMI1	Cell cycle, DNA damage response and anti-senescence
12q13	?	?	16-30	CDK4	Cell cycle
18q11-q23	15-17	18	11–26‡	BCL2	Anti-apoptosis
Losses					
1p13-p31	29–52	18	24-52	?	?
2q13	17	?	?	BIM§	Pro-apoptosis
6q23-q27	23-38	18	?	?	?
8p21-pter	17–34	?	13-30	?	?
9p21-p22	18–31	27	16-30	CDKN2A	Cell cycle and anti-senescence
9q21-qter	29	?	18	?	?
10p14-15	18-31	18	18	?	?
11q22-q23	21-59	23	16-30	ATM	DNA damage response
13q11-q13	25-55	27	17-74	?	?
13q14-q34	43-51	?	44-70	?	?
17p13-pter	21-45	18	13-16	TP53	Cell cycle, DNA damage response and anti-senescence
22q12	17-50	?	?	?	?

***Minimal altered regions vary slightly among different studies. ‡High-level DNA amplifications have been identified in these regions. §Homozygous deletions of this gene have been identified in mantle cell lymphoma cell lines but not in primary tumors. BAC, bacterial artificial chromosome; CGH, comparative genomic hybridization; SNP, single nucleotide polymorphism; ?, not known.**

The main distinguishable feature of MCL is the overexpression of nuclear cyclin D1. This is caused by a translocation between chromosomes 11 and 14 that puts the *CCND1* gene under the control of the enhancer of the heavy chain of the immunoglobulins (Raffeld and Jaffe, 1991). The t(11;14)(q13;q32) translocation is found in the vast majority of MCL patients, it is considered the hallmark of the disease (Jares et al., 2007) and probably facilitates the

deregulation of the cell cycle at the G_1-S transition. In those patients that do not carry the t(11;14) translocation, other genetic abnormalities seem to cause excess production of cyclin D1. However, there are rare examples in which MCL seems to initiate from the overexpression of other cyclins (e.g., cyclin D2 and cyclin D3) (Fu et al., 2005). However, this characteristic molecular event does not explain fully the clinical and biological features of the tumor and is not sufficient for malignant transformation, as has been demonstrated in experimental models (Bodrug et al., 1994).

Moreover, several secondary chromosomal gains and losses are found in MCL samples and surely account for the varying survival of these patients (Table 1.2). The most frequently altered chromosomal regions in MCL identified up to now are gains of chromosomal fragments in 3q, 7q and 8q and losses in 1p, 6q, 8p, 9p, 9q, 11q, 13q and 17p (Ferrer et al., 2007; Jares et al., 2007). These alterations affect the expression of several proteins involved in regulation of cell cycle (BMI1, INK4a, ARF, CDK4 and RB1), proteins involved in DNA damage repair (ATM, CHK2 and p53) and apoptosis (BCL2, BIM) (Jares et al., 2007). NF-κB activation has been also implied in the pathogenesis of MCL (Martinez et al., 2003). Nevertheless, there are still various MCL oncogenic features that are not explained by the alterations so far identified.

1.1.3 DIFFUSE LARGE B CELL LYMPHOMA

Diffuse large B cell lymphoma (DLBCL) is a high-grade large cell lymphoma. It is characterized by the proliferation of mature B cells that can have different origins.

However, classical DLBCL is already a heterogeneous disease. The molecular heterogeneity of DLBCL has been explored through the use of microarrays and has lead to the definition of three different molecular subtypes of DLBCL: germinal centre B-like DLBCL (GCB DLBCL), activated B-like DLBCL (ABC DLBCL) and primary mediastinal B cell lymphoma (PMBL) (Lenz et al., 2008b). Each subtype has different prognosis and survival rates.

1.1.3.1 EPIDEMIOLOGY

DLBCL is the most common form of lymphoma accounting for 30-40% of all newly diagnosed lymphomas. Approximately 5-6 DLBCL new cases per 100,000 people are diagnosed in Europe each year. Median age at presentation for the two most common subtypes is around

60 years old with male predominance. It often involves the lymph nodes, spleen, liver, and bone marrow, though this differs from patient to patient (Swerdlow et al., 2008).

The cell of origin is thought to be a B cell in different stages of differentiation depending on the DLBCL subtype. GCB subtype is thought to arise from germinal-center B cells whereas de ABC subtype may arise from a post-germinal center B cell that is blocked during plasmacytic differentiation. The cells of origin for PMBL are probably rare thymic B cells.

DLBCL is considered curable with anthracycline-based chemotherapy regimens such as a combination of cyclophosphamide, doxorubicin, vincristine, and prednisone (CHOP) (Fisher et al., 1993), but addition of rituximab immunotherapy (R-CHOP) increases significantly the survival rate of patients (Coiffier et al., 2002). However only 50% of patients achieve complete response (Lenz and Staudt). The prognosis depends mainly on the molecular subtype of DLBCL. Thus, overall survival is favorable for GCB and PMBL subtypes and worse for those patients with the ABC subtype (Lenz et al., 2008a) (Figure 1.2).

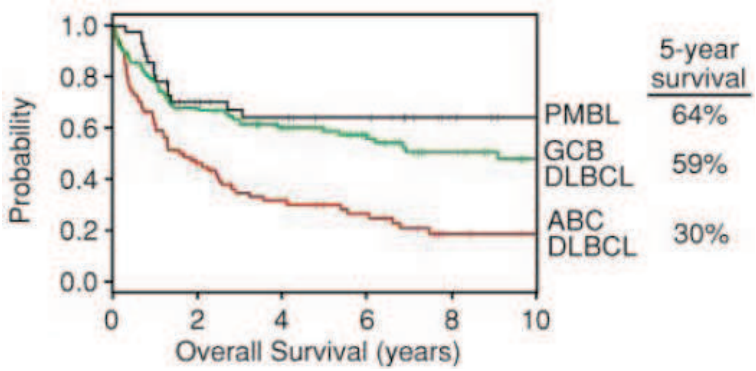

Figure 1.2. Kaplan-Meier plot of overall survival of PMBL, GCB, and ABC DLBCL patients after chemotherapy (reproduced from Rosenwald A et al., 2003)

1.1.3.2 MOLECULAR PATHOGENESIS

Chromosomal translocations involving the *BCL6* gene on band 3q27 are the most common genetic abnormalities in DLBCL, occurring in 35% to 40% of cases (Pasqualucci et al., 2003). The chromosomal partner is usually the immunoglobulin heavy-chain promoter on chromosome 14, thus the consequence is the overexpression of BCL6 which is normally tightly regulated during B cell differentiation. Dysregulated constitutive expression of BCL6 may lead to maturation arrest and confer a proliferative advantage.

However, each DLBCL subtype relies in a different oncogenic program. Although some alterations are common for more than one subtype there are several features that are

exclusive of one subtype. For instance the GCB subtype is characterized by the t(14;18) translocation that puts the anti-apoptotic gene *BCL2* under the control of the promoter of immunoglobulins (Lenz et al., 2008b; Rosenwald et al., 2002). Other genetic aberrations are p53 mutations (Young et al., 2008), deletion of the tumor suppressor gene *PTEN* and the amplification of the oncogenic miR-17-92 cluster (which also downregulates PTEN) (Xiao et al., 2008).

In the case of ABC lymphomas, some of them bear amplification of the *BCL2* locus and almost all overexpress BCL2 protein (Lenz et al., 2008b). Other frequent cytogenetic alterations are the deletion of the *CDKN2A* locus (Lenz et al., 2008b; Tagawa et al., 2005) which encodes for two different proteins INK4a and ARF both of which are able to restrict cell proliferation upon aberrant mitotic signaling. However the mechanism is different for each protein. Whereas INK4a acts through the activation of RB, ARF inhibits the function of MDM2, a known repressor of p53. Thus, deletion of the *CDKN2A* locus provides resistance to cell cycle arrest and p53-induced apoptosis.

The third entity, PMBL is characterized by the 9p24 amplification, an alteration that is common to HL (Joos et al., 2000; Lenz et al., 2008b; Rosenwald et al., 2003a). This region encompasses several megabases of DNA and involves many genes, but it is thought that one of the most important targets of this amplification is *JAK2* which encode for a tyrosine kinase involved in the inhibition of apoptosis among other functions (Meier et al., 2009).

1.1.3.3 RELATIONSHIP WITH EPSTEIN BARR VIRUS

Epstein Barr virus (EBV) is a virus belonging to the γ-herpesvirus family that infects 90% population worldwide and persists for life in the infected host. Its genome is constituted by a 172 kb molecule of double stranded DNA. The main target of the virus is the subpopulation of B cells but it can also infect other cell types, especially epithelial cells. The virus exploits the physiological hierarchy of the normal B cell differentiation to ensure its permanence in memory B cell pool of the immunocompetent host where the viral DNA stays as an episome in the nucleus of the infected cell (Kurth et al., 2000). Sometimes the virus switches to a lytic cycle and new viruses are produced resulting in death of the infected cell.

In most cases the infection is harmless, however EBV has been associated to the development of many cancers including nasopharyngeal cancer (Young and Rickinson, 2004)

and several lymphomas such as Burkitt lymphoma (BL), post-transplant lymphoproliferative disease (PTLD) and HL (Kuppers, 2003). EBV positive DLBCLs are normally associated to circumstances of immunosupression such as in PTLD; however the WHO has recently included a new entity as a variant of DLBCL, the Epstein-Barr virus positive DLBCL of the elderly which is also closely related to EBV infection (Swerdlow et al., 2008).

The virus preferentially infects B lymphocytes through the binding of the major viral envelope glycoprotein gp350 to the CD21 receptor on the surface of B cells (Nemerow et al., 1987) and through the binding of a second glycoprotein, gp42, to human leukocyte antigen (HLA) class II molecules as a co-receptor (Borza and Hutt-Fletcher, 2002). However, as mentioned before, other cell types can be infected such as epithelial cells but in a much lower efficient process.

The expression pattern of EBV-encoded genes depends on the differentiation stage of the infected B-cell. This has led to the description of different types of latency that also apply to tumor cells (Babcock et al., 2000).

The oncogenic potential of the EBV resides in several of the virus-encoded proteins and RNAs. For instance, the latent membrane protein 1 (LMP1), which is able to block B cells from differentiating into germinal-centre B cells, has been shown to mimic a constitutively active CD40 receptor and activate the NF-κB pathway that protect the cells from apoptosis (Gires et al., 1997; Kilger et al., 1998; Mosialos et al., 1995; Uchida et al., 1999). Moreover, its expression inversely correlates with the expression of BCL6, a key transcriptional repressor that is essential for germinal centre differentiation, in B-cell lymphomas (Capello et al., 2003; Carbone et al., 1997). The viral protein LMP2a functionally resembles a B cell receptor (BCR) and has immunoreceptor tyrosine-based motifs (ITAMs) in its cytoplasmic domain that can replace the survival signals for B cells that are normally provided by the BCR (Caldwell et al., 1998). This is especially important for Hodgkin and Reed-Sternberg (HRS) cells which are thought to be rescued from apoptosis by this viral BCR-mimicry phenomenon (Kuppers and Rajewsky, 1998). EBV also expresses several transcripts that do not translate into protein. These are the EBV-encoded RNAs (EBERs), the BamH1-H Right Fragment 1 (BHRF1) RNAs and the BamH1-A rightward transcripts (BARTs). The function of these RNAs is not as well-studied as the coding sequences, however on one hand, EBERs have been associated to the induction of IL-10 expression (Kitagawa et al., 2000), the relocalization of the ribosomal L22 protein from nucleoli to the nucleoplasm (Houmani et al., 2009) and the resistance to interferon-α (IFN-α) (Nanbo et al., 2002). It is thought that the antiapoptotic activity of EBERs can counteract the

proapoptotic effect of the MYC translocation in BL (Niller et al., 2003). On the other hand, BHFR1 RNAs and BARTs have been demonstrated to be microRNAs (miRNAs), being EBV the first virus discovered to express miRNAs (Pfeffer et al., 2004).

1.2 MECHANISMS OF EPIGENETIC REGULATION

The enormous complexity of life even at the cellular level requires a complex traffic of information between external and internal signals and a coordinated response mediated by systems to read the information and execute the response. Although the genetic information that determines the response is contained in the sequence of nucleotides of DNA, the structure of chromatin is crucial in the way this information is read. The effective organization of the genomic information is the object of study of epigenetic.

There are several existing definitions of epigenetic and more than one sense is given to this word. In this work, the concept of epigenetic refers to the heritable changes (heritable in the sense of transmissible over rounds of cell divisions, but in some cases also over generations of organisms) that do not involve changes in DNA sequence. In other words, epigenetic defines all the heritable information that is not directly codified in the sequence of nucleotides.

The most fundamental epigenetic mechanisms are DNA methylation and histone tail modification. There are additional epigenetic mechanisms such as the presence of histone variants, and displacement and reposition of nucleosomes. Non-coding RNAs (ncRNAs) are also considered an epigenetic mechanism because in some organisms they can direct DNA methylation (Bao et al., 2004) and participate in some epigenetic processes such as the inactivation of X chromosome in mammals. However, in mammals the relationship between miRNAs and DNA methylation is still under debate although some examples are described in the literature (Kim et al., 2008).

1.2.1 LEVELS OF EPIGENETIC REGULATION

The functional unit for epigenetic regulation is chromatin. Chromatin is a highly ordered structure consisting of DNA molecules organized in nucleosomes. Chromatin is constituted by DNA, histones and non-histone proteins. It adopts two main structures: heterochromatin and euchromatin. Heterochromatin is a densely compacted conformation that impedes the transcription for those loci contained in it. In contrast, euchromatin is characterized by a

decondensed conformation and is normally associated to active transcription (Huisinga et al., 2006). The main mechanisms of epigenetic regulation rely on two different levels: modification of histone tails and DNA methylation.

The best known epigenetic mechanism of gene regulation is DNA methylation. DNA methylation does not occur in a stochastic manner. It is targeted to specific bases in the genome. In the mammalian genome DNA methylation takes place only at the 5 position of the pyrimidine ring of a cytosine and is mediated by DNA methyl transferases (DNMTs) (Bird, 2002; Goll and Bestor, 2005). This cytosine must be followed by a guanosine in the 3' direction forming the so called CpG dinucleotides (Weber et al., 2007). DNA methylation is executed by DNMTs. DNMT3A and DNMT3B are responsible for *de novo* methylation whereas DNMT1 is responsible for maintenance of DNA methylation during DNA replication (Okano et al., 1999) by methylating the hemimethylated strands. In healthy cells, DNA methylation represses the expression of deleterious sequences that have been incorporated to our genomes over the time such as transposons and viral sequences. It is also important for the regulation of development and cell differentiation (Li et al., 1992), genomic imprinting (Li et al., 1993) and X-chromosome inactivation in females (Heard et al., 1997). Having these global functions it is not surprising that DNA methylation has been implicated in several diseases, especially in cancer. Regarding DNA methylation, two different phenomena occur in cancer cells: first there is a global DNA hypomethylation that affects mainly repetitive sequences, coding regions and introns and produces chromosomal instability (Feinberg et al., 1988; Tuck-Muller et al., 2000); second there is a DNA hypermethylation at special CpG-rich sites called CpG islands that are present at the promoter of many genes. The CpG islands are normally unmethylated in normal cells but become methylated in cancer leading to the repression of tumor suppressor genes (Toyota et al., 1999).

Another epigenetic mechanism of transcriptional regulation is histone modification. Histones are the small basic proteins that form the core of the nucleosomes. A typical nucleosome contains an octamer of histones composed of two copies of each of the core histones i.e. H2A, H2B, H3 and H4 that is wrapped by 146 base pairs of DNA (Luger et al., 1997). Nucleosomes are connected by stretches of linker DNA which can vary on their extension and the linker histone H1. Histones contain a globular domain and a flexible tail with a charged NH_2 terminus that projects out of the nucleosome and is the main substrate of histone modifications. There are more than 60 different modification sites but histone modifications can be classified in eight categories: lysine acetylation, lysine and arginine methylation, serine and threonine phosphorylation, lysine ubiquitination, lysine sumoylation,

arginine deimination, proline isomerization, and glutamate poly-ADP ribosylation (Kouzarides, 2007). They suppose a highly dynamic regulatory process that act either by disrupting chromatin contacts or by modifying the recruitment of non-histone proteins and ATP-dependent chromatin remodeling complexes to chromatin. All these modifications constitute a complex language that governs the structure of chromatin and the transcriptional status of the genes contained in a particular locus. In terms of transcription, modifications can be grouped in those that correlate with activation of transcription and those that correlate with repression of transcription. Thus, acetylation, methylation, phosphorylation and ubiquitination have been associated to active transcription whereas methylation, ubiquitination, sumoylation, deimination and proline isomerization have been implicated in gene repression. However, each modification has its own meaning in a defined context and the same modification can be associated to gene activation or repression depending on the context. Two good examples are methylation of H3K36 and H3K9 that have a positive effect on gene transcription when they are located in the coding region but a negative effect if they are located in the promoter of the gene (Vakoc et al., 2005).

Some authors claim that all these modifications, acting alone or in combinations, constitute a histone code that provide a binding platform for chromatin-associated proteins that initiates or block the transcription (Turner, 2007). Nevertheless, this concept probably only defines the need for specific histone modifications to carry on a specific function, and does not reflect the presence of a real code of modifications with a predictable outcome (Liu et al., 2005). In the end, the crosstalk between the histone modifications and the status of DNA methylation is what determines if a particular gene is going to be transcriptionally active or not. Similar to DNA methylation, histone modification has several important functions including DNA repair, replication and chromosome condensation, but the most versatile function is regulation of transcription (Kouzarides, 2007).

1.2.2 THE POLYCOMB GROUP AS A REGULATOR OF GENE EXPRESSION

There are several enzymes involved in histone modification such as histone acetylases, methylases, demethylases, deacetylases, ubiquitinases and so on. Nevertheless most of them act in the form of (or associated to) complexes. The Polycomb (PcG) and trithorax (trxG) complexes are major modifiers of chromatin structure through histone modification and have opposing roles. They were first described in *Drosophila* as systems that regulate body

segmentation during fly development through the direct control of *HOX* genes (Lewis, 1978) and alterations in these proteins provoke homeotic transformations. On one hand trxG activates gene expression through the methylation of lysine 4 of histone H3 (H3K4) and through the chromatin remodeling activity of some of their members. On the other hand PcG proteins, the repressive counterpart of trxG, induce two different histone modifications associated to repression counteracting the nucleosome remodeling activity of SWI/SNF complex (Shao et al., 1999) and blocking the association of RNA polymerase II to the gene promoter (Dellino et al., 2004; Stock et al., 2007), preventing gene transcription (Schuettengruber et al., 2007). The regulation of *HOX* genes is a PcG function that is conserved from flies to human. Notwithstanding in *Drosophila* there are specific consensus sequences called PRE (Polycomb Repressed Elements) to which PcG proteins bind (Muller and Kassis, 2006) but these sequences have not been identified in mammals yet although a recent work shows the existence of a genomic region in the human genome that shares some characteristics with the PREs (Woo et al., 2010). Polycomb proteins form DNA-binding complexes to exert their function. Expression studies as well as the use of immunoprecipitation assays has led to the postulation that the composition of these complexes is variable and dynamic depending on the cell or tissue type or the differentiation status of the cell (Gunster et al., 2001; Otte and Kwaks, 2003; Sanchez-Beato et al., 2006) but at least two different complexes have been clearly identified: the Polycomb Repressive Complex 1 (PRC1) and the Polycomb Repressive Complex 2 (PRC2) (Lund and van Lohuizen, 2004).

The PRC2 is thought to be the first complex acting on gene promoters. It has as core members EZH2, EED and SUZ12. EZH2 carries the histone methyl transferase activity in its SET domain that trimethylates the lysine 27 of histone H3 (H3K27me3 mark) (Kuzmichev et al., 2002). The composition of this complex is variable and some authors have proposed the existence of a PRC3 and PRC4 regarding the molecular partners of the core proteins that include several EED isoforms and the proteins RBBP4, RBBP7, PHF1, AEBP2, SIRT1, HDAC1 and HDAC2 amongst others (Kuzmichev et al., 2004; Kuzmichev et al., 2005) but its presence is associated to specific differentiation status or malignant conditions (Kuzmichev et al., 2005).

The composition of PRC1 is also highly variable but it is constituted by combinations of member of the PC (CBX2, CBX4, CBX7 and CBX8), PSC (BMI1, MEL18, MBLR, NSPC1, PCGF5 and PCGF3), RING (RING1 and RNF2), PH (HPH1, HPH2 and HPH3) and SCML (SCML1 and SCML2) families (Bracken and Helin, 2009). The PRC1 is recruited to the H3K27me3 mark through the chromodomain of PC proteins (Min et al., 2003) and ubiquitinates histone H2A at lysine 119

(H2AK119Ub) thanks to the ubiquitin E3 ligase activity of RNF2 (Wang et al., 2004). This ubiquitination is thought to be important for gene repression (Cao et al., 2005; Wang et al., 2004). The PRC1 eventually provokes changes in chromatin structure (Francis et al., 2004).

In embryonic stem (ES) cells PRC1 and PRC2 are both present at the promoters of several key developmental regulators. In these promoters the Polycomb-mediated H3K27m3 mark co-exist with the methylation of lysine 4 of histone H3 (H3K4me) associated to trxG activity (Bernstein et al., 2006a). This bivalent mark keeps the genes poised to rapidly switch gene status upon differentiation. This is not exclusive of ES cells and some adult cells also harbor bivalent promoters such as T cells and fibroblasts (Araki et al., 2009; Barski et al., 2007; Roh et al., 2006; Wei et al., 2009).

As suggested by this model the activities of PRC2 and PRC1 are closely related and it has been demonstrated high levels of co-occupancy of proteins belonging to the PRC1 and PRC2 complexes at promoters with the H3K27me3 mark (Bernstein et al., 2006b; Lee et al., 2007; Terranova et al., 2008). However, this is a simplistic description of reality. Even though the H3K27me3 mark has been demonstrated to recruit the PRC1 to gene promoters, independence from this mark has also been described for PRC1 recruitment (Pasini et al., 2007; Schoeftner et al., 2006). Moreover there are additional complexes that contain PcG as well as non-PcG proteins. For instance, several factors of the E2F family can be found associated to PcG proteins such as E2F6 (Trimarchi et al., 2001), MGA, MAX and TFDP1. The formation of these complexes can be regulated in a cell cycle-dependent manner (Ogawa et al., 2002) revealing the limitations of the model in which the action of PRC2 and PRC1 complexes is sequential. Probably it will be more correct to say that gene repression mediated by PcG proteins rely on the activity of PRC1 and PRC2 alone or in association.

Moreover there are additional enzymatic activities associated to PRCs that are not directly executed by PcG members. For instance, EED is able to interact with histone deacetylases (HDACs) that collaborate to repress gene expression (van der Vlag and Otte, 1999). It seems that PcG proteins can also regulate DNA methylation, although this question is now under active debate. Two main direct evidences support the role of PcG in DNA methylation. First, murine Bmi1 has been found to interact directly with Dmap1 and form a ternary complex with Dmap1 and Dnmt1. In this interaction, Bmi1 collaborate with Dmap1 to repress target genes as demonstrated by the fact that *Hox* genes are derepressed not only in the absence of Bmi1 but also in the absence of Dmap1 (Negishi et al., 2007). Second, EZH2 by GST pull-down assays and immunoprecipitation has been shown to interact directly with the

three DMNTs in the context of PRC2/3 and to be required for DNA methylation at EZH2-target promoters (Vire et al., 2006). However it does not mean that DNA methylation is required for PcG activity since the H3K27me3 mark can be found out of CpG islands (Kondo et al., 2008).

1.2.2.1 POLYCOMB TARGETING TO GENE PROMOTERS

Despite the huge advance in the understanding of the mechanism of action of PcG proteins, there are still many facts that remain obscure. For instance it is still a mystery how PcG complexes are driven to the correct places in the mammalian genome. Neither PRC1 nor PRC2 contain DNA-binding domains and, as commented before, human PREs have been only recently described in the HOXD cluster. One of the best candidates to drive PcG function is YY1. YY1 is the human homologue of *Drosophila* Pho and can interact with several PcG proteins. In fact, YY1 knockdown in mouse myoblasts impedes the recruitment of Ezh2 to target promoters and prevents H3K27 trimethylation (Caretti et al., 2004). However, studies in mouse ES cells showed very limited overlap suggesting that recruitment by YY1 might not be a general mechanism. In fact, in ES cells OCT4 could be more important for PcG function since OCT4 knockdown diminishes the binding capacity of PRC1 and PRC2 in these cells (Endoh et al., 2008; Squazzo et al., 2006). However, the biochemical evidence for the interaction between OCT4 and PcG members is very weak (Lee et al., 2006). Other transcription factors that can recruit PcG complexes are E2F6 and BCOR. E2F6 is a repressor member of the E2F family of transcription factors. E2F6 can repress its targets by direct interaction with RING1, RNF2, YAF2 and DP1 (Ogawa et al., 2002). BCOR (BCL-6 interacting co-repressor) is a co-repressor that is essential for repression of BCL6 targets. It has been associated to several PcG members such as RING1, RNF2 and RYBP (Gearhart et al., 2006).

Another type of molecules, the ncRNAs, have also been implicated in PcG targeting (Bernstein et al., 2006b; Grimaud et al., 2006; Kanhere et al., 2010; Pandey et al., 2008; Rinn et al., 2007; Yap et al., 2010). For instance the long ncRNAs HOTAIR (encoded in *HOXC* cluster) interacts directly with PRC2 and is required for SUZ12 recruitment, and trimethylation of H3K27 in *HOXD* loci (Rinn et al., 2007). Another long RNA, Kcnq1ot1 functions in placenta interacting with PRC2 and chromatin (Pandey et al., 2008). This interaction correlates with the presence of the repressive marks H3K27me3 and H3K9me3. Another long ncRNA, ANRIL which is codified in a region that overlaps the INK4b/ARF/INK4a loci is bound by the PRC1 protein CBX7 in order to repress the INK4a/ARF locus. CBX7 uses distinct regions and residues of its

chromodomain for binding RNA or H3K27me3 (Yap et al., 2010). The RepA RNA that is transcribed from *Xist* has also been shown to interact with PRC2. This interaction is necessary for H3K27me3 and X chromosome inactivation (Zhao et al., 2008). Two reports indicate that this mechanism might be general and long ncRNAs (Khalil et al., 2009) as well as short RNAs (Kanhere et al., 2010) can physically interact with PcG members and influence the activity of PRCs. It seems that these RNAs frequently form stem loop structures that serve as a docking platform for PcG binding.

Finally, RNAi machinery adds even more complexity to the PcG system. RNAi when directed to gene promoters has been associated to PcG activity. For instance, in *Drosophila* AGO1, a protein which plays an important role in RNAi, is able to drive gene silencing of promoters targeted by specific small interfering RNAs (siRNAs) by recruiting EZH2 (Kim et al., 2006).

1.2.2.2 POLYCOMB FUNCTIONS

Polycomb genes are highly conserved through plants, flies and vertebrates. The best studied function of PcG is the regulation of *HOX* gene expression through cell division and during development and this function is also conserved in the aforementioned groups. Actually, most of PcG members were initially identified because their mutations produce homeotic phenotypes.

However PcG functions go far beyond the regulation of *HOX* genes. Several genome-wide studies have revealed the numerous target genes regulated by the PRCs (Boyer et al., 2006; Bracken et al., 2006; Lee et al., 2006; Schwartz et al., 2006; Squazzo et al., 2006; Tolhuis et al., 2006). Among the PcG targets there is an evident enrichment in transcription factors and proteins that regulate development, differentiation, stemness, and cell fate decisions. The role of PcG in the self renewal of stem cells has been widely demonstrated not only in ES cells but also in a variety of adult stem cells (for a review see (Sparmann and van Lohuizen, 2006)).

PcG play a major role in the regulation of adult hematopoietic stem cells (HSC) and several alterations in PcG proteins affect this cellular compartment (Jacobs and van Lohuizen, 2002; Kajiume et al., 2004; Ohta et al., 2002; Orlando, 2003; Park et al., 2003). Levels of BMI1 and MEL18 determine to a great extent the capability of HSCs to function as progenitors (Kajiume et al., 2009) with opposing roles. BMI1 enhances HSC potential whereas MEL18

restricts HSC self renewal and is increased in differentiated cells which agrees with the fact that BMI1 is expressed in more primitive cells and during differentiation, there is an upregulation of MEL18, RAE28, and EZH2 (Lessard et al., 1998). Moreover, mouse models using Bmi1 knockout (Lessard and Sauvageau, 2003; Park et al., 2003; van der Lugt et al., 1994) and transgenic mice (Iwama et al., 2004) have demonstrated the key role of Bmi1 in the function of HSCs. Many of the Bmi1 effects on HSC function are mediated through the repression of the Ink4a/Arf locus. $Bmi^{-/-}$ HSCs have markedly higher levels of Ink4a and Arf (Jacobs et al., 1999) two proteins that induce cell cycle arrest and p53-mediated apoptosis in HSCs (Park et al., 2003). In fact, deletion of the Cdkn2a locus in $Bmi1^{-/-}$ mice partially restores the proliferative capacity of HSCs (Oguro et al., 2006). In accordance to the opposed role of Mel18 in HSC activity, Mel18 downregulation in bone marrow-derived HSCs promotes their self-renewal, while its forced expression reduces the self-renewal capacity of HSCs (Kajiume et al., 2004). However Mel18 is still necessary for the development of the hematopoietic system as shown in $Mel18^{-/-}$ mice (Akasaka et al., 1997). Many other PcG proteins are important for HSC function such as EZH2 (Kamminga et al., 2006) and EDD (Lessard et al., 1999). Likewise, Rnf2 affects hematopoiesis, but this time in a dual way. On one hand Rnf2 is able to restrict proliferation of progenitor cells; on the other hand it enhances the proliferation of the maturing progeny (Cales et al., 2008).

Polycomb also regulates cell proliferation as demonstrated by several facts. First, as mentioned before, the formation of some PRC complexes is dependent on the cell cycle suggesting a role in proliferation (Ogawa et al., 2002); second, among PcG targets there are some cell cycle regulators including INK4a/ARF, MYC, JUN, FOS, CDC25, hTERT, several cyclins and CDKs, CHEK1, MAD2L1, and BUB3 (Bruggeman et al., 2005; Jacobs et al., 1999). Some recent works also show the implication of PcG proteins in the regulation of proliferation through the control of the JAK/STAT pathway in *Drosophila* (Classen et al., 2009; Gonzalez et al., 2009).

1.2.2.3 POLYCOMB AND CANCER

Cancer is a complex disease in which cells are transformed by genetic and epigenetic alterations and proliferate in an uncontrolled way. There is increasing evidence that many cancer cells present some characteristics of stem cells including unlimited self renewal capacity and activation of several pathways that are active in stem cells. This is supported by the fact

Table 1.3. Common members of PRCs and their alterations in cancer. Bold text indicates members known to be frequently altered in cancer.

Human	Mouse homologue	Alteration in cancer	Tumor type
PRC1 complex			
BMI1	Bmi1	Overexpression/Amplification	Acute myeloid leukemia, Hodgkin lymphoma, B cell non-Hodgkin lymphoma, gastrointestinal tumors, pituitary adenoma, parathyroid adenoma, breast cancer, glioma, neuroblastoma, medulloblastoma, non-small cell lung cancer, skin cancer
MEL18/RNF110/PCGF2	Mel18	Loss	Cutaneous squamous-cell carcinoma, gynecological tumors, prostate cancer
RING1A	Ring1a	Overexpression	Large B cell lymphoma
		Loss	Clear-cell renal-cell carcinoma and testicular germ-cell tumors
RNF2	Ring1b	Overexpression	Gastric and colonic tumors, melanoma, lung cancer, gynecological tumors, diffuse large B cell lymphoma, follicular lymphoma, Burkitt lymphoma, Hodgkin lymphoma
HPH1, HPH2, HPH3	Rae28/Mph1, Phc2, Phc3	Lack of expression	Acute lymphocytic leukemia
		Overexpression	Large B cell lymphoma, central nervous system tumors
CBX2, CBX4, CBX6, **CBX7**, CBX8	M33/Cbx2, Cbx4, Cbx6, Cbx7, Cbx8	Loss	Pancreatic cancer, aggressive thyroid carcinomas
		Overexpression	Follicular lymphoma
PCGF6	Pcgf6	Loss	Mantle cell lymphoma
RYBP	Rybp	Overexpression	Oligodendroglioma, pituitary adenoma, T cell lymphoma, Hodgkin Lymphoma
PRC2 complex			
EZH2/EZH1	Ezh2/Ezh1	Overexpression/Amplification	Prostate carcinoma, breast carcinoma, melanoma, bladder cancer, glioma, endometrial carcinoma, lymphomas, colon carcinoma, glioblastoma, Ewing tumor
		Deletion/Mutation/Uniparental disomy	Linfomas, myeloid malignancies.
		Altered localization	Acute myeloid leukemia
SUZ12	Suz12	Overexpression/Amplification/ Translocation	Gastrointestinal tumors, lung tumors, thyroid follicular carcinoma, pituitary adenoma, parathyroid adenoma, skin tumors, breast and gynecological tumors, mantle cell lymphoma, chronic myeloid leukemia, endometrial stromal tumor
EED	Eed	Overexpression	Salivary gland adenoid cystic carcinoma, Hodgkin lymphoma, prostate cancer
		Lack of expression	Prostate cancer
RBBP7	Rbbp7	Overexpression	Non-small cell lung cancer, breast cancer
RBBP4	Rbbp4	Downregulation	Cervical cancer
PCL3	Phf19	Overexpression	Cancers of colon, skin, lung, rectum, cervix, uterus, and liver

that tumors contain heterogeneous population of cells although they originate from a single clone. It is also true that several pathways that are aberrantly activated in tumors, such as Sonic Hedgehog (Shh), Notch, and Wnt, also regulate self-renewal in stem cells (reviewed in (Taipale and Beachy, 2001)), and some embryonic genes are re-expressed in human cancers (Monk and Holding, 2001).

Taking into account the role of Polycomb in the control of stem cell properties, development and cell cycle, it is not surprising that several reports have linked this system to cancer and that the expression of many PcG proteins is altered in several malignancies (Table 1.3). A plausible model is that alterations in PcG could allow malignant cells to acquire stem cell properties (Figure 1.3). The first example is BMI1. It was initially described in mice to collaborate with c-MYC in the development of lymphomas (Haupt et al., 1991; van Lohuizen et al., 1991) and it has been found to be deregulated in some lymphoid malignancies such as MCL, HL and DLBCL (Bea et al., 2001; Dukers et al., 2004; Raaphorst et al., 2004; Sanchez-Beato et al., 2004; Sanchez-Beato et al., 2006). Anomalous expression of EZH2 has been described in prostate cancer where EZH2 levels also correlate with the progression of the tumor. Moreover, EZH2 is also important for the neopastic transformation of breast epithelial cells (Kleer et al., 2003; Varambally et al., 2002). Other PRC2 members such as EED and RbAp48 are upregulated in colon and breast tumors (Kirmizis et al., 2003), and SUZ12 is translocated in endometrial stromal tumors (Koontz et al., 2001b). The oncogenic role of BMI1 might rely on the aforementioned repression of INK4a/ARF, a role that seems to be shared with other PcG members such as EZH2 (Paul et al., 2010) and CBX7 (Dimri et al., 2002; Gil et al., 2004).

Noteworthy, EZH2 plays a major role in hematologic malignancies. It is upregulated in MCL (Visser et al., 2001) and other non-Hodgkin lymphomas (Dukers et al., 2004; Raaphorst et al., 2001; Raaphorst et al., 2000). More importantly there are mutations that affect the catalytic domain of this protein in follicular lymphoma and DLBCL of GCB origin (Morin et al., 2010). Since these mutations reduce the enzymatic activity of EZH2 one may think that the oncogenic mechanism of EZH2 in these tumors might be different from that of prostate cancer and, in this case, EZH2 would behave as a tumor suppressing gene. However it remains to be explored whether these mutations alter the target specificity of this protein. Two very recent studies also report genetic alterations at the EZH2 locus in myeloid malignancies (Ernst et al., 2010; Nikoloski et al., 2010). Both studies show that EZH2 is the target of deletion, uniparental disomy and mutation. In all cases, the alterations were EZH2-inactivating and, taking into account that many of them are deletions, the major effect must be a loss of function rather than a change in the target specificity. This means that EZH2 may have a tumor suppressor role

in these malignancies. In line with this, recent investigations show that the Drosophila E(z) and other PRC2 and PRC1 components play a tumor suppressor role through the suppression of the oncogenic JAK-STAT (Classen et al., 2009) and Notch (Martinez et al., 2009) pathways.

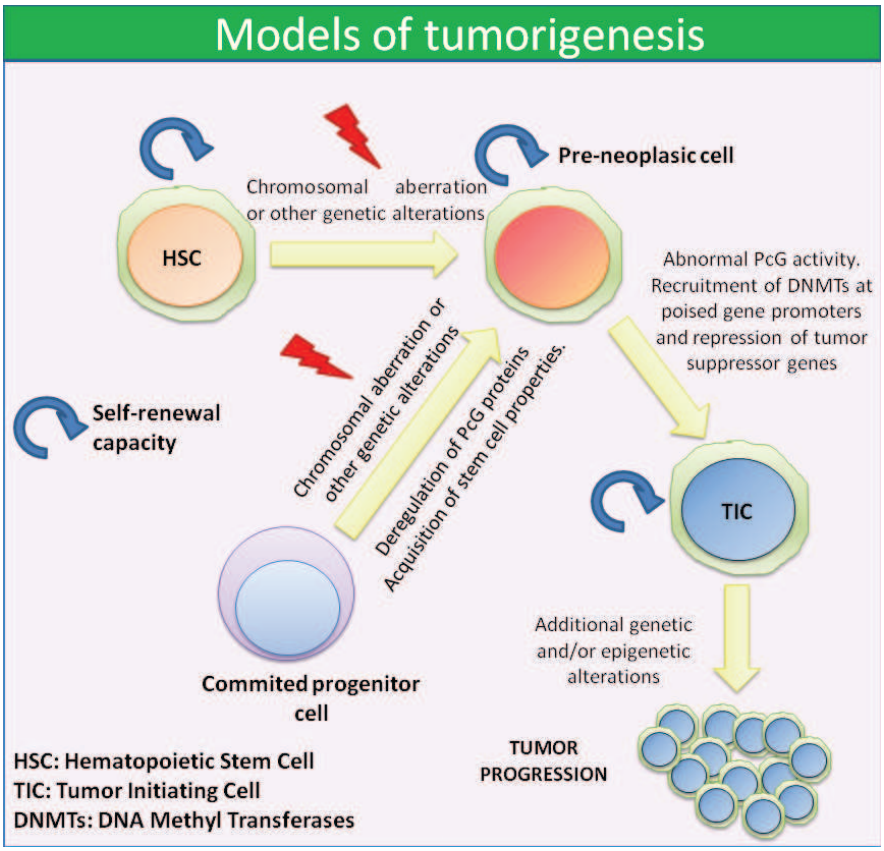

Figure 1.3. Cancer cells can originate from a stem cell such as a HSC that acquire an altered phenotype through chromosomal aberrations and/or mutations. PcG aberrant activity promotes tumor development. Alternatively, the first chromosomal aberration and/or mutation occur in a commited progenitor cell in which the abnormal PcG activity confers stem cell properties.

There are also alterations described in PcG-regulating genes. For instance, several miRNAs that regulate the expression of PcG components are altered in cancer. Two examples are miR-101 and miR-26a which target EZH2, but are downregulated in prostate cancer and in BL (Friedman et al., 2009; Sander et al., 2008). The downregulation of miR-26a comes from the upregulation of MYC due to a common translocation in BL. MYC represses miR-26a and therefore EZH2 can be expressed at higher levels. MiR-200c, miR-203, and miR-183 target BMI1 and are downregulated in cancer cells and mouse embryonic stem cells (Shimono et al., 2009; Wellner et al., 2009).

In the last few years several studies that have come up suggest a more profound impact of Polycomb in cancer. In fact, among the genes that are repressed in cancer there is a significant enrichment in those which are PcG targets in ES cells. This has led to propose the existence of a "Polycomb signature" in cancer.

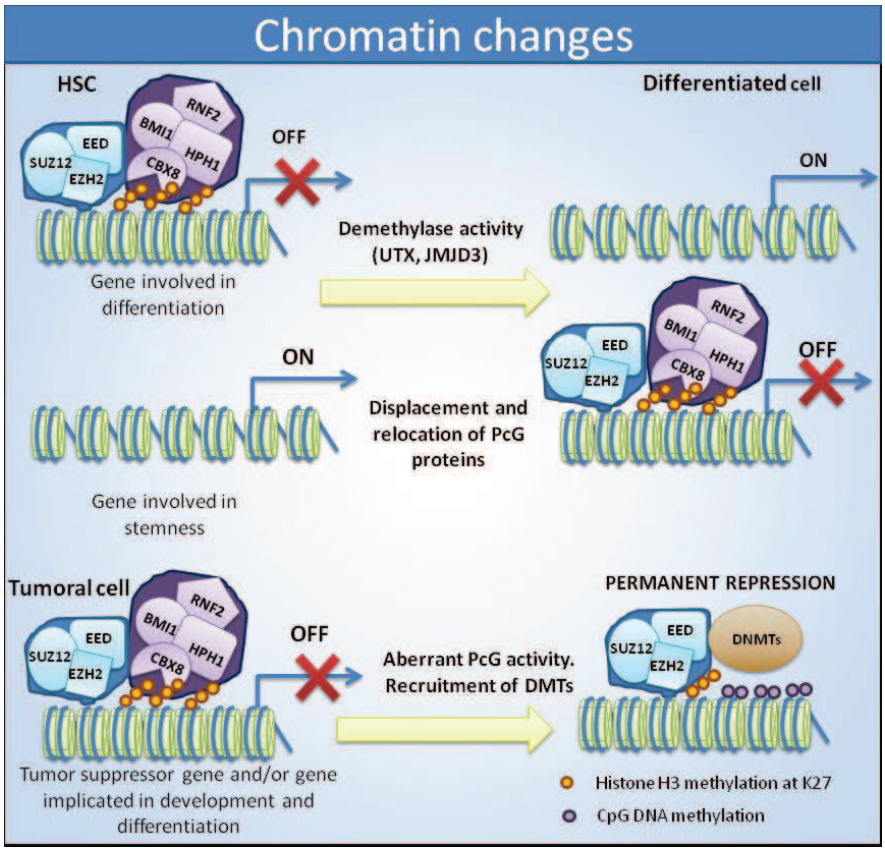

Figure 1.4. Cell identity is reflected by changes in chromatin status. In HSCs PRCs repress genes involved in differentiation to allow a stem cell phenotype. During differentiation PcG proteins target genes involved in stemness. In cancer the aberrant PcG activity blocks differentiation and repress tumor suppressor genes. In this case the recruitment of DNMTs induces permanent repression of the genes.

This molecular signature consists of those PRC2 target genes identified by chIP-on-chip analysis in cancer (most of which coincide with PcG targets identified in ES cells) that are also found downregulated in tumors by gene expression profile analysis.

This Polycomb fingerprint can predict clinical outcome in several tumors (Yu et al., 2007). Other reports have studied the methylation pattern of promoters in human tumors in a genome-wide scale. In these studies, among the genes that suffer promoter hypermethylation

in human tumors, there is an enrichment for PcG target genes described in ES cells (Dunwell et al., 2010; Martin-Subero et al., 2009a; Martin-Subero et al., 2009b; O'Riain et al., 2009; Richter et al., 2009; Schlesinger et al., 2007; Wang et al., 2010; Wu et al., 2010a). Some examples of PcG target genes that accumulate DNA methylation at their promoters in cancer are WT1, RARB, KLF4, ID4, GATA3, CHD5 and SPI1 (Bracken and Helin, 2009). This can be explained, as commented before, because EZH2 can directly control DNA methylation in some models by serving as a recruitment platform for DNA methyltransferases (Vire et al., 2006), and suggests a model in which PcG proteins recruits DNA methylation machinery to induce permanent repression of target genes (Figure 1.4).

1.2.3 MicroRNAS AND REGULATION OF GENE EXPRESSION

MiRNAs are one of the most abundant regulatory gene families. They are endogenously codified as long transcripts from RNA polymerase II promoters (Lee et al., 2004). These long transcripts called primary miRNAs (pri-miRNA) form imperfect stem loop structures that are processed by the RNAse III-type complex Drosha-DGCR8 (Lee et al., 2003) to remove the flanking sequences, and liberate the stem–loop precursor miRNA (pre-miRNA). At this step the pre-miRNA needs to be transported to the cytoplasm. This step is carried out by the Ran-dependent nuclear transport receptor exportin-5 (Bohnsack et al., 2004; Lund et al., 2004; Yi et al., 2003). Once in the cytoplasm the pre-miRNA is processed by the RNAse III-type Dicer into approximately 22-nucleotides long double stranded RNAs that constitute the mature miRNA. The mature miRNA is now loaded into the miRISC (miRNA-containing RNA-induced silencing complex). During incorporation to the RISC complex, the miRNAs are converted into single stranded molecules. The strand that do not enter into the RISC complex is usually short-lived and rapidly disappears whereas the other strand remains as mature miRNA (Khvorova et al., 2003).

The mature miRNA guides the miRISC complex to the target mRNA through sequence complementarity to the 3’ UTR. If the miRNA have perfect or nearly perfect complementarity to the 3’ UTR it normally induces mRNA cleavage (Llave et al., 2002; Yekta et al., 2004) whereas in those cases where complementarity is not perfect, translation blockade is normally achieved (Pillai et al., 2005) (Figure 1.5). As an exception to this biogenesis pathway, the less abundant “mirtrons” bypass the normal nuclear Drosha processing and are processed exclusively by Dicer (Okamura et al., 2008). From the point of view of evolution, miRNAs are only expressed by plants and animals and the viruses that infect them(Bartel and Chen, 2004).

Most miRNAs are phylogenetically conserved between several species and their number correlates with the complexity of the organism.

Actually, expansions of the miRNA repertoire appear to be associated with major body-plan innovations during animal evolution (Niwa and Slack, 2007). Until the elaboration of this work, 940 human miRNAs can be found at the miRbase (www.mirbase.org). Each miRNA can regulate hundreds of target genes, so this group of short sequences can actually regulate a big part of the transcriptome even though the system seems to be redundant (Lim et al., 2005). The consequence is that miRNAs are virtually implicated in every cellular process. In fact miRNAs have been shown to regulate quite different functions such as development, cell proliferation, cell death, fat metabolism, pattering of the nervous system and modulation of hematopoietic differentiation (Ambros, 2004; Bartel and Chen, 2004; Niwa and Slack, 2007). Many miRNAs are tissue specific, highlighting their role in the development and differentiation.

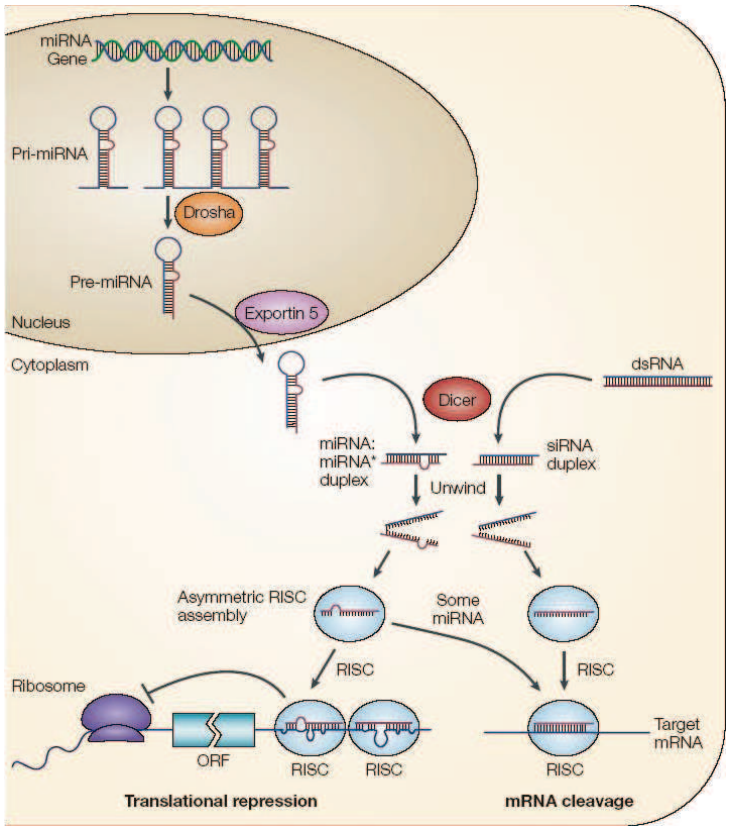

Figure 1.5. Scheme of miRNA biogenesis (reproduced from (He and Hannon, 2004))

MiRNAs have been also implicated in several diseases including cancer. The first evidence of the role of miRNAs in cancer came from a study on B-cell chronic lymphocytic leukemia

where miR-15 and miR-16 were downregulated due to hemi- or homozygous chromosomal deletion at 13q14 (Calin et al., 2002). Several miRNA loci reside on chromosomal fragile sites that are frequently altered in cancer: for instance the aforementioned miR-15a/16 cluster which is also deleted in pituitary adenomas; miR-143 and miR-145 that are located in the 5q33 region which is deleted in lung cancer (Calin and Croce, 2006) and the miR-17-92 cluster which is frequently amplified in B-cell lymphomas (Ota et al., 2004) and lung cancers (Hayashita et al., 2005). Methylation is another cause of abnormal miRNA expression in cancer. Hypomethylation of miR-21, miR-203 and miR-205 has been suggested as the mechanism by which these miRNAs are overexpressed in ovarian carcinomas (Iorio et al., 2007). The decreased miR-124a expression has been attributed to DNA hypermethylation in colon, breast and lung carcinomas (Lujambio and Esteller, 2007). Several oncogenic viruses also express miRNAs although the function of most of these miRNAs is largely unknown. This is especially important in oncogenic viruses like EBV. EBV expresses more than 20 miRNAs that are organized in two clusters within the EBV genome: one in the intronic region of the BART (BamH1-A Rigthward Transcript) gene, and another in the untranslated regions (UTRs) of the BHRF1 (BamHI-H right reading frame) gene (Cai et al., 2006; Grundhoff et al., 2006; Pfeffer et al., 2004). These miRNAs are important for the biological cycle of the virus and control several viral genes such as BALF5, LMP1 and LMP2a (Barth et al., 2008; Lo et al., 2007; Lung et al., 2009). Some of these viral miRNAs promote survival of the host cell by targeting cellular transcripts. An example is ebv-miR-BART5 which targets the p53 up-regulated modulator of apoptosis (PUMA) rendering the infected cells less sensitive to apoptosis (Choy et al., 2008).

OBJECTIVES

Cancer arises from the accumulation of both genetic and epigenetic events. Much attention has been paid to the molecular events that cause cancer from the genetic point of view (e.g. mutations, translocations, deletions, amplifications), but there is increasing evidence that epigenetic alterations play also a very important role in cancer.

Two main epigenetic mechanisms could play a key role in the development of lymphomas: the Polycomb group of proteins and the microRNAs.

Further investigation in these areas may be useful to elucidate new mechanisms of oncogenesis, thus helping to the understanding of the disease and proposing new therapeutic targets.

Initial studies with several members of the Polycomb Repressive Complex 1 highlighted the importance of this system in lymphomas therefore promoting investigation of the Polycomb Repressive Complex 2. The objectives of the first part of this work are the following:

a) To analyze the SUZ12 expression pattern in normal and malignant lymphoid tissues, investigating a possible oncogenic role for SUZ12.
b) To analyze SUZ12 target genes in order to elucidate the exact mechanism by which SUZ12 can confer advantages to tumor cells or influence the tumorigenic process.

On the other hand, the unexplained mutually exclusive relationship observed between the presence of the Epstein Barr Virus and the expression of the BCL6 protein in diffuse large cell lymphomas pointed to new mechanisms of regulation to explain this phenomenon.

Hence, the objectives of the second part of this work are the following:

c) To investigate the role of Epstein Barr virus and its correlation with BCL6 in diffuse large B cell lymphomas.
d) To search microRNAs encoded by the Epstein Barr virus that could repress the expression of BCL6 protein and test functionally this hypothesis.

2. MATERIAL AND METHODS

2.1 HUMAN TISSUE SAMPLES. ORIGIN, PROCESSING AND DIAGNOSIS

All human tissue samples used in this work were collected through the archive of the CNIO tumor bank with the collaboration of the hospitals integrating the tumor bank network. The complete protocol for sample collection can be found in the following web address http://www.cnio.es/ing/programas/progTumor11.asp and are summarized in the following lines. Immediately after the surgery the tumor is divided in several pieces and processed in two different ways:

Fixation in 10% formalin for 16-48 hours followed by inclusion in paraffin by standard techniques

Freezing: The sample is properly identified in plastic cryomolds (Cryomold standard; Tissue-Tek 4557) and embedded in a cryosolidifiable medium (OCT-Compound, Tissue-Tek 4583, Bayer S.A). The sample is subsequently fast-frozen through immersion in isopentane at -160º C.

In this work formalin-fixed, paraffin-embedded (FFPE) tissue sections were used for immunohistochemical (IHC) studies as well as analysis of microRNA expression by RT-PCR. Frozen tissues were used for gene expression profiling by microarray hybridization. Diagnosis of all samples was revised in a centralized manner using FFPE tissue sections by means of hematoxylin/eosin and immunohistochemical staining according to the WHO criteria (Swerdlow et al., 2008). For the first project, we used in total, 154 non-malignant and 550 malignant samples of human tissues. Three different samples of each of the following non-malignant human samples were collected:

- *Central nervous system*: parietal lobes, cerebellum, basal nuclei, brain stem, choroid plexus.
- *Gastrointestinal tract*: esophagus, stomach, small bowel, colon, appendix, liver, pancreas, gallbladder.
- *Respiratory tract*: parotid, larynx, trachea, lung (pleura and bronchi).
- *Endocrine system*: pituitary, thyroid, parathyroid and adrenal glands.
- *Skin and soft tissue*: skin, muscle.
- *Lymphoid tissue*: tonsil, spleen, thymus.
- *Breast and gynecological tissue*: breast, ovary, uterus (cervix, endometrium, myometrium), fallopian tubes, placenta, umbilical cord.
- *Male reproductive system and urinary tract*: kidney, bladder, prostate, testis, seminal vesicles, epididymis.

- *Hyperplasic and inflammatory tissue*: nodular thyroid hyperplasia, parathyroid hyperplasia, seborrheic keratosis, ulcerative colitis, hyperplasic polyp of the colon.

The following tumors were represented in the malignant samples:

- *Central nervous system*: low- and high-grade astrocytomas, oligodendroglioma, ependymoma, meningioma (10 cases per type).
- *Gastrointestinal tract and annexes*: gastric adenocarcinoma (10 well differentiated and eight poorly differentiated cases); gastric signet-ring adenocarcinoma (10 cases), colonic villous adenoma (10 low-grade and 10 high-grade dysplasia cases); colonic tubular adenoma (10 cases); well-differentiated colorectal adenocarcinoma (10 cases); mucinous colorectal adenocarcinoma (10 cases), poorly differentiated colorectal adenocarcinoma (5 cases); hepatocellular carcinoma (10 cases); gallbladder adenocarcinoma (9 cases); carcinoid tumor of the appendix (3 cases); endocrine pancreatic tumor (5 cases); exocrine pancreatic adenocarcinoma (5 cases).
- *Respiratory tract tumors*: parotid pleomorphic adenoma (10 cases), squamous cell carcinoma of the larynx (10 cases), lung adenocarcinoma (10 cases), lung squamous cell carcinoma (10 cases), lung undifferentiated large-cell carcinoma (10 cases), lung neuroendocrine small-cell carcinoma (6 cases), mesothelioma (10 cases).
- *Endocrine tumors*: pituitary adenoma (10 cases), thyroid papillary carcinoma (10 cases), thyroid follicular carcinoma (8 cases), thyroid medullary carcinoma (9 cases), adrenal cortex carcinoma (3 cases), adrenal pheochromocytoma (8 cases), parathyroid adenoma (10 cases).
- *Skin and soft tissue tumors*: cutaneous basal cell carcinoma (10 cases), cutaneous squamous cell carcinoma (10 cases), malignant melanoma (10 cases), capillary haemangioma (10 cases), Kaposi's sarcoma (10 cases), fibrous solitary tumor (4 cases), leiomyosarcoma (6 cases), liposarcoma (7 cases) and atypical lipomas (3 cases).
- *Lymphomas*: non-Hodgkin's lymphomas (FL, MCL, DLBCL, BL and peripheral T-cell lymphomas) and Hodgkin's lymphomas (HL) (10 cases of each type).
- *Breast and gynecological tumors*: breast ductal carcinoma (10 cases), breast lobular carcinoma (8 cases), squamous cell carcinoma of the cervix (10 cases), endometrial adenocarcinoma (8 cases) and serous endometrial carcinoma (2 cases), uterus leiomyoma (4 cases); ovary mucinous cystadenoma (5 cases) and cystadenocarcinomas (4 cases), ovary serous cystadenomas (4 cases) and cystadenocarcinomas (6 cases), ovary endometrioid adenocarcinoma (7 cases) and cystadenocarcinomas (3 cases), ovary clear-cell carcinoma (10 cases).
- *Tumors of the urinary and male reproductive system*: bladder urothelial carcinoma, clear-cell renal-cell carcinoma (10 cases), prostate adenocarcinoma (10 cases), seminoma (10 cases), embryonal carcinoma (5 cases), teratocarcinoma (5 cases).

Additional samples of MCL were used for the second TMA (76 samples) and the hybridization onto miRNA microarrays (24 samples, frozen tissues).

In the second project, a first series of 36 cases of DLBCL (frozen tissues) was used to perform the analysis of miRNA expression and a second series of 149 DLBCL patients (FFPE tissues) was used for the immunohistochemical analysis as well as for the validation of miRNA expression. All the studies were carried out under the supervision of the institutional review board of the Instituto de Salud Carlos III.

2.2 CELL CULTURE

2.2.1 CELL LINES

HEK293T (Graham et al., 1977) cells derived from human embryonic kidney were obtained from the American Type Culture Collection. Human cell lines derived from MCL patients Jeko-1 (Jeon et al., 1998) and Z-138 (Estrov et al., 1998) and from DLBCL patients HBL1 (Nozawa et al., 1988), HLY-1 (Al Saati et al., 1989), MD901 (Miki et al., 1994), OCI-LY10 (Alizadeh et al., 2000), OCI-LY3 (Yee et al., 1989), RIVA and U2932 (Amini et al., 2002) were kindly provided by Dr. Martínez-Climent from the Centro de Investigación Médica Aplicada, Navarra. Human cell line derived from BL patient AKATA (Takada et al., 1991) was a kind gift of Dr. Campanero from the Instituto de Investigaciones Biomédicas “Alberto Sols”, Madrid. NAMALWA (Henderson et al., 1983), RAJI (Pulvertaft, 1964), RAMOS (Benjamin et al., 1982) and TOLEDO (Gabay et al., 1999) cell lines were purchased from the American Type Culture Collection (Rockville, MD) and GRANTA-519 (Jadayel et al., 1997), DB (Beckwith et al., 1990), DOHH-2 (Kluin-Nelemans et al., 1991), FARAGE (Baruch et al., 1996), KARPAS-422 (Dyer et al., 1990), OCI-LY19 (Chang et al., 1995), SU-DHL-4 (Epstein et al., 1978) and SU-DHL-6 (Epstein et al., 1978) from the Deutsche Sammlung von Mikroorganismen und Zellkulturen (Braunschweig, Germany).

Table 2.1 summarizes all the characteristics of the cell lines used in this work including the origin, description and culture conditions for each one.

Table 2.1. Description of all cell lines used in this study.

Cell line	Species	Source	Culture medium	Growth	Origin
HEK293T	Human	Embryonic kidney	DMEM + 10% FBS	Adherent	ATCC
GRANTA-519	Human	Mantle Cell Lymphoma	DMEM + 10% FBS	Suspension	DSMZ
Jeko-1	Human	Mantle Cell Lymphoma	RPMI 1640 + 10% FBS	Suspension	Martínez-Climent
Z-138	Human	Mantle Cell Lymphoma	RPMI 1640 + 10% FBS	Suspension	Martínez-Climent
AKATA	Human	Burkitt's Lymphoma	RPMI 1640 + 10% FBS	Suspension	Campanero
NAMALWA	Human	Burkitt's Lymphoma	RPMI 1640 + 10% FBS	Suspension	ATCC
RAJI	Human	Burkitt's Lymphoma	RPMI 1640 + 10% FBS	Suspension	ATCC
RAMOS	Human	Burkitt's Lymphoma	RPMI 1640 + 10% FBS	Suspension	ATCC
DB	Human	Diffuse Large B Cell Lymphoma	RPMI 1640 + 20% FBS	Suspension	DSMZ
DOHH-2	Human	Diffuse Large B Cell Lymphoma	RPMI 1640 + 10% FBS	Suspension	DSMZ
FARAGE	Human	Diffuse Large B Cell Lymphoma	RPMI 1640 + 10% FBS	Suspension	ATCC
HBL-1	Human	Diffuse Large B Cell Lymphoma	RPMI 1640 + 10% FBS	Suspension	Martínez-Climent
HLY-1	Human	Diffuse Large B Cell Lymphoma	RPMI 1640 + 10% FBS	Suspension	Martínez-Climent
KARPAS-422	Human	Diffuse Large B Cell Lymphoma	RPMI 1640 + 20% FBS	Suspension	DSMZ
MD901	Human	Diffuse Large B Cell Lymphoma	RPMI 1640 + 10% FBS	Suspension	Martínez-Climent
OCI-LY10	Human	Diffuse Large B Cell Lymphoma	IMDM + 10% FBS	Suspension	Martínez-Climent
OCI-LY19	Human	Diffuse Large B Cell Lymphoma	RPMI 1640 + 20% FBS	Suspension	DSMZ
OCI-LY3	Human	Diffuse Large B Cell Lymphoma	RPMI 1640 + 20% FBS	Suspension	Martínez-Climent
RIVA	Human	Diffuse Large B Cell Lymphoma	RPMI 1640 + 10% FBS	Suspension	Martínez-Climent
SU-DHL-4	Human	Diffuse Large B Cell Lymphoma	RPMI 1640 + 10% FBS	Suspension	DSMZ
SU-DHL-6	Human	Diffuse Large B Cell Lymphoma	RPMI 1640 + 10% FBS	Suspension	DSMZ
TOLEDO	Human	Diffuse Large B Cell Lymphoma	RPMI 1640 + 10% FBS	Suspension	ATCC
U2932	Human	Diffuse Large B Cell Lymphoma	RPMI 1640 + 10% FBS	Suspension	Martínez-Climent

2.2.2 CULTURE AND CONSERVATION OF CELL LINES

All cell lines were grown in RPMI 1640 (Sigma Chemical, St Louis, MO), DMEM (Sigma Chemical) or IMDM medium (Gibco, Billings, MT) supplemented with 10-20% heat-inactivated fetal bovine serum – FBS (Euroclone, Ltd, UK), 2mM L-glutamine (Life Technologies, Inc., Grand Island, NY), 40 units/mL

penicillin (Gibco), 40 µg/mL streptomycin (Gibco) and 1 µg/mL fungizone (amphotericin B, Gibco) in a humidified incubator (Nuaire, Inc., Plymouth, MN) at 37º C with a 5% CO2 atmosphere. Cell lines in suspension were grown in 25-150 cm^2 flasks (Corning, Corning, NY) and were subcultured by diluting cells 1:3 to 1:6 every other day. All cell manipulations were performed in a Telstar Biological Safety Cabinets (Bio IIA) with the laminar air flow systems. For long storage, cells were preserved in a liquid nitrogen container using DMSO as a cryoprotectant to avoid crystal formation and rupture of cell membrane. Briefly, 2.5-5 million cells were resuspended in 1 mL of freezing medium (90% FBS, 10% DMSO) and aliquoted in cryotubes. Aliquots where then put into a chilling jar and stored for 24 h in a -80º C freezer to achieve a -1º C/minute cooling rate. To defrost the cells, a cryotube was quickly thawed in a 37º C water bath and DMSO was removed by a 5 minutes centrifugation step at 1,200 rpm. Cells were then resuspended in the proper amount of fresh medium.

2.3 ANTIBODIES

The antibodies utilized in the present work together with its origin, type, clone, application, dilution and manufacturer are shown in table 2.2.

Table 2.2. Characteristics of the antibodies used.

Antibody	Species	Type	Clone	Dilution	Manufacturer
BCL6	Mouse	Monoclonal	PG-B6p	1:500 (WB)	DAKO
BCL6	Mouse	Monoclonal	GI 191E/A8	1:300 (IHC)	CNIO
EZH2	Rabbit	Polyclonal	ZMD.309	1:25 (IHC)	Zymed
Histone H3	Mouse	Monoclonal	6.6.2	1:1000 (WB)	Upstate
H3K27me3	Rabbit	Polyclonal	07-499	1:1000 (WB)	Upstate
Ki67	Mouse	Monoclonal	MIB-1	Ready to use (IHC)	DAKO
LMP-1	Mouse	Monoclonal	CS.1-4	Ready to use (IHC)	DAKO
PARP	Mouse	Monoclonal	P248	1:1000 (WB)	Sigma-Aldrich
SUZ12	Mouse	Monoclonal	220A/A3	1:2000 (WB & ChIP, concentrated) 1:2 (IHC, supernatant)	CNIO
SUZ12	Mouse	Monoclonal	07-379	1:1000 (ChIP)	Upstate
Tubulin	Mouse	Monoclonal	DM1A	1:10000 (WB)	Sigma-Aldrich

2.3.1 PRODUCTION OF SUZ12 MONOCLONAL ANTIBODY

A cDNA encoding the full-length human SUZ12 protein was obtained from the laboratory of Dr Yi Zhang (pGEX-KG-SUZ12). The human SUZ12 gene was amplified by polymerase chain reaction (PCR) and introduced into the pDEST-TH1 expression vector (Invitrogen, Carlsbad, CA, USA) by means of Gateway® technology. The MBP-SUZ12 fusion protein was then expressed in E. coli strain BL21 (DE3) with 0.4 mM IPTG overnight at 30ºC. The bacteria were lysed with BugBuster reagent. The soluble fraction was purified with amylase resin (New England Biolabs, Ipswich, MA, USA), and the joined protein was eluted with 10 mM maltose. The protein-containing fractions were concentrated by Vivaspin ultrafiltration and used as an immunogen.

Three BALB/c mice were injected intraperitoneally (three times at 14-day intervals) with 100 µg 6 x MBP-SUZ12 fusion protein and Freund's adjuvant. A 150-µg booster of the recombinant SUZ12 protein was injected intraperitoneally, and fused three days later, as described previously (Garcia et al., 2006; Montes-Moreno et al., 2008)

To confirm that 220A/A3 mAb recognized the human SUZ12 protein, immunohistochemistry on frozen cytospin preparations of V5-tagged human SUZ12 expressed in HEK-293T cells was performed. Labeling with the anti-V5 mAb confirmed the efficiency of transfection. A Cytospin preparation of V5-tagged human SOX4 protein was used as a negative control (Figure 3.1). Hybridoma supernatants were screened by ELISA. The mouse mAb raised against SUZ12 (220A/A3) was cloned by the limiting dilution technique. Animal experiments were performed under the experimental protocol approved by the Institutional Committee for Care and Use of Animals, CEUCA nº 001/02.

2.4 IMMUNOHISTOCHEMISTRY

In general, immunohistochemical staining was performed in the Histology and Immunohistochemistry Core Unit at the CNIO as follows. Immunohistochemical staining was carried out on FFPE tissue slides using a robotized system (Techmate 500; DAKO) and the LSAB Visualization System protocol (labeled streptavidin-biotin; DAKO). The slides were dried at 56º C and paraffin removed by successive immersion in xylene (2 x 10 minutes), 100% ethanol (5 minutes), 95% ethanol (5 minutes), 70% ethanol (5 minutes) and water (2 minutes). A Heat-Induced Epitope Retrieval (HIER) step was performed in a 10mM solution of sodium citrate buffer pH 6.5 with 0.01M tri-sodium citrate solution, and heated for 2min in a conventional pressure cooker. After heating, slides were rinsed in cool running water for 5min. They were then quickly washed in Tris-buffered-saline pH 7.4, and incubated with monoclonal primary antibodies at appropriate dilutions for approx. 40min. The primary monoclonal antibodies used in this study and their dilutions are included in the table 2.7.

Following incubation with the primary antibody, immunodetection was performed with biotinylated secondary antibody (25 minutes), followed by peroxidase-labelled streptavidin-biotin (DAKO-Cytomation, Glostrup, Denmark) with diaminobenzidine chromogen as substrate and contra stained with hematoxilin (1 minute and washed with distilled water). The preparations were dehydrated through consecutive incubations with ethanol 95% (30 seconds), ethanol 100% (30 seconds) and xylene (1 hour), and mounted using automatic mounting Tissue-Tek SCA. Incubation omitting the specific antibody and incubation with unrelated antibodies was used as a control of the technique.

2.5 TISSUE MICROARRAYS

Tissue Microarrays (TMA) technology allows for the simultaneous analysis of multiple individual tissue samples on a single slide through immunohistochemistry, *in situ* hybridization and fluorescence *in situ* hybridization techniques (Kallioniemi et al., 2001; Kononen et al., 1998). A TMA consist of the arrayed disposition of a variable number of circular biopsies (0.6-2 mm diameter) originated from different PFFE blocks into a unique block. This technology takes advantage of the possibility of analyzing a big number of samples in homogeneous experimental conditions with a minimum destruction of the original tissue sample and a low time and money consumption. The possibility of bias due to non-representative tissue sections is overcame by the number of tumors analyzed as demonstrated by several studies (Camp et al., 2000).

To construct the TMAs we used a Tissue Arrayer device (Beecher Instruments, Sun Prairie, WI) as previously described (Kallioniemi et al., 2001; Sanchez-Beato et al., 2006). All cases were histologically reviewed and representative areas were selected. In each case, 2 selected 1-mm-diameter cylinders from 2 different areas were included, along with 43 different controls to ensure the quality, reproducibility, and homogenous staining of the slides.

Two independent researchers evaluated the staining of TMA sections for SUZ12, EZH2, and Ki67 proteins using uniform criteria. Discrepancies in the scoring of cases were resolved after joint examination on a multi-headed microscope. To ensure the reproducibility of this method, we employed straightforward, clear-cut criteria, and cases were scored as positive (1) or negative (0) for SUZ12 and EZH2 antibodies. The threshold was 5% of positive cells for both antibodies. For Ki67, the values were scored as negative (0) for fewer than 5% of proliferating cells, positive (1) for 5-25%, and strongly positive (2) if more than 25% of cells were positive for Ki67.

Whole-tissue sections from reactive lymph node, thymus, spleen, and tonsillectomy specimens were used for the examination of benign lymphocyte subpopulations.

2.6 BACTERIAL STRAINS AND CULTURE

2.6.1 PROPAGATION CONDITIONS

All Gateway™ destination vectors with the ccdB toxic gene were propagated in *Escherichia coli* One Shot® ccdB Survival™ T1 Phage-Resistant Cells (Invitrogen, San Diego, CA) which genotype is: F- mcrA Δ(mrr-hsdRMS-mcrBC) Φ80lacZΔM15 ΔlacX74 recA1 araΔ139 Δ(ara-leu)7697 galU galK rpsL (StrR) endA1 nupG tonA::Ptrc-ccdA.

All other vectors including Gateway™ destination vectors without the ccdB toxic gene were propagated in One Shot® TOP10 Chemically Competent E. coli (Invitrogen) which genotype is: F- mcrA Δ(mrr-hsdRMS-mcrBC) ϕ80lacZΔM15 ΔlacX74 recA1 araD139 Δ(araleu) 7697 galU galK rpsL (StrR) endA1 nupG.

All bacteria strains were normally growth in Luria-Bertani (LB) broth (10 g/L tryptone, 5 g/L yeast extract, 200 mM NaCl, pH 7.0) at 37º C in continuous shaking (225 rpm) for 16-20 hours approximately. Low salt LB broth (10 g/L tryptone, 5 g/L yeast extract, 100 mM NaCl, pH7.0) was used for propagating those bacteria carrying lentiviral plasmids.

2.7 POLYMERASE CHAIN REACTION (PCR)

The amplification of DNA fragments was carried out following a standard procedure. A general mixture was prepared with the following components: 1X polymerase buffer, 1.5 mM MgCl2, 0.2 mM dNTPs, 0.2 mM of each primer, 100 ng of DNA and 1 unit of polymerase. The typical reaction volume was 25 µL. The polymerase was different depending on the use of the PCR product and will be described in the proper section. PCR reactions took place in a GeneAmp® PCR System 9700 (Applied Biosystems, Foster City, CA). The conditions for each reaction will be described in the corresponding section.

2.8 CLONING OF PCR PRODUCTS

2.8.1 CLONING IN PENTR/D-TOPO VECTOR

The pEntr/D-TOPO (Invitrogen) is a linear vector with a 5’ overhang in one side that contains the sequence GGTG and allows the directional cloning of a PCR product with a CACC 5’ end. Moreover it

contains a molecule of topoisomerase I covalently bound to each end of the vector that catalyzes the formation of a phosphodiester bond. The reactions were carried out in a volume of 3 µL that contained 1 µL of PCR product (in which one of the primers contained the CACC 5' end), 0.5 µL of salt solution (1.2 M NaCl, 0.06 M MgCl2), 0.3 µL of the vector and 1.2 µL of water. This mix was incubated at room temperature for 5 minutes and 2 µL were used to transform chemocompetent TOP10 cells. The plasmid DNA of the resulting colonies was extracted by the miniprep procedure and analyzed by restriction analysis and sequencing.

2.8.2 CLONING IN PGL3 CONTROL VECTOR

The pGL3 Control vector (Promega) is an expression vector that contains the luc+ gene from the Firefly luciferase under the control of the SV40 promoter and enhancer sequences, resulting in the strong expression of the luc+ gene in many types of mammalian cells. For cloning of PCR products, the vector was digested with the XbaI restriction enzyme (New England Biolabs, Ipswich, MA). The vector was separated by electrophoresis in a 0.8 % agarose gel to ensure the correct digestion and purified. Vector was then subjected to blunting using the T4 DNA polymerase. For this, 1 unit of T4 polymerase was mixed with 1 µg of digested vector and 100 µM dNTPs in a final volume of 50 µL. This mix was incubated at 12º C for 20 minutes and then T4 DNA polymerase was inactivated by heating at 75º C for 10 minutes. Then the blunt PCR product was ligated overnight at 16º C.

2.9 CLONING OF shRNA IN LENTIVIRAL VECTORS

The lentiviral vector pA179.Helix (Figure 2.1) was developed by the Genomics Unit at the CNIO by introducing a Gateway cassette into the pFUGW vector (Lois et al., 2002) deposited by David Baltimore to Addgene's plasmid repository (http://www.addgene.org/14883). Different shRNAs were designed using the SIDE program (http://side.bioinfo.cipf.es). The shRNAs were designed within the ORF sequence of the gene to avoid off-target effects associated with imperfect matching in the 3' UTR of the target gene.

As a first step for cloning, the H1 promoter is added to a shRNA-coding oligo by overlap extension PCR using the pSUPER vector (Brummelkamp et al., 2002) (Oligoengine, Seattle, WA) as a mold. The shRNA-coding oligo carries a CACC sequence at the 5' end to allow the cloning into the pENTR/D-TOPO vector. The PCR is normally carried out using the Pfu Turbo DNA polymerase (Stratagene, La Jolla, CA) derived from the DNA polymerase of the hyperthermophilic archaeon *Pyrococcus furiosus* or the KOD DNA polymerase (Toyobo Co., Osaka, Japan) derived from the DNA polymerase of the hyperthermophilic archaeon *Thermococcus kodakaraensis* if reaction with Pfu Turbo was unproductive.

The constructions are separated by gel electrophoresis, extracted and cloned into the pENTR/D-TOPO vector as described in the sections 2.9 and 2.10.1.

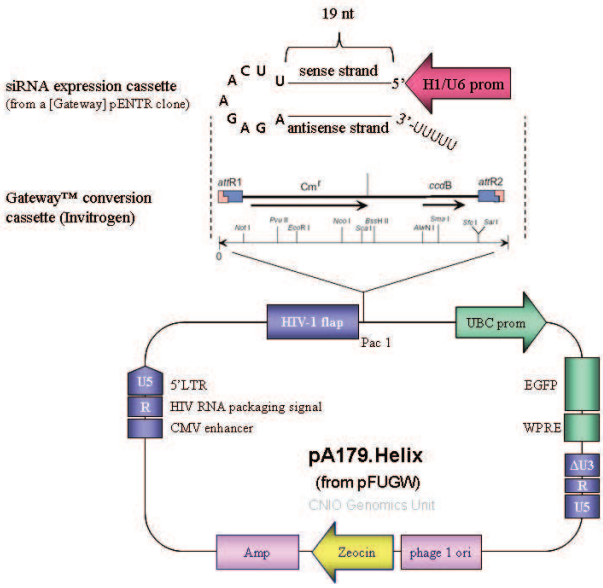

Figure 2.1. Vector map for the lentiviral vector pA179

After successful cloning in the pENTR/D-TOPO vector, the plasmid is propagated, isolated and sequence-verified as described in the sections 2.6.1 and 2.7.2.

The insert is then subcloned into the pA179.Helix vector by using the Gateway® LR Clonase™ II enzyme mix (Invitrogen). This enzyme mix contains the Int (Integrase), IHF (Integration Host Factor) and Xis (Excisionase) enzymes that catalyze the in vitro recombination between the pENTR/D-TOPO and pA179.Helix vectors. For the reaction to occur 150 ng of each vector were mixed and TE buffer (10 mM Tris, pH 8.0; 1 mM EDTA) was added up to 8 µL. Then 2 µL of enzyme mix were added and the mixture was briefly vortexed and spun down. The reaction was incubated at room temperature overnight and 2 µL of the mix were used to transform TOP10 chemocompetent cells.

2.10 TRANSFECTION AND TRANSDUCTION TECHNIQUES

2.10.1 TRANSFECTION WITH FUGENE® HD

HEK293T cells were transfected with FuGene® HD (Roche, Basel, Switzerland) for the production of viral particles. FuGene® HD is a multi-component reagent for the transient and stable transfection of animal and insect cells. It contains lipids and other components that form complexes with DNA that are

transported into the cells. The HD formulation allows transfection of cells cultured at high density (80-90% confluence). The transfection was done following the manufacturer's recommendations. Briefly, the day before the assay 4.5 million cells were seeded in a 10 cm plate. The next day the medium was replaced by 10 mL of fresh medium and the cells were put back into the incubator. 9 µg of plasmid were mixed in 500 µL of prewarmed OPTIMEM® (Invitrogen) with 27 µL of FuGene® HD. The mixture was incubated for 30 minutes with gentle shaking every 5-10 minutes at room temperature. The mixture was added drop by drop to the cells and the cells were cultured normally.

2.10.2 CALCIUM PHOSPHATE PRECIPITATION

For transfection of luciferase plasmids and/or microRNAs in HEK293T cells calcium phosphate precipitation protocol was used since it showed superior performance than FuGene for simultaneous transfection of plasmids and microRNAs. In this case 1 million cells were seeded the day before transfection in a 35 mm diameter plate. The following day the old medium was removed and 2 mL of fresh medium were added. Cells were put back again into the incubator at least for 30 minutes to allow pH equilibration. In the meantime the following mix was prepared (per sample):

- 400 ng of pGL3 derived vector.
- 50 ng of pRL-CMV vector containing the R*luc* gene coding for the *Renilla* luciferase.
- The proper amount of microRNA.
- Up to 87 µL of distilled water.
- 13 µL of 1M $CaCl_2$

Prior to transfection cells were taken out the incubator and 100 µL of 2X HBS were added to the CaCl2 mix. The blend was mixed by directly bubbling for 15 seconds with the pipette. Then, it was added drop by drop to the cells. 16-20 hours after the transfection the cells were washed twice with 1X PBS (NaCl 137 mM, Na2HPO4 10 mM, KCl 2.7 mM, KH2PO4 2 mM, pH 7.4) to remove calcium phosphate precipitates and 2 mL of fresh medium were added.

2.10.3 MICROPORATION

Microporation is a novel electroporation technique that achieves high levels of transfection while keeping high levels of cell viability. Electroporation is an effective technique for transfection in which an electric field is applied to increase the permeability of the cell membrane. The increased permeability

allows the nucleic acids to pass through the cell membrane and enter into the cell. However, during the electroporation there are some processes that affect cell viability such as heat generation, dissolution of metal ions, variations in pH and oxide formation avoiding its use for sensitive cell lines such as lymphoid ones. The microporator (Digital Bio Technology, Seoul, Korea) is an electroporation device that uses a pipette tip as the electroporation space. This allows the generation of a uniform electric field with minimum heat generation, dissolution of metal ions, variation in pH or oxide formation. Thus we were able to get high transfection efficiency and survival rates with this method.

For microporation one day prior to the assay the cells were cultured in a fresh growth medium without antibiotics in order to reach 60 to 80% confluence. The following day $2x10^6$ cells (100 µL tips) or $3x10^5$ cells (10 µL tips) were harvested and washed with PBS. The pellet was resuspended in 110 µL (100 µL tip) or 11 µL (10 µL tip) of buffer R and mixed with the proper amount of nucleic acids. 3 mL of buffer E2 (100 µL tip) or E (10 µL tip) were added to the microporation tube. 100 µL or 10 µL were taken with the gold tip, the pipette was inserted in the microporation tube and the electric field was applied. For microporation of the cell lines used in this study the following conditions were applied: 1250 volts, 30 ms, 2 pulses.

2.10.4 TRANSDUCTION WITH LENTIVIRAL PARTICLES

Retroviral vectors are attractive tool for gene delivery. They have three characteristics that make them an ideal tool for stable expression of DNA elements. First, they stably integrate their cargo in the target cell which is important for the stable expression of the gene. Second, they have a large capacity (close to 10 Kb) that allows the expression of most cDNAs. Last, current retroviral vectors are free of pathogenic sequences and they do not transfer genes encoding for viral proteins thus minimizing the risk for the operator. Lentiviruses are a subtype of retroviruses with some specific features that render them very interesting for gene transduction of difficult-to-transfect cell lines. Transduction with lentiviruses also allows the stable delivery of DNA elements in a wide variety of cell lines, including primary cells and lymphoid cells. They are more efficient than other retroviral vectors because they are able to transduce both dividing as well non dividing cells. Lentivectors are derived from the HIV-1 genome and have evolved to increase their safety and versatility.

Production of lentiviral particles requires the use of a packaging cell line. In this case the HEK293T cell line was used to produce the viruses. This cell line allows the production of non-replicative units of the virus that are able to infect target cells but do not have the potential of producing more viral particles as normal viruses.

There are several genes that are needed to produce the virus but are not codified by the lentivector. These are structural and enzymatic genes (*gag*, *pol* and *env*; necessary for the formation and

the replication of the virus that are provided in separate vectors for safety reasons). In lentiviruses, the efficient expression of Gag and Pol also requires a virally-encoded post-transcriptional activator called Rev. The gene *gag-pol* encodes for the capside, nucleocapside, integrase and retrotranscriptase of the virus whereas the *env* gene encodes for the glycoprotein that is present in the envelope of the virus. This protein determines the tropism of the virus since it is recognized by cell surface receptors and mediates the entry of the vector particle on its target. In this work we used the G protein of vesicular stomatitis virus (VSV-G) to pseudotype lentiviral vector particles because it is highly stable and because its receptor is ubiquitously expressed in mammalian cells (Salmon and Trono, 2007).

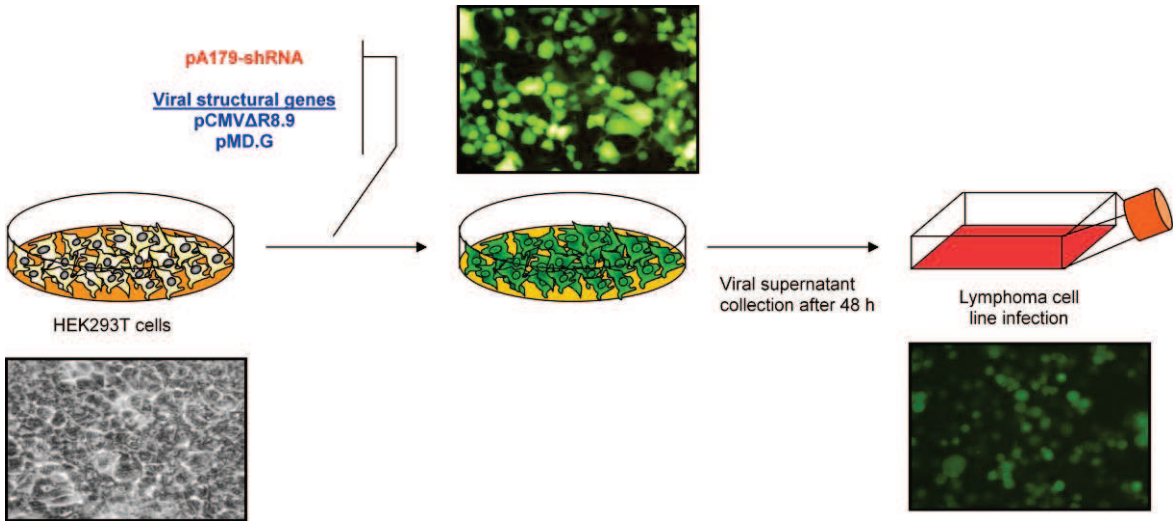

Figure 2.2. Schematic representation of the steps followed for viral production and transduction of lymphoid cell lines.

The first step to produce the viruses is to co-transfect the lentivector (pA179.Helix, described above) with the structural vectors (pCMVdeltaR8.91 derived from the pCMVdeltaR8.9 (Lois et al., 2002) and encoding the *gag-pol* gene and pMD.G codifying for the *env* gene encoding the VSV-G protein) following the protocol described in the section 2.14.1.1 of this thesis. 48 hours after the transfection the cell supernatant already contains a high viral titer and can be used to infect target cells. For this, the supernatant is recovered and filtered through 0.45 µm cellulose acetate filter and 1 mL of viral supernatant was mixed with 10^6 lymphoid target cells in a 6-well plate (NUNC, Roskilde, Denmark). Several protocols include the addition of polybrene (a polycation that reduces the electrostatic repulsion between the virus and the cell membrane) at this step, however it is not necessary when viral particles are pseudotyped with the VSV-G protein (Salmon and Trono, 2007). Then the cells are centrifuged with the viruses at 1,000 xg for 90 minutes (spinoculation). The cells are recovered and centrifuged to remove the viral supernatant and resuspended in 2 mL of fresh medium. The protocol is summarized in figure 2.2.

2.11 LUCIFERASE ASSAYS

To measure luciferase activity, $5x10^5$ cells were transfected with 400 ng of pGL3 vector and 40 ng of Renilla vector. 48h later, cells were lysed in 250 µL of Passive Lysis Buffer for 15 minutes (Promega) and cell debris was removed by brief centrifugation. 50 µL of Luciferase Assay Reagent II (LARII, Promega) were added to 50 µL of cell lysate and the firefly luciferase activity was measured in a lumminometer. Then, 50 µL of STOP&Glo reagent (Promega) were added to measure the activity of the Renilla luciferase. Total luciferase activity was represented as the ration between firefly and Renilla signals.

2.12 CHROMATIN IMMUNOPRECIPITATION (CHIP) AND CHIP-ON-CHIP

Chromatin immunoprecipitation (ChIP) is a technique that allows the analysis of protein binding to DNA sequences in a physiological context. It has been widely used to identify specific proteins or protein modifications in a region of the genome or the other way around, i.e. to identify regions of the genome associated with specific proteins. The technique is based on the immunoprecipitation of proteins that have been previously fixed with a cross linking agent and sonicated to shear DNA, allowing the precipitation of DNA sequences bound by these proteins. Standard PCR is commonly used to identify the DNA sequences associated to the immunoprecipitated protein. ChIP-on-chip, also known as location analysis (LA) is a variant of the ChIP assay that complements ChIP with hybridization in an oligonucleotide microarray. Both techniques have four common steps:

- Fixation: It is one of the most critical steps. By fixing cells, proteins are cross linked to the molecules with which they are interacting. This permits protein-DNA complexes to keep their interactions throughout the entire process.
- Cell lysis and sonication: It is necessary not only to release the DNA-protein complexes but also to shear DNA in adequate size fragments that are suitable for subsequent analysis.
- Immunoprecipitation (IP): It is the differential step that will purify the protein-DNA complexes. The use of a high-quality antibody is crucial to get high signal-to-noise ratios.
- Hydrolysis: Once the DNA fragments are co-immunoprecipitated with the protein, it is necessary to reverse the cross-links as a previous step to the analysis.

After this point, in standard ChIP, DNA fragments are analyzed by standard PCR. In the case of ChIP-on-chip, DNA is amplified to get enough starting material and later on labeled and hybridized in an oligonucleotide microarray (Figure 2.3).

The detailed protocol is described below. All used buffers are described at the end of the protocol.

2.12.1 CHROMATIN IMMUNOPRECIPITATION (CHIP)

First of all, 1-2 x 107 cells are harvested in a Falcon tube to have enough material for 5-10 immunoprecipitations (approximately 2 x 106 cells are used per antibody). Cells are fixed by directly adding fresh 18.5% formaldehyde to get a final concentration of 1% formaldehyde. After addition of the fixating agent, cells are incubated for 15 minutes in a rotating platform. Afterwards, the cross linking reaction is stopped by direct addition of glycine powder to a final concentration of 0.125M. The samples are incubated 5 more minutes in a rotating platform, centrifuged for 5 minutes at 2,000 rpm to remove medium and washed twice with 10 mL of ice cold 1X PBS supplemented with 1X Protease Inhibitor Cocktail II (Milipore, Billerica, MA) and transferred to a 2 mL eppendorf tube. The pellet is disrupted by addition of SDS Lysis Buffer supplemented with 1X Protease Inhibitor Cocktail II (Milipore) and incubation for 10 minutes on ice. The amount of SDS Lysis Buffers depends on cell density and size but in this protocol 300 µL of lysis buffer is added to every 5 x 106 cells. Lysates can be frozen at -80º C at this step.

The second step is to sonicate the cells. For this, lysates were divided in 300 µL aliquots and sonicated in a Bioruptor sonication device (Diagenode, Liège, Belgium) under the following conditions:

- Intensity: High (H).
- Time: 20 minutes.
- Intervals: 30 seconds on, 30 seconds off.

Prior to sonication, half of the water of the Bioruptor was replaced with ice to avoid sample heating. These conditions have been previously optimized to yield chromatin fragments between 200-1000 bp with an average of 400 bp.

Sonicated samples were centrifuged for 10 minutes at 15,000 xg to precipitate cell debris and insoluble chromatin. The chromatin can be stored at this point at -80º C. The third step is the immunoprecipitation. For this chromatin was measured in a NanoDrop (NanoDrop) just as an estimation of the yield and all the samples were put at a concentration of 750 ng/µL by diluting with SDS Lysis Buffer supplemented with protease inhibitors. 200 µL of chromatin were diluted with 1800 µL of Dilution Buffer supplemented with protease inhibitors and pre-cleared by addition of 60 µL of Salmon sperm DNA/Protein A/G 50% Slurry (Millipore). The samples were incubated for 1 hour in a rotating platform at 4º C. Agarose beads were pelleted by brief centrifugation (3000-5000 x g for 1 minute) and the supernatants were collected. 5 µg of the antibody were added to the sample (For the negative control, normal mouse IgG was used) and incubate overnight in a rotating platform at 4º C. After this, antibody-protein-DNA complexes are collected by addition of 80 µL of Salmon sperm DNA/Protein A/G 50% Slurry (Millipore) for 1 hour at 4º C with rotation. . Agarose beads were pelleted by brief centrifugation (3000-5000 x g for 1 minute). 1 mL of supernatant of the negative control was collected

as the input. The beads were washed in 1ml each of the cold buffers in the order listed below and incubating for 3-5 minutes on a rotating platform followed by brief centrifugation (3000-5000 x g for 1 minute) and careful removal of the supernatant fraction:

- Low Salt Immune Complex Wash Buffer
- High Salt Immune Complex Wash Buffer
- LiCl Immune Complex Wash Buffer
- TE Buffer (two washes)

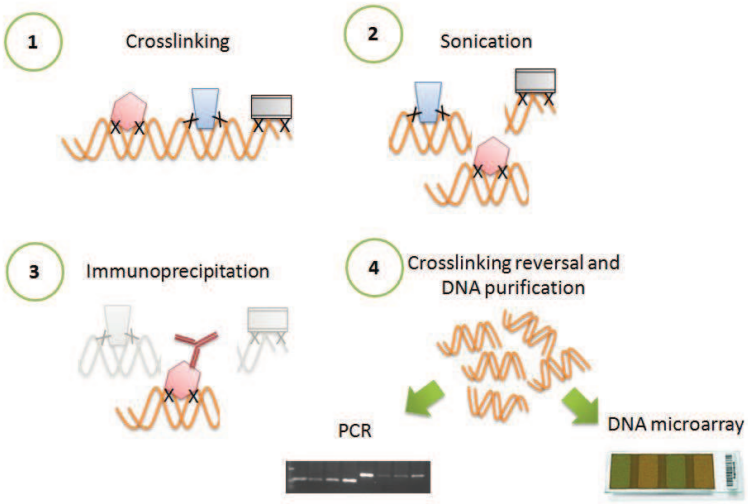

Figure 2.3. Schematic representation of the ChIP and ChIP-on-chip protocols with the four common steps.

To elute the protein-DNA complexes, Elution Buffer was prepared prior to the elution step. 250 µL of elution buffer were added to each sample and incubated for 15 minutes in a rotating platform. Agarose was pelleted by brief centrifugation (3000-5000 x g for 1 minute) and supernatants were collected into new microfuge tubes. This step was repeated and eluates were combined to get a final volume of 500 µL.

To reverse the cross linking, 20 µL 5M NaCl were added to each tube (40 µL for inputs) and incubated at 65°C for 4-5 hours or overnight. After this, 10 µl 0.5M EDTA, 20 µl 1M Tris-HCl and 2.5 µl of 10 µg/µL Proteinase K were added to each sample (double for the inputs) and incubated at 45°C for 1-2 hours. DNA was extracted by phenol:chlorophorm extraction as described in section 2.18 resuspending the DNA in a final volume of 20 µL.

For ChIP analysis, 1 µL of immunoprecipitated material was subjected to PCR using 1 unit of EcoStart Taq polymerase (Ecogen). The PCR program is described in table 2.3:

Table 2.3. PCR conditions for ChIP analysis.

Temperature	**Time**	**Step**	
95º C	5 minutes	Denaturation	
94º C	30 seconds	Denaturation	35 cycles
60º C	30 seconds	Annealing	
72º C	30 seconds	Extension	
72º C	10 minutes	Final extension	

Table2.4 List of PCR primers used for ChIP analysis.

Gene name	Sense strand	Antisense strand
ATM	GTTGTGCAAAGGGGTCAACT	TTGGCGGAACTGAAAGAAG
BCOR	GCAAAAGACAGGCGAGCAAG	ACCCCCAGAAAGACCAGGAA
BIRC2	CCCAGGTGCATTTTTGGAAG	TGCCTGCCAGTCAGTCACAG
CBX2	TTCTCCCCGCTGTAACCTGA	GCCCGAGATCCAGAACAATG
E2F5	TGGATTGCAGTGGCAGGA	CGTGGTAGTGCACACTTG
GADD45G	GTGCCAGCGTGTATGGTCAA	CGAGTAAGGGCTGCAAAACG
H2AFZ	AGGGCCTGGGAGTTTTCTTG	CTGTGTACAGCGCAGCCATC
HDAC2	CTGGAGAAGGAGGCCGTTTC	GCAGACCTGAGGGGGAGAAC
JMJD2D	AAATATGTACGGGGCAACCA	TGACATCTCCCCTCCCACTA
VAV3	GCTCAGCGCACCTAGACGTT	GGCTCAGGTGTTCGACCTTG

Buffers composition and preparation of other reagents.

- SDS Lysis Buffer: 1% SDS, 10 mM EDTA, 50 mM Tris, pH 8.1.
- ChIP Dilution Buffer: 0.01% SDS, 1.1% Triton X-100, 1.2mM EDTA, 16.7mM Tris-HCl, pH 8.1, and 167 mM NaCl.
- Low Salt Immune Complex Wash Buffer: 0.1% SDS, 1% Triton X-100, 2 mM EDTA, 20 mM Tris-HCl, pH 8.1, 150 mM NaCl.
- High Salt Immune Complex Wash Buffer: 0.1% SDS, 1% Triton X-100, 2 mM EDTA, 20 mM Tris-HCl, pH 8.1, 500 mM NaCl.
- LiCl Immune Complex Wash Buffer: 0.25 M LiCl, 1% IGEPAL-CA630, 1% deoxycholic acid (sodium salt), 1 mM EDTA, 10 mM Tris, pH 8.1.
- TE buffer: 10 mM Tris-HCl, 1 mM EDTA, pH 8.0.
- Preparation of fresh 18.5 % formaldehyde: 0.925g paraformaldehyde (Sigma-Aldrich) was dissolved in a 50 mL Falcon tube with 4.8 mL of distilled water and 35 µL of 1N KOH. The tube was put in a glass beaker with 400-600 mL of water and heated in the microwave until the water in the beaker began boiling. The dissolved paraformaldehyde was cooled down on ice.

2.12.2 CHIP-ON-CHIP

For ChIP-on-chip immunoprecipitated DNA was amplified using the GenomePlex Whole Genome Amplification kit (Sigma-Aldrich) following the protocol described by O'Geen and colleagues (O'Geen et al., 2006):

Library preparation: 10 µL of immunoprecipitated material or 10 ng of the input were mixed with 2 µL of 1X Library Preparation Buffer and 1 µL Library Stabilization Solution. Samples were incubated at 95º C for 2 minutes and immediately cooled on ice. Then 1 µL Library Preparation Enzyme was added and the samples were incubated as follows in a thermal cycler:

- 16° C for 20 minutes (cycler should be precooled to this temperature)
- 24° C for 20 minutes
- 37° C for 20 minutes
- 75° C for 5 minutes

- 4° C hold

Amplification: A master mix was prepared containing 7.5 µL of 10X Amplification Master Mix, 47.5 µL Nuclease-free H_20 and 5 µL WGA DNA polymerase per sample. 60 µL of this master mix were added to each sample and incubated in a thermal cycler as follows:

- 95° for 3' , then 14 cycles of
- 94° for 15"
- 65° for 5', then
- 4° hold

DNA was purified using the QIAquick PCR Purification Kit (Qiagen) and 15 ng of amplified material were subjected to a second amplification step as described above. Biological triplicates were amplified with this method. The same quantity of each replicate was mixed in a single tube. 2µg of DNA were labeled with the Bioprime Total Genomic Labeling System (Invitrogen) following the manufacturer's recommendations. Briefly, input material and samples were labeled through random primer extensions by Exo-minus Klenow DNA polymerase in the presence of either Alexa Fluor 5 or Alexa Fluor 3 propargyl linked fluorophores. Labeled samples were purified with silica-based PureLink spin columns (Invitrogen). The samples were hybridized onto the Human Promoter ChIP-on-chip Microarray Set (Agilent Technologies Inc., Santa Clara, CA) that covers -5.5 kb upstream to +2.5 kb downstream of the transcriptional start sites of every gene with a total of 487,008 probes, following the instructions provided by the manufacturer. Briefly the samples were hybridized on a SureHyb hybridization chamber (Agilent Technologies) for 40 hours at 10 rpm and 65º C.

2.12.3 DATA ANALYSIS

Raw data from the images was extracted using the Feature Extraction software (v. 9.5.3.1, Agilent Technologies). ChIP Analytics program (v. 1.3.1, Agilent Technologies) was used for the analyses. A whole-chip error model was used to calculate confidence values from the enrichment ratio and the signal intensity of each probe (probe p-value) and of each set of three neighboring probes (probe set p-value). Probe sets with significant probe-set p-values ($p < 0.001$) and significant individual probe p-values ($p < 0.01$) were judged to be bound. Bound regions were assigned to genes if they were within 1 kb of the transcription start site registered in at least one of five genomic databases.

2.13 FLOW CYTOMETRY TECHNIQUES

2.13.1 ANALYSIS OF TRANSDUCTION EFFICIENCY

For analysis of transduction efficiency, cells were counted and 200,000 cells were washed twice with 1X PBS (NaCl 137 mM, Na2HPO4 10 mM, KCl 2.7 mM, KH2PO4 2 mM, pH 7.4) by centrifugation at 300 xg for five minutes. The cells were resuspended in 200 µL of PBS and acquired in a FACScalibur (Becton Dickinson, Franklin Lakes, NJ). Acquisition and analysis was carried out using the CellQuest™ Pro software (Becton Dickinson). 10,000 events were acquired and EGFP signal was detected in the FL-1 channel.

2.13.2 CELL COMPETITION ASSAYS

To determine if viability or proliferative capacity of cells infected with a lentivirus carrying a shRNA against SUZ12 or a scramble control, we designed a competitive proliferation assay similar to that previously described (Ivanova et al., 2006). In short, GFP expression was analyzed by FACS 72 hours after infection of the cell lines with lentivirus carrying either the empty vector, or a scrambled control or either of the two shRNAs against SUZ12. This was done every 2 to 4 days. The evolution of GFP expression was compared with the third day using the following formula:

$$\%Initial\ Ratio = \frac{Ratio\ \ GFP^+/GFP^-\ _{day\ n}}{Ratio\ \ GFP^+/GFP^-\ _{day\ 3}} \times 100$$

2.13.3 ANALYSIS OF APOPTOSIS BY ANNEXIN V STAINING

Double staining with annexin V and propidium iodide (PI) was carried out in order to measure apoptosis. Annexin V is a 35-36 kDa Ca^{2+} dependent phospholipid-binding protein that has a high affinity for phosphatidylserine (PS), and binds to cells with exposed PS. Loss of plasma membrane asymmetry, that includes flipping of PS from the inner to the outer leaflet of the plasma membrane, is an early event in apoptosis. Thus annexin V stains cells that are undergoing apoptosis. PI is a DNA intercalating molecule that stains nucleic acids. It is used to stain death cells that have lost their membrane integrity. Since PI is a cell membrane impermeable compound, it is excluded from alive and early apoptotic cells while staining late apoptotic and necrotic cells. Double staining with these two compounds allows the discrimination between alive (double negative), early apoptotic (annexin V positive, PI negative) and late apoptotic/necrotic cells (double positive). In brief, 200,000 cells were washed twice with 1X PBS and

resuspended in 200 µL of 1X binding buffer (10 mM HEPES, pH 7.4; 140 mM NaCl; 2.5 mM $CaCl_2$). To this suspension, 2 µL of Annexin V (BD Pharmingen) plus 2 µL of 1 mg/mL PI (Sigma-Aldrich, ST. LOUIS, MO) were added and cells were incubated for 30 minutes prior to acquisition in a FACScalibur (Becton Dickinson). Acquisition and analysis was carried out using the CellQuest™ Pro software (Becton Dickinson). 10,000 events were acquired. Propidium iodide signal was detected in the FL-2 channel and annexin V signal was detected in the FL-4 channel.

2.13.4 CELL CYCLE ANALYSIS BY PI STAINING

Cell distribution in cell cycle stages was analyzed by PI staining in a flow cytometer. PI is able to indicate the amount of DNA in permeabilized cells. PI fluorescence signal is directly proportional to the amount of DNA inside the cell. For the experiments, 10^6 cells were washed once with 1X PBS and resuspended in 330 µL of cold PBS. Then 670 µL of chilled absolute ethanol was added drop by drop with continuous and gentle vortex. The cells were kept in this suspension for a minimum of 30 minutes and up to several days. Prior to analysis the cells are washed twice with 1X PBS and resuspended in 500 µL of PBS plus 1 µL of RNAse A (100 mg/mL, Qiagen) and incubated at room temperature for 30 minutes. 10 µL of 1mg/mL PI were added prior to acquisition in a FACScalibur (Becton Dickinson). Acquisition and analysis was carried out using the CellQuest™ Pro software (Becton Dickinson). 20,000 events were acquired. Propidium iodide signal was detected in the FL-2 channel.

2.14 GENOMIC DNA EXTRACTION

1-2 x 10^6 cells were washed twice with 1X PBS centrifugating at 300 xg for 5 minutes. The pellet was disrupted by addition of 500 µL of Tissue and Cell lysis solution (Epicentre, Madison, WI) and 4 µL of 50 µg/µL proteinase K and incubated overnight at 65º C. After the digestion the solution was observed to ensure that the entire pellet is digested. If that was not the case, 2 µL of proteinase K were added and the solution was incubated for 10 minutes at 65º C. After successful digestion of the samples, the solution was transferred to a 2 mL phase lock gel light tube (Eppendorf, Hamburg, Germany) and DNA was extracted by addition of 500 µL of phenol:chloroform:isoamyl alcohol 25:24:1 (Sigma-Aldrich), inverting the tube for 2 minutes to mix and centrifugation for 5 minutes at 10,000 rpm in a microcentrifuge. Aqueous phase was then extracted and 500 µL of chloroform:isoamyl alcohol 24:1 (Sigma-Aldrich) were added. The tubes were inverted again for a couple of minutes and centrifuged 5 minutes at 10,000 rpm in a microcentrifuge. Organic phase was discarded and 1 mL of ice cold ethanol, 50 µL of 7.5 M sodium acetate and 0.5 µL of linear acrylamide were added to the aqueous phase. The solution was inverted several times to mix and kept at -20º C to allow DNA precipitation for 30 minutes to one hour. DNA was subsequently pelleted by centrifugation at 12,000 rpm for 15 minutes and

washed with 1 mL of cold 70% ethanol. After washing, pellet was left to dry and later resuspended in 100-200 µL of water. DNA concentration and quality was measured using a NanoDrop (Nanodrop Technologies, Wilmington, DE).

2.15 RNA EXTRACTION

2.15.1 CELL LINES

2.15.1.1 EXTRACTION OF mRNA

RNA was extracted using the RNAeasy Mini-Kit (Qiagen) following the manufacturer's recommendations. Briefly, 10^6 cells were harvested and washed twice in 1X PBS. The pellet was lysed and homogenized using 350 µL of the highly denaturing RLT buffer (containing guanidine isothiocyanate that inhibits RNAse activity) supplemented with 10 µL of ß-mercaptoethanol. Cells were homogenized in a QIAshredder spin column (Qiagen) by centrifugation at top speed for 1 minute in a microfuge. Ethanol was added to the samples and the sample was passed through an RNeasy mini column that contains a silica-gel membrane that selectively binds RNA. The contaminant DNA is then digested using DNAse I (RNase-free DNase I Set; Qiagen) for 20 minutes and RNA is washed with an ethanol-containing buffer. As a last step, RNA is eluted in 50 µL of RNAse-free water.

If RNA concentration or quality was not optimal, RNA was precipitated by addition of 0.5 µl of linear acrylamide, 25 µL of 7.5 M ammonium acetate and 125 µL of chilled absolute ethanol. The mix was kept at -20º C for 12-16 hours and RNA was recovered by centrifugation at top speed for 30 minutes in a microfuge. The RNA was washed twice with 70% cold ethanol, air-dried and resuspended in 20-30 µL of RNAse-free water. Purified RNA was stored at -80º C in all cases.

2.15.1.2 EXTRACTION OF microRNA

RNA extraction protocol described in section 2.19.1.1 is not suitable when analyzing small RNAs because small RNAs are lost through the RNAeasy column. Thus, for analysis of miRNA expression, a different protocol was used. Since the detection of microRNA expression was performed using TaqMan miRNA probes (Applied BioSystems) that can discriminate mature from immature miRNAs and do not bind the microRNA gene, no DNA removal step is done in this protocol.

First, 1-2 x 10^6 cells were washed twice with 1X PBS and the pellet was disrupted by addition of 1 mL of TRIzol reagent (Invitrogen) and 5 minutes incubation at room temperature. TRIzol is a mono-phasic solution of phenol and guanidine isothiocyanate that maintains the integrity of the RNA, while disrupting cells and dissolving cell components. Then, 200 µL of chloroform were added, mixed and the sample was centrifuged at 1,200 rpm for 15 minutes at 4º C. Aqueous phase was recovered and the same volume of isopropanol is added to precipitate the RNA. The sample is then centrifuged and washed with 70% ethanol.

The pellet is dried and resuspended in 50 µL of RNAse-free water.

2.15.2 TISSUES

2.15.2.1 FROZEN TISSUES

Frozen tissues were cut with a cryostat to get 20-30 slides depending on the size of the frozen piece. The slides were homogenized using a Polytron homogenizer (Capitol scientific, Inc; Austin, TX). The homogenized samples were lysed by addition of 1 mL and the following steps are common to the protocol described in section 2.19.1.2. The RNA extracted by this method was purified again using the protocol described in section 2.19.1.1.

2.15.2.2 FFPE TISSUES

RNA form paraffin embedded tissues is usually not well conserved because the process of fixing the tissue sample and embedding it in paraffin can cause severe degradation of the RNA. The quality of the RNA from paraffin embedded tissues is usually much lower than RNA from frozen tissues. The RNA isolated from FFPE tissues use to be shorter (primarily as fragments of less than 300 bases in length), and the yields are lower than those obtained from the same mass of fresh tissue. However, RNA from FFPE tissues is still suitable for some applications such as RT-PCR. Paraffin blocks were cut in a microtome to get 20-30 sections of 10µm thickness depending on the size of the fixed piece. The sections were desparaffinized by incubating twice with 1 mL of xilol for 10 minutes at 65º C. Then the samples were centrifuged at 10,000 rpm for 10 minutes and sections were washed twice with 1 mL of absolute ethanol for 10 minutes at 65º C. The samples were centrifuged again for 10 minutes at 10,000 rpm and the pellets were left drying at 65º C.

500 µL of lysis buffer (10mM Tris ph8, 0.1 mM EDTA ph8, 2%SDS) and 4 µL of 50 µg/µL of proteinase K were used to lyse the samples and incubated for 16 hours at 65º C with shaking. RNA was purified by addition of 500 µL of phenol:chloroform:isoamyl alcohol (25:24:1) and centrifugation at 10,000 rpm for 10 minutes in a microfuge. The aqueous phase was collected, 500 µL of chloroform:isoamyl alcohol were added and the sample was centrifuged again at 10,000 rpm for 10 minutes. The aqueous phase was collected and 1 mL of isopropanol plus 1 µL of linear acrylamide were added to precipitate the RNA. The sample was stored at -20º C overnight and then centrifuged for 30 minutes at 4º C. The supernatant was discarded and the pellet was washed with 70% ethanol. The pellet was dried and resuspended in 30-50 µL of RNAse-free water.

2.16 RETROTRANSCRIPTION

2.16.1 mRNA

cDNA synthesis from RNA was performed using the SuperScript II Reverse Transcriptase enzyme (Invitrogen), following the instructions provided by the manufacturer. Briefly, 500 ng of RNA were mixed with 50 ng of random hexamers, 1 µL of 10 mM dNTPs mix and water was added to a final volume of 12 µL. Then, after a 5-minutes denaturation step at 65º C the following components were added: 4 µl of 5X first strand buffer, 2 µL of 0.1 M DTT and 1 µL of ribonuclease inhibitor (RNAsin) at 40 U/µL and the mixture was incubated for 2 minutes at 25º C prior to adding 1 µL of 200 U/µL SuperScript retrotranscriptase. The samples were then put in a thermocycler with the following program:

Temperature	**Time**
25º C	10 minutes
42º C	50 minutes
70º C	15 minutes
4º C	∞

2.16.2 MicroRNA

cDNA synthesis from miRNAs raises several problems attributable to the structure of the miRNA. First, miRNAs are 22 nucleotides long on average. Thus designing primers with the necessary melting temperature is very difficult. A second problem is that miRNAs are synthesized as primary miRNAs (pri-miRNAs) and processed to precursor miRNAs (pre-miRNAs) through Drosha-mediated cleavage (Lee et al., 2003). After export to the cytosol the pre-miRNA is then processed by Dicer to the mature miRNA (McManus and Sharp, 2002). However the only form that is biologically active is the mature miRNA and to measure its abundance is necessary to discriminate the mature form.

In this work we have used TaqMan microRNA Assays to measure specifically the mature form of the miRNAs. The cDNA synthesis step is carried out with a specific primer for each miRNA. This primer contains a specific sequence that anneals on the miRNA in the 3' end and a general sequence in the 5' end that do not anneal on the miRNA. Instead, this general sequence forms a hairpin impedes the annealing to the immature forms. In the other hand, the primer yields a product much larger than the original miRNA allowing for an easier design of the PCR primers.

The retrotranscription was carried out using the TaqMan® MicroRNA Reverse Transcription Kit (Applied Biosystems). Briefly, 1 µL of 2ng/µL RNA solution was mixed with 0.05 µL of 100 mM dNTPs, 0.33 µL of 50 U/µL MultiScrib Reverse Transcriptase, 0.5 µL of Reverse Transcription Buffer, 0.063 µL of 20 U/µL of RNAse inhibitor and 1 µL of the specific RT primer in a final volume of 5 µL. The samples were put in a thermocycler with the following program:

Program	Time (min)	Temperature
HOLD	30	16º C
HOLD	30	42º C
HOLD	5	85º C
HOLD	∞	4º C

2.17 REAL-TIME QUANTITATIVE PCR

Quantification of RNA expression by RT-PCR was carried out in a similar manner for mRNA and miRNA but the volumes of each reagent differ slightly. For mRNA, 2 µL of cDNA (0.66 µL for miRNAs) were mixed with 7.5 µL (5 µL for miRNAs) of 2X Universal Master Mix (Applied Biosystems) and 0.75 µL (0.5 µL for miRNAs) of the specific 20X TaqMan Assay (Applied Biosystem) in a final volume of 15 µL (10 µL for miRNAs). The PCR cycling conditions were standard: 95º C for 10 minutes (one step), 95º C for 15

seconds, and 60º C for 1 minute (40 cycles). The relative changes in gene expression were calculated by the ΔΔCt method using the Sequence Detection System (SDS) 2.1 software (Applied Biosystems). The ΔΔCt method gives the amount of target normalized to an endogenous reference and relative to a calibrator. The expression of each of the genes in all specimens was related to its expression in a reference RNA pool (Stratagene) used as a calibrator. The level of each transcript was quantified by the cycle at which the PCR amplification was in log phase where there was significant fluorescent signal (Ct) with HGUSB as the endogenous control (RNU19, RNU44 and RNU48 for miRNAs). All standards and samples were run in triplicate.

2.18 GENE EXPRESSION MICROARRAYS

Gene expression microarrays are powerful techniques, which allow the analysis of the expression of thousands of genes simultaneously. The past decade has witnessed a revolution in the field of expression profiling in cancer. Microarray technology has changed both the view of cancer and how research in molecular oncology can be conducted (Raetz and Moos, 2004). In this work the Whole Human Genome Microarray Kit (1x44K, Agilent Technologies) was used.

2.18.1 cDNA SYNTHESIS FROM TOTAL RNA

2µg of total RNA were mixed with 2µl of a 5,000-fold dilution of Agilent's Two-Color Spike-in RNA control and amplified using Agilent Low RNA Input Fluorescent Amplification Kit (Agilent Technologies, Inc., Santa Clara, CA). The mixture in a final volume of 6.5µl (total concentration at least 5ng/µl) was mixed with 5µl of T7 promoter primer. The primer and the template were denatured by incubating the reaction at 65º C for 10min and placing on ice for 5min. Following, 8.5µl of cDNA Master Mix was added and the samples were incubated first at 40OC in a circulating water bath for 2h and then at 65º C in a heating block for 15min to inactivate MMLV-RT. Following that time, the samples were incubated on ice for 5min.

cDNA Master Mix composition: 4µl of 5X First strand buffer, 0.1M DTT 2µl, 10mM dNTP mix 1µl, 1µl of MMLV-RT and 0.5µl of RNaseOUT.

2.18.2 FLUORESCENT cRNA SYNTHESIS: IN VITRO TRASNSCRIPTION AND INCORPORATION OF FLUOROCHROMES

To each sample tube, either 2.4µl of 10mM cyanine 3-CTP (sample) or 2.4µl of 10mM cyanine 5-CTP (Stratagene Universal Human Reference RNA) was added and mixed. Following, to each sample, 57.6µl

of Transcription Master Mix was added an incubated in a circulated water bath at 40º C for 2h. Following amplification and labeling, each sample was assessed on the Nanodrop ND-1000 to measure yield and specific activity.

Transcription Master Mix composition: 15.3µl of Nuclease-free water, 20µl of 4X Transcription buffer, 0.1M DTT 6µl, 8µl of NTP mix, 50% PEG 6.4µl, 0.5µl of RNase OUT, 0.6µl of Inorganic pyrophosphatase and 0.8µl T7 RNA Polymerase.

2.18.3 HYBRIDIZATION

cRNA target was prepared as follows: 0.75µg cyanine 3-labeled, linearly amplified sample cRNA was mixed with 0.75µg cyanine 5-labeled, linearly amplified reference pool cRNA, 50µl of 10X control targets and Nuclease-free water to final volume of 240µl. The hybridization solution was prepared by adding 240µl of 2X target solution to 10µl of 25X fragmentation buffer. The mixture was incubated at 60º C in the heating block for 30min. Following, 250µl of 2X hybridization buffer (from In situ Hybridization kit) to the final volume of 500µl, mixed, spinned and 490µl of the hybridization solution was applied to 60-mer Agilent 44K (or 4X 44K) Human Whole Genome oligonucleotide microarrays and assembled in microarray hybridization chamber (G2534A).

Once fully assembled, the chambers were loaded into the hybridization rotator rack and set to rotate at 4rpm. The hybridization was performed in a rotating oven at 60º C for 17h. All the washing steps were performed at room temperature. First the sandwiched slides were submerged in Wash Solution 1 to remove oligo microarray slide. The slides were washed for 1min in the Wash Solution 1 with the magnetic stir. The slides were then transferred to the staining dish containing Wash Solution 2 and washed for 1min. Following, the slides were transferred to the staining dish containing the Wash Solution 3 and washed for 30 seconds. All steps were performed in the dark. The dried slides were scanned with a G2565BA Microarray Scanner System (Agilent Technologies, Palo Alto, CA).

Wash solution 1 composition: 6X SSPE, 0.005% N-Lauroylsarcosine, deionized nuclease free water.

Wash solution 2 composition: 0.06X SSPE, 0.005% N-Lauroylsarcosine, deionized nuclease free water.

The buffers 1 and 2 are passed through a 0.2µm sterile filtration unit before use.

Wash solution 3 composition: The Agilent Stabilization and Drying Solution contains an ozone scavenging compound dissolved in acetonitrile.

2.19 MicroRNA EXPRESSION MICROARRAYS

2.19.1 LABELING

100 ng of total RNA were hybridized onto an Agilent 8x15K Human microRNA Microarray Kit for the detection of 470 human and 64 viral microRNAs, following the manufacturer's instructions (Agilent Technologies). Briefly, this procedure consisted of a RNA dephosphorylation step where the mixture of 100 ng RNA, 10X CIP Buffer and CIP (16 U/µl) was incubated at 37º C for 30min. Following, a denaturation step was performed through addition of DMSO to samples carried out at 100º C for 5min. Samples were then treated with T4 ligase (15 U/µl) and labeled with Cy3 at 16º C for 2 hours. The reaction was performed in a total volume of 20 µl. Subsequently, RNA was purified with Bio-spin 6 columns (BioRad, Hercules, CA) and dried in a speed vacuum (45º C, 45 minutes).

Ligation master mix composition: 10X T4 ligase Buffer 2 µl, 0.1% BSA 2 µl, pCp-Cy3 3 µl and T4 ligase diluted (15 U/µl) 1 µl.

2.19.2 HYBRIDIZATION

Labeled RNA was resuspended in the appropriate volume of hybridization mix (H_2O 18 µl, blocking agent 4.5 µl and hybridization buffer 22.5 µl) to a final volume of 45 µl and incubated at 100º C for 5 minutes, quickly cooled and pipetted into the 8X gasket, closed with the Agilent 8x15K Human miRNA platform, and locked with the appropriate support. Hybridization was carried out at 55º C for 20 hours at 20 rpm. After that time the slides were washed first with WB1 buffer and then with WB2 buffer. Both washing steps were performed at 37º C for 7 minutes each, with shaking. Finally, the array was submerged in acetonitrile for 1 minute and dried. The arrays were scanned for Cy3 fluorescence with a G2565BA Microarray Scanner System (Agilent Technologies, Palo Alto, CA).

2.20 BIOINFORMATIC TOOLS

2.20.1 MICROARRAY DATA ANALYSIS

2.20.1.1 GENE EXPRESSION MICROARRAYS

The data were processed and normalized with the use of Feature Extraction (v.9.5.3.1) software (Agilent technologies). The data were subsequently combined and filtered for saturated and non-uniformly stained flags using the combine program (http://combine.bioinfo.cnio.es/). Filtered data were analyzed with the T-Rex program included in the Gene Expression Pattern Analysis Suite (http://www.gepas.org/) (Montaner et al., 2006) calculating the Pearson correlation between identified SUZ12-target genes and SUZ12 expression.

2.20.1.2 MICRORNA EXPRESSION MICROARRAYS

Data from miRNA microarrays were extracted using Feature Extraction (v. 9.5.3.1) software (Agilent technologies). Following, the average values of the replicate spots of each miRNA were background subtracted, normalized, and subjected to further analysis. MicroRNA was normalized using Loess within array normalization and quantile between-array normalization. MicroRNAs were retained when present in at least 30% of samples, (meaning the miRNAs were measured as present in at least the smallest group in the dataset) and when at least 30% of the miRNA had fold change of more than 1.5 from the gene median. Following the data was analyzed using the bioinformatics tools included in the Gene Expression Pattern Analysis Suite (http://www.gepas.org/) (Montaner et al., 2006). T-test statistic was calculated with the T-Rex program included in the aforementioned package.

2.20.2 GENE SET ENRICHMENT ANALYSIS

The Gene Set Enrichment Analysis (GSEA) tool (http://www.broad.mit.edu/gsea/) (Subramanian et al., 2005) was used to explore functional gene sets, allowing the interpretation of complete gene-expression data in relation to SUZ12 expression. The gene sets coregulated with SUZ12 expression were identified using Pearson correlation, with a minimum of 10 and a maximum of 500 genes in a gene set being required to qualify them for further analysis. The selected gene sets corresponded to Biocarta pathways (http://www.biocarta.com/), excluding those that were not relevant to either lymphoid cell biology or cancer. Gene sets with an FDR less than 0.25 were considered significant.

2.20.3 INGENUITY PATHWAYS

We identified Functions/Pathways classification terms enriched for SUZ12-bound genes using Ingenuity Pathways Analysis (http://www.ingenuity.com). The probability associated with a biological process is a measure of its statistical significance with respect to the Functions/Pathways/Lists Eligible molecules for the dataset and a Reference Set of molecules that defines the molecules that could possibly have been Functions/Pathways/Lists Eligible. The probability is that associated with a right-tailed Fisher's exact test

2.21 TOTAL PROTEIN EXTRACTION

Total protein extraction was performed by lysis with RIPA buffer (150mM NaCl, 1.0% IGEPAL® CA-630, 0.5% sodium deoxycholate, 0.1% SDS, and 50mM Tris, pH 8.0; Sigma-Aldrich) supplemented with Complete Protease Inhibitor Cocktail (Roche, Basel, Switzerland). Briefly, 10^6 cells were lysed by addition of 50 µL of RIPA with cocktail inhibitor for 20 minutes on ice. Cell debris was removed by 4º C centrifugation at top speed for 30 minutes in a microfuge. Proteins were quantified using the A, B and C reagents of the BioRad protein assay (BioRad, Hercules, CA) following the manufacturer's instructions and using bovine seroalbumin (BSA) as a standard. Briefly, 1ml of Agent A was mixed with 20µl of Agent S. First, the adequate amount of either standard (BSA) or sample was applied to each well of 96-well plate, following 25µl of previously prepared mixture was added. Finally, 200µl of Agent B was added and the whole preparation was incubated for 15min at RT and measured at a wavelength of 750nm.

2.22 HISTONE EXTRACTION

Histones were isolated by acidic extraction in 0.25 M HCl and precipitation with acetone. Briefly, 10^6 cells were harvested and incubated overnight in 200 µl of 0.25 M HCl at 4ºC with shaking. For histone precipitation, eight volumes of acetone were added to the supernatant, and histones were pelleted by centrifugation and washed with acetone. Histones were air-dried and resuspended in 0.25 M HCl for subsequent immunoblot analysis.

2.23 WESTERN BLOTTING

The list of antibodies used for Western blot can be found in table 2.7. For Western blot, 15-40 µg of protein were subjected to electrophoresis on sodium dodecyl sulfate polyacrylamide (SDS-PAGE) gels using the acrylamide concentration adequate for the size of the detected proteins (15% for histones, 12% for PARP, 10% for SUZ12 and BCL6) using Mini-Protean 3 system (BioRad).

Electrophoresis buffer 5X composition: TrisHCl 0.13M, glycine 0.95M, SDS 0.5%.

Sample buffer (Laemmli buffer) 4X composition: 62.5mM TrisHCl pH 6.8, glycerol 20%, SDS 2%, 2-mercaptoethanol 5%, bromophenol blue 0.025%.

After the electrophoresis, the proteins were transferred to a nitrocellulose membrane (Hybond ECL; Amersham) using the Mini Trans-blot Cell system (BioRad). Transference conditions were 40 mA for 16 hours at room temperature or 400 mA for 1.5 hours at 4º C.

Transference buffer 10X composition: TrisHCl 0.025M, glycine 0.2M, 20% of methanol

Membranes were blocked in PBS-T (phosphate-buffered saline with 0.1% Tween-20) for 1 hour with continuous shaking and sequentially immunoprobed with primary antibodies at adequate dilution. Antibody detection was carried out using fluorescent-labeled secondary antibodies (Alexa 680 and Alexa 800, Rockland, Gilbertsville, PA, USA) and an Odyssey Infrared System Scanner (LI-COR Biosciences, Lincoln, NE, USA). Band intensities were quantified using the ImageJ 1.34S software (National Institute of Health, Bethesda, MD, USA).

2.24 ANALYSIS OF THE PRESENCE OF THE EPSTEIN-BARR VIRUS (EBV)

2.24.1 ANALYSIS BY PCR

Analysis of the presence of the EBV genome in cell lines was carried out by standard PCR using 1 unit of EcoStart Taq polymerase (Ecogen, Truro, England) and 100 ng of DNA in a reaction volume of 25 µL as described in section 2.8. The PCR conditions are the followings:

Temperature	**Time**	**Step**	
95º C	5 minutes	Denaturation	
94º C	30 seconds	Denaturation	30 cycles
55º C	30 seconds	Annealing	
72º C	30 seconds	Extension	
72º C	10 minutes	Final extension	

The primer sequences are described below and gave an amplicon of 122 bp. The PCR products were analyzed by electrophoresis in a 2% agarose gel.

Primer sequences (5' → 3'):

EBV1: CCA GAG GTA AGT GGA CTT TA

EBV2: GAC CGG TGC CTT CTT AGG AG

2.24.2 ANALYSIS BY IN SITU HYBRIDIZATION (ISH)

EBV detection in FFPE tissue sections was carried out by the Histology and Immunohistochemistry Core Unit at the Spanish National Cancer Research Center (CNIO). EBV was detected by ISH using an Epstein Barr Virus encoded RNA (EBER) specific probe (Bond ISH EBER Probe; Vision BioSystem, Wetzlar, Germany). The probe was hybridized in a Bond-maX autostainer (Vision BioSystem), an automated IHC staining system.

2.25 FLUORESCENCE *IN SITU* HYBRIDIZATION (FISH)

FISH was performed by the Molecular Cytogenetics Group at the CNIO. The technique was used to detect SUZ12 copy-number changes in malignant samples. To study SUZ12 amplification we used the Bacterial Artificial Chromosome clones RP11-290N17 and RP11-640N20 from the BACPAC resources center (Children's Hospital Oakland Research Institute, Oakland, CA), which spans the entire 17q11.2 genomic region, and a commercial centromeric probe for chromosome 17 (Vysis Inc., Downers Grove, IL), which was used as a control for the ploidy level of chromosome 17.

The probes were labeled using the Nick Translation kit (Abbot Inc., Abbott Park, IL) following the protocol provided by the manufacturer and purified with the QIAquick PCR Purification kit (Qiagen) as indicated by the manufacturer's instructions. The probes were hybridized on FFPE tissue slides that were previously desparaffinized as follows:

First, slides were incubated overnight at 65º C. Then the slides were treated with xilol for 10 minutes (twice at 65º C in the oven), ethanol 100% for 5 minutes (twice), ethanol 80% for 5 minutes and ethanol 70% for 5 minutes and kept in distilled water. After this, the samples were boiled in pre-warmed EDTA 0,5mM pH 8 for 6-10 minutes and the slides were washed with 1X PBS. The last step is digestion with 40 µL of pepsin for 30 minutes at 37º C. The reaction was stopped by putting the slides in STOP solution (1X PBS, 50 mM Mg_2Cl). Slides were washed with water and dehydrated by progressively

increasing the ethanol concentration in the washing solution (70% ethanol, 80% ethanol, 100% ethanol; 3 minutes each).

The protocol for hybridization is summarized here. A hybridization mix was prepared with the following components: 1 µL of the probe, 2 µL of sterile water and 7 µL of the proper buffer. In the case of SUZ12 probe Vysis LSI (Abbot Inc.) was used and Vysis CEP (Abbot Inc.) for the centromeric probe. This mix was heated at 96º C for 5 minutes and 10 µL of it were put in each slide and incubated overnight at 37º C. The following day, the slides were washed with 0.4X SSC, 0.3% NP-40 for 2 minutes at 75º C and later on with 2X SSC, 0.1% NP-40 for 5 minutes under agitation. A last wash with phosphate buffered detergent (PBD) at room temperature was performed. Chromosomes were revealed by addition of 10 µL of 4',6-diamidino-2-phenylindole (DAPI).

Fluorescence signals were scored in each sample by counting the number of single-copy gene and centromeric signals in an average of 130 (60–210) well-defined nuclei. SUZ12 amplification was recognized if the SUZ12/chromosome 17 ratio was greater than 2 in at least 20% of tumor cells. A sample was considered to feature a SUZ12 gene gain if the SUZ12/chromosome 17 ratio was greater than 1.5 but less than 2 (Sholl et al., 2007; Singh et al., 2002).

3. RESULTS

RESULTS I

Deregulated expression of the Polycomb-group protein SUZ12 target genes characterizes Mantle Cell Lymphoma

Cancer is the result of a series of genetic and epigenetic alterations that lead to the uncontrolled proliferation of malignant cells. Polycomb proteins are known to be of great importance in different tumors. SUZ12, a component of the PRC2 complex, is essential for the H3K27me trimethylation mark that is catalized by EHZ2 and both are involved in embryonic stem cell differentiation. In spite of the discovery that EZH2 plays an oncogenic role in several tumors a similar causative role has not been demonstrated for SUZ12. Using tissue microarray in a large cohort of normal and tumor samples it has been found that EZH2 and SUZ12 are not expressed at the same time in many tumors and normal tissues. Whereas EZH2 seemed to be almost ubiquitously expressed, SUZ12 showed a much more limited pattern of expression restricted mainly to proliferating cells in normal tissues such as germinal centers in lymph nodes and cycling epithelial cells. Changes in expression associated with tumoral transformation were found for SUZ12, which exhibited increased expression in different types of tumors including mantle cell lymphomas. Moreover, amplification of the SUZ12 locus was found in some cases. Using MCL cell lines as a model, functional and genomic studies were performed. Knock down of SUZ12 by shRNA demonstrated that SUZ12 loss compromises cell viability and increases apoptosis. By chIP-on-chip it was found that SUZ12 targets genes that are essential in the pathogenesis of MCL, including ATM, CDKN2A, CHEK1, BCL10 and RB. A high number of SUZ12 target genes were involved in cell cycle and proliferation, DNA replication and repair, development, cell death and control of gene expression. This results support the hypothesis that the abnormal expression of SUZ12 accounts for some of the unexplained features of MCL, such as abnormal DNA repair and increased resistance to apoptosis.

3.1 SUZ12 AND EZH2 PROTEIN EXPRESSION IN NORMAL HUMAN TISSUES

Taking into account the fundamental role of the PcG repressing complexes in cancer and the fact that the relevance as well as the function of the PRC2 member SUZ12 in cancer has not yet been clarified, we decided to investigate the potential role of SUZ12 in human tumors.

With the aim of exploring a possible abnormal expression pattern of SUZ12 in human tumors, we first characterized the expression of this protein in normal tissues. As first step, in collaboration with the Monoclonal Antibodies Core Unit of the CNIO, we generated a monoclonal antibody (mAb) against SUZ12 (clone 220A/A3; described in the section 2.3.1) that was used in subsequent experiments. To confirm that 220A/A3 mAb recognized de human SUZ12 protein, immunohistochemistry on frozen cytospin preparations of V5-tagged human SUZ12 expressed in HEK-293T cells was performed. Labeling with the anti-V5 mAb confirmed the efficiency of transfection. A Cytospin preparation of V5-tagged human SOX4 protein was used as a negative control (Figure 3.1).The immunohistochemical results were confirmed by western blot using cell lysate of SUZ12 and SOX4-transfected cells. The specificity of the mAb generated was also demonstrated in the shRNA experiments described below using several shRNAs designed against the coding sequence of SUZ12 transcripts and comparing with an unrelated scramble control sequence. The antibody was found to be suitable for immunohistochemistry, immunofluorescence (data not shown), western blot detection, and chromatin immunoprecipitation.

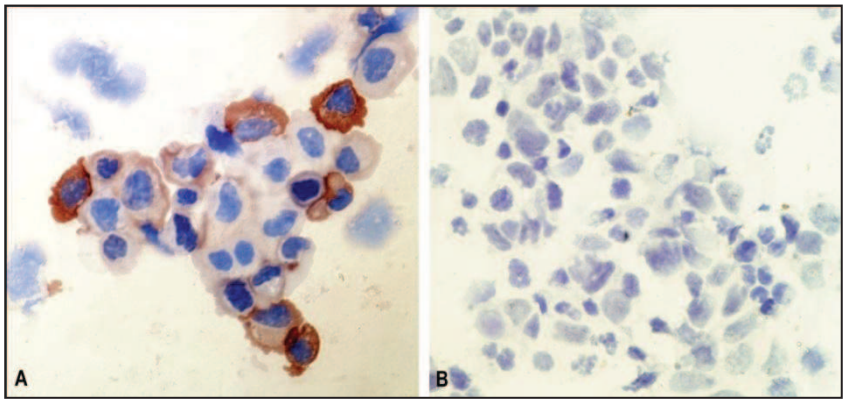

Figure 3.1. SUZ12 220A/A3 antibody validation in cytospin slides of transfected HEK-293T cells. (A) The transfected HEK-293T cell line with SUZ12-cDNA showed specific staining with SUZ12 220A mAB. (B) However, the same cell line transfected with SOX4–cDNA was negative with SUZ12 220A mAB.

This antibody was used in a TMA that contained around 50 different normal tissues (154 samples) as described previously (Sanchez-Beato et al., 2006). Since EZH2 is the molecular partner of SUZ12 that carries the enzymatic activity, we decided to characterize the expression of EZH2 as well. Strikingly, EZH2 expression was detected in a large proportion of tissues with very few exceptions, while SUZ12 was detected in a more limited number of samples and usually in proliferating cells such as centroblasts in reactive lymphoid tissue, germinal cells in the testis, and the epithelium of various organs (Figure 3.2 & 3.3; Table 3.1).

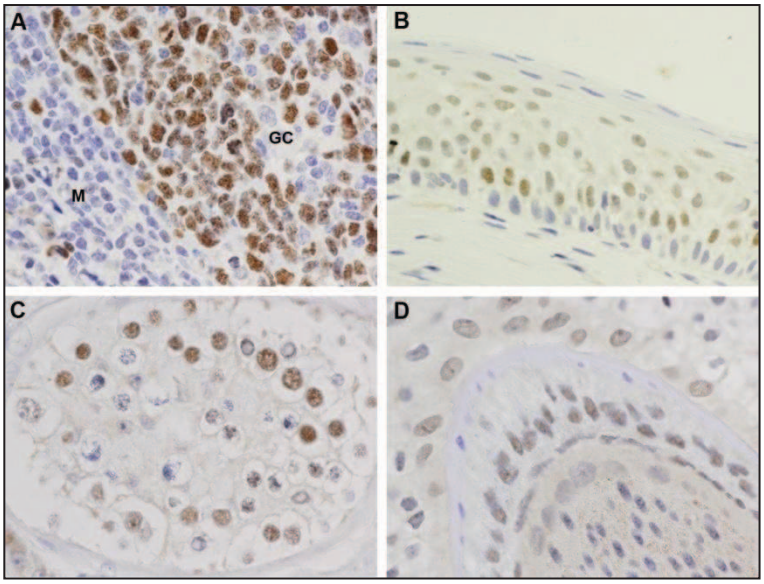

Figure 3.2. Expression of SUZ12 in non-tumoral human tissues. SUZ12 protein is preferentially detected in proliferating cells of various non-tumoral human tissues such as proliferating cells of tonsil's germinal center (A), proliferating cells of tonsil's squamous epithelium (B), germinal cells of the testis (C), and hair follicle (D). (Objective 100x, immersion). (M: Mantle Zone; GC: Germinal Center)

3.2 SUZ12 AND EZH2 PROTEIN EXPRESSION IN HUMAN TUMORS

At the same time, we also studied the expression of these two proteins in TMAs containing representative paraffin sections from 569 cases of different human tumors encompassing up to 69 different tumor types (Sanchez-Beato et al., 2006). Similar to normal tissues, the pattern of expression was different in human tumors for both proteins and we found no significant association between them. EZH2 was again more ubiquitously expressed in most tumors (489 out of 521 -94%- were positive) although with different intensities, however SUZ12 expression was mainly detected in tumors arising from lymphoid, lung, vascular, germinal and skin tissues (250 out of 497 -50.3%- had detectable expression). In summary, SUZ12-positive cases used to

be also EZH2-positive but not vice versa. A small fraction of the tumors (16/497, 3.2%) showed expression of SUZ12 but not EZH2 suggesting that SUZ12 can have additional EZH2-independent functions (Figure 3.3 & 3.4; table 3.2).

SUZ12 was detected mainly in lymphomas (91%) (especially in MCL), germinal cell-derived tumors (70%) (seminomas, teratocarcinomas, and embryonic carcinomas), skin tumors (88%) (melanomas and skin carcinomas), vascular tumors (83%) and pulmonary neuroendocrine small-cell carcinomas (70%) (Figure 3.3; Table 3.2). Most of these tumors are characterized by the presence of a high growth fraction.

Table 3.1. SUZ12, EZH2 and Ki67 expression in non-tumoral human tissues. 0: Negative expression. 1: positive expression. 1*: isolated cells. - 1: No data.

	ORGAN	CELL TYPE	SUZ12	EZH2	Ki67
CENTRAL NERVOUS SYSTEM	Cerebral cortex	neurons	0	1	0
		glia	0	1	0
		molecular layer	0	1	0
		Purkinje cells	0	1	0
		granular layer	0	1	0
	Basal nuclei	neurons	0	1	0
		glia	0	1	0
	Brain stem	neurons	0	1	0
		glia	0	1	0
	Choroid plexus		0	1	0
DIGESTIVE TRACT	Esophageal mucose	basal	0	1	-1
		superficial	0	1	-1
	Gastric mucose	glands	0	1	1
		crypts	0	1	0
	Small intestine-mucose	glands	0	1	1
		villi	0	1	0
	Large intestine-mucose	crypts	0	1	1
		surface epithelium	0	1	0
	Parotid	glands	0	1	0
		ducts	0	1	0
	Liver	hepatocytes	0	-1	0
		bile duct	0	1	0
	Pancreas	acini	0	1	1
		duct	0	1	0
		Langerhans islets	0	1	0
	Gallbladder	glands	0	1	1
		surface epithelium	0	1	0
RESP. TRACT	Larynx	basal	0	1	1
		superficial	1	0	0
	Lung-pleura & bronchi	bronchi	-1	-1	-1
		pneumocytes	0	1	0
ENDOCRINE SYSTEM	Pituitary gland	adenohypophisis	0	1	0
		neurohypophisis	-1	-1	0
	Thyroid gland	follicles	0	1	1
	Parathyroid gland	chief cells	0	1	1

		cortex	0	1	0
		medulla	0	1	0
SKIN & SOFT TISSUES	Skin	basal	1	1	1
		spinous	1	1	0
		hair follicle	1	1	1
	Adipose tissue	adipocytes	0	1	0
	Striated muscle		0	1	0
LYMPHOID TISSUE	Spleen	red pulp	0	1	0
		germinal center cells	1	1	1
		marginal cells	0	1*	1
	Thymus	epithelial cells	1*	1	0
		lymphocytes	1	1*	1
	Tonsil & Lymph node	interfollicular cells	1*	1	1
		germinal center cells	1	1	1
		mantle cells	0	1*	1
BREAST	Breast	ducts	0	1	0
		acini	0	-1	0
		stroma	0	1*	0
GINECOLOGICAL TISSUES	Ovary	follicles	-1	1	-1
		stroma	0	1	0
	Fallopian tubes		0	1	0
	Myometrium		0	1	0
	Proliferative endometrium	glands	0	1	1
		stroma	0	1	1
	Secretor edometrium	glands	0	1	1
		stroma	0	1	1
	Endocervix		0	1	-1
	Exocervix	basal	0	1	1
		superficial	1	0	0
	Placenta	syncytiotrophoblast	0	1	0
		cytotrophoblast	1	1	1
	Umbilical cord	stroma	0	1*	-1
URINARY TRACT	Kidney	glomerulus	0	0	0
		tubule	0	1	0
	Bladder	urothelium	0	1	-1
	Prostate	glands	0	1	0
		stroma	0	1	0
MALE & REPRODUCTIVE SYSTEM	Testis	germinal cells	1	1	1
		Sertoli cells	0	1	1
		Leydig cells	0	1*	0
	Epididymis	ducts	0	1	0
	Seminal vesicles	epithelium	0	1	0
	Endothelium	endotehlial cells	0	1	1

3.3 COPY NUMBER CHANGES AT THE SUZ12 LOCUS

SUZ12 gene has been described to suffer several cytogenetic abnormalities in some tumors such as recurrent translocations in endometrial stromal tumors (Koontz et al., 2001a) and a wide spectrum of cytogenetic abnormalities in other tumors (Douglas et al., 2004; Espinet et

al., 1999; Kraggerud et al., 2002; Onciu et al., 2001; Starczynowski et al., 2008). Therefore, we thought that amplification of the gene locus might be a mechanism that could explain the high level of expression of SUZ12 and we decided to study the copy number of the chromosomal region containing the *SUZ12* gene in our series of tumors.

To study copy number variations at the *SUZ12* locus we performed FISH analysis in TMA paraffin sections, in collaboration with the Molecular Cytogenetics Group of the CNIO. The TMAs were the same as used for the immunohistochemical analysis. We used standard criteria for definition of amplification (ratio *SUZ12*/centromeric 17 > 2.0), copy gains (2>ratio *SUZ12*/centromeric 17 > 1.5) and trisomies (Sholl et al., 2007; Singh et al., 2002).

We found five cases with amplification of *SUZ12*, and two cases with copy gains. These chromosomal aberrations affected several tumor types: mesothelioma (amplification in 1/10), melanoma (amplification in 1/10), skin basal cell carcinoma (gain in 1/10), thyroid follicular carcinoma (amplification in 1/8), leiomyosarcoma (gain in 1/6), MCL (amplification in 1/10) and ovary serous cystoadenocarcinoma (amplification in 1/6). The results are summarized in table 3.2.

SUZ12 protein expression in MCL was positive in 9 out of 10 samples while it was not detected in non-malignant mantle zone cells. This result together with the finding of one case with amplification of the *SUZ12* locus that was associated to strong SUZ12 protein expression prompted us to extend the study to a larger cohort of cases for further validation.

Additionally, SUZ12 expression was detected in lymphomas that derive from germinal center B-cells with a high growth fraction (BL and DLBCL), or was restricted to proliferating cells in chronic lymphocytic leukemia, follicular lymphoma and splenic marginal zone lymphoma cases (Figure 3.3 & 3.4) while MCL is a tumor characterized by lower or intermediate proliferation, and their normal cell counterparts, mantle zone cells, show undetectable levels of SUZ12 protein expression.

3.4 SUZ12 IN MANTLE CELL LYMPHOMAS

Therefore, we extended our previous observations and checked SUZ12 protein expression and gene locus alterations in an additional TMA containing 76 MCL cases. In total, 46 out of 81 (56%) MCL cases (10 in the general multitumor TMA and 71 new evaluable cases in MCL-specific TMA) showed SUZ12 protein expression (Table 3.3).

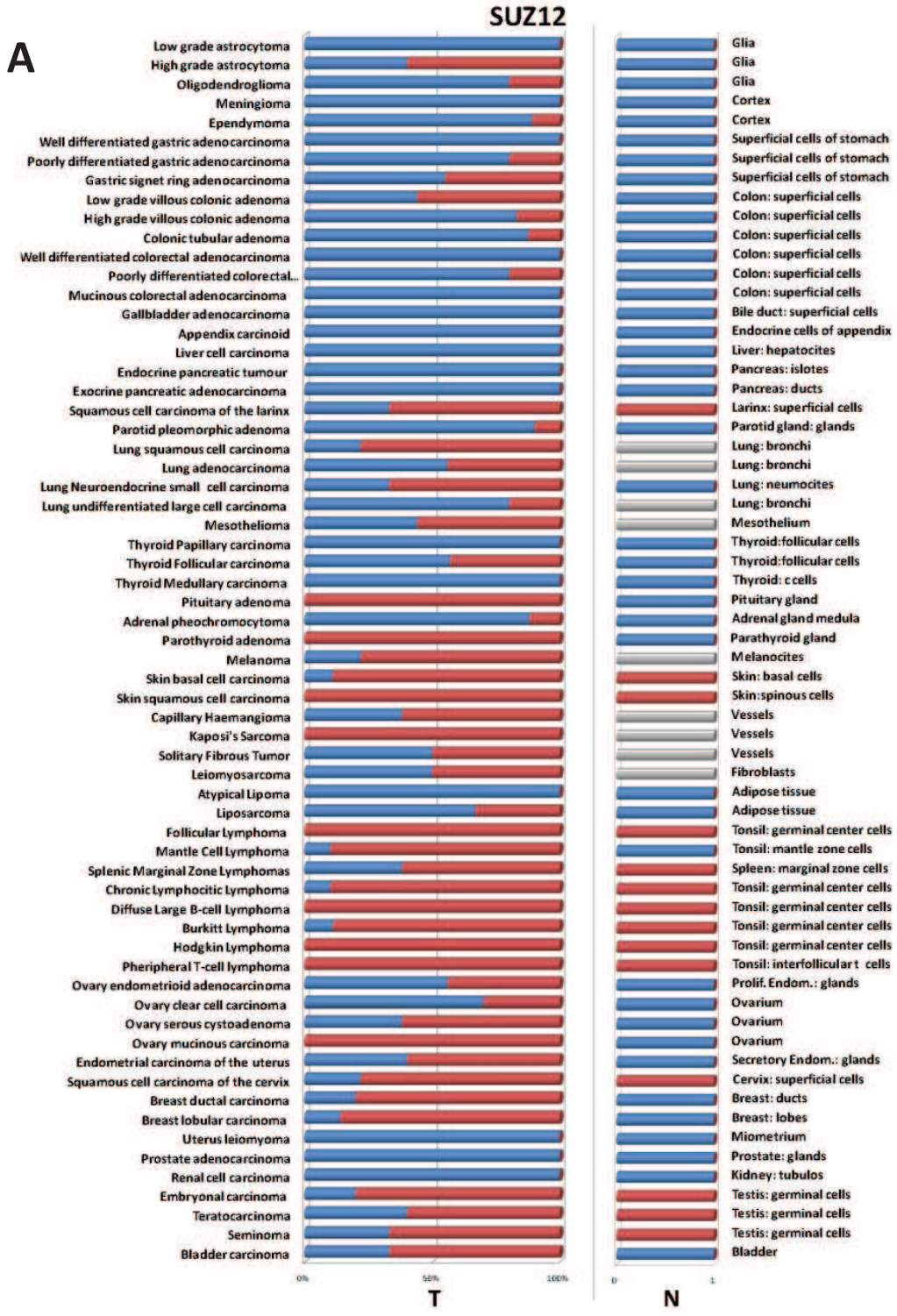
A
SUZ12
Low grade astrocytoma
High grade astrocytoma
Oligodendroglioma
Meningioma
Ependymoma
Well differentiated gastric adenocarcinoma
Poorly differentiated gastric adenocarcinoma
Gastric signet ring adenocarcinoma
Low grade villous colonic adenoma
High grade villous colonic adenoma
Colonic tubular adenoma
Well differentiated colorectal adenocarcinoma
Poorly differentiated colorectal...
Mucinous colorectal adenocarcinoma
Gallbladder adenocarcinoma
Appendix carcinoid
Liver cell carcinoma
Endocrine pancreatic tumour
Exocrine pancreatic adenocarcinoma
Squamous cell carcinoma of the larinx
Parotid pleomorphic adenoma
Lung squamous cell carcinoma
Lung adenocarcinoma
Lung Neuroendocrine small cell carcinoma
Lung undifferentiated large cell carcinoma
Mesothelioma
Thyroid Papillary carcinoma
Thyroid Follicular carcinoma
Thyroid Medullary carcinoma
Pituitary adenoma
Adrenal pheochromocytoma
Parothyroid adenoma
Melanoma
Skin basal cell carcinoma
Skin squamous cell carcinoma
Capillary Haemangioma
Kaposi's Sarcoma
Solitary Fibrous Tumor
Leiomyosarcoma
Atypical Lipoma
Liposarcoma
Follicular Lymphoma
Mantle Cell Lymphoma
Splenic Marginal Zone Lymphomas
Chronic Lymphocitic Lymphoma
Diffuse Large B-cell Lymphoma
Burkitt Lymphoma
Hodgkin Lymphoma
Pheripheral T-cell lymphoma
Ovary endometrioid adenocarcinoma
Ovary clear cell carcinoma
Ovary serous cystoadenoma
Ovary mucinous carcinoma
Endometrial carcinoma of the uterus
Squamous cell carcinoma of the cervix
Breast ductal carcinoma
Breast lobular carcinoma
Uterus leiomyoma
Prostate adenocarcinoma
Renal cell carcinoma
Embryonal carcinoma
Teratocarcinoma
Seminoma
Bladder carcinoma
0%
50%
100%
T
0
1
N
Glia
Glia
Glia
Cortex
Cortex
Superficial cells of stomach
Superficial cells of stomach
Superficial cells of stomach
Colon: superficial cells
Colon: superficial cells
Colon: superficial cells
Colon: superficial cells
Colon: superficial cells
Colon: superficial cells
Bile duct: superficial cells
Endocrine cells of appendix
Liver: hepatocites
Pancreas: islotes
Pancreas: ducts
Larinx: superficial cells
Parotid gland: glands
Lung: bronchi
Lung: bronchi
Lung: neumocites
Lung: bronchi
Mesothelium
Thyroid:follicular cells
Thyroid:follicular cells
Thyroid: c cells
Pituitary gland
Adrenal gland medula
Parathyroid gland
Melanocites
Skin: basal cells
Skin:spinous cells
Vessels
Vessels
Vessels
Fibroblasts
Adipose tissue
Adipose tissue
Tonsil: germinal center cells
Tonsil: mantle zone cells
Spleen: marginal zone cells
Tonsil: germinal center cells
Tonsil: germinal center cells
Tonsil: germinal center cells
Tonsil: germinal center cells
Tonsil: interfollicular t cells
Prolif. Endom.: glands
Ovarium
Ovarium
Ovarium
Secretory Endom.: glands
Cervix: superficial cells
Breast: ducts
Breast: lobes
Miometrium
Prostate: glands
Kidney: tubulos
Testis: germinal cells
Testis: germinal cells
Testis: germinal cells
Bladder

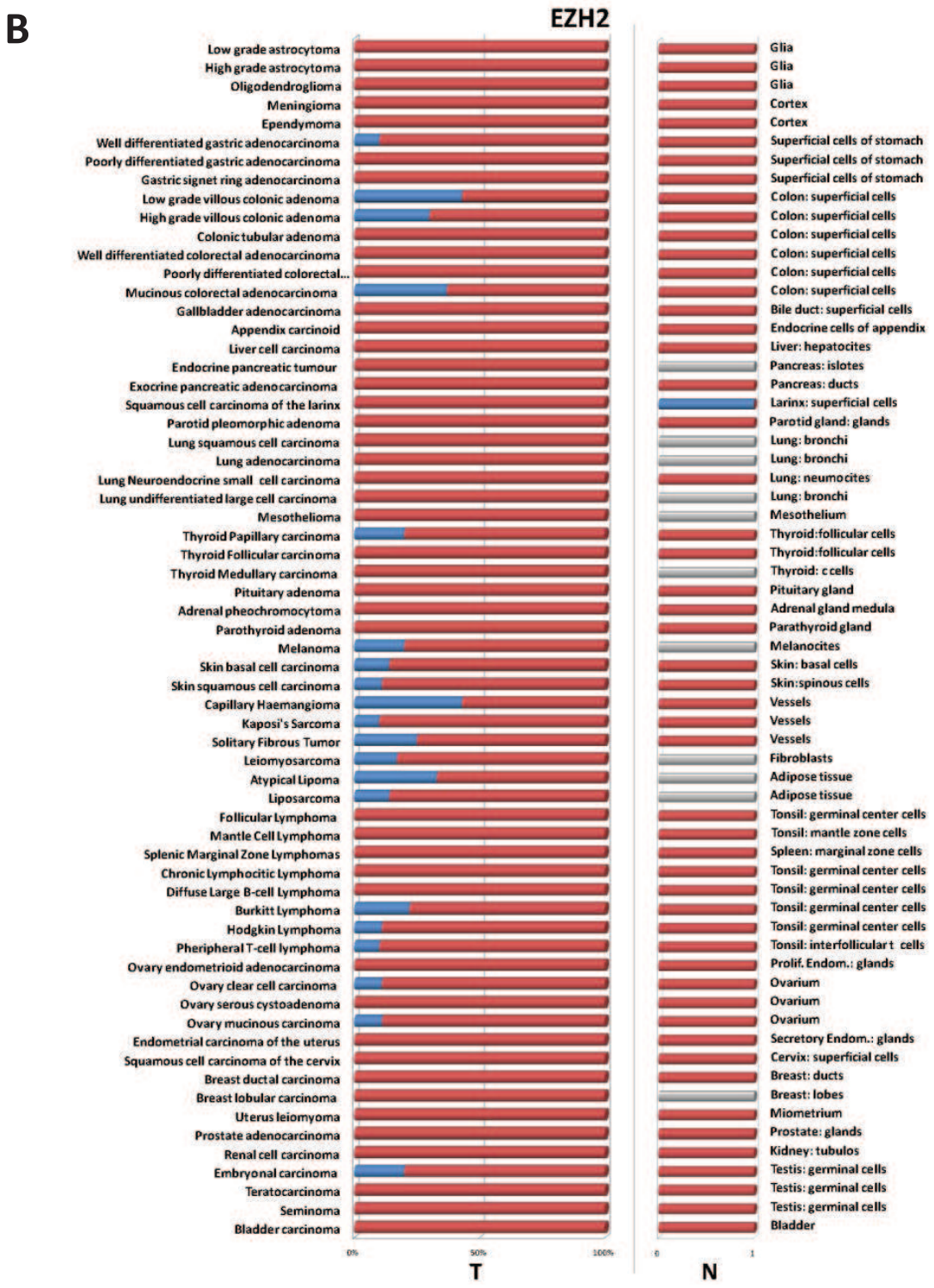

Figure 3.3. Expression of SUZ12 (A) and EZH2 (B) proteins in human tumors (T) and in corresponding normal tissue counterparts (N). Red color represents positive expression; blue indicates absence of expression. In the case of tumors, the length of red/blue bars is proportional to the percentage of positive/negative cases, respectively, for each tumor type. Grey indicates no sample.

For FISH analysis, 67 new samples from the TMA gave evaluable results. In total, three MCL samples (the previous one and two cases in the new TMA) showed gene amplification (Figure 3.4) and four cases had copy gains affecting *SUZ12* locus. Strikingly, the three cases with amplification had more than 80% of SUZ12 positive cells and remarkably, two of them were diagnosed as aggressive (blastoid) variant MCL cases. In summary, around 9% of MCL cases had cytogenetic alterations at the *SUZ12* locus. Additionally polysomy of chromosome 17 was found in twelve MCL samples.

Table 3.2. Summary of SUZ12 and EZH2 expression, and *SUZ12* locus (17q11.2) alterations in human tumors. Values are the number of positive samples for SUZ12 or EZH2 staining.

TUMORAL TYPE	EZH2 EXPRESSION	SUZ12 EXPRESSION	SUZ12 GAINS (AMP+GAIN)	SUZ12 AMPS	SUZ12 GAINS	Chr 17 POLY
CENTRAL NERVOUS SYSTEM	**48/48**	**9/48**	**---**	**---**	**---**	**---**
Ependymoma	9/9	1/9	---	---	---	---
High grade astrocytoma	10/10	6/10	---	---	---	---
Low grade astrocytoma	9/9	0/9	---	---	---	---
Meningioma	10/10	0/10	---	---	---	---
Oligodendroglioma	10/10	2/10	---	---	---	---
GASTROINTESTINAL TRACT	**87/97**	**12/95**	**---**	**---**	**---**	**---**
Gastric signet ring adenocarcinoma	10/10	4/9	---	---	---	---
Poorly differentiated gastric adenocarcinoma	6/6	0/6	---	---	---	---
Well differentiated gastric adenocarcinoma	9/10	0/9	---	---	---	---
Exocrine pancreatic adenocarcinoma	5/5	0/5	---	---	---	---
Endocrine pancreatic tumor	5/5	0/5	---	---	---	---
Appendix carcinoid	3/3	0/3	---	---	---	---
Gallbladder adenocarcinoma	6/6	0/5	---	---	---	---
Colonic tubular adenoma	5/5	1/8	---	---	---	---
Liver cell carcinoma	9/9	0/7	---	---	---	---
Low grade villous colonic adenoma	4/7	5/9	---	---	---	---
High grade villous colonic adenoma	7/10	1/6	---	---	---	---
Poorly differentiated colorectal adenocarcinoma	4/4	1/5	---	---	---	---
Well differentiated colorectal adenocarcinoma	9/9	0/9	---	---	---	---

Mucinous colorectal adenocarcinoma	5/8	0/9	---	---	---	---
RESPIRATORY TRACT	**57/57**	**37/73**	**1/71**	**1**	**0**	**15**
Lung adenocarcinoma	9/9	4/9	0/10	0	0	3
Parotid pleomorphic adenoma	9/9	1/10	0/10	0	0	0
Squamous cell carcinoma of the larinx	10/10	6/9	0/10	0	0	3
Lung squamous cell carcinoma	10/10	7/9	0/10	0	0	2
Lung undifferentiated large cell carcinoma	9/9	2/10	0/10	0	0	4
Lung neuroendocrine small cell carcinoma	5/5	12/17	0/11	0	0	3
Mesothelioma	5/5	5/9	1/10	1	0	0
ENDOCRINE SYSTEM	**52/56**	**31/48**	**1/52**	**1**	**0**	**6**
Parathyroid adenoma	10/10	9/9	0/10	0	0	3
Pituitary adenoma	9/9	9/9	0/10	0	0	2
Thyroid follicular carcinoma	8/8	3/7	1/8	1	0	0
Thyroid medullar carcinoma	8/8	3/8	0/8	0	0	0
Thyroid papillary carcinoma	8/10	2/5	0/10	0	0	1
Adrenal cortex Carcinoma	1/3	1/1	---	---	---	---
Adrenal pheochromocytoma	8/8	1/8	0/6	0	0	0
SKIN & SOFT TISSUE	**45/62**	**45/63**	**3/64**	**1**	**2**	**4**
Capillary haemangioma	4/7	5/8	0/9	0	0	0
Kaposi's sarcoma	9/10	10/10	0/10	0	0	0
Skin squamous cell carcinoma	8/9	8/8	0/9	0	0	2
Skin basal cell carcinoma	6/7	8/9	1/9	0	1	0
Solitary fibrous tumor	3/4	2/4	0/3	0	0	0
Leiomyosarcoma	5/6	3/6	1/6	0	1	1
Atypical lipoma	2/3	0/3	0/2	0	0	0
Liposarcoma	6/7	2/6	0/6	0	0	0
Malignant melanoma	8/10	7/9	1/10	1	0	1
LYMPHOMAS	**131/146**	**100/140**	**7/121**	**3**	**4**	**16**
Follicular lymphoma	9/9	9/9	0/10	0	0	1
Mantle cell lymphoma	70/81	46/81	7/77	3	4	12
Chronic lymphocytic lymphoma	9/9	9/10	---	---	---	---
Splenic marginal zone lymphoma	9/9	5/8	---	---	---	---
Diffuse large B-cell lymphoma	10/10	7/7	0/9	0	0	2
Burkitt lymphoma	7/9	8/9	0/6	0	0	0
Hodgkin lymphoma	8/9	8/8	0/10	0	0	0
Peripheral T-cell lymphoma	9/10	8/8	0/9	0	0	1
GYNECOLOGICAL & BREAST TISSUES	**77/78**	**46/73**	**1/73**	**1**	**0**	**8**
Ovary endometrioid adenocarcinoma	9/9	4/9	0/9	0	0	0
Ovary clear cell carcinoma	8/9	3/10	0/10	0	0	3

Ovary serous cystoadenocarcinoma	10/10	5/8	1/8	1	0	0
Ovary mucinous cystoadenoma	9/9	7/7	0/9	0	0	0
Endometrial carcinoma	10/10	6/10	0/10	0	0	0
Squamous cell carcinoma of the cervix	10/10	7/9	0/10	0	0	4
Breast ductal carcinoma	9/9	8/10	0/8	0	0	1
Breast lobular carcinoma	8/8	6/7	0/5	0	0	0
Uterus leiomyoma	4/4	0/3	0/4	0	0	0
URINARY & MALE REPRODUCTIVE SYSTEM	**45/46**	**19/45**	**0/45**	**0**	**0**	**11**
Prostate adenocarcinoma	9/9	0/8	0/8	0	0	0
Clear cells renal cell carcinoma	9/9	0/9	0/10	0	0	1
Embryonic carcinoma	4/5	4/5	0/5	0	0	2
Seminoma	10/10	6/9	0/10	0	0	4
Teratocarcinoma	3/3	3/5	0/4	0	0	2
Bladder carcinoma	10/10	6/9	0/8	0	0	2

These findings suggest that alterations in SUZ12 leading to the overexpression of the gene product are important in the pathogenesis of MCL. However, the percentage of cytogenetically altered cases does not account for the overexpression of SUZ12 in many MCL cases. In those cases with cytogenetically normal *SUZ12* locus, other mechanisms may be responsible for SUZ12 overexpression.

Table 3.3. SUZ12, EZH2 and Ki67 expression in MCL-specific TMA. NA: not available. 0: negative. 1 and 2: positive expression. AMPL: Amplification; 1N: haploid; 2N: diploid; 3r/2g: gain; Poly; polysomy.

POS TMA	TMA	ORGAN	TUMORAL TYPE	Ki67	EZH2	SUZ12	FISH SUZ12
2	216	lymph node	Mantle Cell Lymphoma	2	1	1	NA
3	216	lymph node	Mantle Cell Lymphoma	2	1	1	NA
5	216	lymph node	Mantle Cell Lymphoma	2	1	1	3R/2G
6	216	lymph node	Mantle Cell Lymphoma	2	1	1	Poly
9	216	lymph node	Mantle Cell Lymphoma	1	1	0	2n
10	216	lymph node	Mantle Cell Lymphoma	0	0	0	NA
11	216	lymph node	Mantle Cell Lymphoma	1	NA	0	NA
12	216	lymph node	Mantle Cell Lymphoma	0	0	NA	2n
13	216	lymph node	Mantle Cell Lymphoma	2	1	1	2n
14	216	lymph node	Mantle Cell Lymphoma_Blastic variant	2	1	1	AMPL
15	216	lymph node	Mantle Cell Lymphoma_Blastic variant	2	1	1	AMPL
16	216	lymph node	Mantle Cell Lymphoma	2	1	1	2n
17	216	lymph node	Mantle Cell Lymphoma	1	1	1	3R/2G
18	216	lymph node	Mantle Cell Lymphoma	2	1	1	2n
19	216	lymph node	Mantle Cell Lymphoma	2	1	0	2n
20	216	lymph node	Mantle Cell Lymphoma	1	0	0	2n

21	216	lymph node	Mantle Cell Lymphoma	1	1	0	Poly
23	216	lymph node	Mantle Cell Lymphoma	2	1	1	Poly
24	216	lymph node	Mantle Cell Lymphoma	0	0	0	2n
26	216	lymph node	Mantle Cell Lymphoma	1	1	NA	2n
27	216	lymph node	Mantle Cell Lymphoma	2	1	1	2n
28	216	lymph node	Mantle Cell Lymphoma	1	1	0	2n
29	216	lymph node	Mantle Cell Lymphoma	1	1	0	Poly
30	216	lymph node	Mantle Cell Lymphoma	2	1	1	2n
31	216	lymph node	Mantle Cell Lymphoma	2	1	1	1n
32	216	lymph node	Mantle Cell Lymphoma	1	1	0	2n
33	216	lymph node	Mantle Cell Lymphoma	1	1	0	2n
34	216	lymph node	Mantle Cell Lymphoma	2	1	1	Poly
35	216	lymph node	Mantle Cell Lymphoma	2	1	1	NA
36	216	lymph node	Mantle Cell Lymphoma	1	0	0	2n
37	216	lymph node	Mantle Cell Lymphoma	2	1	0	Poly
38	216	lymph node	Mantle Cell Lymphoma	1	0	0	NA
40	216	lymph node	Mantle Cell Lymphoma	1	0	0	2n
41	216	lymph node	Mantle Cell Lymphoma	2	1	0	2n
42	216	lymph node	Mantle Cell Lymphoma	0	0	0	2n
43	216	lymph node	Mantle Cell Lymphoma	1	0	0	2n
44	216	lymph node	Mantle Cell Lymphoma	1	1	1	2n
46	216	lymph node	Mantle Cell Lymphoma	NA	NA	NA	2n
47	216	lymph node	Mantle Cell Lymphoma	1	1	0	2n
49	216	lymph node	Mantle Cell Lymphoma	0	NA	0	2n
50	216	lymph node	Mantle Cell Lymphoma	1	1	0	2n
51	216	lymph node	Mantle Cell Lymphoma	0	0	0	NA
52	216	lymph node	Mantle Cell Lymphoma	0	0	NA	Poly
53	216	lymph node	Mantle Cell Lymphoma	NA	NA	NA	3R/2G
55	216	lymph node	Mantle Cell Lymphoma	0	NA	1	poly
56	216	lymph node	Mantle Cell Lymphoma_Blastic variant	2	1	1	2n
57	216	lymph node	Mantle Cell Lymphoma	2	1	1	2n
58	216	lymph node	Mantle Cell Lymphoma	2	1	0	2n
59	216	lymph node	Mantle Cell Lymphoma	1	1	0	2n
60	216	lymph node	Mantle Cell Lymphoma	2	1	1	2n
61	216	lymph node	Mantle Cell Lymphoma	2	1	1	NA
62	216	lymph node	Mantle Cell Lymphoma	2	1	1	2n
63	216	lymph node	Mantle Cell Lymphoma_Blastic variant	2	1	1	Poly
64	216	lymph node	Mantle Cell Lymphoma	1	1	0	2n
65	216	lymph node	Mantle Cell Lymphoma	2	1	1	Poly
66	216	lymph node	Mantle Cell Lymphoma	2	1	1	2n
67	216	lymph node	Mantle Cell Lymphoma	2	1	1	2n
68	216	lymph node	Mantle Cell Lymphoma	1	1	1	2n
69	216	lymph node	Mantle Cell Lymphoma	1	1	1	2n
70	216	lymph node	Mantle Cell Lymphoma	2	1	1	2n
71	216	lymph node	Mantle Cell Lymphoma	1	1	1	Poly
72	216	lymph node	Mantle Cell Lymphoma	2	1	1	2n
73	216	lymph node	Mantle Cell Lymphoma	1	1	0	2n
74	216	lymph node	Mantle Cell Lymphoma	2	1	0	2n
75	216	lymph node	Mantle Cell Lymphoma	2	1	0	2n
76	216	lymph node	Mantle Cell Lymphoma	1	1	0	NA
77	216	lymph node	Mantle Cell Lymphoma	2	1	0	2n
78	216	lymph node	Mantle Cell Lymphoma	2	1	1	2n
79	216	lymph node	Mantle Cell Lymphoma	1	1	0	2n
80	216	lymph node	Mantle Cell Lymphoma	1	1	0	2n
81	216	lymph node	Mantle Cell Lymphoma	2	1	1	Poly
82	216	lymph node	Mantle Cell Lymphoma	2	1	1	2n
83	216	lymph node	Mantle Cell Lymphoma	2	1	1	1n
84	216	lymph node	Mantle Cell Lymphoma	1	1	0	2n
85	216	lymph node	Mantle Cell Lymphoma	1	1	0	3R/2G
86	216	lymph node	Mantle Cell Lymphoma	1	1	1	2n

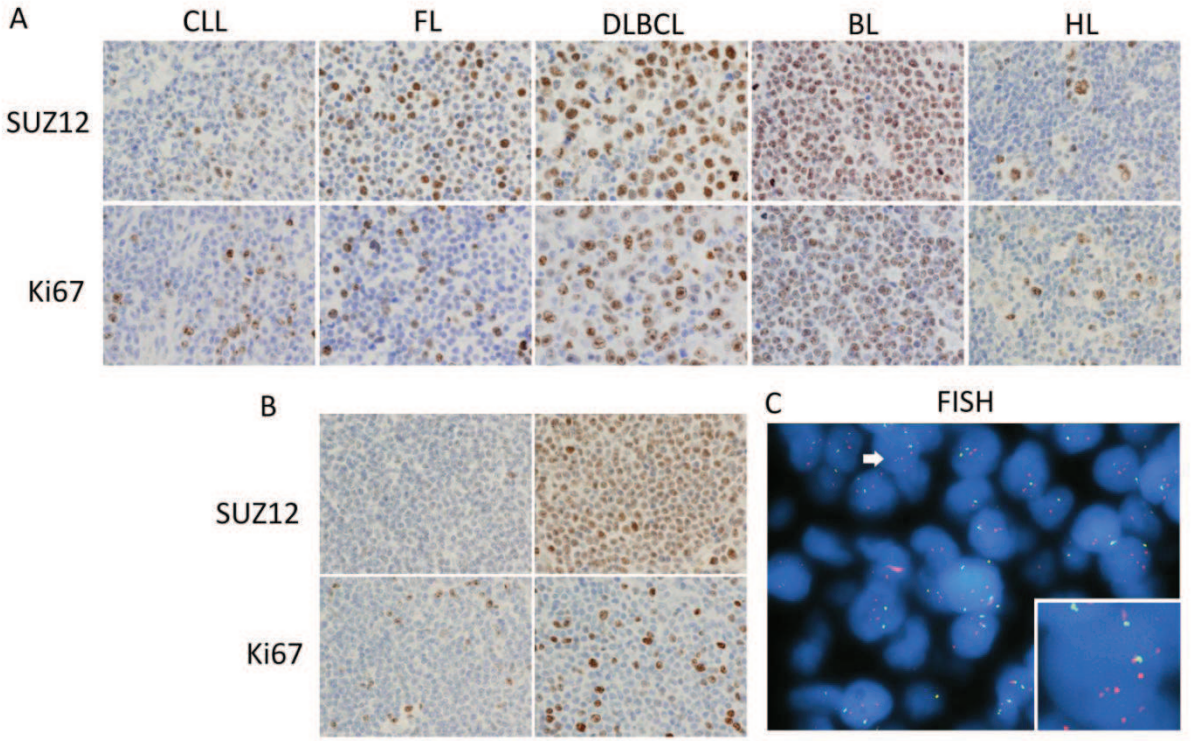

Figure 3.4. SUZ12 in B-cell lymphomas. (A) SUZ12 and Ki67 expression in different types of B-cell lymphoma, showing the correlation between the strength of SUZ12 expression and proliferation index. (B) However, in MCL samples, a tumor with a relatively low proliferation index, some cases showed increased SUZ12 expression, in contrast to the absence of its expression from normal mantle zone cells (Figure 1A), which are the benign counterpart of MCL. C) SUZ12 gene amplification detected by FISH in an SUZ12-positive MCL case. Several copies of SUZ12 (in red) are detected, compared with only two centromeric copies for chromosome 17 (in green). Objective 100X, immersion.

3.5 MicroRNA LOSSES MAY ACCOUNT FOR UPREGULATION OF SUZ12 IN SOME MCL CASES

Although cytogenetic alterations are an important mechanism of aberrant gene expression, SUZ12 locus cytogenetic abnormalities do not fully explain the gene overexpression seen in most of the cases.

A potential role for microRNAs in regulating the expression of multiple oncogenes and tumor suppressor genes has been demonstrated (Croce, 2008). Therefore we decided to investigate microRNAs putatively regulating SUZ12 by studying their expression level in MCL cases.

To this end we used the MicroCosm Targets tool (formerly miRBase Targets; http://www.ebi.ac.uk/enright-srv/microcosm/htdocs/targets/v5/), which contains computationally predicted targets for microRNAs across many species using the miRanda algorithm (Griffiths-Jones, 2004; Griffiths-Jones et al., 2006; Griffiths-Jones et al., 2008). The MicroCosm analysis proposed hsa-miR-27b*, hsa-miR-126, hsa-miR-200b, hsa-miR-210, hsa-miR-323-3p, hsa-miR-429, and hsa-miR-573 as putative regulators of SUZ12 expression.

Therefore, we looked for the expression of these miRNAs in a group of 24 MCL cases and MCL-derived cell lines (Jeko-1 and Z138) using data generated in our laboratory with the Human miRNA Microarray platform from Agilent Technologies. As controls, we used reactive lymphoid tissue for MCL cases, and sorted IgD+ cells for cell lines. Probes for hsa-miR-323-3p and hsa-miR-27b* were not included in the chip.

Expression of two of the five miRNAs included in the array showed lower levels than control samples in nearly all MCL cases studied (Figure 3.5).

We found that hsa-mir-126 and hsa-miR-200b genes were downregulated in MCL cases relative to reactive lymphoid tissues (FDR < 0.01), and hsa-miR-200b was also downregulated in MCL-derived cell lines compared with IgD cells ($p = 0.002$). Hsa-mir-210 was not significantly deregulated in MCL with respect to control samples, and hsa-mir-429 and hsa-mir-573 were not detected in any normal or tumor sample.

These data suggest an alternative mechanism that would explain SUZ12 overexpression in those cases that do not harbor cytogenetic abnormalities. However, further functional studies will be needed to mechanistically confirm our hypothesis.

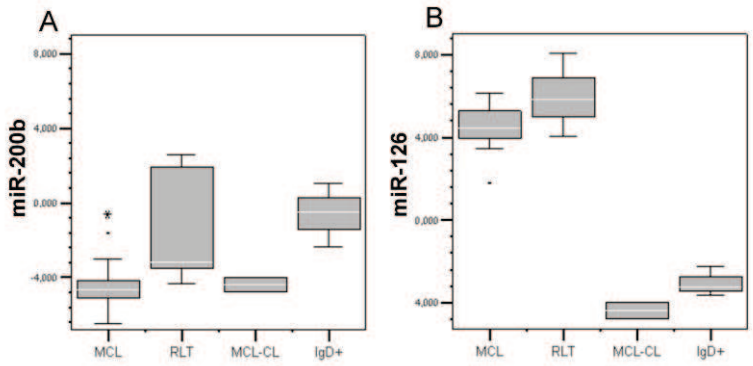

Figure 3.5. Loss of expression of miRs regulating SUZ12 in MCL and MCL-derived cell lines. (A) Relative levels of hsa-mir-200b (A) and hsa-mir-126 (B) in tumoral MCL samples vs. normal controls (FDR < 0.01 for both miRs) and MCL-derived cell lines JEKO and Z138, (p = 0.002 for hsa-mir-200b, and not significant for hsa-mir-126) compared with normal controls. For MCL, the normal control used was reactive lymphoid tissue, and for cell lines IgD+ isolated cells. (MCL-CL: MCL-derived cell lines; RLT: reactive lymphoid tissue).

3.6 SUZ12 DEFICIENCY COMPROMISES MCL VIABILITY

Having in mind a possible oncogenic role for SUZ12 in MCL we wondered if SUZ12 was really needed for MCL cells to survive. Thus, to further asses the significance of SUZ12 overexpression in MCL we performed an RNAi analysis using a lentiviral (HIV)-based RNA interference vector in two MCL-derived cell lines: Jeko-1 and Z138. The vector, as described in section 2.8 harbors the *EGFP* gene under the regulation of the UBC promoter allowing for the selection of infected cells by FACS.

Two sequences (shSUZ12.783 and shSUZ12.2076) successfully knocked SUZ12 down in both cell lines with a residual expression of less than 20% (Figure 3.6A). Additionally, specificity of the shRNAs was assessed by measuring the levels of trimethylation at lysine 27 of histone H3 (H3K27me3), a hallmark of the PRC2 complex activity. Taking into account that SUZ12 is required for the methyltransferase activity of EZH2 (Cao and Zhang, 2004), SUZ12 knock down should abrogate this mark. Levels of H3K27me3 were significantly affected 72 hours (decreased around 50% or less) after the infection with the lentivirus carrying shRNAs against SUZ12 compared with controls (Figure 3.6B).

To determine whether the inhibition of SUZ12 had any effect on the survival of MCL derived cell lines, we followed several strategies. First we studied the growth potential of these cells compared with control cells. To this end we designed a strategy based on competitive

proliferation similar to that previously described (see section 2.10.2) (Ivanova et al., 2006). When we infected Jeko-1 and Z138 with lentivirus carrying shRNAs against SUZ12 or scramble controls, we could observe a decrease in the infected EGFP-positive population only in those experiments in which we used shRNAs against SUZ12 (Figure 3.6C). This decrease was slight but constant along the time, meaning that although SUZ12 deficiency does not have a dramatic effect on cell viability, it is necessary for the long-term survival of these cells. In addition, we tested the effects of SUZ12 silencing on cell growth directly through measurement of cell number by trypan blue exclusion counting. For that, we previously sorted the EGFP-positive fraction. The results show that SUZ12-deficient cells grew less than cells either expressing a scramble control or infected with the empty vector (Figure 3.6D). This was mainly due to an increase in apoptosis, because cell cycle analysis by FACS in these GFP+-sorted cells showed either slight but not significant decrease in G2/M or increase in SubG1 phase in cells deficient for SUZ12 (Figure 3.7C). Thus we decided to study levels of apoptosis by means of annexin V staining. Levels of apoptosis augmented in Jeko-1 and Z138 cells upon silencing of SUZ12 (Figure 3.7B). Apoptosis was also demonstrated by Western blot using antibodies against PARP that were able to detect the cleavage of this protein upon apoptosis induction (Figure 3.7A). PARP was more efficiently cleaved in cells lacking SUZ12. We could observe that one of the hairpins was more efficient killing the cells. This efficiency correlated well with the levels of H3K27me3 suggesting that the effect on cell survival is mediated by the loss of this epigenetic mark. Actually, we could not detect PARP cleavage in Jeko-1 with the less efficient hairpin, although this probably occurred due to a matter of sensitivity of the antibody, since we still observed a mild increase in apoptosis by annexin V staining.

3.7 IDENTIFICATION AND FUNCTIONAL CLASSIFICATION OF SUZ12 GENOMIC TARGET GENES IN MCL

SUZ12 is known to exert its function on the Polycomb-PRC2 complex through the direct repression of many target genes. Although some genome-wide mapping of SUZ12 targets has been previously performed (Boyer et al., 2006; Bracken et al., 2006; Lee et al., 2006; Squazzo et al., 2006), it has been demonstrated that SUZ12 targets vary among developmental states,

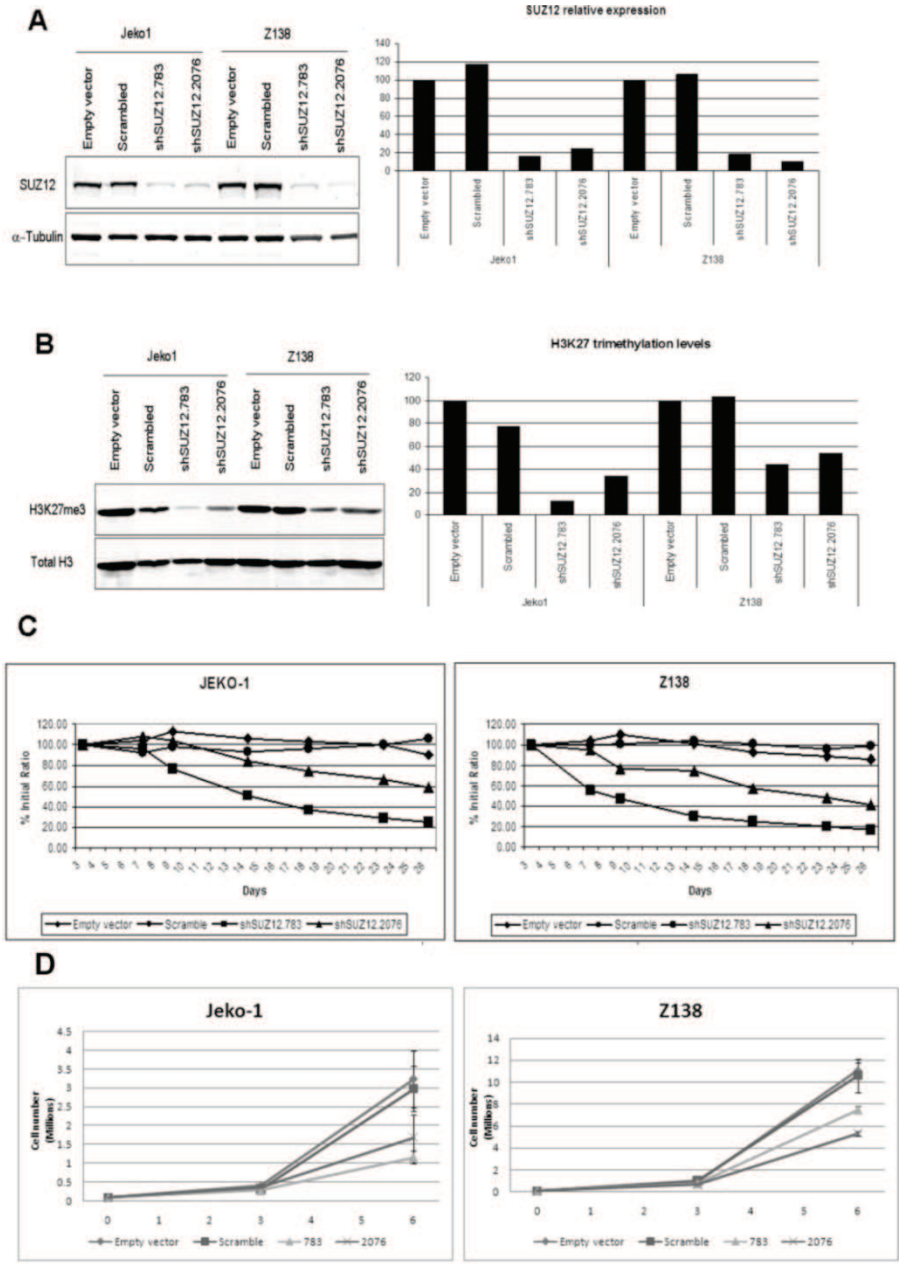

Figure 3.6. (A) (left) Anti-SUZ12 immunoblot of Jeko-1 and Z138 cell lines transduced either with the empty vector, a scrambled sequence or with two different hairpins against SUZ12. Band signals were normalized with tubulin as a loading control (right). (B) Depletion of SUZ12 affects the function of the PRC2 complex as assessed by immunoblot using an antibody against histone H3 trimethylation at lysine 27 (left). Total histone H3 was used to normalize band signals (right). (C) Expression of EGFP that marks transduced cells was tracked over time in order to observe differences in viability between cells transduced either with the empty vector or with a scramble control and cells transduced with two different hairpins against SUZ12. (D) GFP+-sorted Jeko1 and Z138 proliferation was assessed by counting viable cells using trypan blue exclusion along the time.

tissues and cell types (Squazzo et al., 2006). To look for potential targets that could explain the role of SUZ12 in MCL we performed chromatin immunoprecipitation (ChIP) and subsequent hybridization on Agilent's Human Promoter Microarray (ChIP-on-chip) with the Z138 MCL-derived cell line.

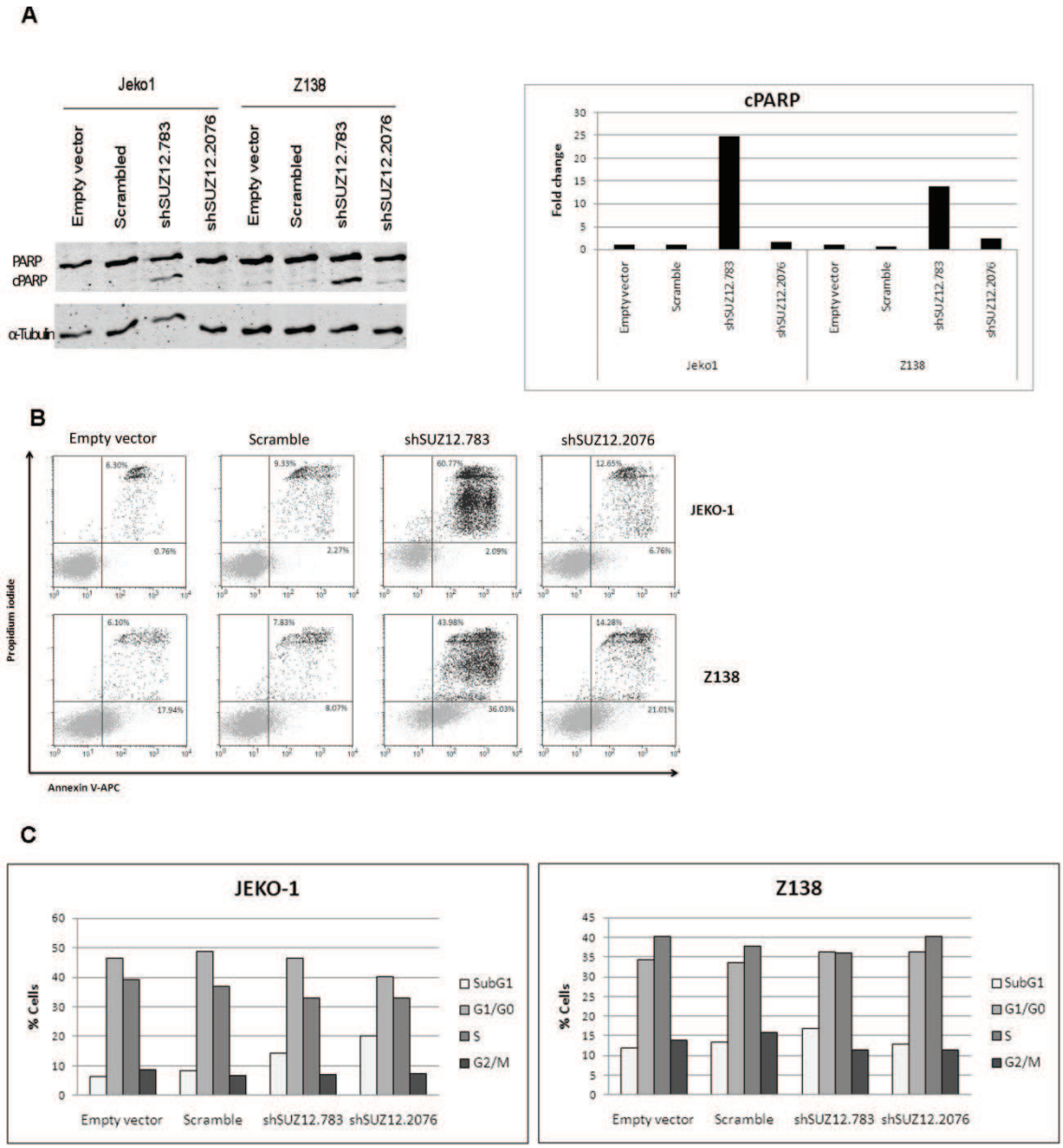

Figure 3.7. (A) Immunoblot showing specific cleavage of poly (ADP-ribose) polymerase (cPARP) in SUZ12-deficient cells after sorting. (B) Flow cytometric analysis of apoptosis using double staining of Annexin V and propidium iodide after cell sorting. (C) Flow cytometric analysis of cell cycle in Jeko1 and Z138 cells after GFP+-sorting. Representative examples of three different measurements for each cell line are shown.

For ChIP experiments the SUZ12 antibody described here (clone 220A/A3) and SUZ12 commercial antibodies (Upstate, 07-379) were used. Triplicates of the immunoprecipitated DNA were amplified using GenomePlex's Whole Genome Amplification kit. Triplicates were then mixed, labeled, and hybridized against the input DNA on the Human Promoter chip.

After data extraction, normalization and processing, we found 17,605 (3.6%) bound probes (peak $p < 0.01$) corresponding to 1,806 genes. As a second filter we used a normalized $\log_2$ ratio above 1 to consider the genes to be potential SUZ12 targets. We found 1,424 gene promoters that passed both criteria including gene promoters of known SUZ12 target genes such as CDKN2A, GADD45G, BMP2, and WNT (Bracken et al., 2006; Kotake et al., 2007; Lee et al., 2006).

However, the chromatin immunoprecipitation technique has some caveats. First, the binding capacity of agarose beads usually overwhelms the amount of antibody used giving high backgrounds that can mask the results. Second, these procedures give, at best, relative enrichment of DNA fragments and not absolute purification (Kuo and Allis, 1999).

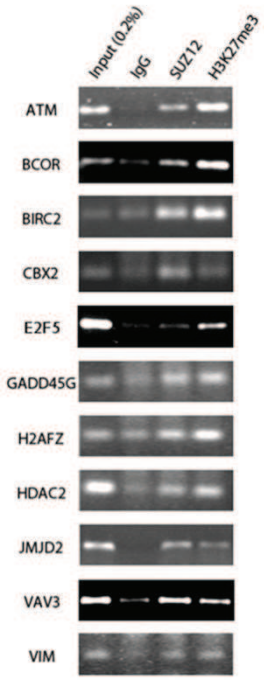

Figure 3.8. Validation of SUZ12 target genes by semi-quantitative ChIP. Single-locus semi-quantitative PCR on ChIP samples was performed on several SUZ12 candidate target genes, with SUZ12 and H3K27me3 antibodies. Mouse IgG was used as a negative control.

Thus, to determine the accuracy of SUZ12 target gene discovery, single-locus semi-quantitative PCR was performed on immunoprecipitated material with SUZ12 and H3K27me3 antibodies on 18 candidate SUZ12 target genes. These target genes included genes with known relevance in MCL or lymphoma pathogenesis such as ATM, BCOR or VAV; genes which play a role on significant processes associated with cancer such as apoptosis or DNA repair (BIRC2,

GADD45G) and genes related to transcriptional regulation, a process in which SUZ12 is supposed to play a critical role (JMJD2, E2F5). GADD45G (a previously described target, (Lee et al., 2006)) was used as the positive control (Figure 3.8).

With this method, eleven out of eighteen targets were validated with both antibodies, SUZ12 and H3K27me3, including ATM, CBX2, VAV3, JMJD2 and BIRC2. These data support the idea that SUZ12 is not only present at these loci but also is functionally active, since the H3K27me3 mark can be found at the same loci.

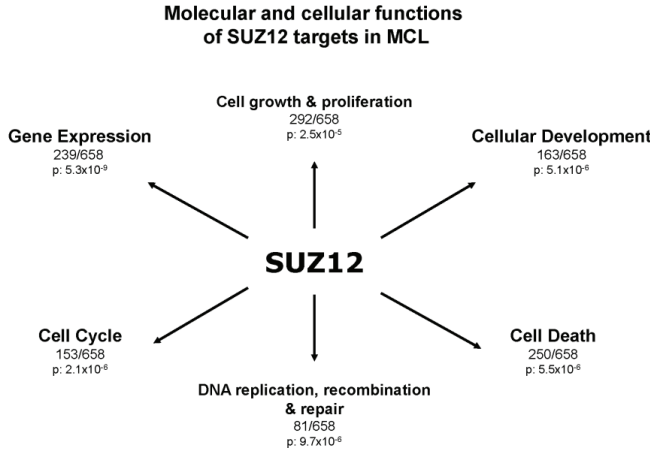

Figure 3.9. Functional classification of SUZ12-targeted genes. Functions of SUZ12 target genes were analyzed using the IPA program. 658 out of 1,424 genes identified by ChIP-on-chip have annotated functions in the IPA database. The number of genes identified as belonging to each category is included. The probability is that associated with a right-tailed Fisher's exact test.

To determine whether SUZ12 controls the expression of essential pathways in the survival of MCL cells as suggested by the functional experiments we decided to explore the functions of SUZ12 target genes using the Ingenuity Pathway Analysis (IPA) program. Only 658 out of 1,424 genes identified by chIP-on-chip had annotated functions in the IPA database and could therefore be functionally classified. Functional classification showed an enrichment of genes controlling gene expression, cell cycle and proliferation, DNA replication and repair and development (Figure 3.9). These findings are consistent with other studies (Bracken et al., 2006; Lee et al., 2006) and can explain the role of SUZ12 in cancer.

Among the SUZ12 target genes that were sorted as having a role in gene expression we mainly found transcription factors and regulators, such as E2F5, POU domain proteins, and SUV39H1, and enzymes regulating transcription and translation, such as DNA and RNA polymerases, jumonji domain (JMJD) proteins, and several eukaryotic translation initiation factors (EIFs). It is interesting that we found members of the E2F family of transcription factors between SUZ12 target genes because several E2F proteins regulate and interact with Polycomb proteins, suggesting a feed-back regulatory loop between E2F factors and Polycomb proteins (Nowak et al., 2006; Sanchez-Beato et al., 2004; Wu et al., 2010b).

Regulation of development is one of the main functions of the PcG proteins. Thus it is not surprising that we found a lot of development regulators among SUZ12, some of which have been previously described as SUZ12 targets in ES cells. These include Sry-related HMG box (SOX) and Forkhead box (FOX) family genes; POU domain transcription factors, including POU2F3 a known tumor suppressor gene that is aberrantly silenced by hypermethylation in cancer (Zhang et al., 2006); and BMP2.

Another interesting finding was the presence of SUZ12 at the promoter of several miR genes, two of which have been identified as SUZ12 targets (hsa-mir-124a and hsa-mir-183 (Lee et al., 2006; Marson et al., 2008). Some of these miRs have a known role in cancer and differentiation such as hsa-miR-148a (Lujambio et al., 2008) and hsa-miR-223 (Stamatopoulos et al., 2009).

Indeed, the most noteworthy finding was many of the most significant genes among the SUZ12 targets were genes with known roles in the pathogenesis of MCL. Some of the genes, like CDKN2A, were previously known to be SUZ12 target genes, but many others have not been previously described as SUZ12 targets. The list of target genes related to MCL pathogenesis included genes regulating cell cycle (CDKN2A and other INK4 family genes, several cyclins and cyclin dependent kinases, CHEK1, MAD2L1, and BUB3), DNA damage and repair genes (ATM, GADD45, several DNA polymerases and topoisomerases, MLH1, XRCC family genes, and ERCC family genes), apoptosis regulators (BCL2 and BCL2 regulator proteins, BID, several BIRC family members, and others). We also found members of NF-κB pathway (BCL10, NF-KB2, and IKBKG) to be regulated by SUZ12. The fine tuning of the NF-κB pathway is altered in several cancers (Karin et al., 2002).

3.8 GENE EXPRESSION PROFILING IN SUZ12 DEFICIENT MCL CELLS AND IN MCL SAMPLES

To really assess the effect of SUZ12 in the gene expression pattern of MCL and elucidate and validate the relevance of the results obtained by chIP-on-chip we decided to look for potential gene expression changes associated to the levels of SUZ12 expression. To this end we performed gene expression profiling in Z138 cell line after SUZ12 silencing and in an additional series of MCL patients, using whole genome expression microarrays.

3.8.1 CHANGES IN SUZ12 TARGETS AFTER SUZ12 SILENCING IN THE Z138 MCL-DERIVED CELL LINE

As a first step we analyzed differentially expressed genes in SUZ12-silenced cells. For that we compared the gene expression profile of cells transduced with lentiviruses encoding for shRNAs against SUZ12 (shSUZ12.783 and shSUZ12.2076) with the gene expression profile of cells transduced with lentiviruses that did not encode for any shRNA. We decided not to use a scramble shRNA in these experiments as a control to exclude the possible off-target effects of the scramble sequence that could mask the effects of SUZ12 on some genes and also give several false positives.

After SUZ12 silencing in the Z138 cell line, some SUZ12 targets were actually unrepressed. 140 transcripts, belonging to the group of SUZ12-target genes, showed an upregulation or downregulation of at least 0.6 (log_2 scale) after 3 or 5 days and were considered to be significantly deregulated after SUZ12 silencing. Among the genes that were differentially expressed we found some genes belonging to pathways altered in MCL such as CDKN2A and GADD45G as well as genes involved in development, such as BMP2 and several GATA binding proteins or differentiation factors like MLLT3 and CBX2 (Figure 3.10).

3.8.2 GENE EXPRESSION PROFILE IN MCL SAMPLES

With the aim of examining the impact of SUZ12 expression in MCL samples, we decided to explore the gene expression changes associated to SUZ12 expression in human samples. Thus we hybridized an additional series of 24 MCL cases onto Agilent's whole human genome microarrays. Then, we looked for genes which expression was inversely or directly correlated with SUZ12 expression and were found to be SUZ12 targets by chIP-on-chip. Using these kind

of analysis we could observe that 188 of 642 known genes suitable for the analysis (30%) were significantly correlated with SUZ12 expression (Pearson R > ±0.4, FDR < 0.15). The correlation of most of these genes with SUZ12 expression was inverse being more downregulated in those cases with more SUZ12 expression and upregulated in those cases that did not express SUZ12 (126 inversely correlated with SUZ12 expression *vs*. 62 with a direct correlation) (Figure 3.11).

Among these target genes we could find genes involved in spindle checkpoint function such as BUB3 and MAD2L1, DNA repair (XRCC6), apoptosis (TP53RK, BNIP2, BIRC2 and TMBIM4), NF-κB pathway (NKAP) and regulators of transcription and translation (SMARCAD1, JMJD2D, EIF1B, EIF4A2, FOXJ2 and E2F5).

3.9 PATHWAYS COREGULATED WITH SUZ12 IN MCL

All these analysis give an idea of the direct targets that are under the control of SUZ12. However, the impact of SUZ12 in tumor cells is composed by the direct as well as indirect effects of its expression. Thus, in order to determine the general characteristics of the tumors associated to the expression of SUZ12, we explored the gene expression profile of MCL samples taking into account all the genes for the analysis and not only those genes that appeared as direct targets of SUZ12.

We focused our attention in identifying functional pathways coregulated with the expression of SUZ12. To this end we performed a gene set-enrichment analysis (GSEA) of SUZ12 expression with all the genes in MCL malignant samples, not restricted to SUZ12 targets identified by ChIP, using GSEA software (http://www.broad.mit.edu/gsea/). GSEA is a computational method that determines whether an a priori defined set of genes shows statistically significant, concordant differences between two biological states. In this case the biological state was the expression of SUZ12 taken as a continuous variable.

This analysis revealed a direct correlation with pathways associated with proliferation, such as cell cycle (including E2F1 and several cyclins and CDKs) and caspase-apoptosis pathways (including BCL2) enforcing the idea that high expression of SUZ12 is associated to more aggressive variants and an inverse correlation with the proteasome pathway (Table 3.4). We also found an inverse correlation with the MAPK pathway, which might be contradictory with previous results, however, some specific genes included in this pathway such as *JUN*, *FOS*, *MAPK4, MAPK7*, and *BRAF* showed stronger expression in SUZ12-expressing tumors.

Figure 3.10. SUZ12 target gene expression was affected in SUZ12-silenced cell lines. Gene-expression profiling was performed in duplicate 3 and 5 days after SUZ12 depletion in Z138, with two different shRNAs (2076 and 783) vs. empty vector. The heat map represents expression levels for each sample. A total of 140 significant genes (Log2 (Cy5/ Cy3) cut-off =+/- 0.6 in at least three samples) were ranked by Euclidean squared distance.

A

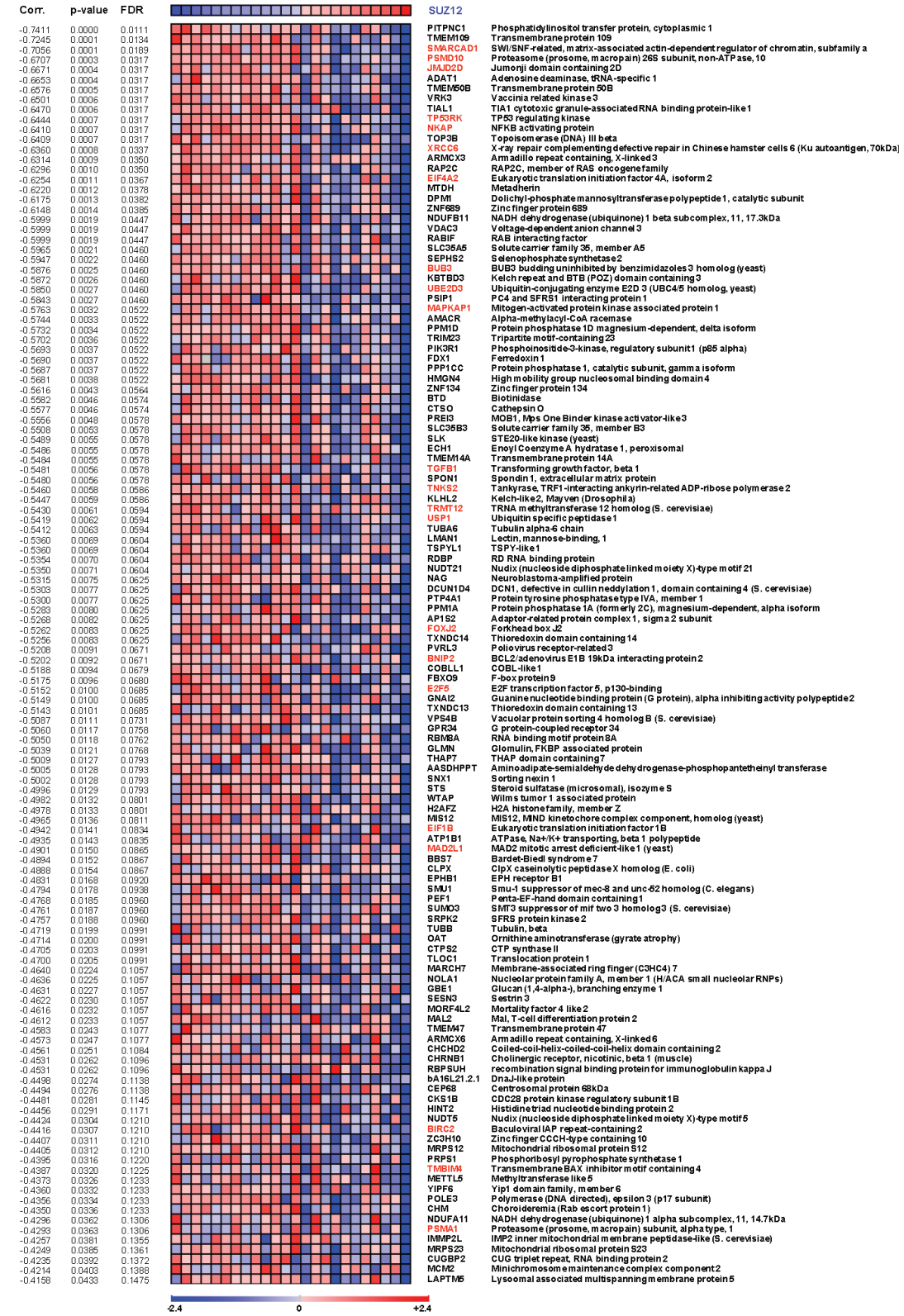

Corr.	p-value	FDR		
-0.7411	0.0000	0.0111	PITPNC1	Phosphatidylinositol transfer protein, cytoplasmic 1
-0.7245	0.0001	0.0134	TMEM109	Transmembrane protein 109
-0.7056	0.0001	0.0189	SMARCAD1	SWI/SNF-related, matrix-associated actin-dependent regulator of chromatin, subfamily a
-0.6707	0.0003	0.0317	PSMD10	Proteasome (prosome, macropain) 26S subunit, non-ATPase, 10
-0.6671	0.0004	0.0317	JMJD2D	Jumonji domain containing 2D
-0.6653	0.0004	0.0317	ADAT1	Adenosine deaminase, tRNA-specific 1
-0.6576	0.0005	0.0317	TMEM50B	Transmembrane protein 50B
-0.6501	0.0006	0.0317	VRK3	Vaccinia related kinase 3
-0.6470	0.0006	0.0317	TIAL1	TIA1 cytotoxic granule-associated RNA binding protein-like 1
-0.6444	0.0007	0.0317	TP53RK	TP53 regulating kinase
-0.6410	0.0007	0.0317	NKAP	NFKB activating protein
-0.6409	0.0007	0.0317	TOP3B	Topoisomerase (DNA) III beta
-0.6360	0.0008	0.0337	XRCC6	X-ray repair complementing defective repair in Chinese hamster cells 6 (Ku autoantigen, 70kDa)
-0.6314	0.0009	0.0350	ARMCX3	Armadillo repeat containing, X-linked 3
-0.6296	0.0010	0.0350	RAP2C	RAP2C, member of RAS oncogene family
-0.6254	0.0011	0.0367	EIF4A2	Eukaryotic translation initiation factor 4A, isoform 2
-0.6220	0.0012	0.0378	MTDH	Metadherin
-0.6175	0.0013	0.0382	DPM1	Dolichyl-phosphate mannosyltransferase polypeptide 1, catalytic subunit
-0.6148	0.0014	0.0385	ZNF689	Zinc finger protein 689
-0.5999	0.0019	0.0447	NDUFB11	NADH dehydrogenase (ubiquinone) 1 beta subcomplex, 11, 17.3kDa
-0.5999	0.0019	0.0447	VDAC3	Voltage-dependent anion channel 3
-0.5999	0.0019	0.0447	RABIF	RAB interacting factor
-0.5965	0.0021	0.0460	SLC35A5	Solute carrier family 35, member A5
-0.5947	0.0022	0.0460	SEPHS2	Selenophosphate synthetase 2
-0.5876	0.0025	0.0460	BUB3	BUB3 budding uninhibited by benzimidazoles 3 homolog (yeast)
-0.5872	0.0026	0.0460	KBTBD3	Kelch repeat and BTB (POZ) domain containing 3
-0.5850	0.0027	0.0460	UBE2D3	Ubiquitin-conjugating enzyme E2D 3 (UBC4/5 homolog, yeast)
-0.5843	0.0027	0.0460	PSIP1	PC4 and SFRS1 interacting protein 1
-0.5763	0.0032	0.0522	MAPKAP1	Mitogen-activated protein kinase associated protein 1
-0.5744	0.0033	0.0522	AMACR	Alpha-methylacyl-CoA racemase
-0.5732	0.0034	0.0522	PPM1D	Protein phosphatase 1D magnesium-dependent, delta isoform
-0.5702	0.0036	0.0522	TRIM23	Tripartite motif-containing 23
-0.5693	0.0037	0.0522	PIK3R1	Phosphoinositide-3-kinase, regulatory subunit 1 (p85 alpha)
-0.5690	0.0037	0.0522	FDX1	Ferredoxin 1
-0.5687	0.0037	0.0522	PPP1CC	Protein phosphatase 1, catalytic subunit, gamma isoform
-0.5681	0.0038	0.0522	HMGN4	High mobility group nucleosomal binding domain 4
-0.5616	0.0043	0.0564	ZNF134	Zinc finger protein 134
-0.5582	0.0046	0.0574	BTD	Biotinidase
-0.5577	0.0046	0.0574	CTSO	Cathepsin O
-0.5556	0.0048	0.0578	PREI3	MOB1, Mps One Binder kinase activator-like 3
-0.5508	0.0053	0.0578	SLC35B3	Solute carrier family 35, member B3
-0.5489	0.0055	0.0578	SLK	STE20-like kinase (yeast)
-0.5486	0.0055	0.0578	ECH1	Enoyl Coenzyme A hydratase 1, peroxisomal
-0.5484	0.0055	0.0578	TMEM14A	Transmembrane protein 14A
-0.5481	0.0056	0.0578	TGFB1	Transforming growth factor, beta 1
-0.5480	0.0056	0.0578	SPON1	Spondin 1, extracellular matrix protein
-0.5460	0.0058	0.0586	TNKS2	Tankyrase, TRF1-interacting ankyrin-related ADP-ribose polymerase 2
-0.5447	0.0059	0.0586	KLHL2	Kelch-like 2, Mayven (Drosophila)
-0.5430	0.0061	0.0594	TRMT12	TRNA methyltransferase 12 homolog (S. cerevisiae)
-0.5419	0.0062	0.0594	USP1	Ubiquitin specific peptidase 1
-0.5412	0.0063	0.0594	TUBA6	Tubulin alpha-6 chain
-0.5360	0.0069	0.0604	LMAN1	Lectin, mannose-binding, 1
-0.5360	0.0069	0.0604	TSPYL1	TSPY-like 1
-0.5354	0.0070	0.0604	RDBP	RD RNA binding protein
-0.5350	0.0071	0.0604	NUDT21	Nudix (nucleoside diphosphate linked moiety X)-type motif 21
-0.5315	0.0075	0.0625	NAG	Neuroblastoma-amplified protein
-0.5303	0.0077	0.0625	DCUN1D4	DCN1, defective in cullin neddylation 1, domain containing 4 (S. cerevisiae)
-0.5300	0.0077	0.0625	PTP4A1	Protein tyrosine phosphatase type IVA, member 1
-0.5283	0.0080	0.0625	PPM1A	Protein phosphatase 1A (formerly 2C), magnesium-dependent, alpha isoform
-0.5268	0.0082	0.0625	AP1S2	Adaptor-related protein complex 1, sigma 2 subunit
-0.5262	0.0083	0.0625	FOXJ2	Forkhead box J2
-0.5256	0.0083	0.0625	TXNDC14	Thioredoxin domain containing 14
-0.5208	0.0091	0.0671	PVRL3	Poliovirus receptor-related 3
-0.5202	0.0092	0.0671	BNIP2	BCL2/adenovirus E1B 19kDa interacting protein 2
-0.5188	0.0094	0.0679	COBLL1	COBL-like 1
-0.5175	0.0096	0.0680	FBXO9	F-box protein 9
-0.5152	0.0100	0.0685	E2F5	E2F transcription factor 5, p130-binding
-0.5149	0.0100	0.0685	GNAI2	Guanine nucleotide binding protein (G protein), alpha inhibiting activity polypeptide 2
-0.5143	0.0101	0.0685	TXNDC13	Thioredoxin domain containing 13
-0.5087	0.0111	0.0731	VPS4B	Vacuolar protein sorting 4 homolog B (S. cerevisiae)
-0.5060	0.0117	0.0758	GPR34	G protein-coupled receptor 34
-0.5050	0.0118	0.0762	RBM8A	RNA binding motif protein 8A
-0.5039	0.0121	0.0768	GLMN	Glomulin, FKBP associated protein
-0.5009	0.0127	0.0793	THAP7	THAP domain containing 7
-0.5005	0.0128	0.0793	AASDHPPT	Aminoadipate-semialdehyde dehydrogenase-phosphopantetheinyl transferase
-0.5002	0.0128	0.0793	SNX1	Sorting nexin 1
-0.4996	0.0129	0.0793	STS	Steroid sulfatase (microsomal), isozyme S
-0.4982	0.0132	0.0801	WTAP	Wilms tumor 1 associated protein
-0.4978	0.0133	0.0801	H2AFZ	H2A histone family, member Z
-0.4965	0.0136	0.0811	MIS12	MIS12, MIND kinetochore complex component, homolog (yeast)
-0.4942	0.0141	0.0834	EIF1B	Eukaryotic translation initiation factor 1B
-0.4935	0.0143	0.0835	ATP1B1	ATPase, Na+/K+ transporting, beta 1 polypeptide
-0.4901	0.0150	0.0865	MAD2L1	MAD2 mitotic arrest deficient-like 1 (yeast)
-0.4894	0.0152	0.0867	BBS7	Bardet-Biedl syndrome 7
-0.4888	0.0154	0.0867	CLPX	ClpX caseinolytic peptidase X homolog (E. coli)
-0.4831	0.0168	0.0920	EPHB1	EPH receptor B1
-0.4794	0.0178	0.0938	SMU1	Smu-1 suppressor of mec-8 and unc-52 homolog (C. elegans)
-0.4768	0.0185	0.0960	PEF1	Penta-EF-hand domain containing 1
-0.4761	0.0187	0.0960	SUMO3	SMT3 suppressor of mif two 3 homolog 3 (S. cerevisiae)
-0.4757	0.0188	0.0960	SRPK2	SFRS protein kinase 2
-0.4719	0.0199	0.0991	TUBB	Tubulin, beta
-0.4714	0.0200	0.0991	OAT	Ornithine aminotransferase (gyrate atrophy)
-0.4705	0.0203	0.0991	CTPS2	CTP synthase II
-0.4700	0.0205	0.0991	TLOC1	Translocation protein 1
-0.4640	0.0224	0.1057	MARCH7	Membrane-associated ring finger (C3HC4) 7
-0.4636	0.0225	0.1057	NOLA1	Nucleolar protein family A, member 1 (H/ACA small nucleolar RNPs)
-0.4631	0.0227	0.1057	GBE1	Glucan (1,4-alpha-), branching enzyme 1
-0.4622	0.0230	0.1057	SESN3	Sestrin 3
-0.4616	0.0232	0.1057	MORF4L2	Mortality factor 4 like 2
-0.4612	0.0233	0.1057	MAL2	Mal, T-cell differentiation protein 2
-0.4583	0.0243	0.1077	TMEM47	Transmembrane protein 47
-0.4573	0.0247	0.1077	ARMCX6	Armadillo repeat containing, X-linked 6
-0.4561	0.0251	0.1084	CHCHD2	Coiled-coil-helix-coiled-coil-helix domain containing 2
-0.4531	0.0262	0.1096	CHRNB1	Cholinergic receptor, nicotinic, beta 1 (muscle)
-0.4531	0.0262	0.1096	RBPSUH	recombination signal binding protein for immunoglobulin kappa J
-0.4498	0.0274	0.1138	bA16L21.2.1	DnaJ-like protein
-0.4494	0.0276	0.1138	CEP68	Centrosomal protein 68kDa
-0.4481	0.0281	0.1145	CKS1B	CDC28 protein kinase regulatory subunit 1B
-0.4456	0.0291	0.1171	HINT2	Histidine triad nucleotide binding protein 2
-0.4424	0.0304	0.1210	NUDT5	Nudix (nucleoside diphosphate linked moiety X)-type motif 5
-0.4416	0.0307	0.1210	BIRC2	Baculoviral IAP repeat-containing 2
-0.4407	0.0311	0.1210	ZC3H10	Zinc finger CCCH-type containing 10
-0.4405	0.0312	0.1210	MRPS12	Mitochondrial ribosomal protein S12
-0.4395	0.0316	0.1220	PRPS1	Phosphoribosyl pyrophosphate synthetase 1
-0.4387	0.0320	0.1225	TMBIM4	Transmembrane BAX inhibitor motif containing 4
-0.4373	0.0326	0.1233	METTL5	Methyltransferase like 5
-0.4360	0.0332	0.1233	YIPF6	Yip1 domain family, member 6
-0.4356	0.0334	0.1233	POLE3	Polymerase (DNA directed), epsilon 3 (p17 subunit)
-0.4350	0.0336	0.1233	CHM	Choroideremia (Rab escort protein 1)
-0.4296	0.0362	0.1306	NDUFA11	NADH dehydrogenase (ubiquinone) 1 alpha subcomplex, 11, 14.7kDa
-0.4293	0.0363	0.1306	PSMA1	Proteasome (prosome, macropain) subunit, alpha type, 1
-0.4257	0.0381	0.1355	IMMP2L	IMP2 inner mitochondrial membrane peptidase-like (S. cerevisiae)
-0.4249	0.0385	0.1361	MRPS23	Mitochondrial ribosomal protein S23
-0.4235	0.0392	0.1372	CUGBP2	CUG triplet repeat, RNA binding protein 2
-0.4214	0.0403	0.1388	MCM2	Minichromosome maintenance complex component 2
-0.4158	0.0433	0.1475	LAPTM5	Lysosomal associated multispanning membrane protein 5

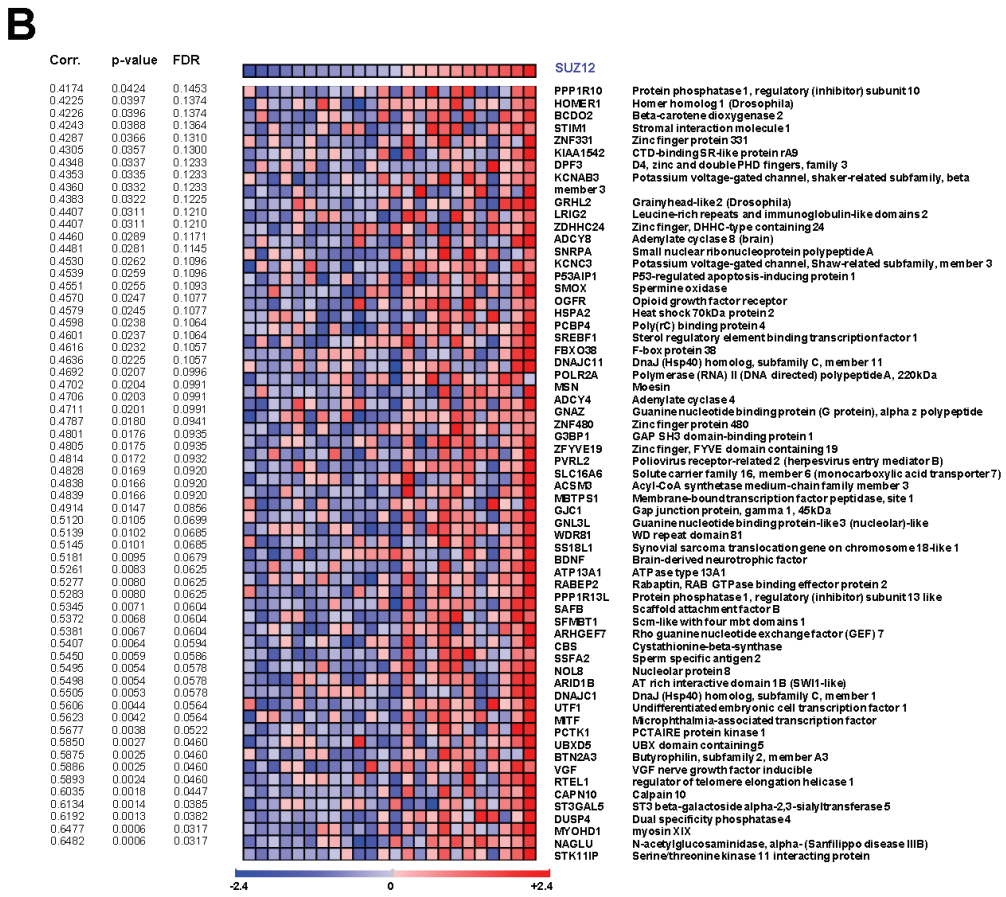

Figure 3.11. SUZ12 target gene expression in MCL samples. (A) Relative expression levels of 126 inversely correlated SUZ12 genes in MCL tumoral samples (FDR < 0.15). (B) Relative expression levels of 62 directly correlated SUZ12 genes in MCL tumoral samples (FDR < 0.15). Pearson correlation coefficients between identified SUZ12-target genes and SUZ12 expression were calculated using the T-Rex program available from the GEPAS site (v. 3.1).

Table 3.4. Pathways coregulated with SUZ12 expression in MCL. GSEA identifies statistically significant functionally relevant pathways ($p < 0.05$, FDR < 0.25) associated with a high level of expression of SUZ12. ES: enrichment score. NES: normalized enrichment score. p-val: Nominal probability. FDR: false discovery rate.

Gene sets positively correlated with SUZ12 expression					
NAME	**SIZE**	**ES**	**NES**	**p-val**	**FDR**
MITOCHONDRIA PATHWAY	21	0.5952	2.4673	0.0000	0.0053
CELL CYCLE PATHWAY	21	0.5622	2.3809	0.0000	0.0075
ARAP PATHWAY	19	0.5528	2.1412	0.0020	0.0283
CASPASE PATHWAY	21	0.5233	2.1399	0.0040	0.0213
CA2+ CAM PATHWAY	12	0.6362	1.9820	0.0043	0.0513
D4GDI PATHWAY	11	0.6060	1.8114	0.0169	0.1118
Gene sets negatively correlated with SUZ12 expression					
NAME	**SIZE**	**ES**	**NES**	**p-val**	**FDR**
MAPK PATHWAY	83	-0.4378	-3.4409	0.0000	0.0000
PROTEASOME PATHWAY	19	-0.7375	-2.8678	0.0000	0.0000
GH PATHWAY	26	-0.4999	-2.2277	0.0000	0.0395
IL1R PATHWAY	29	-0.4244	-2.0417	0.0080	0.0779
CHREBP PATHWAY	15	-0.5951	-2.0912	0.0038	0.0832
CK1 PATHWAY	12	-0.6534	-2.0431	0.0056	0.0916
ARF PATHWAY	16	-0.5428	-1.9669	0.0056	0.1074
RARRXR PATHWAY	14	-0.5157	-1.7385	0.0177	0.1367
RAB PATHWAY	10	-0.5956	-1.7550	0.0220	0.1392
ERK PATHWAY	30	-0.3620	-1.7652	0.0203	0.1402
AKAP-CENTROSOME PATHWAY	10	-0.6027	-1.7413	0.0198	0.1413
TPO PATHWAY	22	-0.4373	-1.8955	0.0096	0.1444
PPARA PATHWAY	51	-0.2753	-1.7689	0.0249	0.1465
CYTOKINE PATHWAY	15	-0.5077	-1.7904	0.0183	0.1473
PDGF PATHWAY	26	-0.3973	-1.7772	0.0149	0.1479
VEGF PATHWAY	26	-0.3992	-1.7929	0.0135	0.1557
TOLL PATHWAY	32	-0.3657	-1.8513	0.0134	0.1642
GATA3 PATHWAY	13	-0.5419	-1.7935	0.0080	0.1678
TOB1 PATHWAY	16	-0.4963	-1.7958	0.0189	0.1797
P38MAPK PATHWAY	37	-0.3407	-1.8065	0.0132	0.1876

RESULTS II

Epstein Barr Virus microRNAs repress BCL6 expression in diffuse large B cell lymphoma.

Epstein Barr Virus (EBV) is able to transform B cells by disrupting the normal B-cell differentiation program leading to the development of different types of B-cell lymphoma. BCL6 is a key transcriptional repressor during normal B-cell differentiation required for germinal centre development that has been shown to repress NF-kB in DLBCL. In some B-cell lymphomas the expression of BCL6 is opposite to the EBV infection, however the mechanism of this phenomenon and its biological meaning remain elusive. In this study, 22 viral microRNAs were found to be upregulated specifically in EBV-positive cases of DLBCL. By applying the miRanda algorithm 10 out of these 22 microRNAs were predicted to potentially target BCL6. To explore this possibility immunohistochemical analysis and in situ hybridization were carried out on 149 cases of DLBCL. The data showed an almost perfect inverse correlation between BCL6 protein expression and EBV infection even in the absence of LMP1 protein expression. From the list of 10 microRNAs, ebv-ebv-miR-BART3, ebv-ebv-miR-BART7, ebv-ebv-miR-BART9 and ebv-ebv-miR-BART17-5p were selected for further functional validation. Thus we transfected synthetic microRNAs and measured the luciferase activity in our reporter system. At least three of the assayed microRNAs were able to decrease luciferase activity of the reporter. Then the effect of these microRNAs over the endogenous BCL6 protein was investigated in lymphoid BCL6-expressing cell lines by Western blot. The four microRNAs were able to downregulate the levels of endogenous BCL6 in several DLBCL cell lines. Inhibition of these microRNAs with synthetic microRNA inhibitors let to the upregulation of BCL6 in an EBV-positive cell line. In summary, EBV-positive DLBCL cases express a restricted set of viral microRNAs. Several of these microRNAs can potentially target the BCL6 gene highlighting the importance of BCL6 downregulation in the context of EBV B-cell transformation. Functional studies demonstrate that at least three of these microRNAs are able to downregulate BCL6 expression. We hypothesize that BCL6 downregulation might be necessary for DLBCL cells to survive in the context of EBV-induced NF-κB pathway activation.

3.10 EBV microRNA EXPRESSION IN DLBCL CASES

EVB is a lymphotropic virus that is associated to the development of several lymphoid malignancies. The discovery that EBV encodes several miRNAs has prompted research in this area. However, the understanding of the effect of these miRNAs and how they work is still very poor. Thus, we decided to study a possible oncogenic role for EBV miRNAs in DLBCL. As a first step, we studied the miRNA expression profile in 36 samples of DLBCL (33 negative for EBV and 3 positive) using a microRNA microarray platform that contains 15,000 probes for 470 human and 64 human viral miRNAs.

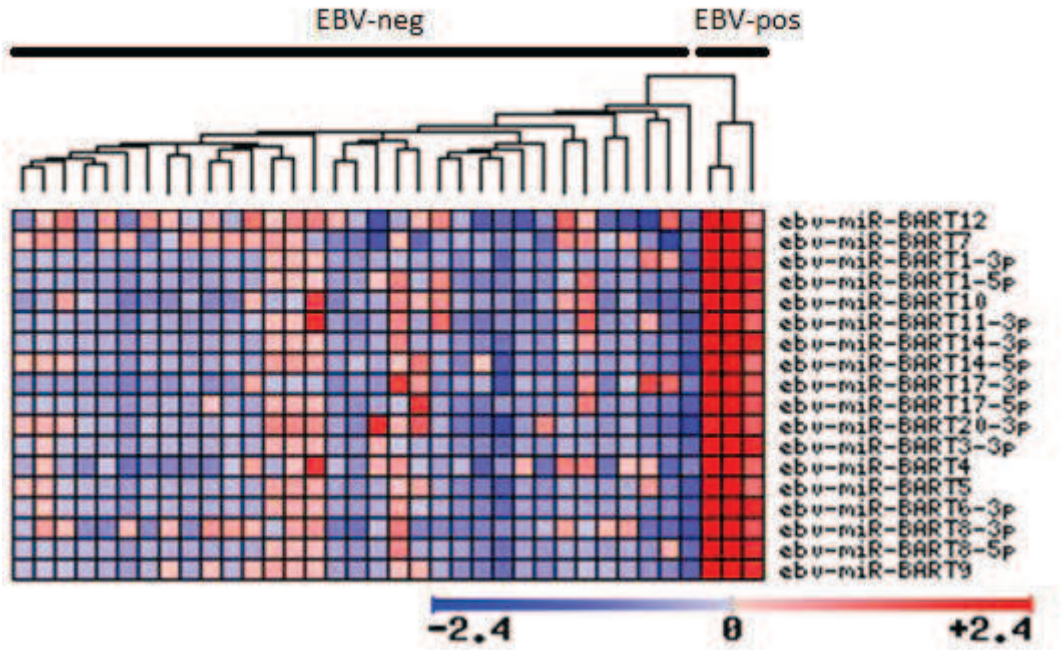

Figure 3.12. Gene clustering demonstrates a very homogenous pattern of expression of EBV-encoded miRNAs in EBV-positive DLBCL patients.

Even though we had just 3 positive samples, the pattern of expression of viral miRNAs was very homogenous (Figure 3.12). 22 EBV-encoded miRNAs were found to be upregulated specifically in EBV-positive cases of DLBCL (Corrected p-value < 0.05, Table 3.5). These 22 miRNAs were the product of 15 pre-miRNAs (Table 3.5). EBV miRNAs are grouped in two different clusters: one in the intronic regions of the BART gene (ebv-miR-BART1 to ebv-miR-BART-20) and the other in the untranslated regions (UTRs) of the BHRF1 gene (ebv-miR-BHRF1-1 to ebv-miR-BHRF1-3) (Cai et al., 2006; Grundhoff et al., 2006; Pfeffer et al., 2004). All the differentially expressed miRNA genes belonged to the BART cluster.

Table 3.5. EBV-encoded miRNAs that show significant differential expression between EBV-positive and EBV-negative DLBCL cases.

SystematicName	p-value	Corrected p-value
ebv-miR-BART3-3p	2.23E-15	1.94E-13
ebv-miR-BART6-3p	4.46E-15	1.94E-13
ebv-miR-BART8-5p	6.71E-15	1.95E-13
ebv-miR-BART14-3p	1.09E-14	2.36E-13
ebv-miR-BART9	2.30E-14	4.01E-13
ebv-miR-BART1-3p	1.01E-13	1.47E-12
ebv-miR-BART1-5p	5.68E-13	7.05E-12
ebv-miR-BART5	1.28E-10	1.40E-09
ebv-miR-BART17-5p	7.19E-10	6.95E-09
ebv-miR-BART14-5p	8.80E-10	7.65E-09
ebv-miR-BART10	4.42E-09	3.50E-08
ebv-miR-BART8-3p	9.48E-09	6.87E-08
ebv-miR-BART4	9.29E-08	6.22E-07
ebv-miR-BART11-3p	1.31E-07	8.13E-07
ebv-miR-BART17-3p	2.42E-07	1.40E-06
ebv-miR-BART7	4.22E-07	2.30E-06
ebv-miR-BART6-5p	1.09E-05	5.60E-05
ebv-miR-BART20-3p	1.76E-05	8.50E-05
ebv-miR-BART3-5p	1.87E-05	8.56E-05
ebv-miR-BART12	2.66E-04	0.001158242
ebv-miR-BART16	0.002387877	0.009442969
ebv-miR-BART11-5p	0.008477309	0.03206634

Among these miRNAs we could find ebv-miR-BART5 which has been described to target the p53 up-regulated modulator of apoptosis (PUMA) (Choy et al., 2008), a proapoptotic protein belonging to the “BH3-only” group of the Bcl-2 family, promoting in this way the survival of the host cell. We also found the expression of ebv-miR-BART1-5p, ebv-miR-BART16 and ebv-miR-BART17-5p which have been described to target the viral LMP1 transcript suppressing protein expression (Lo et al., 2007). These miRNAs also promote cell survival since LMP1 overexpression can be growth-inhibitory (Liu et al., 2002; Lu et al., 1996).

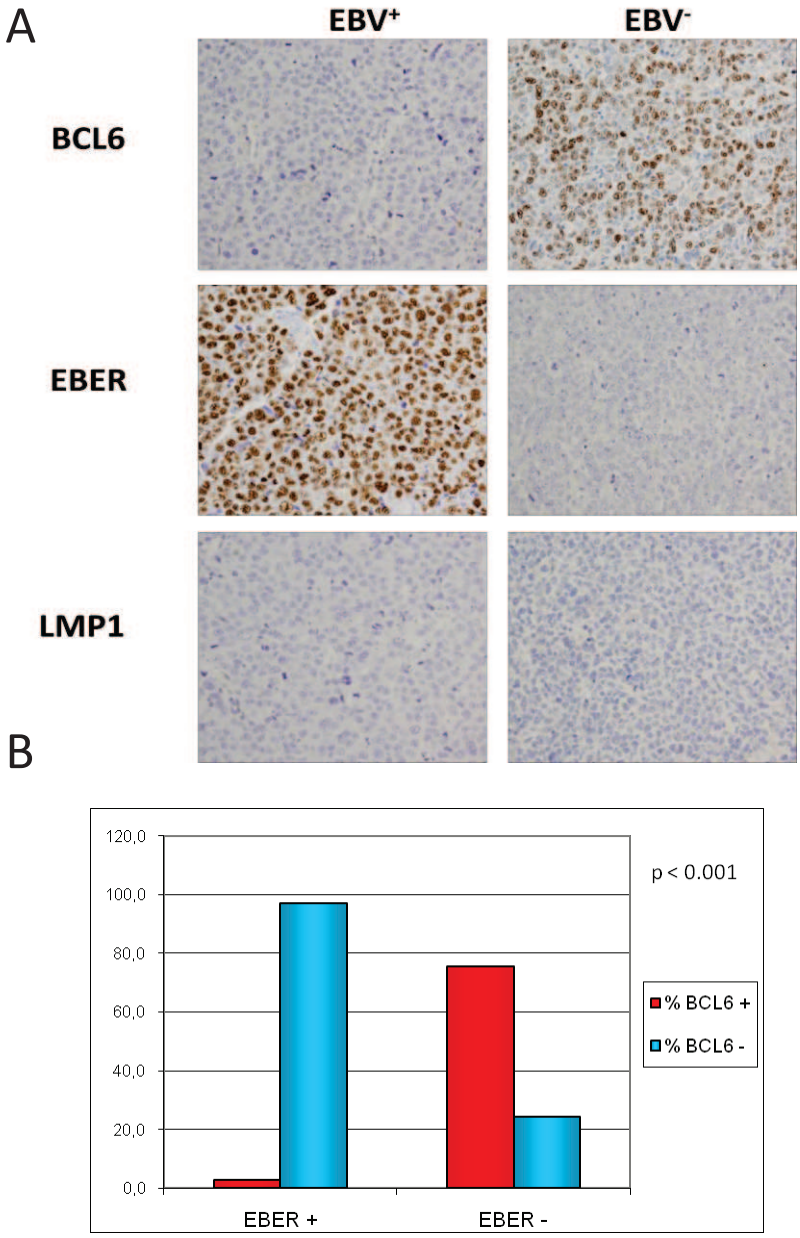

Figure 3.13. BCL6 is not expressed in EBV positive cases of Diffuse Large B-Cell Lymphoma even in the absence of LMP1 protein expression, suggesting other regulatory mechanisms. A) Immunohistochemical staining of two cases of DLBCL showing opposite pattern of BCL6 expression and EBV infection. B) Statistical analysis on a series of 149 DLBCL patients.

Surprisingly, we did not find expression of two important viral miRNAs: ebv-miR-BART2 that down-regulates the viral DNA polymerase BALF5 and inhibits the transition from latent to lytic cycle (Barth et al., 2008) and ebv-miR-BART22 which down-regulates LMP2A allowing the virus to escape from host immune surveillance (Lung et al., 2009). With the few exceptions that

have been commented before, the function as well as the viral or cellular targets of most viral miRNAs discovered here remain unknown.

3.11 EBV INFECTION CORRELATES WITH THE ABSENCE OF BCL6 PROTEIN

It has been observed that in several lymphomas, the expression of BCL6, a key transcription repressor that is essential for germinal center reaction and is frequently translocated or hypermutated in DLBCL (Pasqualucci et al., 2003), and the presence of the EBV genome are mutually exclusive occurrences (Capello et al., 2003; Carbone et al., 1997). In these studies, BCL6 expression was inversely correlated with LMP1 expression, and some evidences suggest that LMP1 can cause down-regulation of BCL6 but other possible mechanisms have not been studied.

Thus to extend previous observations and to explore the possibility that EBV can repress BCL6 in DLBCL cases we performed an immunohistochemical analysis and in situ hybridization on 149 samples of DLBCL to detect BCL6 expression and EBV-encoded EBERs expression in these cases. Expression of EBERs was used as a marker of EBV positivity because it has been described that EBERs are expressed in all EBV latency types (Kuppers, 2003).

From the 149 cases, 34 were found to be EBV positive and 115 were found to be EBV negative. When we looked at the results with the BCL6 antibody, we found an almost perfect inverse correlation between BCL6 expression and the presence of EBV ($p<0.001$, Figure 3.13). Only one out of 34 (2.94%) EBV-positive cases expressed BCL6, however 87 out of 115 (75.65%) EBV-negative cases expressed BCL6.

We also checked the expression of LMP1 viral antigen. Noteworthy, although the expression of LMP1 in our series was variable, many of the DLBCL cases studied were LMP1 negative (Figure 3.13). In these cases, the absence of BCL6 cannot be explained by a putative LMP1-mediated repression of BCL6 and additional mechanisms can be proposed.

3.12 MicroRNA TARGET PREDICTION

Our data in human DLBCL samples suggest that EBV down-regulates BCL6 by a LMP1-independent mechanism. Having in mind the restricted cluster of EBV-encoded miRNAs expressed by EBV-positive DLBCL patients, we hypothesized that some viral miRNAs could account for this phenomenon. To test this hypothesis we decided to look for EBV-encoded miRNAs that could potentially down-regulate BCL6 protein expression. Thus, we extracted BCL6 3'UTR and EBV-encoded miRNAs sequences from public databases (Ensembl, http://www.ensembl.org; and miRBase, http://www.mirbase.org/) and applied the miRanda bioinformatic algorithm V3 (http://cbio.mskcc.org/microrna_data/miRanda-sept2008.tar.gz).

With this approach we identified 21 hits with a score threshold over 50 and an energy threshold below -20 Kcal/mol (Table 3.6). The 21 hits corresponded to 18 different mature miRNAs, three of which presented more than one possible binding site. In order to have a clearer picture, we filtered the list of predicted miRNAs with the list of differentially expressed genes in DLBCL patients (Table 3.5). In common, we identified 10 miRNAs that matched both criteria (Table 3.6).

Table 3.6. List of viral miRNAs that are predicted to target BCL6 as calculated using the miRanda algorithm. Bold indicates miRNAs that are differentially expressed in EBV-positive patients.

Query	Ref	Score	Energy (kCal/Mol)	Quey Pos	RefPos	Align Len
ebv-miR-BART18-5p	BCL6_3UTR	148	-21	1 22	887 911	24
ebv-miR-BART3	BCL6_3UTR	146	-23.59	3 23	121 145	23
ebv-miR-BART17-5p	BCL6_3UTR	145	-20.4	1 23	368 393	26
ebv-miR-BART9	BCL6_3UTR	143	-21.3	1 24	898 919	25
ebv-miR-BART10*	BCL6_3UTR	133	-21.61	1 22	111 142	32
ebv-miR-BART19-5p	BCL6_3UTR	129	-20.38	3 24	270 297	26
ebv-miR-BART14*	BCL6_3UTR	126	-22.56	3 23	126 148	21
ebv-miR-BART11-5p	BCL6_3UTR	122	-20.89	1 24	860 886	26
ebv-miR-BART2-5p	BCL6_3UTR	122	-20.39	2 23	286 306	21
ebv-miR-BART5	BCL6_3UTR	122	-22.92	2 25	856 883	27
ebv-miR-BART16	BCL6_3UTR	120	-21.61	1 24	863 886	23
ebv-miR-BART1-3p	BCL6_3UTR	114	-20.95	3 23	135 156	20
ebv-miR-BART10*	BCL6_3UTR	114	-21.37	1 22	408 429	21
ebv-miR-BART12	BCL6_3UTR	114	-20.02	1 23	980 998	22
ebv-miR-BART7*	BCL6_3UTR	113	-20.27	1 17	132 153	16
ebv-miR-BART15	BCL6_3UTR	104	-21.84	1 22	286 311	25
ebv-miR-BART11-5p	BCL6_3UTR	102	-22.57	6 25	106 132	22

ebv-miR-BART20-3p	BCL6_3UTR	100	-22.02	2 23	989 1021	32
ebv-miR-BART10*	BCL6_3UTR	99	-20.89	2 22	146 167	22
ebv-miR-BART7	BCL6_3UTR	99	-21.62	3 22	153 170	19
ebv-miR-BART7	BCL6_3UTR	76	-26.34	1 21	123 143	20

There are several miRNA target prediction algorithms published that look for potential miRNA targets. All the algorithms follow very similar rules such as near-perfect sequence match between the first 8 nucleotides of the 5' end of the miRNA (the so-called "seed region"), conservation of the binding site between related species and thermodynamic parameters. However, the consequences of varying so many parameters are that many times there is little overlap between different predictions making it difficult to distinguish true targets from false positive (Alexiou et al., 2009).

Figure 3.14. Venn diagram showing the overlap between the predictions of different algorithms. 13 out of 18 miRNAs predicted by miRanda were also predicted by other methods.

Even though a site is predicted by several programs, it is possible that the miRNA does not really bind to the target site and a site predicted by just one algorithm can be potently bound by a defined miRNA. Nonetheless it is widely accepted that targets predicted by more than one algorithm have more chances to be true targets than those predicted by just one algorithm. Hence we also tested if other algorithms predicted that EBV-encoded miRNAs could potentially regulate BCL6. To this end we performed an additional bioinformatic analysis to complement the results obtained with miRanda using three target prediction programs: TargetScan

(http://www.targetscan.org/), PITA (http://genie.weizmann.ac.il/pubs/mir07/32bit_exe_pita_prediction.tar.gz) and another algorithm developed at CNIO's bioinformatic Unit called SequenceMatch. With these three algorithms we could confirm the majority of the results obtained with miRanda. 13 out of 18 miRNAs predicted with miRanda were also predicted by at least one of the complementary algorithms that we have used (Figure 3.14).

Consequently, we selected four miRNAs for further validation. These miRNAs were selected according to the following parameters: 1) The miRNAs presented a good score in the miRanda algorithm and 2) the miRNAs were differentially expressed between EBV-positive and EBV-negative cases of DLBCL. In this way, we selected ebv-miR-BART3, ebv-miR-BART9 and ebv-miR-BART17-5p.We also selected ebv-miR-BART7 because, although it does not present one of the highest scores in the miRanda algorithm, this program predicts two binding sites for the miRNA in the 3' UTR of BCL6, increasing the probability of being a *bona fide* regulator of BCL6 protein expression. The potential pairing between the selected EBV-encoded miRNAs and the 3' UTR of BCL6 is shown in Figure 3.15.

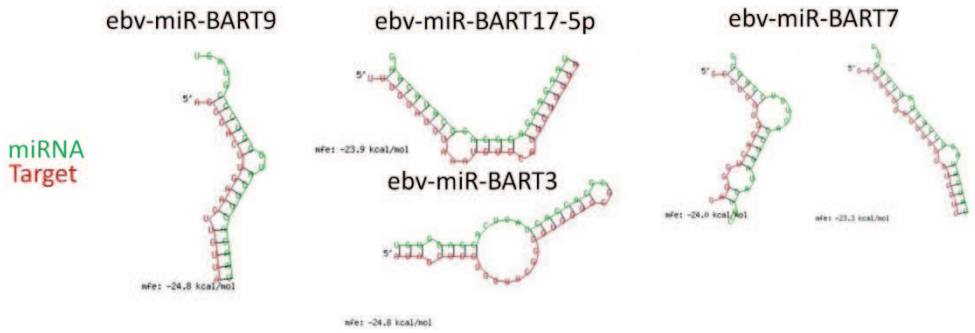

Figure 3.15. Representation of the theoretical binding of selected miRNAs to the 3'UTR of BCL6 using the RNAhybrid software.

3.13 EXPRESSION OF SELECTED microRNAS IN DLBCL PATIENTS

Before continuing with mechanistic experiments, we wanted to validate the results of the microarray in another series of patients by RT-PCR. As a first step we measured the levels of expression of 5 miRNAs in 40 samples of this new cohort of DLBCL patients (15 EBV-positive and 25 EBV-negative) to ensure that viral miRNAs were expressed. The selected miRNAs for validation were the four we selected before plus ebv-miR-BART10*, that was selected for three reasons: first, miRanda algorithm gave a good score for this miRNA; second, there were two binding sites predicted for the miRNA in the 3' UTR of BCL6 and third, although the miRNA

probe was not printed onto the microarray platform, DLBCL patients showed differential expression of the complementary strand of the pre-miR, the ebv-miR-BART10, suggesting that ebv-miR-BART10* could be also expressed at high levels.

Thus, we applied RT-PCR to measure the amount of ebv-miR-BART3, ebv-miR-BART7, ebv-miR-BART9, ebv-miR-BART10*, ebv-miR-BART17-5p transcripts in DLBCL samples. As expected, the selected miRNAs were expressed by EBV-positive cases (Figure 3.16). Intriguingly, although the difference in expression between positive and negative cases was roughly around 100-fold we still could detect expression of viral miRNAs in several EBV-negative cases by this technique.

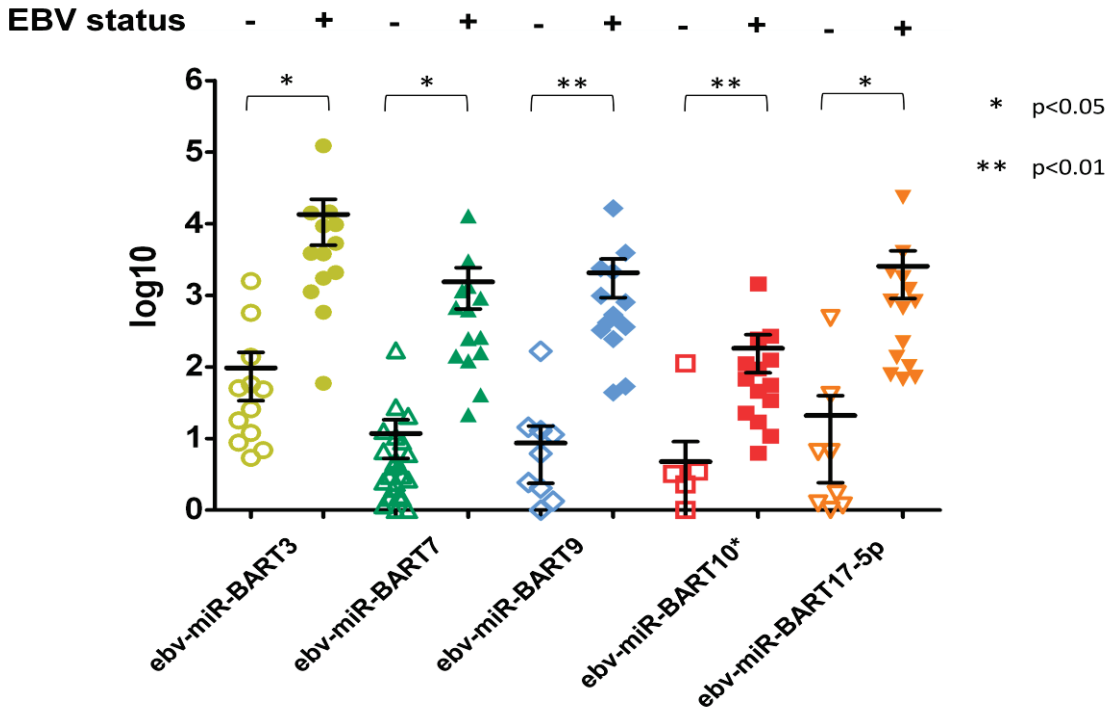

Figure 3.16. RT-PCR was carried out on 40 DLBCL samples using probes for five different microRNAs. Black bars indicate mean and standard deviation.

This unexpected result could be due to a technical limitation of the method used here. However, the fact that some cases were EBV-negative does not mean that EBV was also absent from non-malignant cells. In fact, since EBV infected cells are very rare (approximately 1–50 per million of B cells (Khan et al., 1996)) it is difficult to study EBV in healthy virus carriers. The presence of non-malignant EBV-positive cells in EBV-negative cases of DLBCL could account for the low although detectable expression of viral miRNAs in these patients. Moreover, the ebv-

miR-BART10* was expressed in EBV-positive patients at very low levels when compared to other miRNAs and in contrast with the complementary strand (ebv-miR-BART10) that showed high expression by microarray analysis.

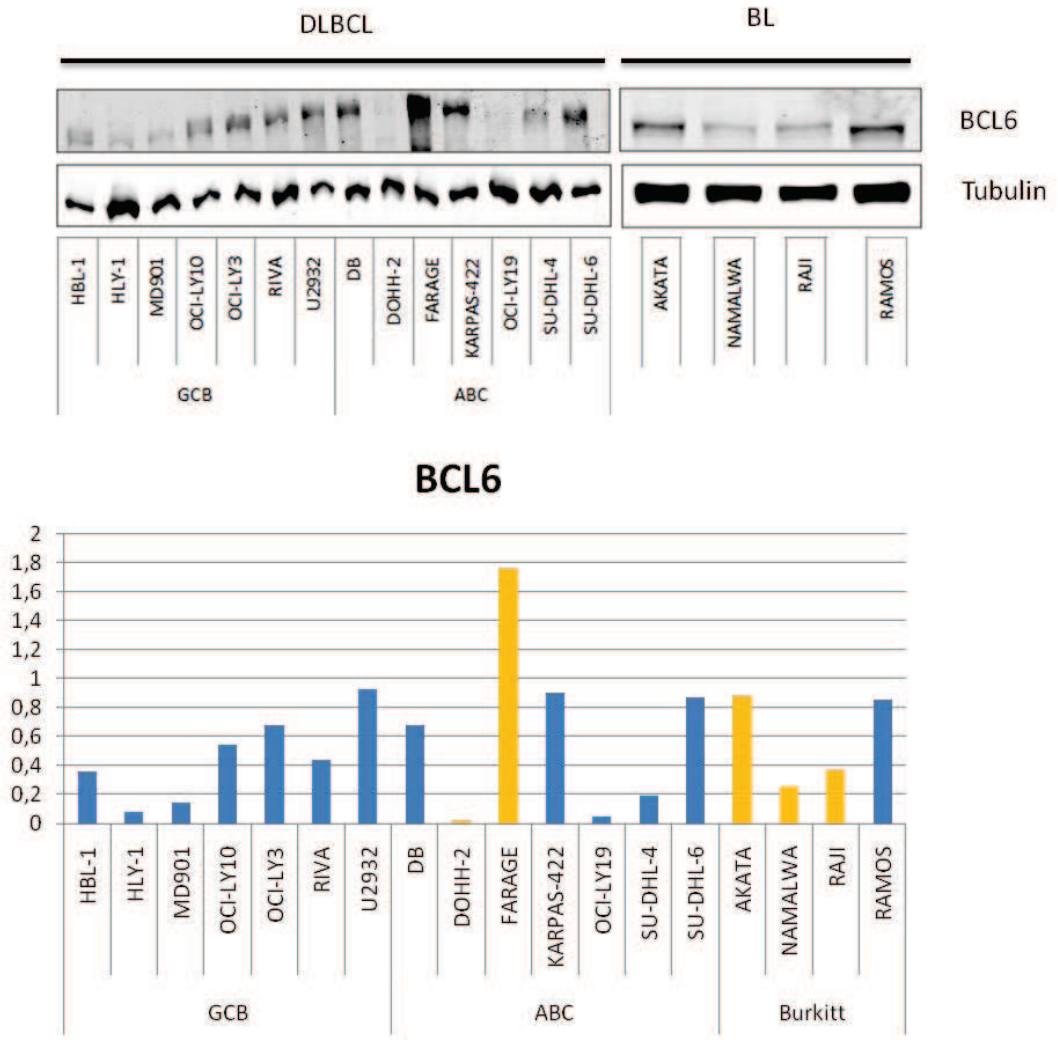

Figure 3.17. The opposite pattern between BCL6 expression and EBV infection is not maintained in DLBCL cell lines. A) Western Blot against BCL6 in several DLBCL and Burkitt cell lines. Tubulin was used as a loading control. B) Quantification of BCL6 protein expression in DLBCL cell lines of Activated B-Cell (ABC) and Germinal Centre B-Cell (GCB) types and Burkitt Lymphoma cell lines. Yellow bars indicate EBV-positive cell lines.

3.14 BCL6 PROTEIN AND microRNA EXPRESSION IN CELL LINES

We wanted to see if this inverse correlation between EBV presence and expression of BCL6 was also observed in cell lines. We performed immunoblot analysis in a panel of DLBCL cell lines (Figure 3.17). We also included 4 BL cell lines because in BL it has been described compatibility between BCL6 expression and EBV presence (Ferry, 2006). We used the EBV-negative cell lines to give an idea of the normal levels of BCL6 in each lymphoma type.

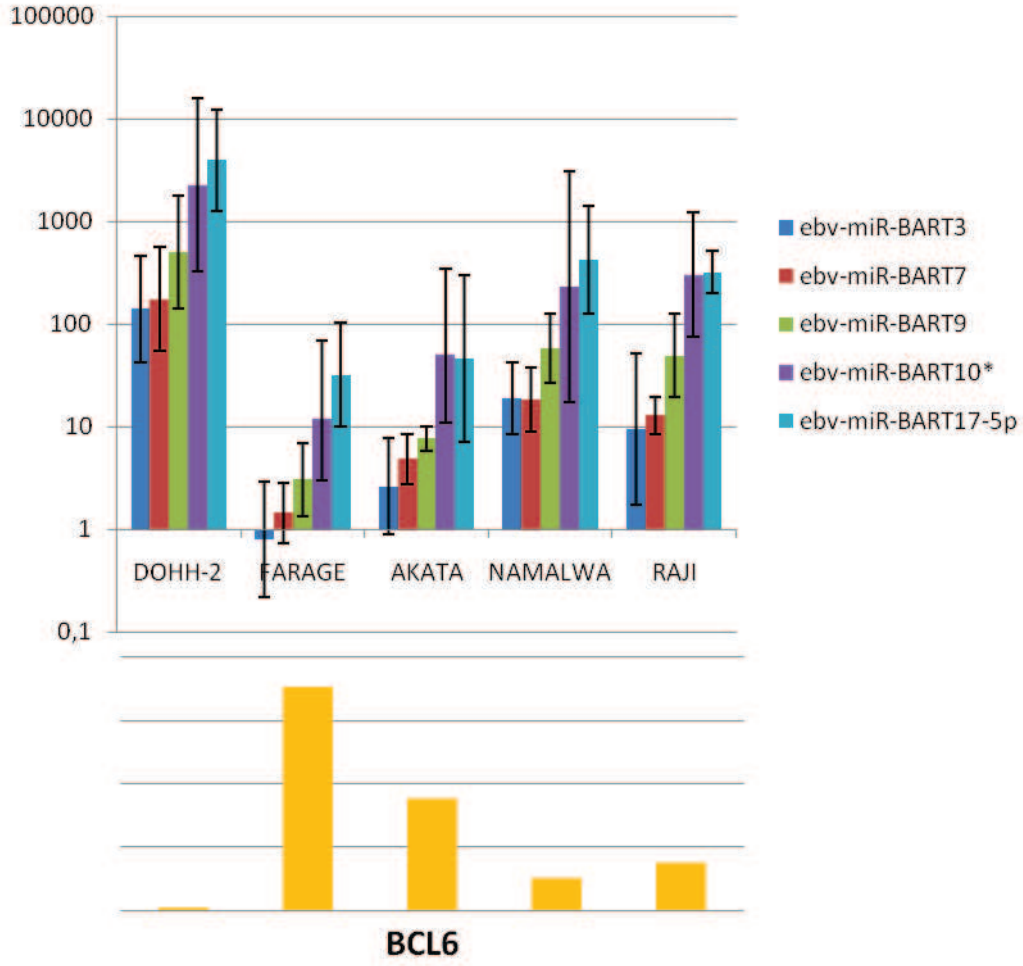

Figure 3.18. RT-PCR analysis of five EBV-encoded miRNAs in DLBCL and BL cell lines demonstrate that levels of BCL6 protein expression (lower panel) correlate with levels of miRNA expression (upper panel). Expression data is represented in a logarithmic scale and has been normalized using the Ramos EBV-negative cell line as background signal.

In BL-derived cell lines, two EBV-positive cell lines (Namalwa and Raji) showed moderate levels of BCL6 and the EBV-positive cell line Akata expressed high levels of BCL6 when compared with the EBV-negative cell line, Ramos (Figure 3.17). In DLBCL cell lines, one of the

EBV-positive cell lines (DoHH-2) showed the lowest levels of BCL6 in the entire panel but the other EBV-positive cell line (Farage) presented the highest levels of BCL6 expression, even higher than the BL-derived cell lines (Figure 3.17). Therefore, the phenomenon that we observe in human samples is not conserved in cell lines.

To look for a reason that could explain the lack of correlation in cell lines, we decided to study the expression of EBV-encoded miRNAs in these cell lines in order to elucidate if the expression of BCL6 still kept an inverse correlation with the levels of viral miRNAs. We measured the expression of ebv-miR-BART3, ebv-miR-BART7, ebv-miR-BART9, ebv-miR-BART10*, ebv-miR-BART17-5p transcripts in EBV-positive DLCBL and BL cell lines by RT-PCR.

Our results show that the relative expression of the five miRNAs still correlates in an inverse fashion with the levels of BCL6 expression. Consequently, the Farage cell line which showed the highest levels of BCL6 expression, expressed very low levels of viral miRNAs; BL-derived cell lines expressed moderate levels of miRNAs, being Akata the one with lower expression; and DoHH-2 expressed the highest levels of EBV-encoded miRNAs (Figure 3.18).

3.15 MULTIPLE VIRAL microRNAS REPRESS BCL6 IN DLBCL

The variability in the results of the different target prediction programs also evidences one of the main caveats of the bioinformatic approach. The use of bioinformatic prediction is reduced to the generation of hypothesis but must be empirically validated. Our hypothesis is supported not only by the bioinformatic predictions but also by the data obtained at the level of miRNA expression in human tumors and the inverse correlation between BCL6 levels and the expression of EBV-encoded miRNAs.

3.15.1 ASSESMENT OF THE INTERACTION BETWEEN EBV-ENCODED microRNAS AND THE 3' UTR OF BCL6

Therefore, to functionally validate the putative BCL6-regulatory role of these miRNAs we amplified the 3' UTR of BCL6 by PCR and cloned the fragment into the pGL3-Control vector. We called the resulting vector pGL3-BCL6. The pGL3-Control vector is a plasmid that contains the *luc+* gene encoding for the firefly luciferase protein under the control of the SV40 promoter, resulting in the constitutive expression of the *luc+* gene. The *luc+* gene does not have a 3' UTR

and only the SV40 polyadenylation signal is added after the coding sequence. This allow the researcher to clone the 3' UTR of interest at the 3' end of the *luc+* gene generating useful tools for the study of the miRNA function.

The following step was to co-transfect the pGL3-BCL6 vector with synthetic Pre-miR miRNA precursor molecules and a vector that contains the R*luc* gene encoding for the Renilla luciferase as a transfection control. The amount of miRNA to transfect was selected based in the optimization with a positive control, the hsa-miR-1 that is able to down-regulate the PRK9 gene. A 50 nM concentration resulted in optimal results for this miRNA and this gene.

As controls we used first, the pGL3-Control vector that does not harbor the 3' UTR of BCL6 to account for the unspecific effects of each miRNA not related to the presence of the BCL6 3' UTR and second a commercial non-targeting control called Pre-miR Negative Control #1.

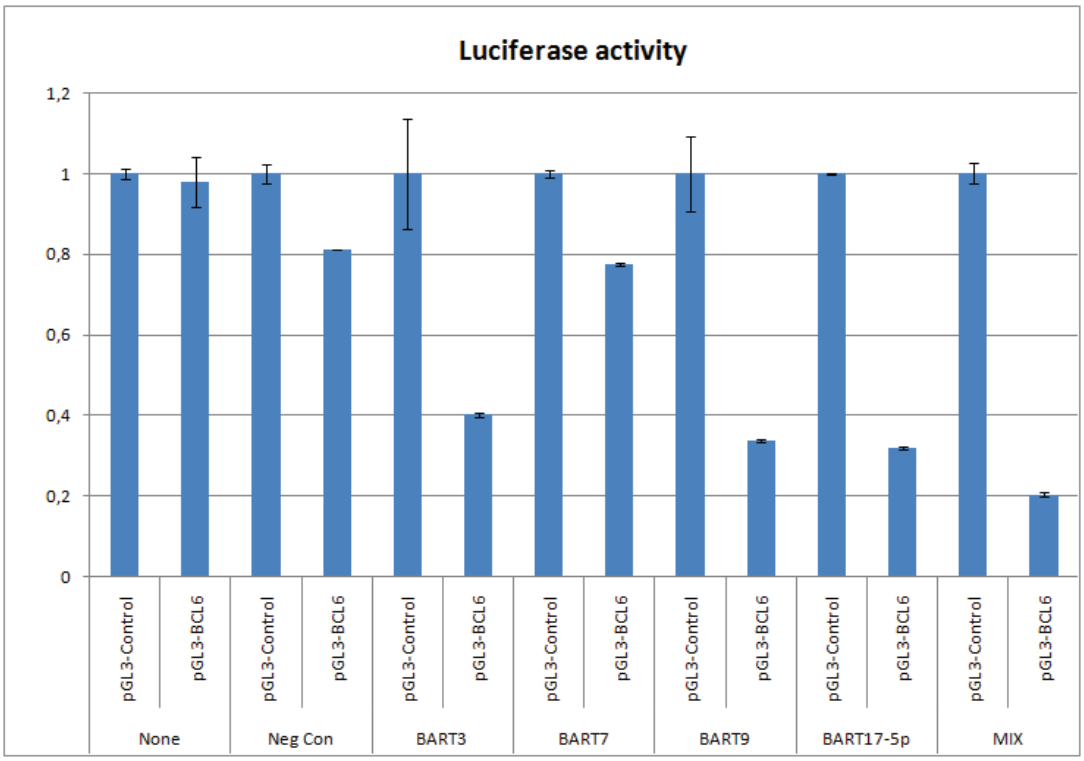

Figure 3.19. Some predicted miRNAs can downregulate BCL6. Cotransfection of several miRNAs with a luciferase reporter with (pGL3-BCL6) or without (pGL3-Co) the 3'UTR of BCL6 led to specific inhibition for miRNAs ebv-miR-BART3, ebv-miR-BART9 and ebv-miR-BART17-5p

With this approach we could identify a significant reduction in luciferase signal with three of the four miRNAs assayed (Figure 3.19). Ebv-miR-BART3, ebv-miR-BART9 and ebv-miR-BART17-5p reduced the luciferase signal around 60%, however the reduction in the signal for

ebv-miR-BART7 was around 20% a value that was similar to the one obtained when we transfected the negative control. We did not explore the effect of the ebv-miR-BART10* because the low expression of this miRNA indicates that the functional miRNA in patients is the complementary strand, ebv-miR-BART10.

Additionally, we also decided to study if these miRNAs could have a collaborative effect to regulate BCL6. To this end we also co-transfected the four miRNAs at a concentration of 10 nM each. With this mix we obtained a reduction of luciferase signal around 80% (Figure 3.19) supporting the hypothesis that these miRNAs can collaborate to repress the same target. The combination of different miRNAs resulted in potent inhibition, especially if we take into account that ebv-miR-BART7 seemed not to be able to reduce the luciferase signal.

Anyway, in order to avoid possible artifacts derived from the forced co-expression of the 3'UTR and the miRNAs we tested our hypothesis on the endogenous protein.

3.15.2 EFFECTS OF microRNAS ON ENDOGENOUS BCL6 PROTEIN

In order to validate the results obtained with the luciferase assays, we investigated the role of EBV-encoded miRNAs on the endogenous BCL6 protein. We first selected several lymphoid cell lines that expressed BCL6 because we thought these models would be more closely related to the situation in the patient than using a cell line derived from non-lymphoid tissues. However, lymphoid cell lines have the disadvantage of being very difficult to transfect. Therefore we used a high-efficiency electroporation device called Microporator (see section 2.14.1.3) that allows the transfection of lymphoid cell lines with minimum levels of cell death.

We transfected each miRNA at a final concentration of 50 nM and looked for changes in BCL6 protein expression 48 hours after the transfection. With this approach we could observe a decrease of BCL6 protein levels with several miRNAs; however the results were not the same in all cell lines (Figure 3.20).

The first striking result was that ebv-miR-BART7 was able to reduce BCL6 expression in most cell lines used. There are two possible explanations: on one hand the effects of ebv-miR-BART7 on the endogenous protein might be indirectly mediated by second players and not due to a direct interaction between the miRNA and the 3' UTR of BCL6; on the other hand, these contradictory results may account for the differences in the cellular context of each cell line. This is also suggested by the variability in the results between different cell lines.

We used three different DLBCL-derived cell lines (DB, SU-DHL-4 and SU-DHL-6) and one BL-derived cell line (Ramos). In the three DLBCL-derived cell lines transfection of the viral miRNAs ebv-miR-BART3, ebv-miR-BART9 and ebv-miR-BART17-5p led to a significant reduction in the levels of BCL6 protein 48 hours after transfection (Figure 3.20). In contrast, ebv-miR-BART7 was able to reduce BCL6 protein expression only in SU-DHL-4 and SU-DHL-6 48 hours after transfection of the miRNA while it had little or no effect in the DB cell line.

In the case of the Ramos cell line, transfection of the miRNAs led to significant reduction of BCL6 protein levels in the case of ebv-miR-BART7, ebv-miR-BART9 and ebv-miR-BART17-5p while the cells showed no response to ebv-miR-BART3 overexpression 48 hours after transfection.

3.15.3 INHIBITION OF ENDOGENOUS EBV-ENCODED microRNAS AUGMENTS THE EXPRESSION OF BCL6 PROTEIN

Finally, we also investigated whether inhibition of EBV-encoded miRNAs could increase the expression f BCL6. This is important for two reasons. First, the fact that EBV-encoded miRNAs can regulate the protein levels of BCL6 does not necessarily mean that this is the main mechanism of BCL6 down-regulation in vivo. Second, our results have shown that the EBV has different and redundant mechanisms to inhibit BCL6 protein expression. Thus, increasing the levels of BCL6 in EBV-positive cells might have an important biological effect.

To this end, we used anti-miR miRNA inhibitors against the ebv-miR-BART3, ebv-miR-BART7, ebv-miR-BART9 and ebv-miR-BART17-5p and transfected two EBV-positive DLBCL-derived cell lines (DoHH-2 and Farage). The anti-miRs are small, chemically modified single-stranded RNA molecules designed to specifically bind to and inhibit the activity of endogenous mature miRNA molecules.

In this case, using a positive control (anti-miR hsa-let7c miRNA inhibitor which inhibits hsa-let7c and induces upregulation of HMGA2) we established an optimum concentration of 200 nM. The results with the two EBV-positive cell lines were very different. On one hand, inhibition of EBV-encoded miRNAs in DoHH-2 cell line, which expresses high levels of miRNAs and almost undetectable levels of BCL6, did not led to any upregulation in the BCL6 protein expression either when we inhibited each miRNA alone or in combination (Figure 3.20). On the other hand, inhibition of EBV-encoded miRNAs in the Farage cell line, which expresses low

levels of viral miRNAs and high levels of BCL6, induced a moderate increase in the levels of BCL6 when ebv-miR-BART9 or ebv-miR-BART17-5p was inhibited but not when we inhibited either ebv-miR-BART3 or ebv-miR-BART7 alone. When we inhibited the four miRNAs with a mixture of anti-miRs at 50 nM concentrations each, we obtained similar results than inhibiting ebv-miR-BART9 or ebv-miR-BART17-5p alone at 200 nM concentrations (Figure 3.20).

The differences between cell lines can be explained in different ways. First, the almost undetectable levels of BCL6 in the DoHH-2 cell line could mean that the gene is regulated by other mechanisms such as the presence of transcription repressors in the promoter of the gene or absence of activators. Second, we cannot forget that DoHH-2 is the cell line that expresses highest levels of EBV-encoded miRNAs. Hence, inhibition of four miRNAs could not be enough to allow the re-expression of BCL6 if other BCL6-targetting miRNAs are at very high concentrations. The increased expression of BCL6 in the Farage cell line after miRNA inhibition did not result in any evident effect on cell viability. However we have experimentally tested that the effect of the synthetic RNAs that we transfect does not last more than 72 hours. This short time window is enough to see effects in the levels of expression but might not be enough to see effects on cell viability, especially in a cell line that already expresses BCL6 and in which the increase in BCL6 protein expression after miRNA inhibition is not dramatic.

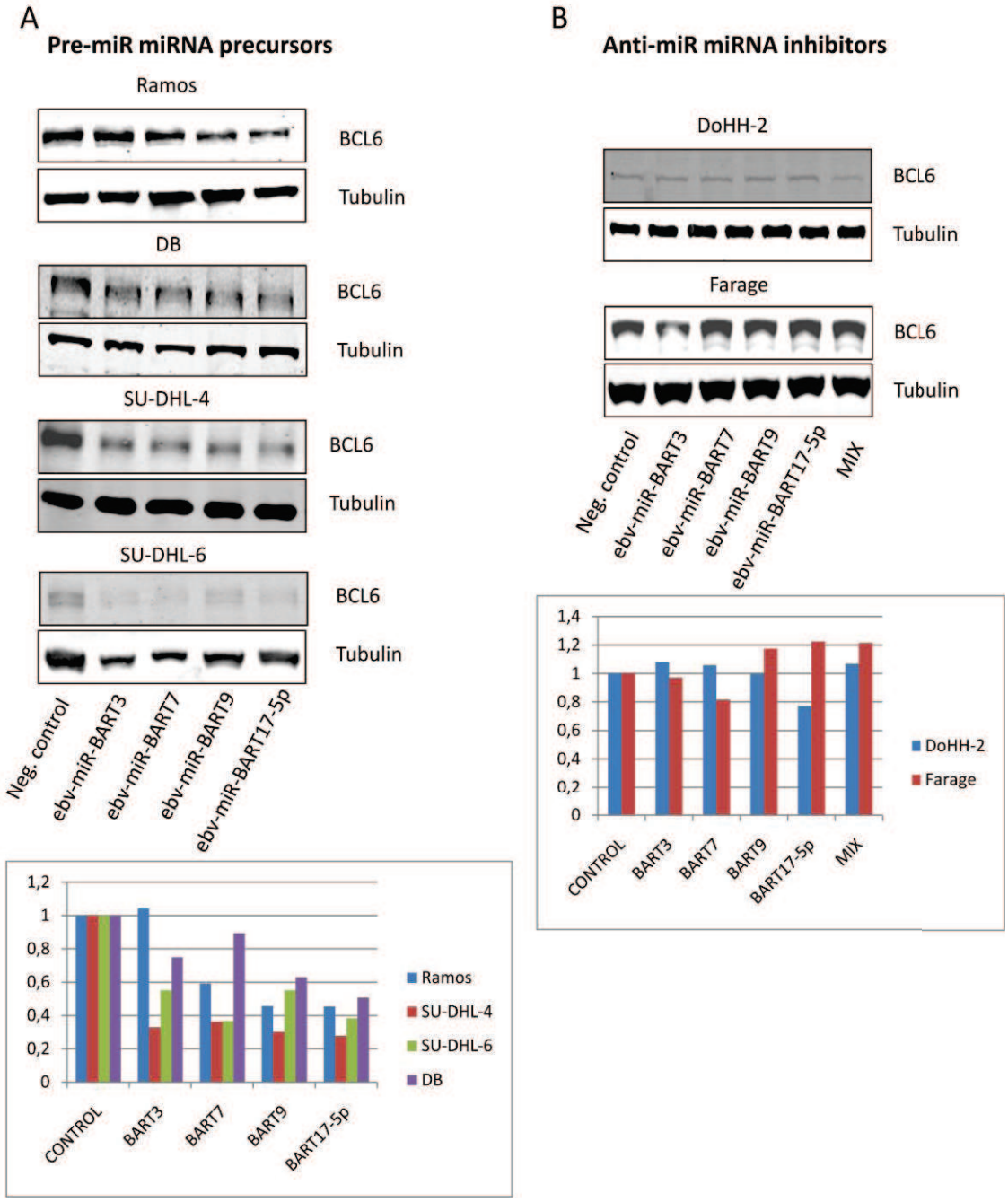

Figure 3.20. (A)Transfection of the DLBCL cell lines with several miRNAs led to a decreased BCL6 expression. BCL6 signal was normalized using tubulin (lower panel). (B) Transfection of anti-miRNA inhibitors led to a moderate upregulation of BCL6 in the Farage cell line. DoHH-2 cell line showed no response to miRNA inhibition. BCL6 signal was normalized using tubulin (lower panel)

4. DISCUSSION

Cancer is a complex disease that follows a multi-step model to develop. This multi-step model encompasses both genetic and epigenetic alterations that finally lead to the development of cancer.

These alterations provide advantages to the tumor cell that allow it to acquire self-sufficiency to growth signals, insensitivity to anti-growth signals, limitless replicative potential, resistance to apoptosis, capacity to sustain angiogenesis and ability to invade tissues and metastasize (Hanahan and Weinberg, 2000). There is increasing evidence that an additional characteristic is the acquisition of stem cell properties. This has led to cancer stem cells (CSCs) being postulated as the origin of some tumors. This is supported by the fact that tumors are composed of a heterogeneous population of cells while being derived from a single clone. Ongoing mutagenesis can only explain part of this process. Thus, many genes and pathways that are active in embryonic stem cells are altered in cancer cells (Taipale and Beachy, 2001).

A CSC can be generated in two ways: the tumor-initiating cell (TIC) with stem cell properties may arise from a stem cell that loses the capacity to regulate its mitotic potential, in contrast it could be a downstream progenitor (or committed progenitor) cell that acquires the ability to self-renew through some molecular alterations. In fact, a recent report suggests that both of these occur (Roesch et al., 2010).

Although a broad spectrum of genetic alterations has been studied in human cancer, it is well documented that progression from normal to malignant cells also involves epigenetic changes, including extensive DNA methylation at promoter-associated CpG islands, an aberrant pattern of histone modifications and changes in the expression of microRNAs. Chromatin structure is crucial for the regulation of DNA accessibility and thus for the regulation of gene expression. Furthermore, an altered chromatin structure provokes altered gene patterns and genomic instability that can be propagated to daughter cells, causing cellular transformation to a malignant status (Jones and Baylin, 2002)

In the present work we provide new insights into the epigenetic mechanisms that lead to development of lymphomas. We focused our attention in the Polycomb group of proteins and microRNAs.

4.1 SUZ12 AND THE PATHOGENESIS OF MANTLE CELL LYMPHOMA

SUZ12 is one of the core components of the PRC2. The other core components are EZH2 and EED and other components that can be molecular partners of SUZ12 are RbAp48, RbAp46, PHF1, AEBP2, SIRT1, HDAC1 and HDAC2 amongst others.

EZH2 has been implicated in several human malignancies such as prostate carcinoma (Bachmann et al., 2006; Varambally et al., 2002), breast carcinoma (Bachmann et al., 2006; Bracken et al., 2003; Puppe et al., 2009), melanoma (Leung et al., 2004), bladder cancer (Bracken et al., 2003; Raman et al., 2005), glioma (Suva et al., 2009), endometrial carcinoma (Bachmann et al., 2006), lymphomas (Bracken et al., 2003; Visser et al., 2001), colon carcinoma (Bracken et al., 2003), glioblastoma (Bracken et al., 2003), Ewing tumor (Burdach et al., 2009), several lymphomas (Morin et al., 2010), myeloid malignancies (Ernst et al., 2010; Nikoloski et al., 2010) and acute myeloid leukemia (Paul et al.).

However, although some studies have demonstrated overexpression of SUZ12 in colon and breast tumors (Kirmizis et al., 2003; Kirmizis et al., 2004), its real relevance in human cancer is yet to be established.

In the first part of this work, we present various results that point to the importance of SUZ12, independently of EZH2, in tumorigenesis in general and MCL pathogenesis in particular.

First, we have studied the expression pattern of SUZ12 and EZH2 in normal human tissues with two different objectives. On one hand, this is important to have a baseline to study tumors. Comparing the expression between normal tissues and tumors gives information about which patterns of expression are associated to malignant transformation. On the other hand, the study of SUZ12 in normal samples can give an idea of the processes in which SUZ12 may be important.

EZH2 was widely detected in most human normal tissues with very few exceptions such as superficial cells of the larynx. This point to an essential function of EZH2 in most tissues and this may be due to the fact that EZH2 is the only PRC2 component that carries methyltransferase activity.

However, the expression pattern of SUZ12 was quite different. This may indicate two things: first, that SUZ12 is dispensable for some of the functions of PRC2. However, it has been described that SUZ12 is essential for the methyltransferase activity (Pasini et al., 2004). This could mean that EZH2 has functions independent of its methyltransferase activity. A second

possibility is that other proteins could partially substitute the absence of SUZ12. Up to our knowledge, it is not known of any protein that could substitute for SUZ12 function.

The expression pattern of SUZ12 in normal tissues indicate that SUZ12 regulates or is regulated by the cell cycle, since SUZ12 expression was mainly restricted to proliferating cells such as germinal centers in reactive lymphoid tissue, thymic cortex, epithelial basal cells and germinal cells in the testis. All these tissues are characterized by their regenerative capacity, suggesting a role for SUZ12 in tissue homeostasis and in cell cycle and proliferation. This regenerative capacity of the tissues could also mean that SUZ12 expression is essential for cells that act as progenitors. It has been published that several Polycomb proteins increase their expression when stem cells begin to differentiate and become committed progenitors (Lessard et al., 1998), so we cannot rule out that the expression of SUZ12 in these tissues could be related to an ongoing differentiation process.

Analysis of malignant samples again showed a very different pattern of expression for the two PRC2 components that we have studied. EZH2 was expressed in all cancer types analyzed and only few tumors showed loss of expression in a percentage of cases. Strikingly, all the tumor types derived from the skin showed loss of expression in a small fraction of tumors, indicating that these tumors might be tolerant to depletion in some PcG components or might have alternative oncogenic mechanisms that can render the cells resistant to a lack of EZH2 expression.

Another finding in human tumors may indicate that the PcG complexes may suffer tissue-dependent changes. The presence of tumors that express SUZ12 but not EZH2 can be an indication that SUZ12 can have EZH2-independent functions under some circumstances. This notion is also supported by the fact that superficial cells of the larynx do express SUZ12 but not EZH2, so the EZH2-independent functions of SUZ12 may be also physiological.

We found overexpression of SUZ12 in several tumors, including germinal cell-derived tumors, tumors from the gastrointestinal tract, astrocytomas, squamous cell carcinomas of the larynx, melanomas, skin basal cell carcinomas, lung neuroendocrine small-cell carcinoma, pituitary and parathyroid adenomas, breast carcinomas and other gynecological tumors and B and T cell lymphomas. A significant proportion of B-cell lymphomas arise from proliferating germinal center B-cells, called centroblasts. These cells normally express SUZ12 so we cannot exclude the possibility that SUZ12 expression in lymphomas may reflect the differentiation status of the cell that gave rise to the tumor. However in MCL, we have found high expression of SUZ12 in contrast with its absence in the non-malignant mantle zone cells in reactive lymph

node. Thus, overexpression of SUZ12 in MCL is a cancer-specific feature. In short, our results extend previous observations of the strong expression of SUZ12 in human tumors (Kirmizis et al., 2003; Kirmizis et al., 2004).

Altered expression of a protein is not sufficient for considering it causally involved in the tumorigenesis. It could be that the altered expression is just a marker of the disease but the underlying oncogenic mechanism could be unrelated to the protein investigated. However, genetic or genomic abnormalities that target directly the gene indicate that the phenomenon is not only a surrogate of other oncogenic mechanisms but has a sense by itself.

Thus our findings of *SUZ12* locus (17q11.2) amplification and copy gains associated with protein overexpression in several tumors such as mesothelioma (amplification in 1/10), melanoma (amplification in 1/10), skin basal cell carcinoma (gain in 1/10), thyroid follicular carcinoma (amplification in 1/8), leiomyosarcoma (gain in 1/6), ovary serous cystoadenocarcinoma (amplification in 1/6) and especially in MCL (3/77 amplifications and 4/77 gains), along with the presence of *SUZ12* translocations in endometrial stromal sarcomas (Koontz et al., 2001a; Oliva et al., 2007), support the hypothesis that SUZ12 has an oncogenic function and contributes to tumor formation and maintenance.

It is interesting to note that amplification of *SUZ12* locus was more frequently found in aggressive variant cases of MCL (two out of four cases showed gene amplification by standard criteria). The gene locus amplification was associated with the highest levels of SUZ12 expression. This could mean that SUZ12 is not only important for MCL pathogenesis but its expression also correlates to aggressiveness of the disease. This phenomenon has already been described for other PRC2 members such as EZH2 which expression is correlated to the aggressiveness of the tumor in prostate cancer (Varambally et al., 2002).

Another interesting issue that focused our attention in MCL is that SUZ12 overexpression was mainly found in lymphomas that derive from germinal center B cells and are characterized by a high growth fraction (like diffuse large B cell lymphomas) or was restricted to proliferating cells in other lymphoid tumors such as chronic lymphocytic leukemia, follicular lymphoma, and splenic marginal zone lymphoma.

MCL seems to be an exception because it is a tumor characterized by lower or intermediate proliferation rate, which do not derive from germinal center B cells and still expresses high levels of SUZ12 in the majority of cases.

Our findings became even more interesting when we looked at the expression of miRNAs in MCL cases. It has been estimated that at least one-third of the genome may be regulated by microRNAs (Lewis et al., 2005; Lim et al., 2005). MicroRNA deregulation has been proposed as a general mechanism of carcinogenesis.

Our data suggest that loss of expression of hsa-miR-126 and hsa-miR-200b may account for the overexpression of SUZ12 in many MCL patients, revealing an even greater complexity of the genetic mechanisms that drive carcinogenesis than previously appreciated. However we are aware that the data provided in this issue is only correlative and the hypothesis that these two miRNAs regulate SUZ12 must be experimentally confirmed by using *in vitro* manipulated cell lines. Anyway, the data obtained from the MicroCosm database indicate that there are very few miRNAs with the potential of inhibiting SUZ12 expression, a fact that increases the probability that hsa-miR-126 and hsa-miR-200b are *bona fide* regulators of SUZ12.

Given the especial characteristics of MCL in relation with SUZ12 expression in the tumor and in the normal counterpart and the finding of genomic abnormalities involving the *SUZ12* locus we decided to use MCL to depict the role of SUZ12 in tumorigenesis and its putative oncogenic function. This has been further supported by the functional assays described here and the integrative genomic analysis performed in cell lines and malignant samples.

To functionally validate the oncogenic role of SUZ12 in MCL, we have silenced SUZ12 expression by RNAi in two different MCL-derived cell lines, and we have evaluated the effect of SUZ12 depletion on levels of H3K27me3, cell proliferation, apoptosis, and cell survival. The clear decrease in H3K27me3 after SUZ12 silencing demonstrated that SUZ12 knockdown affects the function of the PRC2 in accordance with previous reports (Pasini et al., 2004).

Moreover this suggests that, SUZ12 is necessary for EZH2-methyltransferase activity in different conditions and models so, if EZH2 have SUZ12-independent functions as commented before, these might not rely on the methyltransferase activity of SUZ12. However it is still possible that EZH2-mediated methyltransferase activity can be restored by other factors in SUZ12 deficient cells in some uncommon situations.

When we studied viability of SUZ12 deficient cells, we could observe that SUZ12 knockdown resulted in an increased apoptosis, as demonstrated by annexin V and PARP cleavage analysis.

The increase in apoptosis was maintained over time leading to a progressive reduction in the SUZ12 deficient population as assessed by cell counting and competition assays. Thus,

SUZ12 knock down compromises cell viability and leads to big decrease in cell number over time. These results indicate that SUZ12 expression contributes to cell survival in MCL through the inhibition of apoptosis and supporting cell proliferation.

SUZ12 is known to exert its function on the Polycomb-PRC2 complex through the direct repression of many target genes. The identification of SUZ12 direct targets and the discovery of genes/pathways co-regulated by SUZ12 are essential to understand their role and relevance in MCL. Although other studies have already tackled this question (Bracken et al., 2006; Lee et al., 2006) in other models, it has been demonstrated that SUZ12 targets vary among different cell types (Squazzo et al., 2006).

Therefore, we decided to identify SUZ12 targets that could mediate the effect on MCL-derived cell line viability and explain their role in MCL pathogenesis. We have approached this question by combining ChIP-on-chip for SUZ12-target identification with gene expression profiling of these targets in SUZ12-silenced cells and MCL samples.

We have found several genes related to apoptosis among SUZ12 targets (including BCL2, BID, cFLIP and several BIRC family members). The fact that some apoptosis-related SUZ12 targets were anti-apoptotic, may lead to the assumption that SUZ12 can have a pro-apoptotic function rather than inhibiting apoptosis. However, the phenotypic effect seen in MCL cell lines after SUZ12 knock down supports the notion that, overall SUZ12 overexpression results in inhibition of apoptosis.

We also found that SUZ12 targets several genes related to cell proliferation (several INK4 family genes, cyclins, and CDKs). Again, the presence of cyclins and CDKs seems contradictory with a putative oncogenic role of SUZ12; however several cyclins and CDKs are tissue or cell type specific and some of them are dispensable depending on the cell (Santamaria et al., 2007). In contrast, SUZ12 targets the CDK inhibitors CDKN2A, CDKN2B, CDKN2C and CDKN2D which is supports the idea of an oncogenic role for SUZ12.

More arguments that favor our hypothesis are the discovery that SUZ12 targets several genes related to checkpoint regulation (CHK1, BUB3, MADL2, GADD45, and CDK6) and DNA damage and repair (ATM, GMNN, and MLHL1) inhibiting two of the key signaling pathways that suppress tumor development.

SUZ12 also targets several transcription factors and genes involved in development and differentiation in MCL cells, which is in accordance with previous results (Bracken et al., 2006; Lee et al., 2006; Squazzo et al., 2006).

Several of these targets are genes of relevance in MCL (Figure 4.1). For instance, CDKN2A, ATM, BCL10, and RBL1, identified here as being SUZ12 targets, are frequently deleted or lost in MCL (reviewed in (Jares et al., 2007)). This means that SUZ12 is collaborating to the inactivation of these genes by epigenetic mechanisms. Other important pathways in MCL such as the NF-κB pathway are targeted by SUZ12 (BLIMP1, IKBKG, and NFKB2) indicating an abnormal regulation of this key pathway.

Many of these genes have been previously described as SUZ12 targets in other cell lines (e.g. BMP2, CDKN2A, SOX3, and GADD45G), but many others not and could be specific of MCL. This is the case for many interesting genes such as ATM, BIRC family genes, BTK, BUB3, MAD2L1, and RBL1, among others, some of which have been validated by classic ChIP suggesting that they are *bona fide* SUZ12-targets, and possibly specific to MCL cells. Moreover, SUZ12 targets several miRNAs, some of which were already known to be involved in cancer.

Many of these genes were confirmed to be inversely correlated with SUZ12 expression in MCL samples, such as BIRC2, TMBIM4, XRCC6, JMJD2D, MAD2L1 and BUB3, among others. Some SUZ12 target genes that do not correlate with SUZ12 expression in MCL cases might be repressed by other mechanisms in SUZ12-negative cases. Some SUZ12 targets were also re-expressed after SUZ12 knockdown in a MCL cell line. The fact that some of the SUZ12 targets remained unaltered after SUZ12 depletion has several possible explanations. For instance, many SUZ12 targets may require not only the depletion of SUZ12 but also additional events like DNA demethylation or the presence of an activator to be expressed again (Bracken et al., 2006; Sparmann and van Lohuizen, 2006).

All these findings strongly indicate that SUZ12 collaborates in deregulating the expression or function of many important pathways controlling MCL pathogenesis and SUZ12 overexpression may account for some of the still unexplained features of MCL, including abnormal DNA repair, increased resistance to apoptosis.

Interestingly, some studies highlight the ability of some drugs to interfere with the PRC2 complex. Tan et al. (Tan et al., 2007) reported how DNZep, a drug that disrupts the function of the PRC2 complex, can induce apoptosis in cancer cells but not in normal cells. The drug also induced the re-expression of several genes involved in development and differentiation (Miranda et al., 2009). The re-expression of these genes can be indicative that cancer cells are losing self-renewal capacity.

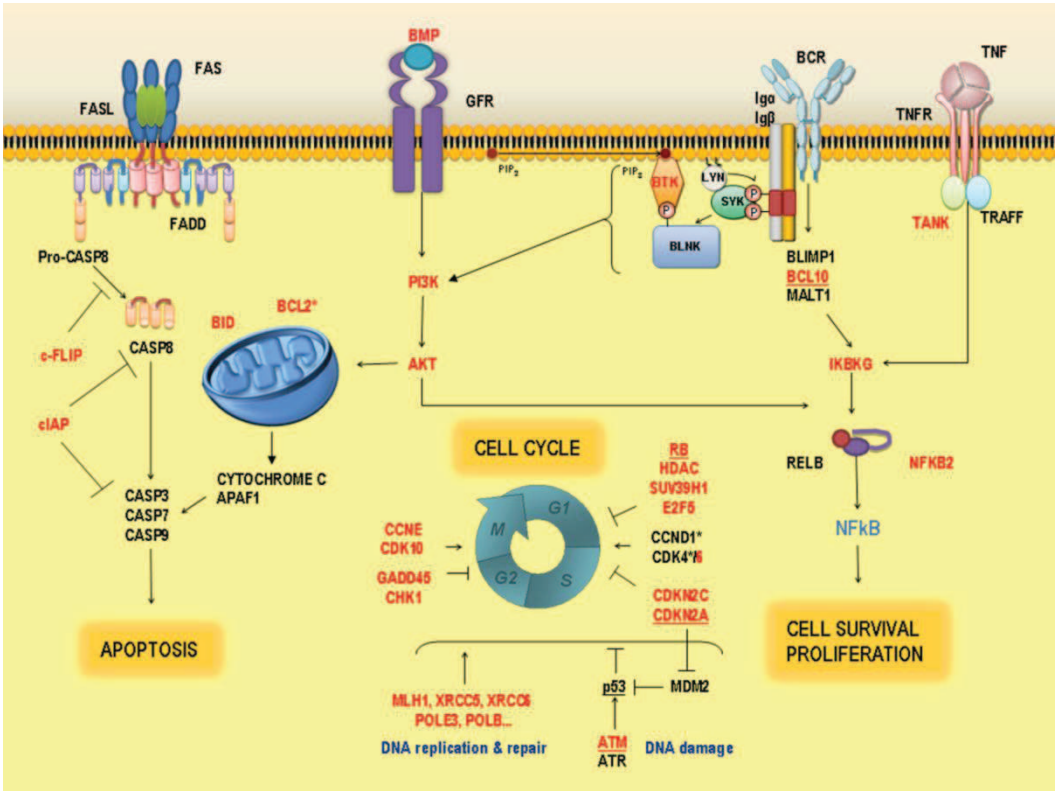

Figure 4.1. SUZ12 regulates the expression or function of multiple important pathways controlling MCL pathogenesis. Genes identified as SUZ12 targets by ChIP-on chip in red. Genes marked with * suffer translocation or overexpression in MCL cases. Genes underlined are frequently deleted in MCL.

Some studies also point to the fact that some histone deacetylase inhibitors (HDACi), such as LBH589 and LAQ824, can also deplete the PRC2 complex in malignant cells in acute myeloid leukemia (AML) (Fiskus et al., 2006). Combination of DNZep with HDACi has been also tested in AML with good results (Fiskus et al., 2009).

4.2 REGULATION OF BCL6 BY EBV-ENCODED microRNAS

EBV is a lymphotropic virus that has been implicated in the development of several lymphoid malignancies. The oncogenic potential of many of the proteins encoded by the virus has been extensively studied (Klein et al., 2010). These investigations has led to the discovery that the latent membrane protein LMP1 and the nuclear antigens EBNA-2, -3, -5 and -6 are essential for immortalization of B lymphocytes (Kaye et al., 1993). However the EBV also expresses several RNAs that do not translate into proteins. On one hand, the Epstein Barr-

encoded RNAs (EBERs) and on the other hand several miRNAs that are grouped in two clusters: the BHRF and the BART clusters. The biological significance as well as the oncogenic potential of these miRNAs has been poorly investigated.

Thus we have investigated the role of EBV-encoded miRNAs in DLBCL where the role of EBV is not well defined.

First we have analyzed the pattern of expression of EBV-encoded miRNAs in a series of 36 patients (33 negative and 3 positive) and we have found a very constant pattern of expression in the positive cases. The EBV-positive cases did not express all the viral miRNAs but only a group of 22 miRNAs that were the product of 15 pre-miRNAs. None of the miRNAs belonged to the BHRF1 cluster, a finding that confirms previous publications that propose that the highest levels of these miRNAs are reached during the lytic cycle (Pfeffer et al., 2004).

Among the EBV-encoded miRNAs that were differentially expressed in these DLBCL cases; we found some miRNAs that has been described to exert a protective function for the host cell. Three of these miRNAs, ebv-miR-BART1-5p, ebv-miR-BART16 and ebv-miR-BART17-5p, target the viral antigen LMP1 (Lo et al., 2007) and avoids the growth inhibitory effect of the overexpression of this protein (Liu et al., 2002; Lu et al., 1996). Another miRNA, ebv-miR-BART5 has a cellular target, PUMA and its inhibition promotes host survival. In both cases it seems clear that one of the main advantages that confer the virus to the host cell is to impede cell death.

BCL6 is the most frequently involved oncogene in the pathogenesis of DLBCL, where it is hypermutated or translocated in a high number of cases (Pasqualucci et al., 2003; Ye, 2000). BCL6 is a key repressor that orchestrates many of the events occurring during the germinal center reaction. However, EBV positive cells seem, in most cases, not to participate in the germinal center reaction (Araujo et al., 1999). BCL6 can be downregulated *in vitro* by transfection of the viral LMP1 protein (Kuppers, 2003), but we have studied the relationship between BCL6 and EBV in a series of 149 patients of DLBCL and we have found an inverse correlation even in the absence of LMP1 expression. The reason why many of these DLBCL did not express LMP1 remains unknown, but we have found the expression of the LMP1-targetting miRNAs ebv-miR-BART1-5p, ebv-miR-BART16 and ebv-miR-BART17-5p in these lymphomas.

Therefore, BCL6 must be down-regulated in these cases by other means. We wanted to test the hypothesis that the down-regulation of BCL6 in DLBCL could be due to the expression of BCL6-targetting miRNAs by the virus. As a first step we have performed a bioinformatic

prediction using the miRanda algorithm. This prediction rendered 21 binding sites in the 3' UTR of BCL6 for 18 EBV-encoded miRNAs. In spite of the stringent thermodynamic criterion that we have used (-20 Kcal/mol) we found a high number of miRNAs. This might be a reflection of a redundant or a synergistic system. From this list, 10 miRNAs were found differentially expressed in the first series of 36 DLBCL patients and therefore we selected four miRNAs for functional validation based on bioinformatic parameters.

However, in the miRNA microarray we had just 3 EBV-positive cases so we decided to study the expression of these four miRNAs plus the ebv-miR-BART10* that had very good score in miRanda but was not included in the microarray, in 40 patients (15 positive and 25 negative) included in the second series of 149 patients by RT-PCR. We found that all the miRNAs analyzed were expressed in the EBV-positive cases. Notably the expression of ebv-miR-BART10* was around 10-fold less than the other miRNAs probably indicating that this strand is not entering into the RISC complex and is being targeted for degradation.

A striking finding is that we still could detect the expression of several of these miRNAs in EBV-negative cases (although at a much lower level). There are several possible explanations for this. The most obvious is that RT-PCR technique applied to miRNAs has some limitations. We used TaqMan probes that use a looped RT primer to increase melting temperature of the primer and to avoid amplification of immature miRNA sequences. However, due to the short extension of miRNAs the design of the primers is difficult and may not be as favorable as in the case of mRNA. The unexpected observations indicated here might be not important in cells expressing the target miRNA because the transcript will efficiently compete with the unspecific background. However, if the miRNA is not present, unspecific amplification could be giving some signal. Another possibility is that there are EBV-positive non-malignant cells in the biopsies that we have used and, although they are uncommon, we still can detect the expression of EBV-encoded miRNAs originated in these cells.

Tumor cell lines are not always adequate models and very often do not resemble some of the features of the original tumors. However, our results of miRNA levels in cell lines explain why the phenomenon observed in patients is not reproduced in cell lines. In cell lines, the presence of EBV does not always result in high expression of the miRNAs. Hence, BCL6 is not repressed in those cell lines with low levels of EBV-encoded miRNAs. These results also offer a possible explanation of why EBV does not induce down-regulation of BCL6 in BL. Nevertheless it remains to be demonstrated that EBV-positive BL patients express lower levels of these miRNAs than EBV-positive DLBCL patients.

Using luciferase assays we have demonstrated that at least three of these miRNAs (ebv-miR-BART3, ebv-miR-BART9 and ebv-miR-BART17-5p) can decrease BCL6 protein expression. This has been also confirmed in BCL6 positive cell lines by measuring the effect of the miRNAs on BCL6 protein levels. The results at the protein level differed slightly from the results obtained in the luciferase assays, especially with ebv-miR-BART7. This could reflect an indirect effect of this miRNA (which also makes sense) or, more probably, a cell context-dependent phenomenon that could be related to target-site accessibility.

Moreover, using anti-miR miRNA inhibitors, we could increase the expression of BCL6. It is interesting that we could not re-express BCL6 in the DoHH-2 cell line, which expresses the highest levels of miRNAs and the lowest levels of BCL6 protein. In this cell line, BCL6 might be transcriptionally inactive because it is being regulated at a different level (i.e. by a co-repressor) or that the concentration of anti-miR that we have used is not enough to inhibit the high levels of EBV-encoded miRNAs in this cell line.

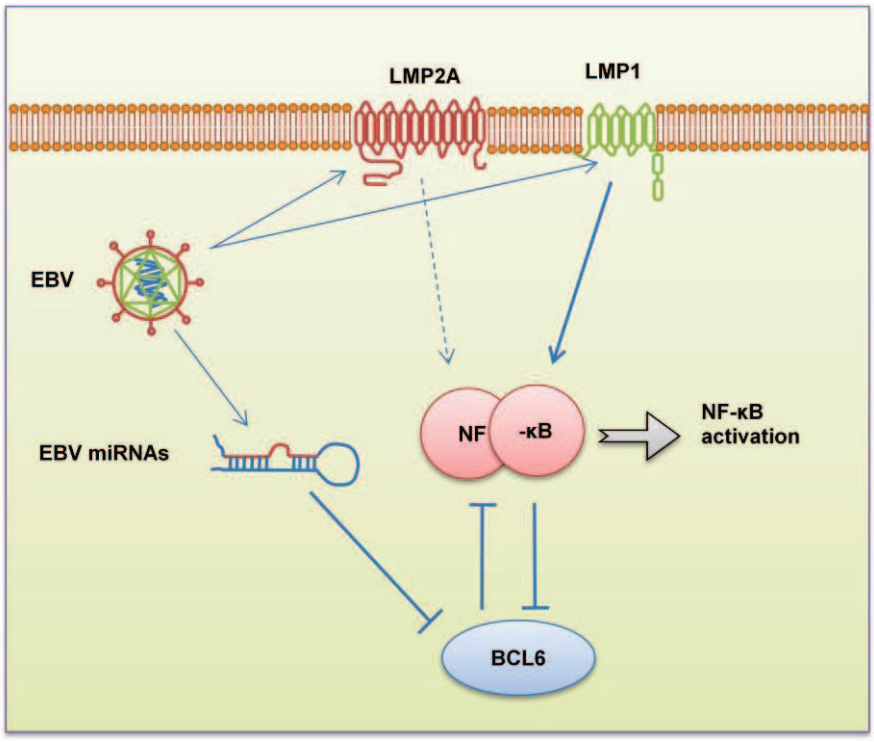

Figure 4.2. EBV activates NF-κB pathway directly (full line arrow) or indirectly (dashed line arrow) through latent membrane proteins (LMP1 and LMP2A) as a survival mechanism. At the same time it inhibits BCL6 to avoid NF-κB repression.

The reason by which EBV-encoded miRNAs down-regulate BCL6 remains unknown. However, we could speculate that it is a mechanism to allow the activation of the NF-κB pathway. BCL6

represses NF-κB in normal and pathogenic conditions (Perez-Rosado et al., 2008). However, several of the viral proteins such as LMP1 and LMP2A can activate directly or indirectly the NF-κB pathway to promote the survival of the host cell (Figure 4.2) (Cahir-McFarland et al., 2004; Cahir McFarland et al., 1999; Keller et al., 2006; Kung and Raab-Traub, 2010; Merchant et al., 2001; Mosialos et al., 1995; Song and Kang, 2010). Thus to down-regulate BCL6 is a pre-requisite for the virus in order to survive in the host cell.

This could have therapeutic implications. Taking into account that BCL6 functions as an oncogene in DLBCL, the presence of the EBV and the down-regulation of BCL6 indicate that, in infected cells, BCL6 confers disadvantages for the tumor cells. Thus inhibiting EBV-encoded miRNAs in these cells to increase the levels of BCL6 could be toxic for the cell. Moreover, in EBV-negative DLBCL cases and cell lines, inhibition of BCL6 by a small-molecule inhibitor leads to the suppression of tumor growth in xenograft models and to cell death in primary DLBCLs from human patients (Cerchietti et al., 2010).

4.3 PERSPECTIVES

In summary, in this work we have shown in first place that alterations in the PRC2 complex are common in human cancer and can be relevant in the pathogenesis of the tumors. It would be interesting to study the expression pattern of the third PRC2 core component, EED, because given the fact that EZH2 and SUZ12 act as oncogenes in many tumors, it is plausible that EED also exerts an oncogenic effect under some conditions. Moreover, we have seen a very different expression pattern for SUZ12 and EZH2 but we still do not know if the EED expression pattern is more similar to EZH2, to SUZ12 or has a distinct pattern.

Second, we have demonstrated that the oncogenic virus EBV takes advantage of the host's molecular machinery and hijacks the miRNA pathway to induce the regulation of BCL6. Although here we have only explored the relationship with BCL6, many other cellular targets may be affected by EBV infection and be relevant to its oncogenic potential. Thus, it would be interesting to study the effect of these miRNAs at the proteome level using quantitative proteomic profiling (Khan et al., 2010) in order to elucidate the exact role of these miRNAs in DLBCL. Moreover, the therapeutic implications of our discoveries also deserve further investigation in the adequate models.

CONCLUSIONS/ CONCLUSIONES

1. SUZ12 and EZH2, although being both core components of the PRC2, are not expressed simultaneously in normal tissues and tumors. EZH2 was ubiquitously expressed in almost every tissue, while SUZ12 showed a most restricted expression pattern, associated to proliferation.

2. SUZ12 is altered in human cancers, including lymphoid, pulmonary cancer, vascular tumor, germ-cell tumors, and skin tumors. The alterations include protein overexpression as well as copy number changes.

3. SUZ12 loss interferes with the H3K27me3 mark and induces a decrease of cell viability in mantle cell lymphoma derived cell lines.

4. Genome-wide mapping of SUZ12 gene targets suggests that SUZ12 controls several important functions such as apoptosis, proliferation, checkpoint regulation and DNA damage and repair.

5. Epstein Barr virus-positive diffuse large B cell lymphoma samples express a restricted cluster of EBV-encoded miRNAs, located within the BART cluster and most of them with unknown function.

6. Epstein Barr virus and BCL6 expression are mutually exclusive phenomena in diffuse large B-cell lymphoma

7. Several of the EBV-encoded miRNAs that are expressed in EBV-positive DLBCL samples target BCL6 and inhibit its expression. *In vitro* studies demonstrate the ability of several EBV-encoded miRNAs to collectively modulate BCL6 expression.

1. Aunque SUZ12 y EZH2 son ambos miembros centrales del complejo PRC2, no siempre se expresan de manera simultánea en tejidos normales y tumores. La expresión de EZH2 se detectó en prácticamente todos los tejidos y tumores, mientras que SUZ12 presentó un patrón asociado a proliferación.

2. SUZ12 se encuentra alterado en cáncer, incluyendo tumores linfoides, pulmonares, vasculares, germinales y de piel. Estas alteraciones incluyen aumentos en los niveles de expresión y variaciones en el número de copias.

3. La deficiencia de SUZ12 interfiere con la modificación epigenética H3K27me3 y produce un descenso en la viabilidad celular de líneas celulares derivadas de linfoma de células del manto.

4. La identificación a nivel genómico de los genes diana de SUZ12 sugiere que SUZ12 controla funciones importantes tales como apoptosis, proliferación, regulación de puntos de control y daño y reparación del ADN.

5. Muestras de pacientes de linfoma difuso de células B grandes positivos para el virus de Epstein Barr expresan un grupo restringido de microARNs codificados por el virus, localizados en el grupo BART, la mayoría de los cuales tiene función desconocida.

6. La presencia del virus de Epstein Barr y la expresión de BCL6 son fenómenos recíprocamente excluyentes en linfoma difuso de células B grandes.

7. Varios de los microARNs codificados por el virus y que son expresados en muestras de pacientes de linfoma difuso están dirigidos contra BCL6 e inhiben su expresión. Estudios *in vit*ro demuestran la capacidad de varios microARNs codificados por el virus para regular colectivamente los niveles de expresión de BCL6.

REFERENCES

Akasaka, T., Tsuji, K., Kawahira, H., Kanno, M., Harigaya, K., Hu, L., Ebihara, Y., Nakahata, T., Tetsu, O., Taniguchi, M., and Koseki, H. (1997). The role of mel-18, a mammalian Polycomb group gene, during IL-7-dependent proliferation of lymphocyte precursors. Immunity *7*, 135-146.

Al Saati, T., Mazerolles, C., and Caspar, S., eds. (1989). Production of two mAb identifying a novel activation antigen (CDw70), using spleen cells from nude mice bearing HLY-1 cell line.

Alexiou, P., Maragkakis, M., Papadopoulos, G. L., Reczko, M., and Hatzigeorgiou, A. G. (2009). Lost in translation: an assessment and perspective for computational microRNA target identification. Bioinformatics *25*, 3049-3055.

Alizadeh, A. A., Eisen, M. B., Davis, R. E., Ma, C., Lossos, I. S., Rosenwald, A., Boldrick, J. C., Sabet, H., Tran, T., Yu, X.*, et al.* (2000). Distinct types of diffuse large B-cell lymphoma identified by gene expression profiling. Nature *403*, 503-511.

Altekruse, S. F., Kosary, C. L., Krapcho, M., Neyman, N., Aminou, R., Waldron, W., Ruhl, J., Howlader, N., Tatalovich, Z., Cho, H.*, et al.* (2009). SEER Cancer Statistics Review, 1975-2007. In, (Bethesda, MD: National Cancer Institute).

Ambros, V. (2004). The functions of animal microRNAs. Nature *431*, 350-355.

Amini, R. M., Berglund, M., Rosenquist, R., Von Heideman, A., Lagercrantz, S., Thunberg, U., Bergh, J., Sundstrom, C., Glimelius, B., and Enblad, G. (2002). A novel B-cell line (U-2932) established from a patient with diffuse large B-cell lymphoma following Hodgkin lymphoma. Leuk Lymphoma *43*, 2179-2189.

Araki, Y., Wang, Z., Zang, C., Wood, W. H., 3rd, Schones, D., Cui, K., Roh, T. Y., Lhotsky, B., Wersto, R. P., Peng, W.*, et al.* (2009). Genome-wide analysis of histone methylation reveals chromatin state-based regulation of gene transcription and function of memory CD8+ T cells. Immunity *30*, 912-925.

Araujo, I., Foss, H. D., Hummel, M., Anagnostopoulos, I., Barbosa, H. S., Bittencourt, A., and Stein, H. (1999). Frequent expansion of Epstein-Barr virus (EBV) infected cells in germinal centres of tonsils from an area with a high incidence of EBV-associated lymphoma. J Pathol *187*, 326-330.

Argatoff, L. H., Connors, J. M., Klasa, R. J., Horsman, D. E., and Gascoyne, R. D. (1997). Mantle cell lymphoma: a clinicopathologic study of 80 cases. Blood *89*, 2067-2078.

Babcock, G. J., Hochberg, D., and Thorley-Lawson, A. D. (2000). The expression pattern of Epstein-Barr virus latent genes in vivo is dependent upon the differentiation stage of the infected B cell. Immunity *13*, 497-506.

Bachmann, I. M., Halvorsen, O. J., Collett, K., Stefansson, I. M., Straume, O., Haukaas, S. A., Salvesen, H. B., Otte, A. P., and Akslen, L. A. (2006). EZH2 expression is associated with high proliferation rate and aggressive tumor subgroups in cutaneous melanoma and cancers of the endometrium, prostate, and breast. J Clin Oncol *24*, 268-273.

Banks, P. M., Chan, J., Cleary, M. L., Delsol, G., De Wolf-Peeters, C., Gatter, K., Grogan, T. M., Harris, N. L., Isaacson, P. G., Jaffe, E. S., and et al. (1992). Mantle cell lymphoma. A proposal for unification of morphologic, immunologic, and molecular data. Am J Surg Pathol *16*, 637-640.

Bao, N., Lye, K. W., and Barton, M. K. (2004). MicroRNA binding sites in Arabidopsis class III HD-ZIP mRNAs are required for methylation of the template chromosome. Dev Cell *7*, 653-662.

Barski, A., Cuddapah, S., Cui, K., Roh, T. Y., Schones, D. E., Wang, Z., Wei, G., Chepelev, I., and Zhao, K. (2007). High-resolution profiling of histone methylations in the human genome. Cell *129*, 823-837.

Bartel, D. P., and Chen, C. Z. (2004). Micromanagers of gene expression: the potentially widespread influence of metazoan microRNAs. Nat Rev Genet *5*, 396-400.

Barth, S., Pfuhl, T., Mamiani, A., Ehses, C., Roemer, K., Kremmer, E., Jaker, C., Hock, J., Meister, G., and Grasser, F. A. (2008). Epstein-Barr virus-encoded microRNA miR-BART2 down-regulates the viral DNA polymerase BALF5. Nucleic Acids Res *36*, 666-675.

Baruch, M., Hochberg, M., Gabay, C., Ben-Bassat, H., Shlomai, Z., and Laskov, R. (1996). Molecular characterization of an unusual non-Hodgkin's B-lymphoma cell line ("Farage") lacking the ability to produce immunoglobulin polypeptide chains. Leuk Lymphoma *21*, 485-495.

Bea, S., Tort, F., Pinyol, M., Puig, X., Hernandez, L., Hernandez, S., Fernandez, P. L., van Lohuizen, M., Colomer, D., and Campo, E. (2001). BMI-1 gene amplification and overexpression in hematological malignancies occur mainly in mantle cell lymphomas. Cancer Res *61*, 2409-2412.

Beckwith, M., Longo, D. L., O'Connell, C. D., Moratz, C. M., and Urba, W. J. (1990). Phorbol ester-induced, cell-cycle-specific, growth inhibition of human B-lymphoma cell lines. J Natl Cancer Inst *82*, 501-509.

Benjamin, D., Magrath, I. T., Maguire, R., Janus, C., Todd, H. D., and Parsons, R. G. (1982). Immunoglobulin secretion by cell lines derived from African and American undifferentiated lymphomas of Burkitt's and non-Burkitt's type. J Immunol *129*, 1336-1342.

Bernstein, B. E., Mikkelsen, T. S., Xie, X., Kamal, M., Huebert, D. J., Cuff, J., Fry, B., Meissner, A., Wernig, M., Plath, K.*, et al.* (2006a). A bivalent chromatin structure marks key developmental genes in embryonic stem cells. Cell *125*, 315-326.

Bernstein, E., Duncan, E. M., Masui, O., Gil, J., Heard, E., and Allis, C. D. (2006b). Mouse polycomb proteins bind differentially to methylated histone H3 and RNA and are enriched in facultative heterochromatin. Mol Cell Biol *26*, 2560-2569.

Bird, A. (2002). DNA methylation patterns and epigenetic memory. Genes Dev *16*, 6-21.

Bodrug, S. E., Warner, B. J., Bath, M. L., Lindeman, G. J., Harris, A. W., and Adams, J. M. (1994). Cyclin D1 transgene impedes lymphocyte maturation and collaborates in lymphomagenesis with the myc gene. Embo J *13*, 2124-2130.

Bohnsack, M. T., Czaplinski, K., and Gorlich, D. (2004). Exportin 5 is a RanGTP-dependent dsRNA-binding protein that mediates nuclear export of pre-miRNAs. RNA *10*, 185-191.

Borza, C. M., and Hutt-Fletcher, L. M. (2002). Alternate replication in B cells and epithelial cells switches tropism of Epstein-Barr virus. Nat Med *8*, 594-599.

Bosch, F., Lopez-Guillermo, A., Campo, E., Ribera, J. M., Conde, E., Piris, M. A., Vallespi, T., Woessner, S., and Montserrat, E. (1998). Mantle cell lymphoma: presenting features, response to therapy, and prognostic factors. Cancer *82*, 567-575.

Boyer, L. A., Plath, K., Zeitlinger, J., Brambrink, T., Medeiros, L. A., Lee, T. I., Levine, S. S., Wernig, M., Tajonar, A., Ray, M. K.*, et al.* (2006). Polycomb complexes repress developmental regulators in murine embryonic stem cells. Nature *441*, 349-353.

Bracken, A. P., Dietrich, N., Pasini, D., Hansen, K. H., and Helin, K. (2006). Genome-wide mapping of Polycomb target genes unravels their roles in cell fate transitions. Genes Dev *20*, 1123-1136.

Bracken, A. P., and Helin, K. (2009). Polycomb group proteins: navigators of lineage pathways led astray in cancer. Nat Rev Cancer *9*, 773-784.

Bracken, A. P., Pasini, D., Capra, M., Prosperini, E., Colli, E., and Helin, K. (2003). EZH2 is downstream of the pRB-E2F pathway, essential for proliferation and amplified in cancer. EMBO J *22*, 5323-5335.

Bruggeman, S. W., Valk-Lingbeek, M. E., van der Stoop, P. P., Jacobs, J. J., Kieboom, K., Tanger, E., Hulsman, D., Leung, C., Arsenijevic, Y., Marino, S., and van Lohuizen, M. (2005). Ink4a and Arf differentially affect cell proliferation and neural stem cell self-renewal in Bmi1-deficient mice. Genes Dev *19*, 1438-1443.

Brummelkamp, T. R., Bernards, R., and Agami, R. (2002). A system for stable expression of short interfering RNAs in mammalian cells. Science *296*, 550-553.

Burdach, S., Plehm, S., Unland, R., Dirksen, U., Borkhardt, A., Staege, M. S., Muller-Tidow, C., and Richter, G. H. (2009). Epigenetic maintenance of stemness and malignancy in peripheral neuroectodermal tumors by EZH2. Cell Cycle *8*, 1991-1996.

Cahir-McFarland, E. D., Carter, K., Rosenwald, A., Giltnane, J. M., Henrickson, S. E., Staudt, L. M., and Kieff, E. (2004). Role of NF-kappa B in cell survival and transcription of latent membrane protein 1-expressing or Epstein-Barr virus latency III-infected cells. J Virol *78*, 4108-4119.

Cahir McFarland, E. D., Izumi, K. M., and Mosialos, G. (1999). Epstein-barr virus transformation: involvement of latent membrane protein 1-mediated activation of NF-kappaB. Oncogene *18*, 6959-6964.

Cai, X., Schafer, A., Lu, S., Bilello, J. P., Desrosiers, R. C., Edwards, R., Raab-Traub, N., and Cullen, B. R. (2006). Epstein-Barr virus microRNAs are evolutionarily conserved and differentially expressed. PLoS Pathog *2*, e23.

Caldwell, R. G., Wilson, J. B., Anderson, S. J., and Longnecker, R. (1998). Epstein-Barr virus LMP2A drives B cell development and survival in the absence of normal B cell receptor signals. Immunity *9*, 405-411.

Cales, C., Roman-Trufero, M., Pavon, L., Serrano, I., Melgar, T., Endoh, M., Perez, C., Koseki, H., and Vidal, M. (2008). Inactivation of the polycomb group protein Ring1B unveils an antiproliferative role in hematopoietic cell expansion and cooperation with tumorigenesis associated with Ink4a deletion. Mol Cell Biol *28*, 1018-1028.

Calin, G. A., and Croce, C. M. (2006). MicroRNAs and chromosomal abnormalities in cancer cells. Oncogene *25*, 6202-6210.

Calin, G. A., Dumitru, C. D., Shimizu, M., Bichi, R., Zupo, S., Noch, E., Aldler, H., Rattan, S., Keating, M., Rai, K.*, et al.* (2002). Frequent deletions and down-regulation of micro- RNA genes

miR15 and miR16 at 13q14 in chronic lymphocytic leukemia. Proc Natl Acad Sci U S A *99*, 15524-15529.

Camacho, F. I., Algara, P., Rodriguez, A., Ruiz-Ballesteros, E., Mollejo, M., Martinez, N., Martinez-Climent, J. A., Gonzalez, M., Mateo, M., Caleo, A.*, et al.* (2003). Molecular heterogeneity in MCL defined by the use of specific VH genes and the frequency of somatic mutations. Blood *101*, 4042-4046.

Camp, R. L., Charette, L. A., and Rimm, D. L. (2000). Validation of tissue microarray technology in breast carcinoma. Lab Invest *80*, 1943-1949.

Cao, R., Tsukada, Y., and Zhang, Y. (2005). Role of Bmi-1 and Ring1A in H2A ubiquitylation and Hox gene silencing. Mol Cell *20*, 845-854.

Cao, R., and Zhang, Y. (2004). SUZ12 is required for both the histone methyltransferase activity and the silencing function of the EED-EZH2 complex. Mol Cell *15*, 57-67.

Capello, D., Cerri, M., Muti, G., Berra, E., Oreste, P., Deambrogi, C., Rossi, D., Dotti, G., Conconi, A., Vigano, M.*, et al.* (2003). Molecular histogenesis of posttransplantation lymphoproliferative disorders. Blood *102*, 3775-3785.

Carbone, A., Gaidano, G., Gloghini, A., Pastore, C., Saglio, G., Tirelli, U., Dalla-Favera, R., and Falini, B. (1997). BCL-6 protein expression in AIDS-related non-Hodgkin's lymphomas: inverse relationship with Epstein-Barr virus-encoded latent membrane protein-1 expression. Am J Pathol *150*, 155-165.

Caretti, G., Di Padova, M., Micales, B., Lyons, G. E., and Sartorelli, V. (2004). The Polycomb Ezh2 methyltransferase regulates muscle gene expression and skeletal muscle differentiation. Genes Dev *18*, 2627-2638.

Cerchietti, L. C., Ghetu, A. F., Zhu, X., Da Silva, G. F., Zhong, S., Matthews, M., Bunting, K. L., Polo, J. M., Fares, C., Arrowsmith, C. H.*, et al.* (2010). A small-molecule inhibitor of BCL6 kills DLBCL cells in vitro and in vivo. Cancer Cell *17*, 400-411.

Chang, H., Blondal, J. A., Benchimol, S., Minden, M. D., and Messner, H. A. (1995). p53 mutations, c-myc and bcl-2 rearrangements in human non-Hodgkin's lymphoma cell lines. Leuk Lymphoma *19*, 165-171.

Choy, E. Y., Siu, K. L., Kok, K. H., Lung, R. W., Tsang, C. M., To, K. F., Kwong, D. L., Tsao, S. W., and Jin, D. Y. (2008). An Epstein-Barr virus-encoded microRNA targets PUMA to promote host cell survival. J Exp Med *205*, 2551-2560.

Classen, A. K., Bunker, B. D., Harvey, K. F., Vaccari, T., and Bilder, D. (2009). A tumor suppressor activity of Drosophila Polycomb genes mediated by JAK-STAT signaling. Nat Genet *41*, 1150-1155.

Coiffier, B., Lepage, E., Briere, J., Herbrecht, R., Tilly, H., Bouabdallah, R., Morel, P., Van Den Neste, E., Salles, G., Gaulard, P.*, et al.* (2002). CHOP chemotherapy plus rituximab compared with CHOP alone in elderly patients with diffuse large-B-cell lymphoma. N Engl J Med *346*, 235-242.

Croce, C. M. (2008). Oncogenes and cancer. N Engl J Med *358*, 502-511.

Dellino, G. I., Schwartz, Y. B., Farkas, G., McCabe, D., Elgin, S. C., and Pirrotta, V. (2004). Polycomb silencing blocks transcription initiation. Mol Cell *13*, 887-893.

Dimri, G. P., Martinez, J. L., Jacobs, J. J., Keblusek, P., Itahana, K., Van Lohuizen, M., Campisi, J., Wazer, D. E., and Band, V. (2002). The Bmi-1 oncogene induces telomerase activity and immortalizes human mammary epithelial cells. Cancer Res *62*, 4736-4745.

Douglas, E. J., Fiegler, H., Rowan, A., Halford, S., Bicknell, D. C., Bodmer, W., Tomlinson, I. P., and Carter, N. P. (2004). Array comparative genomic hybridization analysis of colorectal cancer cell lines and primary carcinomas. Cancer Res *64*, 4817-4825.

Dukers, D. F., van Galen, J. C., Giroth, C., Jansen, P., Sewalt, R. G., Otte, A. P., Kluin-Nelemans, H. C., Meijer, C. J., and Raaphorst, F. M. (2004). Unique polycomb gene expression pattern in Hodgkin's lymphoma and Hodgkin's lymphoma-derived cell lines. Am J Pathol *164*, 873-881.

Dunwell, T., Hesson, L., Rauch, T. A., Wang, L., Clark, R. E., Dallol, A., Gentle, D., Catchpoole, D., Maher, E. R., Pfeifer, G. P., and Latif, F. (2010). A genome-wide screen identifies frequently methylated genes in haematological and epithelial cancers. Mol Cancer *9*, 44.

Dyer, M. J., Fischer, P., Nacheva, E., Labastide, W., and Karpas, A. (1990). A new human B-cell non-Hodgkin's lymphoma cell line (Karpas 422) exhibiting both t (14;18) and t(4;11) chromosomal translocations. Blood *75*, 709-714.

Endoh, M., Endo, T. A., Endoh, T., Fujimura, Y., Ohara, O., Toyoda, T., Otte, A. P., Okano, M., Brockdorff, N., Vidal, M., and Koseki, H. (2008). Polycomb group proteins Ring1A/B are functionally linked to the core transcriptional regulatory circuitry to maintain ES cell identity. Development *135*, 1513-1524.

Epstein, A. L., Levy, R., Kim, H., Henle, W., Henle, G., and Kaplan, H. S. (1978). Biology of the human malignant lymphomas. IV. Functional characterization of ten diffuse histiocytic lymphoma cell lines. Cancer *42*, 2379-2391.

Ernst, T., Chase, A. J., Score, J., Hidalgo-Curtis, C. E., Bryant, C., Jones, A. V., Waghorn, K., Zoi, K., Ross, F. M., Reiter, A*., et al.* (2010). Inactivating mutations of the histone methyltransferase gene EZH2 in myeloid disorders Nature genetics.

Espinet, B., Sole, F., Woessner, S., Bosch, F., Florensa, L., Campo, E., Costa, D., Lloveras, E., Vila, R. M., Besses, C*., et al.* (1999). Translocation (11;14)(q13;q32) and preferential involvement of chromosomes 1, 2, 9, 13, and 17 in mantle cell lymphoma. Cancer Genet Cytogenet *111*, 92-98.

Estrov, Z., Talpaz, M., Ku, S., Harris, D., Van, Q., Beran, M., Hirsch-Ginsberg, C., Huh, Y., Yee, G., and Kurzrock, R. (1998). Z-138: a new mature B-cell acute lymphoblastic leukemia cell line from a patient with transformed chronic lymphocytic leukemia. Leuk Res *22*, 341-353.

Feinberg, A. P., Gehrke, C. W., Kuo, K. C., and Ehrlich, M. (1988). Reduced genomic 5-methylcytosine content in human colonic neoplasia. Cancer Res *48*, 1159-1161.

Fernandez, V., Salamero, O., Espinet, B., Sole, F., Royo, C., Navarro, A., Camacho, F., Bea, S., Hartmann, E., Amador, V*., et al.* (2010). Genomic and gene expression profiling defines indolent forms of mantle cell lymphoma. Cancer Res *70*, 1408-1418.

Ferrer, A., Salaverria, I., Bosch, F., Villamor, N., Rozman, M., Bea, S., Gine, E., Lopez-Guillermo, A., Campo, E., and Montserrat, E. (2007). Leukemic involvement is a common feature in mantle cell lymphoma. Cancer *109*, 2473-2480.

Ferry, J. A. (2006). Burkitt's lymphoma: clinicopathologic features and differential diagnosis. Oncologist *11*, 375-383.

Fisher, R. I., Gaynor, E. R., Dahlberg, S., Oken, M. M., Grogan, T. M., Mize, E. M., Glick, J. H., Coltman, C. A., Jr., and Miller, T. P. (1993). Comparison of a standard regimen (CHOP) with three intensive chemotherapy regimens for advanced non-Hodgkin's lymphoma. N Engl J Med *328*, 1002-1006.

Fiskus, W., Pranpat, M., Balasis, M., Herger, B., Rao, R., Chinnaiyan, A., Atadja, P., and Bhalla, K. (2006). Histone deacetylase inhibitors deplete enhancer of zeste 2 and associated polycomb repressive complex 2 proteins in human acute leukemia cells. Mol Cancer Ther *5*, 3096-3104.

Fiskus, W., Wang, Y., Sreekumar, A., Buckley, K. M., Shi, H., Jillella, A., Ustun, C., Rao, R., Fernandez, P., Chen, J.*, et al.* (2009). Combined epigenetic therapy with the histone methyltransferase EZH2 inhibitor 3-deazaneplanocin A and the histone deacetylase inhibitor panobinostat against human AML cells. Blood *114*, 2733-2743.

Francis, N. J., Kingston, R. E., and Woodcock, C. L. (2004). Chromatin compaction by a polycomb group protein complex. Science *306*, 1574-1577.

Friedman, J. M., Liang, G., Liu, C. C., Wolff, E. M., Tsai, Y. C., Ye, W., Zhou, X., and Jones, P. A. (2009). The putative tumor suppressor microRNA-101 modulates the cancer epigenome by repressing the polycomb group protein EZH2. Cancer Res *69*, 2623-2629.

Fu, K., Weisenburger, D. D., Greiner, T. C., Dave, S., Wright, G., Rosenwald, A., Chiorazzi, M., Iqbal, J., Gesk, S., Siebert, R.*, et al.* (2005). Cyclin D1-negative mantle cell lymphoma: a clinicopathologic study based on gene expression profiling. Blood *106*, 4315-4321.

Gabay, C., Ben-Bassat, H., Schlesinger, M., and Laskov, R. (1999). Somatic mutations and intraclonal variations in the rearranged Vkappa genes of B-non-Hodgkin's lymphoma cell lines. Eur J Haematol *63*, 180-191.

Garcia, J. F., Roncador, G., Garcia, J. F., Sanz, A. I., Maestre, L., Lucas, E., Montes-Moreno, S., Fernandez Victoria, R., Martinez-Torrecuadrara, J. L., Marafioti, T.*, et al.* (2006). PRDM1/BLIMP-1 expression in multiple B and T-cell lymphoma. Haematologica *91*, 467-474.

Gearhart, M. D., Corcoran, C. M., Wamstad, J. A., and Bardwell, V. J. (2006). Polycomb group and SCF ubiquitin ligases are found in a novel BCOR complex that is recruited to BCL6 targets. Mol Cell Biol *26*, 6880-6889.

Gil, J., Bernard, D., Martinez, D., and Beach, D. (2004). Polycomb CBX7 has a unifying role in cellular lifespan. Nat Cell Biol *6*, 67-72.

Gires, O., Zimber-Strobl, U., Gonnella, R., Ueffing, M., Marschall, G., Zeidler, R., Pich, D., and Hammerschmidt, W. (1997). Latent membrane protein 1 of Epstein-Barr virus mimics a constitutively active receptor molecule. EMBO J *16*, 6131-6140.

Goll, M. G., and Bestor, T. H. (2005). Eukaryotic cytosine methyltransferases. Annu Rev Biochem *74*, 481-514.

Gonzalez, I., Simon, R., and Busturia, A. (2009). The Polyhomeotic protein induces hyperplastic tissue overgrowth through the activation of the JAK/STAT pathway. Cell Cycle *8*, 4103-4111.

Graham, F. L., Smiley, J., Russell, W. C., and Nairn, R. (1977). Characteristics of a human cell line transformed by DNA from human adenovirus type 5. J Gen Virol *36*, 59-74.

Griffiths-Jones, S. (2004). The microRNA Registry. Nucleic Acids Res *32*, D109-111.

Griffiths-Jones, S., Grocock, R. J., van Dongen, S., Bateman, A., and Enright, A. J. (2006). miRBase: microRNA sequences, targets and gene nomenclature. Nucleic Acids Res *34*, D140-144.

Griffiths-Jones, S., Saini, H. K., van Dongen, S., and Enright, A. J. (2008). miRBase: tools for microRNA genomics. Nucleic Acids Res *36*, D154-158.

Grimaud, C., Bantignies, F., Pal-Bhadra, M., Ghana, P., Bhadra, U., and Cavalli, G. (2006). RNAi components are required for nuclear clustering of Polycomb group response elements. Cell *124*, 957-971.

Grundhoff, A., Sullivan, C. S., and Ganem, D. (2006). A combined computational and microarray-based approach identifies novel microRNAs encoded by human gamma-herpesviruses. RNA *12*, 733-750.

Gunster, M. J., Raaphorst, F. M., Hamer, K. M., den Blaauwen, J. L., Fieret, E., Meijer, C. J., and Otte, A. P. (2001). Differential expression of human Polycomb group proteins in various tissues and cell types. J Cell Biochem Suppl *Suppl 36*, 129-143.

Hanahan, D., and Weinberg, R. A. (2000). The hallmarks of cancer. Cell *100*, 57-70.

Haupt, Y., Alexander, W. S., Barri, G., Klinken, S. P., and Adams, J. M. (1991). Novel zinc finger gene implicated as myc collaborator by retrovirally accelerated lymphomagenesis in E mu-myc transgenic mice. Cell *65*, 753-763.

Hayashita, Y., Osada, H., Tatematsu, Y., Yamada, H., Yanagisawa, K., Tomida, S., Yatabe, Y., Kawahara, K., Sekido, Y., and Takahashi, T. (2005). A polycistronic microRNA cluster, miR-17-92, is overexpressed in human lung cancers and enhances cell proliferation. Cancer Res *65*, 9628-9632.

He, L., and Hannon, G. J. (2004). MicroRNAs: small RNAs with a big role in gene regulation. Nat Rev Genet *5*, 522-531.

Heard, E., Clerc, P., and Avner, P. (1997). X-chromosome inactivation in mammals. Annu Rev Genet *31*, 571-610.

Henderson, A., Ripley, S., Heller, M., and Kieff, E. (1983). Chromosome site for Epstein-Barr virus DNA in a Burkitt tumor cell line and in lymphocytes growth-transformed in vitro. Proc Natl Acad Sci U S A *80*, 1987-1991.

Houmani, J. L., Davis, C. I., and Ruf, I. K. (2009). Growth-promoting properties of Epstein-Barr virus EBER-1 RNA correlate with ribosomal protein L22 binding. J Virol *83*, 9844-9853.

Huisinga, K. L., Brower-Toland, B., and Elgin, S. C. (2006). The contradictory definitions of heterochromatin: transcription and silencing. Chromosoma *115*, 110-122.

Iorio, M. V., Visone, R., Di Leva, G., Donati, V., Petrocca, F., Casalini, P., Taccioli, C., Volinia, S., Liu, C. G., Alder, H.*, et al.* (2007). MicroRNA signatures in human ovarian cancer. Cancer Res *67*, 8699-8707.

Ivanova, N., Dobrin, R., Lu, R., Kotenko, I., Levorse, J., DeCoste, C., Schafer, X., Lun, Y., and Lemischka, I. R. (2006). Dissecting self-renewal in stem cells with RNA interference. Nature *442*, 533-538.

Iwama, A., Oguro, H., Negishi, M., Kato, Y., Morita, Y., Tsukui, H., Ema, H., Kamijo, T., Katoh-Fukui, Y., Koseki, H*., et al.* (2004). Enhanced self-renewal of hematopoietic stem cells mediated by the polycomb gene product Bmi-1. Immunity *21*, 843-851.

Jacobs, J. J., Scheijen, B., Voncken, J. W., Kieboom, K., Berns, A., and van Lohuizen, M. (1999). Bmi-1 collaborates with c-Myc in tumorigenesis by inhibiting c-Myc-induced apoptosis via INK4a/ARF. Genes Dev *13*, 2678-2690.

Jacobs, J. J., and van Lohuizen, M. (2002). Polycomb repression: from cellular memory to cellular proliferation and cancer. Biochim Biophys Acta *1602*, 151-161.

Jadayel, D. M., Lukas, J., Nacheva, E., Bartkova, J., Stranks, G., De Schouwer, P. J., Lens, D., Bartek, J., Dyer, M. J., Kruger, A. R., and Catovsky, D. (1997). Potential role for concurrent abnormalities of the cyclin D1, p16CDKN2 and p15CDKN2B genes in certain B cell non-Hodgkin's lymphomas. Functional studies in a cell line (Granta 519). Leukemia *11*, 64-72.

Jaffe, E. S. (2009). The 2008 WHO classification of lymphomas: implications for clinical practice and translational research. Hematology Am Soc Hematol Educ Program, 523-531.

Jares, P., and Campo, E. (2008). Advances in the understanding of mantle cell lymphoma. Br J Haematol *142*, 149-165.

Jares, P., Colomer, D., and Campo, E. (2007). Genetic and molecular pathogenesis of mantle cell lymphoma: perspectives for new targeted therapeutics. Nat Rev Cancer *7*, 750-762.

Jeon, H. J., Kim, C. W., Yoshino, T., and Akagi, T. (1998). Establishment and characterization of a mantle cell lymphoma cell line. Br J Haematol *102*, 1323-1326.

Jones, P. A., and Baylin, S. B. (2002). The fundamental role of epigenetic events in cancer. Nat Rev Genet *3*, 415-428.

Joos, S., Kupper, M., Ohl, S., von Bonin, F., Mechtersheimer, G., Bentz, M., Marynen, P., Moller, P., Pfreundschuh, M., Trumper, L., and Lichter, P. (2000). Genomic imbalances including amplification of the tyrosine kinase gene JAK2 in CD30+ Hodgkin cells. Cancer Res *60*, 549-552.

Kajiume, T., Ninomiya, Y., Ishihara, H., Kanno, R., and Kanno, M. (2004). Polycomb group gene mel-18 modulates the self-renewal activity and cell cycle status of hematopoietic stem cells. Exp Hematol *32*, 571-578.

Kajiume, T., Ohno, N., Sera, Y., Kawahara, Y., Yuge, L., and Kobayashi, M. (2009). Reciprocal expression of Bmi1 and Mel-18 is associated with functioning of primitive hematopoietic cells. Exp Hematol *37*, 857-866 e852.

Kallioniemi, O. P., Wagner, U., Kononen, J., and Sauter, G. (2001). Tissue microarray technology for high-throughput molecular profiling of cancer. Hum Mol Genet *10*, 657-662.

Kamminga, L. M., Bystrykh, L. V., de Boer, A., Houwer, S., Douma, J., Weersing, E., Dontje, B., and de Haan, G. (2006). The Polycomb group gene Ezh2 prevents hematopoietic stem cell exhaustion. Blood *107*, 2170-2179.

Kanhere, A., Viiri, K., Araujo, C. C., Rasaiyaah, J., Bouwman, R. D., Whyte, W. A., Pereira, C. F., Brookes, E., Walker, K., Bell, G. W*., et al.* (2010). Short RNAs are transcribed from repressed polycomb target genes and interact with polycomb repressive complex-2. Mol Cell *38*, 675-688.

Karin, M., Cao, Y., Greten, F. R., and Li, Z. W. (2002). NF-kappaB in cancer: from innocent bystander to major culprit. Nat Rev Cancer *2*, 301-310.

Kaye, K. M., Izumi, K. M., and Kieff, E. (1993). Epstein-Barr virus latent membrane protein 1 is essential for B-lymphocyte growth transformation. Proc Natl Acad Sci U S A *90*, 9150-9154.

Keller, S. A., Hernandez-Hopkins, D., Vider, J., Ponomarev, V., Hyjek, E., Schattner, E. J., and Cesarman, E. (2006). NF-kappaB is essential for the progression of KSHV- and EBV-infected lymphomas in vivo. Blood *107*, 3295-3302.

Khalil, A. M., Guttman, M., Huarte, M., Garber, M., Raj, A., Rivea Morales, D., Thomas, K., Presser, A., Bernstein, B. E., van Oudenaarden, A.*, et al.* (2009). Many human large intergenic noncoding RNAs associate with chromatin-modifying complexes and affect gene expression. Proc Natl Acad Sci U S A *106*, 11667-11672.

Khan, A. P., Poisson, L. M., Bhat, V. B., Fermin, D., Zhao, R., Kalyana-Sundaram, S., Michailidis, G., Nesvizhskii, A. I., Omenn, G. S., Chinnaiyan, A. M., and Sreekumar, A. (2010). Quantitative proteomic profiling of prostate cancer reveals a role for miR-128 in prostate cancer. Mol Cell Proteomics *9*, 298-312.

Khan, G., Miyashita, E. M., Yang, B., Babcock, G. J., and Thorley-Lawson, D. A. (1996). Is EBV persistence in vivo a model for B cell homeostasis? Immunity *5*, 173-179.

Khvorova, A., Reynolds, A., and Jayasena, S. D. (2003). Functional siRNAs and miRNAs exhibit strand bias. Cell *115*, 209-216.

Kienle, D., Krober, A., Katzenberger, T., Ott, G., Leupolt, E., Barth, T. F., Moller, P., Benner, A., Habermann, A., Muller-Hermelink, H. K.*, et al.* (2003). VH mutation status and VDJ rearrangement structure in mantle cell lymphoma: correlation with genomic aberrations, clinical characteristics, and outcome. Blood *102*, 3003-3009.

Kilger, E., Kieser, A., Baumann, M., and Hammerschmidt, W. (1998). Epstein-Barr virus-mediated B-cell proliferation is dependent upon latent membrane protein 1, which simulates an activated CD40 receptor. EMBO J *17*, 1700-1709.

Kim, D. H., Saetrom, P., Snove, O., Jr., and Rossi, J. J. (2008). MicroRNA-directed transcriptional gene silencing in mammalian cells. Proc Natl Acad Sci U S A *105*, 16230-16235.

Kim, D. H., Villeneuve, L. M., Morris, K. V., and Rossi, J. J. (2006). Argonaute-1 directs siRNA-mediated transcriptional gene silencing in human cells. Nat Struct Mol Biol *13*, 793-797.

Kirmizis, A., Bartley, S. M., and Farnham, P. J. (2003). Identification of the polycomb group protein SU(Z)12 as a potential molecular target for human cancer therapy. Mol Cancer Ther *2*, 113-121.

Kirmizis, A., Bartley, S. M., Kuzmichev, A., Margueron, R., Reinberg, D., Green, R., and Farnham, P. J. (2004). Silencing of human polycomb target genes is associated with methylation of histone H3 Lys 27. Genes Dev *18*, 1592-1605.

Kitagawa, N., Goto, M., Kurozumi, K., Maruo, S., Fukayama, M., Naoe, T., Yasukawa, M., Hino, K., Suzuki, T., Todo, S., and Takada, K. (2000). Epstein-Barr virus-encoded poly(A)(-) RNA supports Burkitt's lymphoma growth through interleukin-10 induction. EMBO J *19*, 6742-6750.

Kleer, C. G., Cao, Q., Varambally, S., Shen, R., Ota, I., Tomlins, S. A., Ghosh, D., Sewalt, R. G., Otte, A. P., Hayes, D. F.*, et al.* (2003). EZH2 is a marker of aggressive breast cancer and

promotes neoplastic transformation of breast epithelial cells. Proc Natl Acad Sci U S A *100*, 11606-11611.

Klein, G., Klein, E., and Kashuba, E. (2010). Interaction of Epstein-Barr virus (EBV) with human B-lymphocytes. Biochem Biophys Res Commun *396*, 67-73.

Kluin-Nelemans, H. C., Limpens, J., Meerabux, J., Beverstock, G. C., Jansen, J. H., de Jong, D., and Kluin, P. M. (1991). A new non-Hodgkin's B-cell line (DoHH2) with a chromosomal translocation t(14;18)(q32;q21). Leukemia *5*, 221-224.

Kondo, Y., Shen, L., Cheng, A. S., Ahmed, S., Boumber, Y., Charo, C., Yamochi, T., Urano, T., Furukawa, K., Kwabi-Addo, B*., et al.* (2008). Gene silencing in cancer by histone H3 lysine 27 trimethylation independent of promoter DNA methylation. Nat Genet *40*, 741-750.

Kononen, J., Bubendorf, L., Kallioniemi, A., Barlund, M., Schraml, P., Leighton, S., Torhorst, J., Mihatsch, M. J., Sauter, G., and Kallioniemi, O. P. (1998). Tissue microarrays for high-throughput molecular profiling of tumor specimens. Nat Med *4*, 844-847.

Koontz, J. I., Soreng, A. L., Nucci, M., Kuo, F. C., Pauwels, P., van Den Berghe, H., Cin, P. D., Fletcher, J. A., and Sklar, J. (2001a). Frequent fusion of the JAZF1 and JJAZ1 genes in endometrial stromal tumors. Proc Natl Acad Sci U S A *98*, 6348-6353.

Koontz, J. I., Soreng, A. L., Nucci, M., Kuo, F. C., Pauwels, P., van Den Berghe, H., Dal Cin, P., Fletcher, J. A., and Sklar, J. (2001b). Frequent fusion of the JAZF1 and JJAZ1 genes in endometrial stromal tumors. Proc Natl Acad Sci U S A *98*, 6348-6353.

Kotake, Y., Cao, R., Viatour, P., Sage, J., Zhang, Y., and Xiong, Y. (2007). pRB family proteins are required for H3K27 trimethylation and Polycomb repression complexes binding to and silencing p16INK4alpha tumor suppressor gene. Genes Dev *21*, 49-54.

Kouzarides, T. (2007). Chromatin modifications and their function. Cell *128*, 693-705.

Kraggerud, S. M., Skotheim, R. I., Szymanska, J., Eknaes, M., Fossa, S. D., Stenwig, A. E., Peltomaki, P., and Lothe, R. A. (2002). Genome profiles of familial/bilateral and sporadic testicular germ cell tumors. Genes Chromosomes Cancer *34*, 168-174.

Kung, C. P., and Raab-Traub, N. (2010). Epstein-Barr virus latent membrane protein 1 modulates distinctive NF- kappaB pathways through C-terminus-activating region 1 to regulate epidermal growth factor receptor expression. J Virol *84*, 6605-6614.

Kuo, M. H., and Allis, C. D. (1999). In vivo cross-linking and immunoprecipitation for studying dynamic Protein:DNA associations in a chromatin environment. Methods *19*, 425-433.

Kuppers, R. (2003). B cells under influence: transformation of B cells by Epstein-Barr virus. Nat Rev Immunol *3*, 801-812.

Kuppers, R., and Rajewsky, K. (1998). The origin of Hodgkin and Reed/Sternberg cells in Hodgkin's disease. Annu Rev Immunol *16*, 471-493.

Kurth, J., Spieker, T., Wustrow, J., Strickler, G. J., Hansmann, L. M., Rajewsky, K., and Kuppers, R. (2000). EBV-infected B cells in infectious mononucleosis: viral strategies for spreading in the B cell compartment and establishing latency. Immunity *13*, 485-495.

Kuzmichev, A., Jenuwein, T., Tempst, P., and Reinberg, D. (2004). Different EZH2-containing complexes target methylation of histone H1 or nucleosomal histone H3. Mol Cell *14*, 183-193.

Kuzmichev, A., Margueron, R., Vaquero, A., Preissner, T. S., Scher, M., Kirmizis, A., Ouyang, X., Brockdorff, N., Abate-Shen, C., Farnham, P., and Reinberg, D. (2005). Composition and histone substrates of polycomb repressive group complexes change during cellular differentiation. Proc Natl Acad Sci U S A *102*, 1859-1864.

Kuzmichev, A., Nishioka, K., Erdjument-Bromage, H., Tempst, P., and Reinberg, D. (2002). Histone methyltransferase activity associated with a human multiprotein complex containing the Enhancer of Zeste protein. Genes Dev *16*, 2893-2905.

Lardelli, P., Bookman, M. A., Sundeen, J., Longo, D. L., and Jaffe, E. S. (1990). Lymphocytic lymphoma of intermediate differentiation. Morphologic and immunophenotypic spectrum and clinical correlations. Am J Surg Pathol *14*, 752-763.

Lee, M. G., Villa, R., Trojer, P., Norman, J., Yan, K. P., Reinberg, D., Di Croce, L., and Shiekhattar, R. (2007). Demethylation of H3K27 regulates polycomb recruitment and H2A ubiquitination. Science *318*, 447-450.

Lee, T. I., Jenner, R. G., Boyer, L. A., Guenther, M. G., Levine, S. S., Kumar, R. M., Chevalier, B., Johnstone, S. E., Cole, M. F., Isono, K*., et al.* (2006). Control of developmental regulators by Polycomb in human embryonic stem cells. Cell *125*, 301-313.

Lee, Y., Ahn, C., Han, J., Choi, H., Kim, J., Yim, J., Lee, J., Provost, P., Radmark, O., Kim, S., and Kim, V. N. (2003). The nuclear RNase III Drosha initiates microRNA processing. Nature *425*, 415-419.

Lee, Y., Kim, M., Han, J., Yeom, K. H., Lee, S., Baek, S. H., and Kim, V. N. (2004). MicroRNA genes are transcribed by RNA polymerase II. EMBO J *23*, 4051-4060.

Lenz, G., and Staudt, L. M. Aggressive lymphomas. N Engl J Med *362*, 1417-1429.

Lenz, G., Wright, G., Dave, S. S., Xiao, W., Powell, J., Zhao, H., Xu, W., Tan, B., Goldschmidt, N., Iqbal, J*., et al.* (2008a). Stromal gene signatures in large-B-cell lymphomas. N Engl J Med *359*, 2313-2323.

Lenz, G., Wright, G. W., Emre, N. C., Kohlhammer, H., Dave, S. S., Davis, R. E., Carty, S., Lam, L. T., Shaffer, A. L., Xiao, W*., et al.* (2008b). Molecular subtypes of diffuse large B-cell lymphoma arise by distinct genetic pathways. Proc Natl Acad Sci U S A *105*, 13520-13525.

Lessard, J., Baban, S., and Sauvageau, G. (1998). Stage-specific expression of polycomb group genes in human bone marrow cells. Blood *91*, 1216-1224.

Lessard, J., and Sauvageau, G. (2003). Bmi-1 determines the proliferative capacity of normal and leukaemic stem cells. Nature *423*, 255-260.

Lessard, J., Schumacher, A., Thorsteinsdottir, U., van Lohuizen, M., Magnuson, T., and Sauvageau, G. (1999). Functional antagonism of the Polycomb-Group genes eed and Bmi1 in hemopoietic cell proliferation. Genes Dev *13*, 2691-2703.

Leung, C., Lingbeek, M., Shakhova, O., Liu, J., Tanger, E., Saremaslani, P., Van Lohuizen, M., and Marino, S. (2004). Bmi1 is essential for cerebellar development and is overexpressed in human medulloblastomas. Nature *428*, 337-341.

Lewis, B. P., Burge, C. B., and Bartel, D. P. (2005). Conserved seed pairing, often flanked by adenosines, indicates that thousands of human genes are microRNA targets. Cell *120*, 15-20.

Lewis, E. B. (1978). A gene complex controlling segmentation in Drosophila. Nature *276*, 565-570.

Li, E., Beard, C., and Jaenisch, R. (1993). Role for DNA methylation in genomic imprinting. Nature *366*, 362-365.

Li, E., Bestor, T. H., and Jaenisch, R. (1992). Targeted mutation of the DNA methyltransferase gene results in embryonic lethality. Cell *69*, 915-926.

Lim, L. P., Lau, N. C., Garrett-Engele, P., Grimson, A., Schelter, J. M., Castle, J., Bartel, D. P., Linsley, P. S., and Johnson, J. M. (2005). Microarray analysis shows that some microRNAs downregulate large numbers of target mRNAs. Nature *433*, 769-773.

Liu, C. L., Kaplan, T., Kim, M., Buratowski, S., Schreiber, S. L., Friedman, N., and Rando, O. J. (2005). Single-nucleosome mapping of histone modifications in S. cerevisiae. PLoS Biol *3*, e328.

Liu, Y., Wang, X., Lo, A. K., Wong, Y. C., Cheung, A. L., and Tsao, S. W. (2002). Latent membrane protein-1 of Epstein-Barr virus inhibits cell growth and induces sensitivity to cisplatin in nasopharyngeal carcinoma cells. J Med Virol *66*, 63-69.

Llave, C., Xie, Z., Kasschau, K. D., and Carrington, J. C. (2002). Cleavage of Scarecrow-like mRNA targets directed by a class of Arabidopsis miRNA. Science *297*, 2053-2056.

Lo, A. K., To, K. F., Lo, K. W., Lung, R. W., Hui, J. W., Liao, G., and Hayward, S. D. (2007). Modulation of LMP1 protein expression by EBV-encoded microRNAs. Proc Natl Acad Sci U S A *104*, 16164-16169.

Lois, C., Hong, E. J., Pease, S., Brown, E. J., and Baltimore, D. (2002). Germline transmission and tissue-specific expression of transgenes delivered by lentiviral vectors. Science *295*, 868-872.

Lu, J. J., Chen, J. Y., Hsu, T. Y., Yu, W. C., Su, I. J., and Yang, C. S. (1996). Induction of apoptosis in epithelial cells by Epstein-Barr virus latent membrane protein 1. J Gen Virol *77 (Pt 8)*, 1883-1892.

Luger, K., Mader, A. W., Richmond, R. K., Sargent, D. F., and Richmond, T. J. (1997). Crystal structure of the nucleosome core particle at 2.8 A resolution. Nature *389*, 251-260.

Lujambio, A., Calin, G. A., Villanueva, A., Ropero, S., Sanchez-Cespedes, M., Blanco, D., Montuenga, L. M., Rossi, S., Nicoloso, M. S., Faller, W. J*., et al.* (2008). A microRNA DNA methylation signature for human cancer metastasis. Proc Natl Acad Sci U S A *105*, 13556-13561.

Lujambio, A., and Esteller, M. (2007). CpG island hypermethylation of tumor suppressor microRNAs in human cancer. Cell Cycle *6*, 1455-1459.

Lund, A. H., and van Lohuizen, M. (2004). Polycomb complexes and silencing mechanisms. Curr Opin Cell Biol *16*, 239-246.

Lund, E., Guttinger, S., Calado, A., Dahlberg, J. E., and Kutay, U. (2004). Nuclear export of microRNA precursors. Science *303*, 95-98.

Lung, R. W., Tong, J. H., Sung, Y. M., Leung, P. S., Ng, D. C., Chau, S. L., Chan, A. W., Ng, E. K., Lo, K. W., and To, K. F. (2009). Modulation of LMP2A expression by a newly identified Epstein-Barr virus-encoded microRNA miR-BART22. Neoplasia *11*, 1174-1184.

Marson, A., Levine, S. S., Cole, M. F., Frampton, G. M., Brambrink, T., Johnstone, S., Guenther, M. G., Johnston, W. K., Wernig, M., Newman, J.*, et al.* (2008). Connecting microRNA genes to the core transcriptional regulatory circuitry of embryonic stem cells. Cell *134*, 521-533.

Martin-Subero, J. I., Ammerpohl, O., Bibikova, M., Wickham-Garcia, E., Agirre, X., Alvarez, S., Bruggemann, M., Bug, S., Calasanz, M. J., Deckert, M.*, et al.* (2009a). A comprehensive microarray-based DNA methylation study of 367 hematological neoplasms. PLoS One *4*, e6986.

Martin-Subero, J. I., Kreuz, M., Bibikova, M., Bentink, S., Ammerpohl, O., Wickham-Garcia, E., Rosolowski, M., Richter, J., Lopez-Serra, L., Ballestar, E.*, et al.* (2009b). New insights into the biology and origin of mature aggressive B-cell lymphomas by combined epigenomic, genomic, and transcriptional profiling. Blood *113*, 2488-2497.

Martinez, A. M., Schuettengruber, B., Sakr, S., Janic, A., Gonzalez, C., and Cavalli, G. (2009). Polyhomeotic has a tumor suppressor activity mediated by repression of Notch signaling. Nat Genet *41*, 1076-1082.

Martinez, N., Camacho, F. I., Algara, P., Rodriguez, A., Dopazo, A., Ruiz-Ballesteros, E., Martin, P., Martinez-Climent, J. A., Garcia-Conde, J., Menarguez, J.*, et al.* (2003). The molecular signature of mantle cell lymphoma reveals multiple signals favoring cell survival. Cancer Res *63*, 8226-8232.

McManus, M. T., and Sharp, P. A. (2002). Gene silencing in mammals by small interfering RNAs. Nat Rev Genet *3*, 737-747.

Meier, C., Hoeller, S., Bourgau, C., Hirschmann, P., Schwaller, J., Went, P., Pileri, S. A., Reiter, A., Dirnhofer, S., and Tzankov, A. (2009). Recurrent numerical aberrations of JAK2 and deregulation of the JAK2-STAT cascade in lymphomas. Mod Pathol *22*, 476-487.

Merchant, M., Swart, R., Katzman, R. B., Ikeda, M., Ikeda, A., Longnecker, R., Dykstra, M. L., and Pierce, S. K. (2001). The effects of the Epstein-Barr virus latent membrane protein 2A on B cell function. Int Rev Immunol *20*, 805-835.

Meusers, P., Hense, J., and Brittinger, G. (1997). Mantle cell lymphoma: diagnostic criteria, clinical aspects and therapeutic problems. Leukemia *11 Suppl 2*, S60-64.

Miki, T., Kawamata, N., Arai, A., Ohashi, K., Nakamura, Y., Kato, A., Hirosawa, S., and Aoki, N. (1994). Molecular cloning of the breakpoint for 3q27 translocation in B-cell lymphomas and leukemias. Blood *83*, 217-222.

Min, J., Zhang, Y., and Xu, R. M. (2003). Structural basis for specific binding of Polycomb chromodomain to histone H3 methylated at Lys 27. Genes Dev *17*, 1823-1828.

Miranda, T. B., Cortez, C. C., Yoo, C. B., Liang, G., Abe, M., Kelly, T. K., Marquez, V. E., and Jones, P. A. (2009). DZNep is a global histone methylation inhibitor that reactivates developmental genes not silenced by DNA methylation. Mol Cancer Ther *8*, 1579-1588.

Monk, M., and Holding, C. (2001). Human embryonic genes re-expressed in cancer cells. Oncogene *20*, 8085-8091.

Montaner, D., Tarraga, J., Huerta-Cepas, J., Burguet, J., Vaquerizas, J. M., Conde, L., Minguez, P., Vera, J., Mukherjee, S., Valls, J.*, et al.* (2006). Next station in microarray data analysis: GEPAS. Nucleic Acids Res *34*, W486-491.

Montes-Moreno, S., Roncador, G., Maestre, L., Martinez, N., Sanchez-Verde, L., Camacho, F. I., Cannata, J., Martinez-Torrecuadrada, J. L., Shen, Y., Chan, W. C., and Piris, M. A. (2008). Gcet1 (centerin), a highly restricted marker for a subset of germinal center-derived lymphomas. Blood *111*, 351-358.

Morin, R. D., Johnson, N. A., Severson, T. M., Mungall, A. J., An, J., Goya, R., Paul, J. E., Boyle, M., Woolcock, B. W., Kuchenbauer, F.*, et al.* (2010). Somatic mutations altering EZH2 (Tyr641) in follicular and diffuse large B-cell lymphomas of germinal-center origin. Nat Genet *42*, 181-185.

Mosialos, G., Birkenbach, M., Yalamanchili, R., VanArsdale, T., Ware, C., and Kieff, E. (1995). The Epstein-Barr virus transforming protein LMP1 engages signaling proteins for the tumor necrosis factor receptor family. Cell *80*, 389-399.

Mozos, A., Royo, C., Hartmann, E., De Jong, D., Baro, C., Valera, A., Fu, K., Weisenburger, D. D., Delabie, J., Chuang, S. S.*, et al.* (2009). SOX11 expression is highly specific for mantle cell lymphoma and identifies the cyclin D1-negative subtype. Haematologica *94*, 1555-1562.

Muller, J., and Kassis, J. A. (2006). Polycomb response elements and targeting of Polycomb group proteins in Drosophila. Curr Opin Genet Dev *16*, 476-484.

Nanbo, A., Inoue, K., Adachi-Takasawa, K., and Takada, K. (2002). Epstein-Barr virus RNA confers resistance to interferon-alpha-induced apoptosis in Burkitt's lymphoma. EMBO J *21*, 954-965.

Negishi, M., Saraya, A., Miyagi, S., Nagao, K., Inagaki, Y., Nishikawa, M., Tajima, S., Koseki, H., Tsuda, H., Takasaki, Y.*, et al.* (2007). Bmi1 cooperates with Dnmt1-associated protein 1 in gene silencing. Biochem Biophys Res Commun *353*, 992-998.

Nemerow, G. R., Mold, C., Schwend, V. K., Tollefson, V., and Cooper, N. R. (1987). Identification of gp350 as the viral glycoprotein mediating attachment of Epstein-Barr virus (EBV) to the EBV/C3d receptor of B cells: sequence homology of gp350 and C3 complement fragment C3d. J Virol *61*, 1416-1420.

Nikoloski, G., Langemeijer, S. M. C., Kuiper, R. P., Knops, R., Massop, M., Tönnissen, E. R. L. T. M., van der Heijden, A., Scheele, T. N., Vandenberghe, P., de Witte, T.*, et al.* (2010). Somatic mutations of the histone methyltransferase gene EZH2 in myelodysplastic syndromes Nature genetics.

Niller, H. H., Salamon, D., Ilg, K., Koroknai, A., Banati, F., Bauml, G., Rucker, O., Schwarzmann, F., Wolf, H., and Minarovits, J. (2003). The in vivo binding site for oncoprotein c-Myc in the promoter for Epstein-Barr virus (EBV) encoding RNA (EBER) 1 suggests a specific role for EBV in lymphomagenesis. Med Sci Monit *9*, HY1-9.

Niwa, R., and Slack, F. J. (2007). The evolution of animal microRNA function. Curr Opin Genet Dev *17*, 145-150.

Nowak, K., Kerl, K., Fehr, D., Kramps, C., Gessner, C., Killmer, K., Samans, B., Berwanger, B., Christiansen, H., and Lutz, W. (2006). BMI1 is a target gene of E2F-1 and is strongly expressed in primary neuroblastomas. Nucleic Acids Res *34*, 1745-1754.

Nozawa, Y., Abe, M., Wakasa, H., Ohno, H., Fukuhara, S., Kinoshita, T., and Osato, T. (1988). Establishment and characterization of an Epstein-Barr virus negative B-cell lymphoma cell line and successful heterotransplantation. Tohoku J Exp Med *156*, 319-330.

O'Geen, H., Nicolet, C. M., Blahnik, K., Green, R., and Farnham, P. J. (2006). Comparison of sample preparation methods for ChIP-chip assays. Biotechniques *41*, 577-580.

O'Riain, C., O'Shea, D. M., Yang, Y., Le Dieu, R., Gribben, J. G., Summers, K., Yeboah-Afari, J., Bhaw-Rosun, L., Fleischmann, C., Mein, C. A*., et al.* (2009). Array-based DNA methylation profiling in follicular lymphoma. Leukemia *23*, 1858-1866.

Ogawa, H., Ishiguro, K., Gaubatz, S., Livingston, D. M., and Nakatani, Y. (2002). A complex with chromatin modifiers that occupies E2F- and Myc-responsive genes in G0 cells. Science *296*, 1132-1136.

Oguro, H., Iwama, A., Morita, Y., Kamijo, T., van Lohuizen, M., and Nakauchi, H. (2006). Differential impact of Ink4a and Arf on hematopoietic stem cells and their bone marrow microenvironment in Bmi1-deficient mice. J Exp Med *203*, 2247-2253.

Ohta, H., Sawada, A., Kim, J. Y., Tokimasa, S., Nishiguchi, S., Humphries, R. K., Hara, J., and Takihara, Y. (2002). Polycomb group gene rae28 is required for sustaining activity of hematopoietic stem cells. J Exp Med *195*, 759-770.

Okamura, K., Chung, W. J., and Lai, E. C. (2008). The long and short of inverted repeat genes in animals: microRNAs, mirtrons and hairpin RNAs. Cell Cycle *7*, 2840-2845.

Okano, M., Bell, D. W., Haber, D. A., and Li, E. (1999). DNA methyltransferases Dnmt3a and Dnmt3b are essential for de novo methylation and mammalian development. Cell *99*, 247-257.

Oliva, E., de Leval, L., Soslow, R. A., and Herens, C. (2007). High frequency of JAZF1-JJAZ1 gene fusion in endometrial stromal tumors with smooth muscle differentiation by interphase FISH detection. Am J Surg Pathol *31*, 1277-1284.

Onciu, M., Schlette, E., Medeiros, L. J., Abruzzo, L. V., Keating, M., and Lai, R. (2001). Cytogenetic findings in mantle cell lymphoma cases with a high level of peripheral blood involvement have a distinct pattern of abnormalities. Am J Clin Pathol *116*, 886-892.

Orchard, J., Garand, R., Davis, Z., Babbage, G., Sahota, S., Matutes, E., Catovsky, D., Thomas, P. W., Avet-Loiseau, H., and Oscier, D. (2003). A subset of t(11;14) lymphoma with mantle cell features displays mutated IgVH genes and includes patients with good prognosis, nonnodal disease. Blood *101*, 4975-4981.

Orlando, V. (2003). Polycomb, epigenomes, and control of cell identity. Cell *112*, 599-606.

Ota, A., Tagawa, H., Karnan, S., Tsuzuki, S., Karpas, A., Kira, S., Yoshida, Y., and Seto, M. (2004). Identification and characterization of a novel gene, C13orf25, as a target for 13q31-q32 amplification in malignant lymphoma. Cancer Res *64*, 3087-3095.

Otte, A. P., and Kwaks, T. H. (2003). Gene repression by Polycomb group protein complexes: a distinct complex for every occasion? Curr Opin Genet Dev *13*, 448-454.

Pandey, R. R., Mondal, T., Mohammad, F., Enroth, S., Redrup, L., Komorowski, J., Nagano, T., Mancini-Dinardo, D., and Kanduri, C. (2008). Kcnq1ot1 antisense noncoding RNA mediates lineage-specific transcriptional silencing through chromatin-level regulation. Mol Cell *32*, 232-246.

Park, I. K., Qian, D., Kiel, M., Becker, M. W., Pihalja, M., Weissman, I. L., Morrison, S. J., and Clarke, M. F. (2003). Bmi-1 is required for maintenance of adult self-renewing haematopoietic stem cells. Nature *423*, 302-305.

Pasini, D., Bracken, A. P., Hansen, J. B., Capillo, M., and Helin, K. (2007). The polycomb group protein Suz12 is required for embryonic stem cell differentiation. Mol Cell Biol *27*, 3769-3779.

Pasini, D., Bracken, A. P., Jensen, M. R., Lazzerini Denchi, E., and Helin, K. (2004). Suz12 is essential for mouse development and for EZH2 histone methyltransferase activity. EMBO J *23*, 4061-4071.

Pasqualucci, L., Bereschenko, O., Niu, H., Klein, U., Basso, K., Guglielmino, R., Cattoretti, G., and Dalla-Favera, R. (2003). Molecular pathogenesis of non-Hodgkin's lymphoma: the role of Bcl-6. Leuk Lymphoma *44 Suppl 3*, S5-12.

Paul, T. A., Bies, J., Small, D., and Wolff, L. Signatures of polycomb repression and reduced H3K4 trimethylation are associated with p15INK4b DNA methylation in AML. Blood.

Paul, T. A., Bies, J., Small, D., and Wolff, L. (2010). Signatures of polycomb repression and reduced H3K4 trimethylation are associated with p15INK4b DNA methylation in AML. Blood *115*, 3098-3108.

Perez-Rosado, A., Artiga, M., Vargiu, P., Sanchez-Aguilera, A., Alvarez-Barrientos, A., and Piris, M. (2008). BCL6 represses NFkappaB activity in diffuse large B-cell lymphomas. J Pathol *214*, 498-507.

Pfeffer, S., Zavolan, M., Grasser, F. A., Chien, M., Russo, J. J., Ju, J., John, B., Enright, A. J., Marks, D., Sander, C., and Tuschl, T. (2004). Identification of virus-encoded microRNAs. Science *304*, 734-736.

Pileri, S. A., and Falini, B. (2009). Mantle cell lymphoma. Haematologica *94*, 1488-1492.

Pillai, R. S., Bhattacharyya, S. N., Artus, C. G., Zoller, T., Cougot, N., Basyuk, E., Bertrand, E., and Filipowicz, W. (2005). Inhibition of translational initiation by Let-7 MicroRNA in human cells. Science *309*, 1573-1576.

Pulvertaft, J. V. (1964). Cytology of Burkitt's Tumour (African Lymphoma). Lancet *1*, 238-240.

Puppe, J., Drost, R., Liu, X., Joosse, S. A., Evers, B., Cornelissen-Steijger, P., Nederlof, P., Yu, Q., Jonkers, J., van Lohuizen, M., and Pietersen, A. M. (2009). BRCA1-deficient mammary tumor cells are dependent on EZH2 expression and sensitive to Polycomb Repressive Complex 2-inhibitor 3-deazaneplanocin A. Breast Cancer Res *11*, R63.

Raaphorst, F. M., Otte, A. P., van Kemenade, F. J., Blokzijl, T., Fieret, E., Hamer, K. M., Satijn, D. P., and Meijer, C. J. (2001). Distinct BMI-1 and EZH2 expression patterns in thymocytes and mature T cells suggest a role for Polycomb genes in human T cell differentiation. J Immunol *166*, 5925-5934.

Raaphorst, F. M., van Kemenade, F. J., Blokzijl, T., Fieret, E., Hamer, K. M., Satijn, D. P., Otte, A. P., and Meijer, C. J. (2000). Coexpression of BMI-1 and EZH2 polycomb group genes in Reed-Sternberg cells of Hodgkin's disease. Am J Pathol *157*, 709-715.

Raaphorst, F. M., Vermeer, M., Fieret, E., Blokzijl, T., Dukers, D., Sewalt, R. G., Otte, A. P., Willemze, R., and Meijer, C. J. (2004). Site-specific expression of polycomb-group genes encoding the HPC-HPH/PRC1 complex in clinically defined primary nodal and cutaneous large B-cell lymphomas. Am J Pathol *164*, 533-542.

Raetz, E. A., and Moos, P. J. (2004). Impact of microarray technology in clinical oncology. Cancer Invest *22*, 312-320.

Raffeld, M., and Jaffe, E. S. (1991). bcl-1, t(11;14), and mantle cell-derived lymphomas. Blood *78*, 259-263.

Raman, J. D., Mongan, N. P., Tickoo, S. K., Boorjian, S. A., Scherr, D. S., and Gudas, L. J. (2005). Increased expression of the polycomb group gene, EZH2, in transitional cell carcinoma of the bladder. Clin Cancer Res *11*, 8570-8576.

Richter, J., Ammerpohl, O., Martin-Subero, J. I., Montesinos-Rongen, M., Bibikova, M., Wickham-Garcia, E., Wiestler, O. D., Deckert, M., and Siebert, R. (2009). Array-based DNA methylation profiling of primary lymphomas of the central nervous system. BMC Cancer *9*, 455.

Rinn, J. L., Kertesz, M., Wang, J. K., Squazzo, S. L., Xu, X., Brugmann, S. A., Goodnough, L. H., Helms, J. A., Farnham, P. J., Segal, E., and Chang, H. Y. (2007). Functional demarcation of active and silent chromatin domains in human HOX loci by noncoding RNAs. Cell *129*, 1311-1323.

Roesch, A., Fukunaga-Kalabis, M., Schmidt, E. C., Zabierowski, S. E., Brafford, P. A., Vultur, A., Basu, D., Gimotty, P., Vogt, T., and Herlyn, M. (2010). A temporarily distinct subpopulation of slow-cycling melanoma cells is required for continuous tumor growth. Cell *141*, 583-594.

Roh, T. Y., Cuddapah, S., Cui, K., and Zhao, K. (2006). The genomic landscape of histone modifications in human T cells. Proc Natl Acad Sci U S A *103*, 15782-15787.

Rosenwald, A., Wright, G., Chan, W. C., Connors, J. M., Campo, E., Fisher, R. I., Gascoyne, R. D., Muller-Hermelink, H. K., Smeland, E. B., Giltnane, J. M.*, et al.* (2002). The use of molecular profiling to predict survival after chemotherapy for diffuse large-B-cell lymphoma. N Engl J Med *346*, 1937-1947.

Rosenwald, A., Wright, G., Leroy, K., Yu, X., Gaulard, P., Gascoyne, R. D., Chan, W. C., Zhao, T., Haioun, C., Greiner, T. C.*, et al.* (2003a). Molecular diagnosis of primary mediastinal B cell lymphoma identifies a clinically favorable subgroup of diffuse large B cell lymphoma related to Hodgkin lymphoma. J Exp Med *198*, 851-862.

Rosenwald, A., Wright, G., Wiestner, A., Chan, W. C., Connors, J. M., Campo, E., Gascoyne, R. D., Grogan, T. M., Muller-Hermelink, H. K., Smeland, E. B.*, et al.* (2003b). The proliferation gene expression signature is a quantitative integrator of oncogenic events that predicts survival in mantle cell lymphoma. Cancer Cell *3*, 185-197.

Salmon, P., and Trono, D. (2007). Production and titration of lentiviral vectors. Curr Protoc Hum Genet *Chapter 12*, Unit 12 10.

Sanchez-Beato, M., Sanchez, E., Garcia, J. F., Perez-Rosado, A., Montoya, M. C., Fraga, M., Artiga, M. J., Navarrete, M., Abraira, V., Morente, M.*, et al.* (2004). Abnormal PcG protein expression in Hodgkin's lymphoma. Relation with E2F6 and NFkappaB transcription factors. J Pathol *204*, 528-537.

Sanchez-Beato, M., Sanchez, E., Gonzalez-Carrero, J., Morente, M., Diez, A., Sanchez-Verde, L., Martin, M. C., Cigudosa, J. C., Vidal, M., and Piris, M. A. (2006). Variability in the expression of polycomb proteins in different normal and tumoral tissues. A pilot study using tissue microarrays. Mod Pathol *19*, 684-694.

Sander, S., Bullinger, L., Klapproth, K., Fiedler, K., Kestler, H. A., Barth, T. F., Moller, P., Stilgenbauer, S., Pollack, J. R., and Wirth, T. (2008). MYC stimulates EZH2 expression by repression of its negative regulator miR-26a. Blood *112*, 4202-4212.

Santamaria, D., Barriere, C., Cerqueira, A., Hunt, S., Tardy, C., Newton, K., Caceres, J. F., Dubus, P., Malumbres, M., and Barbacid, M. (2007). Cdk1 is sufficient to drive the mammalian cell cycle. Nature *448*, 811-815.

Schlesinger, Y., Straussman, R., Keshet, I., Farkash, S., Hecht, M., Zimmerman, J., Eden, E., Yakhini, Z., Ben-Shushan, E., Reubinoff, B. E.*, et al.* (2007). Polycomb-mediated methylation on Lys27 of histone H3 pre-marks genes for de novo methylation in cancer. Nat Genet *39*, 232-236.

Schoeftner, S., Sengupta, A. K., Kubicek, S., Mechtler, K., Spahn, L., Koseki, H., Jenuwein, T., and Wutz, A. (2006). Recruitment of PRC1 function at the initiation of X inactivation independent of PRC2 and silencing. EMBO J *25*, 3110-3122.

Schuettengruber, B., Chourrout, D., Vervoort, M., Leblanc, B., and Cavalli, G. (2007). Genome regulation by polycomb and trithorax proteins. Cell *128*, 735-745.

Schwartz, Y. B., Kahn, T. G., Nix, D. A., Li, X. Y., Bourgon, R., Biggin, M., and Pirrotta, V. (2006). Genome-wide analysis of Polycomb targets in Drosophila melanogaster. Nat Genet *38*, 700-705.

Shao, Z., Raible, F., Mollaaghababa, R., Guyon, J. R., Wu, C. T., Bender, W., and Kingston, R. E. (1999). Stabilization of chromatin structure by PRC1, a Polycomb complex. Cell *98*, 37-46.

Shimono, Y., Zabala, M., Cho, R. W., Lobo, N., Dalerba, P., Qian, D., Diehn, M., Liu, H., Panula, S. P., Chiao, E.*, et al.* (2009). Downregulation of miRNA-200c links breast cancer stem cells with normal stem cells. Cell *138*, 592-603.

Sholl, L. M., John Iafrate, A., Chou, Y. P., Wu, M. T., Goan, Y. G., Su, L., Huang, Y. T., Christiani, D. C., and Chirieac, L. R. (2007). Validation of chromogenic in situ hybridization for detection of EGFR copy number amplification in nonsmall cell lung carcinoma. Mod Pathol *20*, 1028-1035.

Singh, B., Stoffel, A., Gogineni, S., Poluri, A., Pfister, D. G., Shaha, A. R., Pathak, A., Bosl, G., Cordon-Cardo, C., Shah, J. P., and Rao, P. H. (2002). Amplification of the 3q26.3 locus is associated with progression to invasive cancer and is a negative prognostic factor in head and neck squamous cell carcinomas. Am J Pathol *161*, 365-371.

Song, Y. J., and Kang, M. S. (2010). Roles of TRAF2 and TRAF3 in Epstein-Barr virus latent membrane protein 1-induced alternative NF-kappaB activation. Virus Genes.

Sparmann, A., and van Lohuizen, M. (2006). Polycomb silencers control cell fate, development and cancer. Nat Rev Cancer *6*, 846-856.

Squazzo, S. L., O'Geen, H., Komashko, V. M., Krig, S. R., Jin, V. X., Jang, S. W., Margueron, R., Reinberg, D., Green, R., and Farnham, P. J. (2006). Suz12 binds to silenced regions of the genome in a cell-type-specific manner. Genome Res *16*, 890-900.

Stamatopoulos, B., Meuleman, N., Haibe-Kains, B., Saussoy, P., Van den Neste, E., Michaux, L., Heimann, P., Martiat, P., Bron, D., and Lagneaux, L. (2009). MicroRNA-29c and microRNA-223 downregulation has in vivo significance in chronic lymphocytic leukemia and improves disease risk stratification. Blood.

Stansfeld, A. G., Diebold, J., Noel, H., Kapanci, Y., Rilke, F., Kelenyi, G., Sundstrom, C., Lennert, K., van Unnik, J. A., Mioduszewska, O., and et al. (1988). Updated Kiel classification for lymphomas. Lancet *1*, 292-293.

Starczynowski, D. T., Vercauteren, S., Telenius, A., Sung, S., Tohyama, K., Brooks-Wilson, A., Spinelli, J. J., Eaves, C. J., Eaves, A. C., Horsman, D. E.*, et al.* (2008). High-resolution whole genome tiling path array CGH analysis of CD34+ cells from patients with low-risk myelodysplastic syndromes reveals cryptic copy number alterations and predicts overall and leukemia-free survival. Blood *112*, 3412-3424.

Stock, J. K., Giadrossi, S., Casanova, M., Brookes, E., Vidal, M., Koseki, H., Brockdorff, N., Fisher, A. G., and Pombo, A. (2007). Ring1-mediated ubiquitination of H2A restrains poised RNA polymerase II at bivalent genes in mouse ES cells. Nat Cell Biol *9*, 1428-1435.

Subramanian, A., Tamayo, P., Mootha, V. K., Mukherjee, S., Ebert, B. L., Gillette, M. A., Paulovich, A., Pomeroy, S. L., Golub, T. R., Lander, E. S., and Mesirov, J. P. (2005). Gene set enrichment analysis: a knowledge-based approach for interpreting genome-wide expression profiles. Proc Natl Acad Sci U S A *102*, 15545-15550.

Suva, M. L., Riggi, N., Janiszewska, M., Radovanovic, I., Provero, P., Stehle, J. C., Baumer, K., Le Bitoux, M. A., Marino, D., Cironi, L.*, et al.* (2009). EZH2 is essential for glioblastoma cancer stem cell maintenance. Cancer Res *69*, 9211-9218.

Swerdlow, S. H., Campo, E., Harris, N. L., Jaffe, E. S., Pileri, S. A., Stein, H., Thiele, J., and Vardiman, J. W. (2008). WHO Classification of Tumours of Haematopoietic and Lymphoid Tissues, Fourth Edition, Vol 2, (Lyon, France: IARC).

Tagawa, H., Suguro, M., Tsuzuki, S., Matsuo, K., Karnan, S., Ohshima, K., Okamoto, M., Morishima, Y., Nakamura, S., and Seto, M. (2005). Comparison of genome profiles for identification of distinct subgroups of diffuse large B-cell lymphoma. Blood *106*, 1770-1777.

Taipale, J., and Beachy, P. A. (2001). The Hedgehog and Wnt signalling pathways in cancer. Nature *411*, 349-354.

Takada, K., Horinouchi, K., Ono, Y., Aya, T., Osato, T., Takahashi, M., and Hayasaka, S. (1991). An Epstein-Barr virus-producer line Akata: establishment of the cell line and analysis of viral DNA. Virus Genes *5*, 147-156.

Tan, J., Yang, X., Zhuang, L., Jiang, X., Chen, W., Lee, P. L., Karuturi, R. K., Tan, P. B., Liu, E. T., and Yu, Q. (2007). Pharmacologic disruption of Polycomb-repressive complex 2-mediated gene repression selectively induces apoptosis in cancer cells. Genes Dev *21*, 1050-1063.

Terranova, R., Yokobayashi, S., Stadler, M. B., Otte, A. P., van Lohuizen, M., Orkin, S. H., and Peters, A. H. (2008). Polycomb group proteins Ezh2 and Rnf2 direct genomic contraction and imprinted repression in early mouse embryos. Dev Cell *15*, 668-679.

Tolhuis, B., de Wit, E., Muijrers, I., Teunissen, H., Talhout, W., van Steensel, B., and van Lohuizen, M. (2006). Genome-wide profiling of PRC1 and PRC2 Polycomb chromatin binding in Drosophila melanogaster. Nat Genet *38*, 694-699.

Toyota, M., Ahuja, N., Ohe-Toyota, M., Herman, J. G., Baylin, S. B., and Issa, J. P. (1999). CpG island methylator phenotype in colorectal cancer. Proc Natl Acad Sci U S A *96*, 8681-8686.

Trimarchi, J. M., Fairchild, B., Wen, J., and Lees, J. A. (2001). The E2F6 transcription factor is a component of the mammalian Bmi1-containing polycomb complex. Proc Natl Acad Sci U S A *98*, 1519-1524.

Tuck-Muller, C. M., Narayan, A., Tsien, F., Smeets, D. F., Sawyer, J., Fiala, E. S., Sohn, O. S., and Ehrlich, M. (2000). DNA hypomethylation and unusual chromosome instability in cell lines from ICF syndrome patients. Cytogenet Cell Genet *89*, 121-128.

Turner, B. M. (2007). Defining an epigenetic code. Nat Cell Biol *9*, 2-6.

Uchida, J., Yasui, T., Takaoka-Shichijo, Y., Muraoka, M., Kulwichit, W., Raab-Traub, N., and Kikutani, H. (1999). Mimicry of CD40 signals by Epstein-Barr virus LMP1 in B lymphocyte responses. Science *286*, 300-303.

Vakoc, C. R., Mandat, S. A., Olenchock, B. A., and Blobel, G. A. (2005). Histone H3 lysine 9 methylation and HP1gamma are associated with transcription elongation through mammalian chromatin. Mol Cell *19*, 381-391.

van der Lugt, N. M., Domen, J., Linders, K., van Roon, M., Robanus-Maandag, E., te Riele, H., van der Valk, M., Deschamps, J., Sofroniew, M., van Lohuizen, M., and et al. (1994). Posterior transformation, neurological abnormalities, and severe hematopoietic defects in mice with a targeted deletion of the bmi-1 proto-oncogene. Genes Dev *8*, 757-769.

van der Vlag, J., and Otte, A. P. (1999). Transcriptional repression mediated by the human polycomb-group protein EED involves histone deacetylation. Nat Genet *23*, 474-478.

van Lohuizen, M., Verbeek, S., Scheijen, B., Wientjens, E., van der Gulden, H., and Berns, A. (1991). Identification of cooperating oncogenes in E mu-myc transgenic mice by provirus tagging. Cell *65*, 737-752.

Varambally, S., Dhanasekaran, S. M., Zhou, M., Barrette, T. R., Kumar-Sinha, C., Sanda, M. G., Ghosh, D., Pienta, K. J., Sewalt, R. G., Otte, A. P.*, et al.* (2002). The polycomb group protein EZH2 is involved in progression of prostate cancer. Nature *419*, 624-629.

Vire, E., Brenner, C., Deplus, R., Blanchon, L., Fraga, M., Didelot, C., Morey, L., Van Eynde, A., Bernard, D., Vanderwinden, J. M.*, et al.* (2006). The Polycomb group protein EZH2 directly controls DNA methylation. Nature *439*, 871-874.

Visser, H. P., Gunster, M. J., Kluin-Nelemans, H. C., Manders, E. M., Raaphorst, F. M., Meijer, C. J., Willemze, R., and Otte, A. P. (2001). The Polycomb group protein EZH2 is upregulated in proliferating, cultured human mantle cell lymphoma. Br J Haematol *112*, 950-958.

Wang, H., Wang, L., Erdjument-Bromage, H., Vidal, M., Tempst, P., Jones, R. S., and Zhang, Y. (2004). Role of histone H2A ubiquitination in Polycomb silencing. Nature *431*, 873-878.

Wang, X. M., Greiner, T. C., Bibikova, M., Pike, B. L., Siegmund, K. D., Sinha, U. K., Muschen, M., Jaeger, E. B., Weisenburger, D. D., Chan, W. C.*, et al.* (2010). Identification and functional relevance of de novo DNA methylation in cancerous B-cell populations. J Cell Biochem.

Weber, M., Hellmann, I., Stadler, M. B., Ramos, L., Paabo, S., Rebhan, M., and Schubeler, D. (2007). Distribution, silencing potential and evolutionary impact of promoter DNA methylation in the human genome. Nat Genet *39*, 457-466.

Wei, G., Wei, L., Zhu, J., Zang, C., Hu-Li, J., Yao, Z., Cui, K., Kanno, Y., Roh, T.-Y., Watford, W. T.*, et al.* (2009). Global Mapping of H3K4me3 and H3K27me3 Reveals Specificity and Plasticity in Lineage Fate Determination of Differentiating CD4+ T Cells. Immunity *30*, 155-167.

Weigert, O., Unterhalt, M., Hiddemann, W., and Dreyling, M. (2009). Mantle cell lymphoma: state-of-the-art management and future perspective. Leuk Lymphoma *50*, 1937-1950.

Weisenburger, D. D., Nathwani, B. N., Diamond, L. W., Winberg, C. D., and Rappaport, H. (1981). Malignant lymphoma, intermediate lymphocytic type: a clinicopathologic study of 42 cases. Cancer *48*, 1415-1425.

Wellner, U., Schubert, J., Burk, U. C., Schmalhofer, O., Zhu, F., Sonntag, A., Waldvogel, B., Vannier, C., Darling, D., zur Hausen, A.*, et al.* (2009). The EMT-activator ZEB1 promotes tumorigenicity by repressing stemness-inhibiting microRNAs. Nat Cell Biol *11*, 1487-1495.

Welzel, N., Le, T., Marculescu, R., Mitterbauer, G., Chott, A., Pott, C., Kneba, M., Du, M. Q., Kusec, R., Drach, J.*, et al.* (2001). Templated nucleotide addition and immunoglobulin JH-gene utilization in t(11;14) junctions: implications for the mechanism of translocation and the origin of mantle cell lymphoma. Cancer Res *61*, 1629-1636.

Woo, C. J., Kharchenko, P. V., Daheron, L., Park, P. J., and Kingston, R. E. (2010). A region of the human HOXD cluster that confers polycomb-group responsiveness. Cell *140*, 99-110.

Wu, X., Rauch, T. A., Zhong, X., Bennett, W. P., Latif, F., Krex, D., and Pfeifer, G. P. (2010a). CpG Island Hypermethylation in Human Astrocytomas. Cancer Res.

Wu, Z. L., Zheng, S. S., Li, Z. M., Qiao, Y. Y., Aau, M. Y., and Yu, Q. (2010b). Polycomb protein EZH2 regulates E2F1-dependent apoptosis through epigenetically modulating Bim expression. Cell Death Differ *17*, 801-810.

Xiao, C., Srinivasan, L., Calado, D. P., Patterson, H. C., Zhang, B., Wang, J., Henderson, J. M., Kutok, J. L., and Rajewsky, K. (2008). Lymphoproliferative disease and autoimmunity in mice with increased miR-17-92 expression in lymphocytes. Nat Immunol *9*, 405-414.

Yap, K. L., Li, S., Munoz-Cabello, A. M., Raguz, S., Zeng, L., Mujtaba, S., Gil, J., Walsh, M. J., and Zhou, M. M. (2010). Molecular interplay of the noncoding RNA ANRIL and methylated histone H3 lysine 27 by polycomb CBX7 in transcriptional silencing of INK4a. Mol Cell *38*, 662-674.

Ye, B. H. (2000). BCL-6 in the pathogenesis of non-Hodgkin's lymphoma. Cancer Invest *18*, 356-365.

Yee, C., Biondi, A., Wang, X. H., Iscove, N. N., de Sousa, J., Aarden, L. A., Wong, G. G., Clark, S. C., Messner, H. A., and Minden, M. D. (1989). A possible autocrine role for interleukin-6 in two lymphoma cell lines. Blood *74*, 798-804.

Yekta, S., Shih, I. H., and Bartel, D. P. (2004). MicroRNA-directed cleavage of HOXB8 mRNA. Science *304*, 594-596.

Yi, R., Qin, Y., Macara, I. G., and Cullen, B. R. (2003). Exportin-5 mediates the nuclear export of pre-microRNAs and short hairpin RNAs. Genes Dev *17*, 3011-3016.

Young, K. H., Leroy, K., Moller, M. B., Colleoni, G. W., Sanchez-Beato, M., Kerbauy, F. R., Haioun, C., Eickhoff, J. C., Young, A. H., Gaulard, P.*, et al.* (2008). Structural profiles of TP53 gene mutations predict clinical outcome in diffuse large B-cell lymphoma: an international collaborative study. Blood *112*, 3088-3098.

Young, L. S., and Rickinson, A. B. (2004). Epstein-Barr virus: 40 years on. Nat Rev Cancer *4*, 757-768.

Yu, J., Rhodes, D. R., Tomlins, S. A., Cao, X., Chen, G., Mehra, R., Wang, X., Ghosh, D., Shah, R. B., Varambally, S.*, et al.* (2007). A polycomb repression signature in metastatic prostate cancer predicts cancer outcome. Cancer Res *67*, 10657-10663.

Zhang, Z., Huettner, P. C., Nguyen, L., Bidder, M., Funk, M. C., Li, J., and Rader, J. S. (2006). Aberrant promoter methylation and silencing of the POU2F3 gene in cervical cancer. Oncogene *25*, 5436-5445.

Zhao, J., Sun, B. K., Erwin, J. A., Song, J. J., and Lee, J. T. (2008). Polycomb proteins targeted by a short repeat RNA to the mouse X chromosome. Science *322*, 750-756.

APPENDIX (Publications)

ARTICLES

The following articles have been published or submitted to scientific journals:

Martín-Pérez D, Vargiu P, Montes S, Pisano DG, Rodríguez-Pinilla SM, Rodríguez R, Mollejo M, Castellvi J, Sánchez-Beato M, Piris MA.

Epstein Barr Virus microRNAs repress BCL6 expression in diffuse large B cell lymphoma. [Manuscript in preparation]

Martín-Pérez D, Piris MA, Sánchez-Beato M. (2010).

Polycomb proteins in hematologic malignancies. Blood. Aug 17. [Epub ahead of print].

Martín-Pérez D, Sánchez E, Maestre L, Suela J, Vargiu P, Di Lisio L, Martínez N, Alves J, Piris MA, Sánchez-Beato M. (2010).

Deregulated Expression of the Polycomb-Group Protein SUZ12 Target Genes Characterizes Mantle Cell Lymphoma. Am J Pathol. *177*(2):930-42.

Wozniak MB, Villuendas R, Bischoff JR, Aparicio CB, Martinez Leal JF, de La Cueva P, Rodriguez ME, Herreros B, **Martin-Perez D**, Longo MI, Herrera M, Piris MA, Ortiz-Romero PL. (2010).

Vorinostat interferes with the signaling transduction pathway of T-cell receptor and synergizes with phosphoinositide-3 kinase inhibitors in cutaneous T-cell lymphoma. Haematologica *95*, 613-621.

Molina-Privado I, Rodríguez-Martínez M, Rebollo P, **Martín-Pérez D**, Artiga MJ, Menárguez J, Flemington EK, Piris MA, Campanero MR. (2009).

E2F1 expression is deregulated and plays an oncogenic role in sporadic Burkitt's lymphoma. Cancer Res. *69(9):*4052-8.

Ruiz-Vela A, Aggarwal M, de la Cueva P, Treda C, Herreros B, **Martin-Perez D**, Dominguez O, and Piris MA. (2008).

Lentiviral (HIV)-based RNA interference screen in human B-cell receptor regulatory networks reveals Mcl-1-induced oncogenic pathways. Blood *111*, 1665-1676.